Paleoenvironmental, paleoecological and thermal metamorphism implications on the organic petrography and organic geochemistry of Tertiary Tanjung Enim coal, South Sumatra Basin, Indonesia

Von der Fakultät für Georessourcen und Materialtechnik
der Rheinisch-Westfälischen Technischen Hochschule Aachen

zur Erlangung des akademischen Grades eines

Doktors der Naturwissenschaften

genehmigte Dissertation

vorgelegt von **M. Tech.**

Donatus Hendra Amijaya

aus Yogyakarta

Berichter: Univ.-Prof. Dr.rer.nat. Ralf Littke
Univ.-Prof. (em) Dr.rer.nat. Detlev Leythaeuser

Tag der mündlichen Prüfung: 23. September 2005

untuk Indonesia…

Acknowledgement

The scholarship to pursue the PhD degree at Aachen University and the German language course at Goethe Institute, Mannheim was granted by the German Academic Exchange Service (DAAD) to which first of all a grateful acknowledgement is made.

I would like to express tremendous gratitude to Prof. Dr. Ralf Littke, Head of the Institute of Geology and Geochemistry of Petroleum and Coal (LEK), Aachen University, for his interest in the research topic and his supervision during my work at LEK. His understanding and patience as he was confronted with my "way of work" deserves great respect. I also extend sincere regards to Prof. Dr. Detlev Leythaeuser for his willingness to be the co-supervisor and his advice for the final version of my dissertation.

I equally thank PD Dr. Jan Schwarzbauer, Head of the Organic Geochemistry Laboratory at LEK, and Dr. Bernd Krooss, Head of the Petrophysics Laboratory at LEK, who granted me unlimited access to the laboratory facilities. They introduced various aspects of organic geochemistry to me, a very exciting subject that never got my attention before. They also delivered a lot of important suggestions for my research.

My knowledge on coal petrography was improved by fruitful discussions with Prof. Dr. Marco Ercegovac (Serbian Academy of Sciences and Arts, Belgrade) and Prof. Dr. Ali Karayigit (Haceteppe University, Turkey) during their visit as guest scientist at LEK, to whom my regards are addressed. I also thank to Dr. Achim Bechtel (Bonn University) for the discussion on organic geochemistry. My gratitudes are addressed to Dr. Jim Hower, Dr. Janet Dehmer, Dr. Sandra Neuzil, Dr. Tim Moore and an anonymous reviewer (International Journal of Coal Geology), also to Dr. Clifford Walters, Dr. Henrik Petersen and Dr. Michael Kruge (Organic Geochemistry) for numerous helpful comments, which enormously improved earlier versions of part of this work.

Kind support from Prof. Peter Kukla and PD Dr. Harald Stollhofen (Institute of Geology, Aachen University) by issuing the letter of recommendation for the prolongation of my scholarship was crucial for the continuity of my work.

I am indebted to PT. Tambang Batubara Bukit Asam (PTBA) Management at Tanjung Enim, Sumatra, Indonesia for the permission to take coal samples in PTBA concession area and also for lodging support during field work. I would like to acknowledge the coal geologists of PTBA, especially Ir. Suhedi and Ir. Pajar Hariadi from Exploration and Development Department and Ir. Roberth Bunga, Head of the Geological Section at Tambang Air Laya mine, for their enormous help and discussions during field work.

Valuable suggestions and support from Ir. Djoko Wintolo, DEA and Ir. Marno Datun (Gadjah Mada University, Yogyakarta) and Dr. Ir. Komang Anggayana (Bandung Institute of Technology, Bandung) are highly appreciated. Assistance on coal sampling at PTBA and preliminary sample preparation at Gadjah Mada University were provided by Pentatok Kuncoro, Lalu Winaran, Rimbun Nainggolan, Tiastomo Ardian and Harry Nugraha.

The electron microscopy analysis was conducted at the Central Facility for Electron Microscopy, Aachen University and the XRD analysis was done at the Institute of Mineralogy, Aachen University. I thank all staff members from both institutions who assisted in these analyses.

Co-operation and technical assistance from my fellow-colleagues at LEK, Dipl. Geol. Ralf Meier, Emmannuel Eseme, M.Sc., Ina Blumenstein, M.Sc., Dipl. Geol. Alex Kronimus, Phillip Weniger and Jens Köster on organic geochemistry analysis, as well as Rolf Mildenberger's assistance to prepare the polished sections for microscopic analysis and his teaching on technical aspects of microscopy, are gratefully acknowledged. I thank Dipl. Geol. Danny Schwarzer, Dipl. Geol. Sabine Rodon, Dipl. Geol. Yvonne Senglaub and Dipl. Geow. Susanne Nelskamp for the German language correction on my annual reports to DAAD and Dr. Dirk Prinz for correcting the “Zusammenfassung” of this dissertation. I was also helped by LEK-secretariat staff, Mrs. Dorit Kanellis and Mrs. Renate Wuropoulos, to handle the administrative subjects.

Special thanks are due to my wife, Sita Yuliastuti Amijaya, for the encouragement she gave between her own activities to finish her study in Cologne and to my parents, for their support and understanding.

Abstract

Organic petrography and organic geochemistry studies have been conducted on Tertiary age coals from Tanjung Enim, South Sumatra Basin. The South Sumatra basin is among the most important coal producing basins in Indonesia since the coal resources represent one third of Indonesian coal resources. The coals are of subbituminous rank and characterized by low vitrinite (huminite) reflectance (VR_r = 0.35 - 0.46%). In this area, the coals were also locally intruded by andesitic sills. The thermally metamorphosed coals are of medium-volatile bituminous to meta-anthracite rank (high vitrinite reflectance, VR_r up to 5.18%).

The studied low rank coals are dominated by huminite (34.6 - 94.6 vol. %). Less abundant are liptinite (4.0 - 61.4 vol. %) and inertinite (0.2 - 43.9 vol. %). Minerals are found only in small amounts (0 - 2 vol. %); mostly as iron sulfide. In the high rank coal, the thermally altered vitrinite composes 82.4 – 93.8 vol.%. Liptinite and inertinite are observed only in very minor amount. Mosaic structures can be recognized as groundmass and crack fillings. The most common minerals found are carbonates, pyrite or marcasite and clay minerals. The latter consist of kaolinite in low rank coal and illite and rectorite in high rank coal.

The coals outside the metamorphism area are characterized by high moisture content (4 - 11 wt.%) and volatile matter content (> 40 wt.%, daf), as well as less than 80 wt.% (daf) carbon content. In contrast, the thermally metamorphosed coals are characterized by low moisture content (only < 3 wt.%) and volatile matter content (< 24 wt.%, daf), as well as high carbon content (>80 wt.%, daf).

Based on maceral assemblages, the low rank coals can be grouped into five classes: (1) humotelinite-rich group, (2) humodetrinite-rich group, (3) humocollinite-rich group, (4) inertinite-rich group and (5) humodetrinite-liptinite-rich group. Comparing the distribution of maceral assemblages to the maceral or pre-maceral assemblages in modern tropical domed peat in Indonesia reveals many similarities. The basal section of the studied coal seams is represented typically by the humodetrinite-liptinite-rich group. This section might be derived from sapric or fine hemic peat often occurring at the base

of modern peats. The middle section of the seams is characterized by humotelinite-rich and humocollinite-rich groups. The precursors of these groups were hemic and fine hemic peats. The top section of the coal seams is typically represented by the humodetrinite-rich or inertinite-rich group. These groups are the counterparts of fibric peat at the top of the modern peats. The sequence of maceral assemblages thus represents the change of topogenous to ombrogenous peat and the development of a raised peat bog.

A comparison between the result of detailed maceral assemblage analysis and the paleodepositional environment as established from coal maceral ratio calculation indicates that the use of coal maceral ratio diagrams developed for other coal deposits fails to deduce paleo-peat development for these young tropical coals. In particular, mineral distribution and composition should not be neglected in coal facies interpretations.

The coalification path of each maceral shows that vitrinite, liptinite and inertinite reflectance converge in a transition zone at VR_{max} of around 1.5%. Significant decrease of volatile matter occurs in the zone between 0.5 – 2.0% VR_{max}. A sharp bend occurs at VR_{max} between 2.0% and 2.5%. Above 2.5%, the volatile matter decreases only very slightly. Between VR_r = 0.5% and 2.0%, the carbon content of the coals is ascending drastically. Above 2.5% VR_r, the carbon content becomes relatively stable (around 95 wt.%, daf).

Using Rock-Eval pyrolysis, it is known that the Oxygen Index values of all studied coals are low (<5 mg CO_2/g TOC) and the high rank coals have a lower Hydrogen Index (< 130 mg HC/g TOC) than the low rank coals (~300 mg HC/g TOC). The T_{max} increases with maturity (420 - 440 °C for low rank coals and 475 - 551^{o}C for high rank coals).

Based on some petrographical and chemical properties, it was calculated that the temperature of contact metamorphism reached 700 - 750ºC in the most metamorphosed coal.

GC/GC-MS analysis has been performed to study the molecular composition of the studied coals. The *n*-alkane distribution as well as the relative amount of phytane and pristane correlate with the organic facies of the studied coals and their maturity. Some identified terpenoid biomarkers, most of all cadinane- and eudesmane-type sesquiterpenoids and oleanane- and ursane-type triterpenoids, indicate the predominance of angiosperm plants in the paleomire, which is in agreement with abundance of *Dipterocarpaceae* family documented in previous palynological studies on Tertiary coal and peat in Indonesia. The distribution of hopanoids is affected by the organic facies of the coal and their maturity, and correlates with the paleomire evolution as derived from petrological studies.

Furthermore the effect of rapid thermal stress on the organic geochemistry of the coals has been quantified. Reversals in the trends of molecular maturity parameters based on aliphatic hydrocarbons (*n*-alkane distribution and pristane/phytane ratio) and aromatic hydrocarbons (methylphenanthrene) with coal rank are observed. This trend is also reflected by the ratio of aromatic C-H to aliphatic C-H absorbances of coals based on FTIR analysis.

Zusammenfassung

An tertiären Kohlen aus Tanjung Enim, Südsumatra Becken, wurden organisch-petrographische und -geochemische Untersuchungen durchgeführt. Das Südsumatra Becken ist eines der wichtigsten Kohle produzierenden Becken Indonesiens, da es ein Drittel der indonesischen Kohleressourcen repräsentiert. Die vorliegenden Kohlen wurden als Mattbraunkohle charakterisiert und zeichnen sich durch die entsprechende Vitrinit- (Huminit-)Reflexion (VR_r = 0.35 - 0.46%) aus. Darüber hinaus fanden in diesem Gebiet Andesit-Intrusionen statt. Durch die damit verbundene Thermometamorphose wurden die Kohlen unterschiedlich stark überprägt und lassen sich dem Fettkohlen- bis Meta-Anthrazit-Stadium zuordnen (hohe Vitrinitreflexion, VR_r bis zu 5.18%).

Unter den Mazeralgruppen dominiert Huminit die niedrig inkohlten Kohlen (34,6 - 94,6 Vol.%). Weniger häufig sind Liptinit (4,0 – 61,4 Vol.%) und Inertinit (0,2 - 43,9 Vol. %) anzutreffen. Minerale sind nur in geringem Maße vorhanden (0 - 2 Vol. %), hauptsächlich Eisensulfide sind mikroskopisch erkennbar. Die hoch inkohlten Kohlen bestehen überwiegend aus thermisch verändertem Vitrinit (82,4 - 93,8 Vol.%). Die Liptinit- und Inertinitanteile sind gering. In Grundmasse und Kluftfüllungen lassen sich Mosaik-Strukturen beschreiben. Häufigste Minerale sind Karbonat, Pyrit oder Markasit sowie Tonminerale. In den niedrig inkohlten Kohlen treten die Tonminerale überwiegend als Kaolinit, in den höher inkohlten als Illit und Rektorit auf.

Die Kohlen, die sich ausserhalb der thermischen Beeinflussungszone befinden, haben einen hohen Gehalt an Feuchtigkeit (4 – 11 Gew.%), flüchtigen Bestandteilen (>40 Gew.%, wasser- und aschefrei Basis: waf) sowie weniger als 80 Gew.% (waf) Kohlenstoffgehalt. Im Gegensatz dazu weisen die von der Thermometamorphose beeinflussten Kohlen einen niedrigen Gehalt an Feuchtigkeit (nur < 3 Gew.%), flüchtigen Bestandteilen (< 24 Gew.%, waf), sowie einen hohen Gehalt an Kohlenstoff (>80 Gew.%, waf) auf.

Anhand der Mazeral-Zusammensetzung können die Kohlen in fünf Gruppen eingeteilt werden: (1) eine Humotelinit-reiche Gruppe, (2) eine Humodetrinit-reiche Gruppe, (3)

eine Humodetrinit-Liptinit-reiche Gruppe, (4) eine Humocollinit-reiche Gruppe sowie (5) eine Inertinit-reiche Gruppe. Vergleicht man die Mazeral-Zusammensetzung der Proben mit der Mazeral- oder Prä-Mazeral-Zusammensetzung rezenter tropischer Hochmoore Indonesiens, lassen sich viele Gemeinsamkeiten herausarbeiten. Der basale Abschnitt der untersuchten Kohlenflöze wird durch Humodetrinit-Liptinit-reiche Kohle charakterisiert. Dieser Abschnitt konnte von feinkörnigem („sapric“) oder etwas grobkörnigerem („fine-hemic“) Torf abgeleitet werden, der häufig im Liegenden des rezenten Torfs auftritt. Der mittlere Abschnitt des Flözes wird von Humotelinit-reichen und Humocollinit-reichen Kohlen gekennzeichnet. Der obere Abschnitt des Kohlenflözes wird von Humodetrinit-reichen oder Inertinit-reichen Kohlen repräsentiert. Im Hangenden des rezenten Torfs ist ein faseriger, stark wurzelhaltiger Torf („fibric“) anzutreffen. Diese Sequenz repräsentiert eine Entwicklung von topogenem zu ombrogenem Torf, die auch die Entwicklung eines Hochmoores widerspiegelt.

Ein Vergleich der Ergebnisse der detaillierten Mazeral-Analyse sowie der zur Bestimmung des Paläoablagerungsmilieus berechneten Mazeral-Verhältnisse zeigt, dass aus der Anwendung der Mazeral-Verhältnisdiagramme, die für andere Kohlelagerstätten entwickelt wurden, die Entwicklung des Paläotorfs dieser jungen tropischen Kohlen nicht hergeleitet werden kann. Darüber hinaus spielt die Mineralverteilung und -zusammensetzung bei der Interpretation der Kohlefazies eine nicht zu vernachlässigende Rolle.

Die Inkohlungskennlinien der Mazerale zeigen, dass die Vitrinit-, Liptinit- und Inertinitreflexion in einer Übergangzone bei VR_{max} von etwa 1,5% konvergieren. Eine bedeutende Abnahme an flüchtigen Bestandteilen tritt in der Zone zwischen 0,5 – 2,0% VR_{max} auf. Ein auffallender Knick wird bei VR_{max} zwischen 2,0% und 2,5% festgestellt, während über 2,5% der Gehalt an flüchtigen Bestandteilen nur wenig abnimmt. Zwischen VR_r = 0.5% und 2.0% steigt der Kohlenstoffgehalt der Proben stark an. Über 2,5% VR_r ist der Kohlenstoffgehalt relativ konstant (etwa 95 Gew.%, waf).

Die Rock-Eval-Pyrolyse zeigt einen niedrigen Sauerstoff-Index der untersuchten Kohlen (< 5 mg CO_2/g TOC). Die hoch inkohlten Kohlen besitzen einen niedrigeren Wasserstoff-Index (< 130 mg HC/g TOC) als die Kohlen geringerer Reife (~300 mg

HC/g TOC). T_{max} nimmt mit steigender Reife zu (420 - 440 °C bei den niedrig inkohlten Kohlen und 475 - 551°C bei den hoch inkohlten Kohlen).

Anhand der petrographischen und chemischen Eigenschaften wurde errechnet, dass die Metamorphosetemperatur der Kohlen, die der höchsten thermischen Beeinflussung ausgesetzt waren, im Kontaktbereich 700 - 750ºC erreichte.

GC/GC-MS-Analysen wurden durchgeführt, um die molekularen Eigenschaften der Kohlen zu untersuchen. Die Verteilung der *n*-Alkane sowie die relative Menge von Phytan und Pristan sind von der organischen Fazies sowie dem entsprechenden Inkohlungsstadium abhängig. Identifizierte Terpenoide-Biomarker, hauptsächlich Sesquiterpenoide vom Cadinan- und Eudesmantyp sowie Triterpenoide vom Oleanan- und Ursantyp, zeigen die Vorherrschaft der Angiospermen im Paläomoor an. Dies korreliert sehr gut mit den reichlich vorhandenen Pflanzenresten der *Dipterocarpaceae*-Familie, die in den bisherigen palynologischen Untersuchungen an tertiären Kohlen und Torfen in Indonesien bereits dokumentiert wurden. Die Hopanoidverteilung wird durch die organische Fazies der Kohle und ihrer Reife beeinflußt, und hängt, wie durch petrologische Untersuchung abgeleitet werden kann, mit der Entwicklung des Paläomoores zusammen.

Ferner ist der Einfluss der schnellen intrusionsbedingten Aufheizung durch organisch-geochemische Untersuchungen der Kohlen quantitativ bestimmt worden. Weiterhin konnte eine Umkehrung der auf aliphatische Kohlenwasserstoffe (*n*-Alkan-Verteilung und Pristan/Phytan-Verhältnis) und aromatische Kohlenwasserstoffe (Methylphenanthren) basierenden Trends der molekularen Reifeparameter mit steigender Inkohlung festgestellt werden. Das Verhältnis der aromatischen C-H zu den aliphatischen C-H Absorptionen der FTIR-Analyse zeigt eine ähnliche Entwicklung.

Contents

Chapter 3 Properties of thermally metamorphosed coal from Tanjung Enim Area, South Sumatra Basin, Indonesia with special reference to the coalification path of macerals

Chapter 4 Organic geochemistry of Lower Suban coal seam, South Sumatra Basin, Indonesia: paleoecological and thermal metamorphism implications

Chapter 5 Final discussion

Chapter 6 Outlook

Chapter 1 Introduction

Coal research in Indonesia had began more than one hundred years ago along with the coal mining history as the first mine was opened in 1894 in Pengaron, East Kalimantan (Borneo). Since then, the coal industry has been rapidly expanding, especially since the government's energy diversification program in the middle seventies. At present more than 100 national and 17 international coal mining companies operate in Indonesia.

Indonesia is the fourth largest coal exporter and the twenty-sixth largest coal consumer of the world. Coal consumption has increased rapidly as a number of new coal-fired power plants have been placed into operation in the nineties. To meet the demand of coal, the government of Indonesia encourages more companies to invest in coal mine development. A lot of new coal exploration and exploitation activities will be carried out. Accordingly, research on the Indonesian coals from a geological point of view always becomes an actual need to provide information of the coal characteristics.

1.1 The significance of coals for Indonesia

1.1.1 Economic significance

With more than 200 million inhabitants, Indonesia experienced a tremendous growth of power use in the past thirty years. This has produced a significant increase in the demand of steam coal for power plants. The government plans to construct more coal and gas power plants (combined cycle) which have been proven to be more economical. The expansion of coal fired steam power plants can be seen in the government's plan to increase their power generation capacity from 1,730 MW by year 1990 to 11,055 MW by year 2000 (Prijono, 1989). According to Directorate of Coal of Indonesia (2000), until 1998 the coal contribution to the power sector was 33%, followed by natural gas (31%), oil (21%) and others.

The increasing domestic consumption of coal is also pushed by the expansion programs in the cement sector. The cement industry consumes approximately 11% of the coal production in Indonesia. Other coal user sectors are pulp industry (4%), metallurgy industry (1%) and various industries and household (13%). The government had also

launched a program to change the dependence of energy fulfillment in household on petroleum with coal briquette.

Based on the data from the Directorate of Coal of Indonesia (2000), Indonesia produced 73.8 Mt of coal and exported 55.3 Mt in 1999. Indonesia is becoming one of the most important producers of surface-mined steam coal in Asia because Indonesia provides low-sulfur, low-nitrogen coal at comparatively low cost to buyer. Indonesia's cost of production is considered to be very low compared to other coal producer countries due to the excellent geologic conditions that enable the use of low-cost surface mining methods (Murrell, 1996). The biggest Indonesian coal importer is Japan, followed by Taiwan, Hongkong and other Asian countries. The main Indonesia coal export destinations outside Asia are Spain and the Netherlands in Europe and USA. However, to fulfill the rapidly expanding demands of particular coals for domestic use, Indonesia imported about 285,000 t coal in 2000 and this number is assumed to increase further (Chadwick, 2001).

1.1.2 Coal geology and resources

The sedimentary basins which contain coal deposits in Indonesia are mainly of Tertiary age, although Paleozoic coal occurrences are known locally in Sumatra, Sulawesi (Celebes) and Irian (Papua) (Koesoemadinata, 2000; Daulay et al., 2000). The location of some important coal basins in Indonesia is shown in Fig. 1.1. The basin formation and inversion in Indonesia owe their origin to the interplay between the India-Australian, Eurasian and Pacific tectonic plates, since Indonesia is the area where those three plates converge (see Daly et al., 1987; Hall, 1995).

The major coal deposits in Indonesia are located mostly in Western Indonesia. Koesoemadinata (2000) described in a tectono-stratigraphic overview three deposition episodes of the Tertiary coal in Western Indonesia which can be recognized: (1) syn-rift deposition (Eocene-Oligocene), (2) post-rift transgressive phase deposition (Oligocene-Early Miocene) and (3) syn-orogenic regressive phase deposition (Neogene).

Fig. 1.1. The location of some important coal basins in Indonesia. The major coal basins are Meulaboh Basin (1), Central Sumatra Basin (2), South Sumatra Basin (3), Tarakan Basin (4), Kutai Basin (5), Barito Basin (6) and Pasir Basin (7). Map is modified from Soehandojo (1989).

Paleogene syn-rift coal deposits are usually associated with fluviatile-lacustrine sediments. A typical coal bearing formation related to this depositional phase is the Sawahlunto Formation of the Central Sumatra Basin. Coal seams formed during the post-rift transgressive phase were deposited mainly in a shelf setting associated with nearshore marshes, tidal flats and deltaic environment. Some post-rift coals are found for example in the Sihapas Formation (Central Sumatra Basin), Upper Talang Akar Formation (South Sumatra Basin) or Lower Tanjung Formation of Barito and Pasir Basins in South-East Kalimantan.

The Miocene-Pliocene Muara Enim Formation in South Sumatra Basin is a well known syn-orogenic regression related coal bearing formation. The coal seams were extensively developed during the deltaic deposition in a back-arc basin setting. In the fore-arc basin setting, the main coal deposit related to the same phase is represented for example in the Meulaboh Basin in North Sumatra (Tutut Formation).

Thick coal seams are also found in the suture related basin setting. For example in the Barito and Pasir Basins, they are found in the regressive phase of the Miocene Warukin Formation. East Kalimantan basinal areas are characterized by a passive margin setting. The coal deposits are usually related to the deltaic floodplain environment which developed during Miocene (Balikpapan and Pulubalang Formations). Kutei and Tarakan Basins are the important coal basins in this area.

The significant coal deposits in Central Indonesia are found in South Sulawesi (Celebes), and were formed in the final stage of the syn-rift stage deposition of peat took place in the Middle to Late Eocene within a series of fluviatile-lacustrine and deltaic deposits. In Eastern Indonesia no major coal occurence has been reported, except in the Bintuni Basin in North-West Papua (Steenkool Formation). This syn-orogenic coal was deposited during Late Miocene to Pliocene.

The coal resources in Indonesia are estimated to be greater than than 38.8 billion tons. Most of them are located in East Kalimantan and South Sumatra (Fig. 1.2). Around 60% of the coal resources is brown coal. The rest of them is bituminous coal and only around 1% is anthracite (Directorate of Coal of Indonesia, 2000).

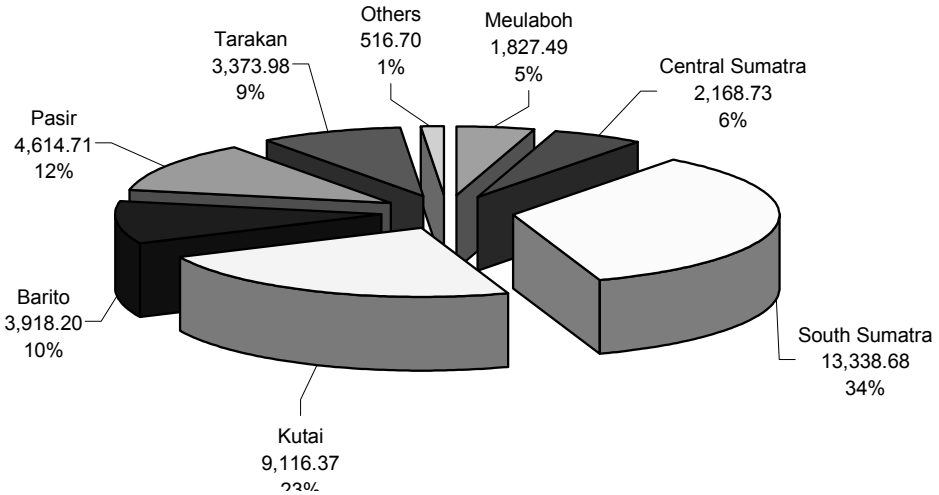

Fig. 1.2. Coal resources of major coal basins in Indonesia (in million tons) and their percentage to the total Indonesian coal resources. Graphic is based on the data published by Directorate of Coal of Indonesia (2000).

1.2 Backgrounds and general goals of the study

South Sumatra Basin is one of the important oil and coal producing sedimentary basins in Indonesia. The coal resources in this basin represent one third of Indonesian coal resources (Directorate of Coal of Indonesia, 2000). The economically valuable coals are found in the Tertiary Muara Enim Formation, which was deposited during the Late Miocene-Early Pliocene. Coal has been mined since the early 20th century in South Sumatra, most of all in Tanjung Enim area.

The South Sumatra Basin is situated in a tectonically active region. The coal-bearing strata were subjected to at least one period of folding and faulting, and later affected by extrusive and intrusive magmatic activity. Intrusion caused further uplift but most importantly subjected the strata to local metamorphism, i.e. rank increase from lignitic through to anthracitic grades in some areas. Previous studies on coal geology in South Sumatra Basin basin were usually conducted for exploration purposes (Shell Mijnbouw, 1976; Bamco, 1983; Kinhil-Otto Gold, 1986). Some other studies have also been done to assess the characteristics of the coal, either using petrographical or geochemical methods (Daulay, 1988; Anggayana, 1996; Daulay et al., 2000; Pujobroto, 2000;

Pujobroto and Hutton, 2000; Nas and Pujobroto, 2000 and others). However, a comprehensive study to assess the coal characteristic based on both organic petrology and organic geochemistry has not been done yet.

Many physical and chemical methods have been used to study the dynamics of coalification and depositional environment of coal. The classical method in coal study is the petrography analysis of coal organic constituents (macerals) and inorganic matter in coal. The degree of coalification has been studied mainly on the basis of vitrinite reflectance (see Teichmüller, 1987; Taylor et al., 1998), although other authors have presented basic petrographic studies of evolution coal macerals during coalification (e.g. Stach, 1953; Teichmüller, 1974; Smith and Cook, 1980). Knowledge of the petrographical composition of the coal can be used also as a key to understand the evolution of coal precursor (paleo-peat) development (Diessel, 1986; Littke, 1987; Littke and ten Haven, 1989; Teichmüller, 1989; Calder et al., 1991 and many others).

Besides optical examination, physicochemical analysis and chemical analysis are applied to determine the characteristics of coal. The Rock-Eval pyrolysis method (Espitalié et al., 1977a, 1977b) has been widely used to characterize the types of organic matter in rock, as well as in coal, and their degree of maturation. It is also well known that the degree of thermal alteration affects the molecular composition of coal. Therefore, many attempts have been made to detect the change of the coal molecular composition due to coalification. Various methods have been applied, for example by using infra red or gas chromatography-mass spectrometry analysis (see van Krevelen, 1993). Moreover, a wide variety of organic geochemical indicators have been proposed to identify paleoenvironmental and paleocological conditions. One of the very useful organic geochemical methods is biological marker (biomarker) analysis, which can provide clues about paleoenvironmental conditions and botanical and bacterial input in the paleomire (see Peters and Moldowan, 1993).

This study deals mainly with the organic petrography and organic geochemistry of coal from Tanjung Enim area in South Sumatra. The general goals are formulated as follows:

(1) to characterize and study the genesis of Tanjung Enim coal from the viewpoint of organic petrography in vertical profiles. Another aspect is to understand the dynamics of the depositional conditions, as Indonesia is an area where the

formation of peat in a tropical climate and the formation of brown and hard coal can be comprehensively studied.

(2) to study the organic petrographical, geochemical and mineralogical characteristics of the thermally metamorphosed Tanjung Enim coal, in particular by applying petrographic properties of coal macerals which change during coalification.

(3) to compare the molecular characteristics of the studied coal with petrological data and to deduce information of paleoecological conditions. Besides that, the effect of the extreme heating by the andesitic intrusion on molecular composition of the coal is also assessed.

1.3 Thesis Overview

As mentioned earlier, this thesis basically discusses the characteristics of coals from Tanjung Enim area from an organic petrographic and organic geochemical point of view, which in turn can provide some clues about the genesis (paleoenvironment and paleoecology) and the coalification of the coals. Chapters 2 to 4 contain the detailed description of the individual studies that had been done to achieve each of the goals stated above. Those chapters are based on several papers written as scientific publication, which can be briefly described as follows:

Chapter 2 – In this chapter, the petrological description of coals from Tanjung Enim is discussed in detail. Microfacies and maceral assemblages were used to determine the evolution of coal precursor (paleo-peat) development in this area. The result of detailed maceral assemblage analysis was also compared with the paleodepositional environment established from coal maceral ratio calculation. The application of several widely used coal maceral ratio calculations to assess the paleomire dynamics of these young tropical coals was evaluated and partly falsified at the end. (Publication to Chapter 2: Amijaya, H., Littke, R., 2005. Microfacies and depositional environment of Tertiary Tanjung Enim low rank coal, South Sumatra Basin, Indonesia. International Journal of Coal Geology 61 (3/4), 197-221)

Chapter 3 – The Tanjung Enim coals were influenced by heat from an andesitic intrusion. The original coals are of sub-bituminous and high-volatile bituminous rank and the thermally metamorphosed coals are of medium-volatile bituminous to meta-

anthracite rank. The result of the investigation by means of petrographic, mineralogical and chemical analyses on those coals are presented in this section. Besides the usual optical examination and proximate – ultimate analysis, Fourier Transform Infrared spectroscopy and Rock-Eval pyrolysis were applied. A special discussion is given with respect to the coalification path of each maceral in relation to the change of optical and chemical properties. To examine the thermal effect to the mineral composition, some selected coals were subjected to X-Ray diffraction. (Publication to Chapter 3: Amijaya, H., Littke, R. Properties of thermally metamorphosed coal from Tanjung Area, South Sumatra Basin, Indonesia with special reference to the coalification path of macerals. International Journal of Coal Geology, in press)

Chapter 4 – This section is specializing in the GC and GC/MS analysis of coal from Lower Suban seam. Lower Suban seam represents an ideal succession of ombrogenous paleo-peat development in a vertical section which is indicated by different maceral assemblages (discussed in Chapter 2). The molecular characteristics gained from GC and GC/MS analysis were then compared with petrographical data to recognize their relationship, especially in terms of the depositional condition effect. The biomarker analysis was done to trace back the paleoecological conditions. Besides that, since Lower Suban seam was locally intruded by andesitic sill, the effect of the andesitic intrusion on the molecular composition of the coals was also studied to complete the characterization of thermally metamorphosed coal which is presented in Chapter 3. (Publication to Chapter 4: Amijaya, H., Schwarzbauer, J., Littke, R. Organic geochemistry of Lower Suban coal seam, South Sumatra Basin, Indonesia: paleoecological and thermal metamorphism implications. Submitted to Organic Geochemistry)

Final Discussion (Chapter 5) is presented to unify all facts and conclusions delivered by each study and build a comprehensively description of the Tanjung Enim coals. It can be clearly deduced from the data that the dynamics of paleodepositional conditions have contributed significantly to the variety of plants in the paleomire, which in turn produced different optical and chemical characteristics of the coals. These were carefully examined then by biomarker analysis, which gave further insight to the paleoecological conditions. The studies also show that later on, the coalification process had extensively changed the optical and chemical properties of coal, especially for the

coals which were subjected to enhanced metamorphism caused by the andesitic intrusion.

At the end of the thesis, some ideas are proposed for the future research especially on South Sumatra coals and Indonesian coals in general. A lot of research has been done to identify the quality of the coals in the framework of coal exploration activity in all Indonesian coal basins. However, this research deals mainly with the optical and some basic physical or chemical properties of coals. More research is still needed to comprehensively study the coals in light of coal petrology and geochemistry to inquire the aspects of coal genesis and coalification in more detail. Only such a complete understanding will allow to develop new and sophisticated exploration and production strategies. These will be summarized in *Outlook (Chapter 6)*.

Chapter 2 Microfacies and depositional environment of Tertiary Tanjung Enim low rank coal, South Sumatra Basin, Indonesia

2.1 Abstract

The South Sumatra basin is among the most important coal producing basins in Indonesia. Results of an organic petrography study on coals from Tanjung Enim, South Sumatra Basin are reported. The studied low rank coals have a mean random huminite reflectance between 0.35-0.46% and are dominated by huminite (34.6-94.6 vol. %). Less abundant are liptinite (4.0-61.4 vol. %) and inertinite (0.2-43.9 vol. %). Minerals are found only in small amounts (0-2 vol. %); mostly as iron sulfide.

Based on maceral assemblages the coals can be grouped into five classes: (1) humotelinite-rich group, (2) humodetrinite-rich group, (3) humocollinite-rich group, (4) inertinite-rich group and (5) humodetrinite-liptinite-rich group. Comparing the distribution of maceral assemblages to the maceral or pre-maceral assemblages in modern tropical domed peat in Indonesia reveals many similarities. The basal section of the studied coal seams is represented typically by the humodetrinite-liptinite-rich group. This section might be derived from sapric or fine hemic peat often occurring at the base of modern peats. The middle section of the seams is characterized by humotelinite-rich and humocollinite-rich groups. The precursors of these groups were hemic and fine hemic peats. The top section of the coal seams is typically represented by the humodetrinite-rich or inertinite-rich group. These groups are the counterparts of fibric peat at the top of the modern peats. The sequence of maceral assemblages thus represents the change of topogenous to ombrogenous peat and the development of a raised peat bog.

A comparison between the result of detailed maceral assemblage analysis and the paleodepositional environment as established from coal maceral ratio calculation indicates that the use of coal maceral ratio diagrams developed for other coal deposits fails to deduce paleo-peat development for these young tropical coals. In particular, mineral distribution and composition should not be neglected in coal facies interpretations.

Key words: coal petrography, microfacies, ash content, Sumatra, Indonesia

2.2 Introduction

Tanjung Enim is an area located in the South Sumatra Basin, one of the important oil and coal producing sedimentary basins in Indonesia. This basin has coal resources of approximately 13.34 Gt, which represent one third of Indonesian coal resources (Directorate of Coal of Indonesia, 2000). In the Tanjung Enim area, which is a part of the coal bearing basin, the coal of the Tertiary Muara Enim formation has been mined since the early 20th century.

The South Sumatra Basin is situated in a tectonically active region. The coal-bearing strata were subjected to at least one period of folding and faulting, and later affected by extrusive and intrusive magmatic activity. Intrusion caused further uplift but most importantly subjected the strata to local metamorphism, i.e. rank increase from lignitic through to anthracitic grades in some areas. Thus, coalification is strongly influenced by the change of geological conditions. Both, conditions of peat accumulation and coalification are reflected in the petrographic characteristics of the coal. Accordingly, knowledge of the petrographical composition of the coal can be used as a key towards a better understanding of the evolution of coal precursor (paleo-peat) development in this area. The goal of this study is to characterize and study the genesis of Tanjung Enim low rank coal from the viewpoint of organic petrography in vertical profiles.

Another aspect is to understand the dynamics of the depositional conditions, as Indonesia is an area where the formation of peat in a tropical climate and the formation of brown and hard coal can be comprehensively studied. Indonesian peat and young coal deposits are probably the best recent or Neogene equivalents of the late Carboniferous coals in the northern hemisphere, which were also deposited in a tropical climate (e.g. Littke, 1987; Grady et al., 1993).

2.3 Geological background

The South Sumatra Basin is located in the southern part of Sumatra island. This basin is regarded as a back-arc basin bounded by the Barisan mountain chain in the southwest

and by the pre-Tertiary of the Sunda Shelf to the northeast (de Coster, 1974). The South Sumatra Basin was formed during east-west extension which took place during pre-Tertiary and early Tertiary times (Daly et al., 1987). The tectonic history and stratigraphy of this basin have been described by Adiwidjaja and de Coster (1973), de Coster (1974), Gafoer and Purbohadiwidjoyo (1986) and Darman and Sidi (2000). The regional tectonic situation and stratigraphy of South Sumatra basin are shown in Figure 2.1.

The coal-bearing Muara Enim Formation was deposited during the Late Miocene – Early Pliocene. The age of Muara Enim Formation cannot be determined directly, as reliable „marker fossils“ are not yet identified. Kinhil-Otto Gold (1986) noted that the Muara Enim Formation is not older and probably younger than N11 and the facies of the formation conforms well with the sea level drops at 13 ma b.p. and 11 ma b.p. (million years before present).

A

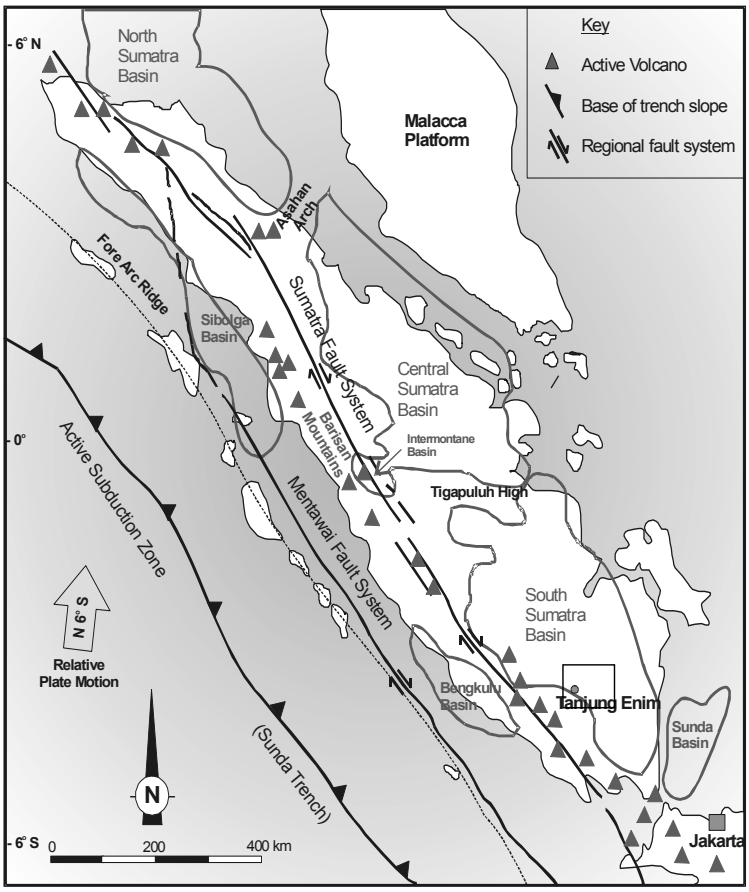

Fig. 2.1. (A) Regional tectonic setting of Sumatra and (B) general stratigraphy of the South Sumatra Basin (modified from Darman & Sidi, 2000). The studied area is indicated by the box.

B

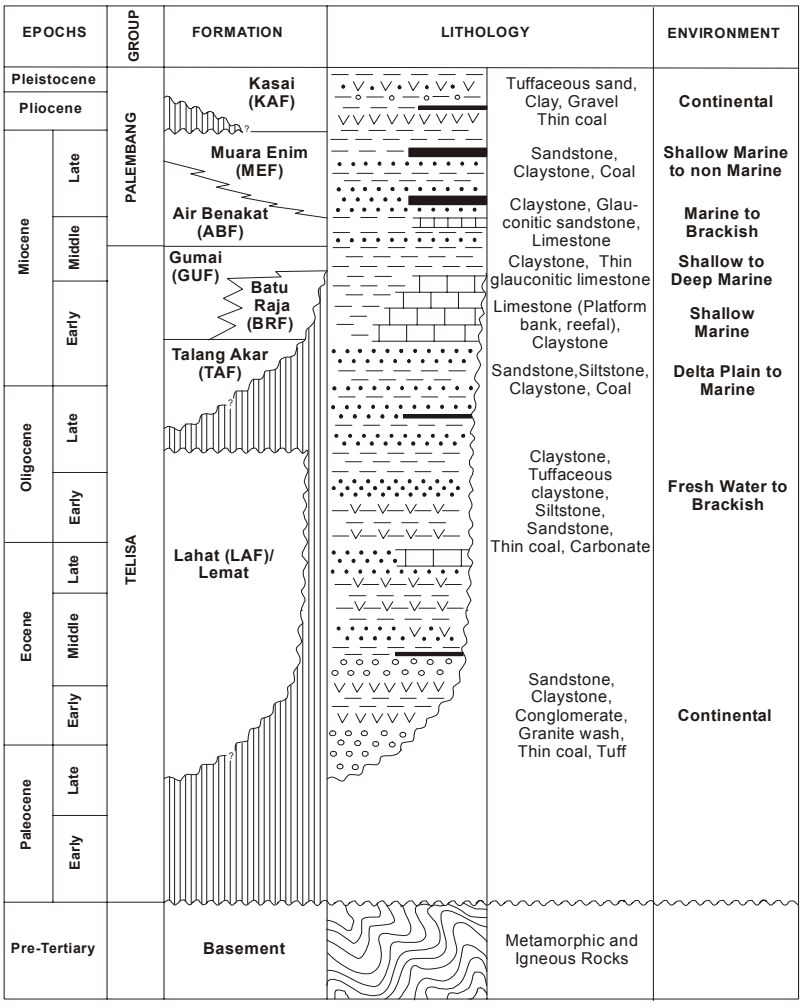

Fig. 2.1. *(continued)*

The Muara Enim Formation consists of claystones and siltstones with several sandstone layers and some coal beds. In detail, the formation consists of stacked shallowing upward parasequences, typically 10 - 30 m thick, with shallow marine or bay clays at the base and shoreline and delta plain facies (sand, silt, clay, coal) at the top. The thickness of Muara Enim formation varies between 450 - 750 m (Darman and Sidi, 2000). Boyd and Peacock (1986) stated that the overall regressive Air Benakat and Muara Enim Formation (Fig.2.1) are interpreted as representing deposition in a humid tropical deltaic system.

Shell Mijnbouw (1976) divided the Muara Enim Formation into two parts (members), known as the lower MPa (Middle Palembang 'a') and the upper MPb (Middle Palembang 'b'). Both members have been subdivided again into M1 – M4 (Fig.2.2).

Both MPa and MPb contain about eight coal seams. It is estimated that the maximum net coal thickness is about 140 m. Some of the coal seams are thin discontinuous layers, whereas others are thick seams. The economically valuable coal seams are those from the upper part of MPa (Mangus, Suban and Petai). In Tanjung Enim, the Mangus, Suban and Petai coal seams each split into two seams, namely Upper (A1) and Lower (A2) Mangus seams, Upper (B1) and Lower (B2) Suban seams and Upper (C1) and Lower (C2) Petai seams.

The coal-bearing strata were subjected to at least one period of folding and faulting, and later to invasion by plug-like masses of andesite. The andesitic intrusions are presumed to be of Pleistocene to early Quaternary age (Gafoer and Purbohadiwidjoyo, 1986; Darman and Sidi, 2000). The intrusions caused further uplift, faulting and folding as well as the formation of some shallow domes, but most importantly altered the local metamorphism of the strata and increased the rank of the coals from lignite through to anthracite in some areas.

2.4 General characteristic of Tanjung Enim coals

Lithologically the coals are mainly composed of vitrain, which has a homogenous appearance and a lustre which varies according to the coal rank, from dull and waxy in the hard lignites, to brilliant in the anthracites. The color varies similarly from dark brown to jet black (Shell Mijnbouw, 1976).

Daulay et al. (2000) divided the coals of the South Sumatra Basin into normal coalification coal and heat affected coal. The normal coalification coal has a sub bituminous rank with a range of Rvmax from 0.40 to 0.50 % while the heat affected coal shows a range from bituminous to anthracite rank with Rvmax of 0.60 to 2.60 %.

Anggayana (1996) studied the A1, A2 and B1 seams of Tanjung Enim coal and found that the coals have a huminite and vitrinite content of 81.6-97.4 vol. %, liptinite content of 0.2-5.2 vol. % and an inertinite content of 0.6-16.6 vol. %. Minerals normally occur only in trace amounts, but one sample had a mineral content of 4.4 vol. %. These data are in general agreement with those of Pujobroto and Hutton (2000), but they also

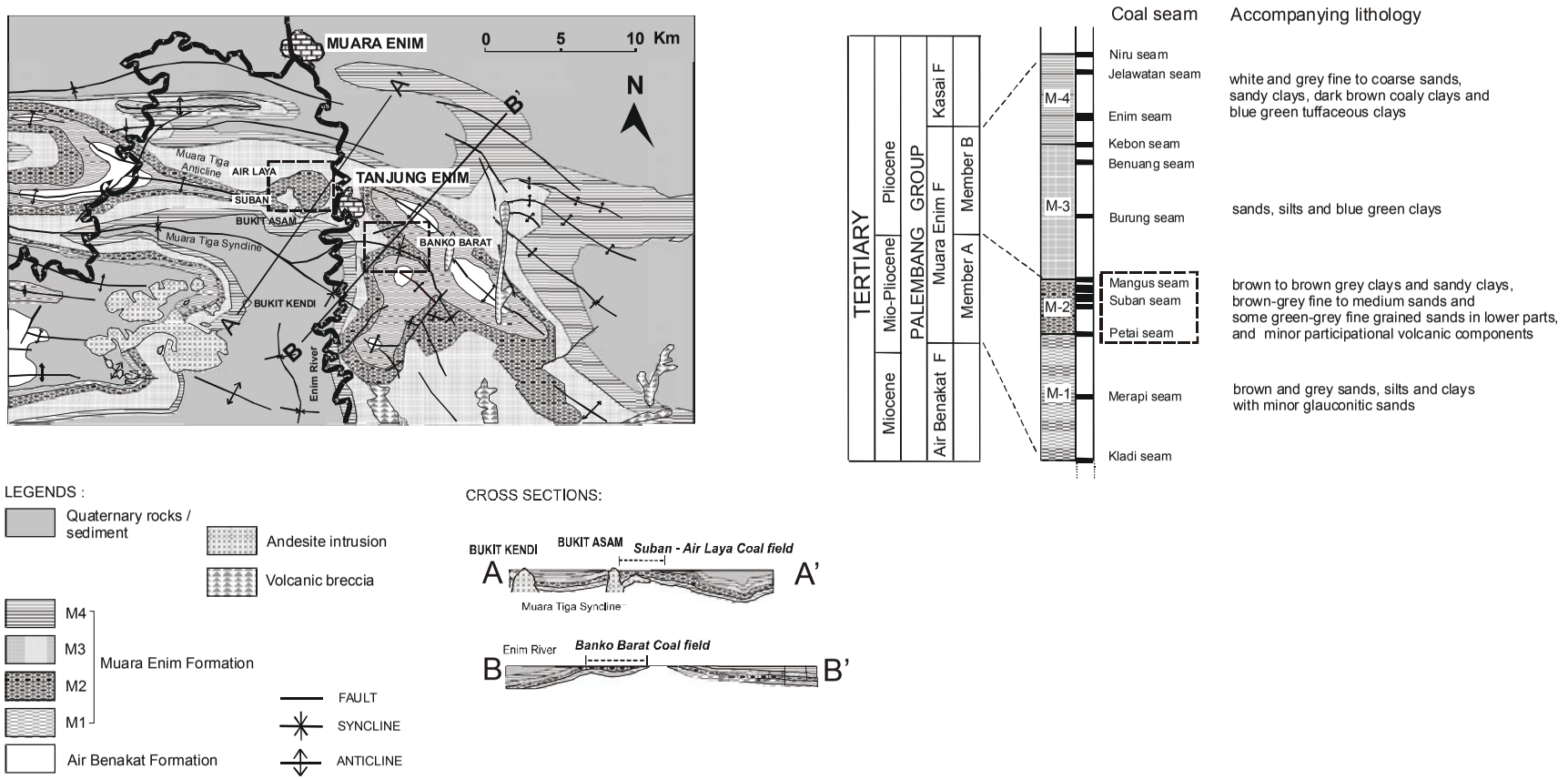

Fig. 2.2. Geological map and general stratigraphy of Tanjung Enim Area (modified from Bamco, 1983 and Gafoer et al., 1986). Broken line rectangles show the mined seams and the studied areas.

described one coal sample that had a mineral content of 20 %. However, their studies also showed that the average mineral content is low (3.4 %).

The ash and sulfur content of Tanjung Enim coal is very low. Anggayana (1996) reported that the mean ash content of A1, A2 and B1 seams are only 2.9 %, 2.1 % and 1.3 % (dry basis; db), respectively. The sulfur content ranges between 0.1 and 2.1 % (db). Other data, for example by Bamco (1983) generally confirm these results. The low rank coal from this area has a sulfur content of less than 1 % (as received; ar). Sulfur content of coal from the area affected by igneous intrusion is slightly higher. The average ash content of the seams is 4.95-7.88 % (ar). Kinhill-Otto Gold (1986) stated that the coal from the Banko Barat field in Tanjung Enim area generally has a low ash content (average 6.3 % db for all seams) and a low to very low sulfur content (average 0.42 % db for all seams).

2.5 Climate and vegetation

During the Miocene Sumatra was located in a tropical area (Morley, 1998; 2000). It can be assumed that the climate during Miocene peat deposition was similar to the modern climate in SE Asia today. In general, peat deposits in Indonesia are situated in a zone of annual rainfall exceeding 2.5 m. Even minimum rainfall usually exceeds evapotranspiration in the peatlands leading to ever wet conditions. Only during exceptional long, drought periods the peat may dry out and sometimes becomes inflammable (see Anderson, 1983; Neuzil et al., 1993).

Anderson (1964) defined two main types of swamp in the Malesian region. Fresh water swamps are regularly or seasonally flooded, whereas true peat swamps are not flooded. The former are basically topogenous swamps and the latter ombrogenous. Topogenous mire refers to peat or vegetation formed under minerotrophic condition (Gore, 1983). This type of mire, which is also called planar mire, occurs generally at or just below the ground-water table and derives most moisture from groundwater (Greb et al., 2002). A significant characteristic of the southeast Asian peat deposit is its occurrence in domes or flat topped mesas that extend upward above the coastal and alluvial plains on which they are formed (Esterle and Ferm, 1994). This ombrogenous mire is formed under conditions, where the nutrients are supplied from rain water (Gore, 1983).

The peat forming vegetation probably has not much changed since the Miocene (Anderson, 1983; Demchuck and Moore, 1993). A vegetation model of tropical peat deposits is described by Anderson (1983, Esterle and Ferm, 1994), where a change in the floral community is recognized as peat accumulates. The succession is characterized by a change from mixed swamp forest consisting of large trees to thin *Shorea albida* trees referred to as 'pole forest' and then to an 'open savanna woodland' vegetation of pandanus, small shrubs and thin trees. Some vegetational successions that show a development from topogenous to ombrogenous peat can also be observed within the raised peat deposits in Kalimantan, Indonesia (Morley, 1981; Dehmer, 1993, 1995).

2.6 Methods

2.6.1 Samples and sample preparation for petrographic analysis

Coal samples were collected from two active surface mines in Tanjung Enim area, Tambang Air Laya (TAL) and Banko Barat (BOB) mine. There, three main coal seams (Mangus, Suban and Petai seams) are mined which have thicknesses ranging from 3 to 14 m.

Forty-three ply samples were taken from TAL and represent all the main seams present. From BOB, 29 ply samples were taken, which represent only the Mangus and Suban seams. The vertical thickness of individual samples depended on the macroscopic appearance of the coal. The macroscopic appearance of the coal was determined using the lithotype classification system from Diessel (1992). Because the coal seams are very thick, the minimum lithotype thickness has been increased to 10 centimeters. Ash content determination on each sample was performed according to DIN 51719-A (1978).

The sample preparation and microscopic examination generally followed the procedures described in Taylor et al. (1998). Coal particles of about 1 mm in diameter were used for preparation of polished sections, which were embedded in a silicone mould (diameter: 3 cm) using epoxy resin as an embedding medium. After hardening, the samples were ground flat and polished.

2.6.2 Microscopy

Vitrinite reflectance measurement was performed on a Zeiss universal microscope equipped with SF photomultiplier. The examination was conducted using a 40x magnification Epiplan objective lens and 12.5x magnification ocular lens under oil immersion (n_e = 1.518 at 23°C). Fifty readings of random vitrinite reflectance were taken on each sample at a wave length of 546 nm. Reflectance was measured on huminite and vitrinite macerals that have a visible structural form (telovitrinite or humotelinite maceral subgroup). The mean random vitrinite reflectance values were then calculated using a computer program.

During maceral analysis, 1000 points with a minimum distance of 0.2 mm between each point were counted on each polished sample. The analysis was conducted in reflected white light and in fluorescence irradiated by blue/violet light (Two-Scan method), with 50x magnification Epiplan objective lens and 10x magnification ocular lens under oil immersion using a Zeiss Axioplan microscope.

Coal rank determination and maceral classification followed Taylor et al. (1998). The terms funginite and secretinite are used to replace the term sclerotinite (see ICCP, 2001). Those terms are used in this paper because both macerals can be found in the studied coal in trace amounts. Mineral matter was only divided into two groups, sulfides and other minerals, since other minerals, such as clay minerals, quartz or carbonate were only found in very small amounts. Sulfides are almost exclusively iron sulfides. In the following these iron sulfides are referred to pyrite, although some marcasite may occur.

2.7 Results

2.7.1 Macroscopic appearance of the coals

Most of the coal seams are predominantly composed of the banded bright coal lithotype. Generally, the coal seams in BOB show less lithotype variations than TAL coals. In TAL, the Mangus A1 seam appears also as banded bright coal, but in the middle part of the vertical section, the seam contains more dull bands. The Mangus A1 seam in BOB

has a relatively homogenous macroscopic appearance and is only comprised of banded bright coal.

In contrast to Mangus A1, the Mangus A2 seam in BOB has a duller appearance. Only the middle part of the vertical section is composed of a brighter lithotype. In the TAL area, this seam is characterized by the banded bright lithotypes with only minor and thinner dull lithotypes. At the top of Mangus A2, the coal is silicified. This silicified coal layer has a thickness of about 10-20 cm. The sedimentary strata between A1 and A2 seams mainly consist of claystone and tuffaceous sandstone. The solution of silica from tuffaceous strata and precipitation at the top of the coal seam was probably the cause of the silification.

The Suban B1 seam in the TAL area has a duller appearance at the top than at the bottom (from banded bright coal to banded dull coal). The Suban B2 shows a different pattern. Dull coal is found at the bottom of the seam and changes into brighter coal towards the top. Both Suban seams in BOB area have a similar macroscopic appearance, characterized by banded bright coal with duller coals in the central part of the seam.

The macroscopic appearance of the studied coals is depicted in Figures. 2.5 and 2.6. In almost all parts of the seams, resin inclusions are visible. Their size varies from a couple of millimeters up to severals centimeters. Sometimes it forms a tabular body up to around 20 centimeters long. Resin rich horizons are occasionally found in A1 seam of TAL and BOB.

The Petai seam is not described here because of its high level of coalification (see below).

2.7.2 Huminite/Vitrinite reflectance

The results of vitrinite and huminite reflectance measurements show that the TAL coals can be classified into two groups of low and high reflectivity (see Table 2.1). Coals from Mangus (A1) seams have mean random huminite reflectance values from 0.35% to 0.40% (mean value 0.37%). Mean random huminite reflectance values of Mangus (A2)

coals range from 0.39% to 0.43% (mean value 0.41%). The Suban (B1) coals have mean random reflectance values between 0.40% and 0.45% (mean value 0.43%) and Suban (B2) coals range between 0.41% and 0.46% (mean value 0.44%). High reflectances of vitrinite are typical of coals from Petai (C) seam, which is located beneath the other seams. Vitrinite reflectance ranges between 1.99% and 2.06% (mean value 2.02%).

In general there is a tendency of increasing vitrinite reflectance with increasing depth at TAL. Reflectance increases from an average of 0.37% (A1 seam) to 0.44% (B2 seam) in a depth interval of only about 55 m and an abrupt change occurs in Petai (C) seam**.** Such change of coal rank from low rank coals (in this case lignite to sub bituminous) to high rank coals (in this case low volatile bituminous to semi anthracite) cannot be explained by normal coalification caused by increasing burial. An explanation for this phenomenon is that this area received additional heat from an intrusive igneous body. The magmatic heat affected coals will not be further discussed in this paper, because detailed microfacies analysis is not possible due to the high level of coalification.

Huminite reflectance values of BOB coals show that all of the samples are characterized by low reflectance values ranging between 0.39% and 0.44%. According to huminite reflectance, all coals are of low rank ranging from lignite to sub-bituminous B-C. In contrast to TAL, there is no tendency of an increasing vitrinite reflectance with increasing depth at BOB. This is reasonable because no significant depth difference exists. Furthermore, no andesitic intrusions have been observed in this area.

Table 2.1. Vitrinite/huminite reflectance of Tambang Air Laya and Banko Barat coals

Seam	Tambang Air Laya		Banko Barat	
	Rr (%)	mean Rr value for each seam	Rr (%)	mean Rr value for each seam
Mangus (A1)	0.35 – 0.40	0.37	0.39 – 0.42	0.40
Mangus (A2)	0.39 – 0.43	0.41	0.39 – 0.44	0.41
Suban (B1)	0.40 – 0.45	0.43	0.39 – 0.43	0.40
Suban (B2)	0.41 – 0.46	0.44	0.39 – 0.42	0.40
Petai (C)	1.99 – 2.06	2.02		

Note: Rr = Random reflectance

2.7.3 Maceral composition

The maceral analysis shows that almost all the low rank coals of TAL are dominated by huminite (34.6-94.6 vol. %). Liptinite (4.0-61.4 vol. %) and inertinite (0.2-43.9 vol. %) are less abundant. Minerals are found only in small amounts (0-2 vol. %); most of them are pyrite. Some clay, carbonate and quartz are observed as well. The BOB coals are also dominated by huminite (68.8-91.7 vol. %), whereas the percentages of liptinite (5.2-23.4 vol. %) and inertinite (1.3-19.6 vol. %) are moderate to low. Minerals are dominated by pyrite but occur only in small amounts (less than 2 vol. %). Table 2.2 shows the maceral composition of each seam.

The huminite maceral group mainly consists of humodetrinite. In TAL coals, it comprises more than 25 vol. % of the macerals, but some samples have lower contents (only 3.3-15.9 vol. %), because of their high contents of humotelinite. Compared with TAL coals, BOB coals have an even higher average content of humodetrinite. It comprises 24.7-66.3 vol. % of the macerals. In both locations, most of the humodetrinite is attrinite. The gelified humodetrinite maceral (densinite) is less abundant.

The gelification process has not reached an advanced stage, since the percentage of the gelified humotelinite (eu-ulminite) ranges between 0.0-15.7 vol. %, which is less than that of ungelified humotelinite (texto-ulminite; 2.0-55.7 vol. % of the coals from both areas). Only one sample from BOB has a relatively high content of eu-ulminite (27.6 vol. %). Humocollinite content varies between 1.0 vol. % and 64.9 vol. % (TAL) and between 2.5 vol. % and 38.5 vol. % (BOB), most of which is corpohuminite. Gelinite is observed in small quantities.

In general, huminite is present in two forms, huminite bands and huminite groundmass. The huminite bands are not only formed by humotelinite macerals, but in many cases they are formed by thick layers of humodetrinite or gelinite that are interbedded with humotelinite layers. Humodetrinite is present mostly as groundmass surrounding liptinite or inertinite particles.

Humocollinite is disseminated throughout the coals mostly as corpohuminite (phlobaphinite and pseudo-phlobaphinite) of globular or tabular shape. Porigelinite occurs usually as thin bands, but sometimes some globular shaped porous gelinite is observed. Most of the pores in porigelinite are filled by micrinite or pyrite.

The liptinite macerals of TAL coals normally range from 4.0 to 28.0 vol. % of the coal. Only two samples have a very high liptinite content (50.8 vol. % and 61.4 vol. %). The liptinite macerals of the coals in BOB comprise 5.2-23.4 vol. % of the coal. The common liptinite macerals in the coals from both locations are sporinite, cutinite, resinite, suberinite and liptodetrinite. Bituminite, fluorinite, exsudatinite and alginite are observed rarely. Bituminite usually occurs as groundmass.

Sporinite content is usually less than 3.5 vol. %, but in the liptinite-rich coal it reaches 8.4 vol. % of the coal. No megaspores were observed and the longest microspores have a length of about 0.2 mm. Most microspores are, however, less than 0.1 mm long. Most of the miospores have thin walls (tenuisporinite), but trace amounts of some thick-walled miospores (crassisporinites) are recognized as well. Cutinite (up to 5.6 vol. %) occurs both as the thin walled (tenuicutinite) and thick walled (crassicutinite) variety.

The maximum content of resinite is 5.8 vol. %. Resinite macerals in the studied coal appear mostly as cell-filling or isolated small globular bodies, but some small resinite layers also occur. Under fluorescence they have pale-brownish-yellow color. Occasionally some resinite bodies appear as groups in distinct layers. Resinite macerals are commonly associated with humotelinite and humodetrinite. Suberinite appears as cell wall tissue associated with corpohuminite (phlobaphinite) and is characterized by dark color in reflected light and a greenish to pale yellow in fluorescent light. Suberinite constitutes 0.0-3.2 vol. % of TAL coals and up to 2.0 vol. % of BOB coals. Fluorinite (up to 2.8 vol. %) can be recognized by its strong fluorescence (yellow color). Fluorinite is not always associated with cutinite.

Table 2.2. Petrographic composition and ash content of Tambang Air Laya and Banko Barat coals.

Petrographic composition	TAL				BOB			
	Mangus (A1) Seam	Mangus (A2) Seam	Suban (B1) Seam	Suban (B2) Seam	Mangus (A1) Seam	Mangus (A2) Seam	Suban (B1) Seam	Suban (B2) Seam
Maceral (vol. %)								
Texto-ulminite	5.9 – 55.7	8.0 – 27.2	2.3 – 32.0	2.0 – 18.3	5.3 – 31.6	6.4 – 27.6	2.8 – 19.3	8.5 – 26.3
Eu-Ulminite	0.0 – 8.8	0.0 – 15.7	0.0 – 13.2	0.3 – 5.3	2.0 – 27.6	0.2 – 9.6	1.0 – 10.9	1.9 – 4.7
(Total Humotelinite)	8.2 – 55.7	8.0 – 42.6	2.3 – 37.4	2.6 – 23.5	14.8 – 42.6	7.8 – 31.9	11.3 – 30.3	10.4 – 29.4
Attrinite	11.9 – 49.2	3.2 – 45.8	13.6 – 50.3	22.2 – 56.8	7.1 – 55.9	27.6 – 58.7	31.5 – 57.6	35.7 – 48.9
Densinite	0.0 – 20.6	0.2 – 21.0	0.0 – 16.8	0.9 – 20.6	1.5 – 31.2	0.4 – 9.7	0.7 – 6.8	1.1 – 6.8
(Total Humodetrinite)	11.9 – 53.3	3.3 – 54.7	15.9 – 67.1	29.8 – 67.8	24.7 – 61.3	32.9 – 66.3	35.0 – 60.0	38.0 – 55.8
Corpohuminite	6.5 – 40.1	6.3 – 59.6	3.3 – 42.4	1.0 – 31.1	7.1 – 19.6	4.3 – 30.3	2.5 – 38.2	5.7 – 24.0
Gelinite	0.0 – 1.5	0.0 – 5.4	0.0 – 3.5	0.0 – 2.2	0.0 – 1.1	0.0 – 1.2	0.0 – 0.6	0.0 – 2.6
(Total Humocollinite)	7.5 – 40.1	6.3 – 64.9	3.3 – 42.4	1.0 – 33.3	7.1 – 19.6	4.3 – 30.7	2.5 – 38.5	5.9 – 24.0
Total Huminite	65.3 – 94.6	49.1 – 91.9	34.6 – 95.8	34.7 – 85.9	82.3 – 87.5	68.8 – 85.3	77.4 – 90.6	70.0 – 91.7
Sporinite	0.0 – 2.0	0.0 – 1.4	0.0 – 3.4	0.4 – 8.4	0.0 – 1.2	0.0 – 2.0	0.0 – 1.6	0.0 – 1.2
Cutinite	0.0 – 2.0	0.0 – 4.4	0.0 – 4.8	1.2 – 3.8	0.0 – 1.6	1.4 – 3.4	0.8 – 5.6	0.0 – 1.2
Suberinite	0.0 – 1.6	0.0 – 1.0	0.0 – 3.2	0.0 – 2.4	0.0 – 2.0	0.0 – 1.0	0.0 – 1.4	0.2 – 0.8
Resinite	0.4 – 2.2	0.0 – 1.8	0.4 – 5.8	0.4 – 1.0	0.0 – 1.0	0.0 – 0.8	0.0 – 1.0	0.2 – 1.0
Fluorinite	0.0 – 0.2	0	0.0 – 2.8	0.0 – 0.4	0.0 – 0.4	0.0 – 0.4	0.0 – 0.6	0
Bituminite	0.0 – 0.6	0.0 – 1.4	0.0 – 6.4	0.0 – 1.0	0.0 – 0.2	0.0 – 0.2	0.0 – 0.2	0.0 – 0.2
Exsudatinite	0.2 – 2.6	0.0 – 5.6	0.0 – 8.4	0.4 – 9.8	0.0 – 3.8	1.0 – 6.2	0.6 – 4.2	0.2 – 3.6
Alginite	0.0 – 0.2	0.0 – 0.2	0	0.0 – 0.4	0	0	0	0
Liptodetrinite	1.6 – 8.2	1.6 – 11.0	1.8 – 32.2	8.2 – 38.0	4.0 – 8.2	4.2 – 15.0	1.4 – 10.6	2.6 – 8.0
Total Liptinite	4.2 – 15.8	5.4 – 17.8	4.0 – 61.4	11.6 – 50.8	8.0 – 14.4	7.4 – 23.4	5.8 – 19.6	5.2 – 12.6
Micrinite	0.0 – 0.2	0.0 – 0.4	0.0 – 0.5	0.0 – 0.3	0.0 – 0.8	0.0 – 0.6	0.0 – 1.1	0
Macrinite	0.0 – 0.2	0.0 – 0.2	0.0 – 0.2	0	0	0	0	0
Semifusinite	0.0 – 2.8	0.0 – 4.2	0.0 – 0.7	0.0 – 2.5	0.0 – 1.1	0.4 – 2.9	0.2 – 0.9	0.0 – 2.1
Fusinite	0.0 – 18.5	0.0 – 38.9	0.0 – 12.6	0.7 – 7.2	0.5 – 3.3	2.4 – 6.9	0.7 – 5.4	0.8 – 16.9
Funginite	0.0 – 0.9	0.0 – 0.9	0.0 – 0.7	0.0 – 0.5	0.0 – 0.4	0.0 – 0.5	0.0 – 0.8	0.0 – 0.4
Secretinite	0.0 – 0.2	0	0	0	0	0	0.0 – 0.2	0
Inertodetrinite	0.0 – 5.0	0.0 – 2.6	0.0 – 1.7	0.2 – 5.9	0.4 – 2.3	0.5 – 3.4	0.0 – 2.7	0.2 – 0.8
Total Inertinite	0.2 – 26.7	0.2 – 43.9	0.2 – 13.4	1.4 – 13.6	1.8 – 6.1	3.9 – 10.3	1.3 – 7.1	1.6 – 19.6
Mineral matter (vol. %)								
Pyrite/Marcasite	0.0 – 0.8	0.0 – 1.0	0.0 – 1.0	0.4 – 1.8	0.2 – 1.8	0.0 – 1.8	0.0 – 1.6	0.2 – 1.4
Other minerals	0.0 – 0.8	0.0 – 0.2	0.0 – 1.0	0.0 – 1.2	0.0 – 0.4	0.0 – 0.4	0	0.0 – 0.4
Total Mineral	0.0 – 1.0	0.0 – 1.2	0.0 – 1.4	0.4 – 2.0	0.2 – 1.8	0.0 – 1.8	0.0 – 1.6	0.6 – 1.4
Ash content (wt.%, dry basis)	1.2 – 3.3	1.2 – 2.9	2.0 – 18.7	0.9 – 10.7	1.1 – 3.9	0.4 – 1.4	1.5 – 5.5	1.2 – 9.7

Bituminite (up to 6.4 vol. % in liptinite-rich coal) is defined as liptinitic maceral without any definite shape and structure. It fluoresces weakly, usually in brownish yellow or brown color. The observed bituminite acts as a groundmass for other liptinitic and inertinitic materials and mainly occurs in attrinite-rich coal. Exsudatinite is a secondary maceral (Teichmüller, 1989; Taylor et al.; 1998) that can be found in almost all samples (up to 9.8 vol. %) as fillings in small cracks or empty cell lumens (mostly in sclerotinite). Exsudatinite exhibits a strong yellow fluorescence. *Botryococcus* alginite was found only in trace amounts in some samples. It has very intense yellow fluorescence color. Liptodetrinite content usually varies between 1.4-16.2 vol. %. In the liptinite-rich samples it reaches 32.2 and 38.0 vol. %. Sometimes liptodetrinite is embedded in bituminite in the bituminite-rich coal. Liptodetrinite is often associated with humodetrinite.

Inertinite macerals constitute 0.2–43.9 vol. % of TAL coals and 1.3–19.6 vol. % of BOB coals. Fusinite is predominant whereas semifusinite, inertodetrinite and funginite are found in small amounts. Micrinite and macrinite are rare. Secretinite is only observed in one sample in trace amounts. Fusinite occurs in the form of discrete lenses and bands. The common fusinite bands have thicknesses from 0.05 mm up to more than 1 mm. The pores are usually empty, but sometimes gelinite, exsudatinite, or pyrite fill those pores. Inertodetrinite is disseminated throughout the coals and comprises usually 0.0–5.9 vol. %.

Funginite, including single and multi-celled fungal spores and sclerotia, compose not more than 1.0 vol. % of studied coals. This maceral is distributed in almost all the samples usually in the oval form funginite. The tubular form of funginite is rarely present. Funginite occurs as single bodies or as colonies. Its pores are often filled by resinite.

2.7.4 Mineral matter and ash contents

The highest content of visually observed mineral matter is only 2 vol. % (Table 2.2). Most common are pyrite and marcasite (up to 1.8 vol. %) which are dispersed throughout the coals. They occur as small, euhedral crystals or in framboidal concretionary form often associated with ulminite. This type of pyrite is usually interpreted as syngenetic pyrite which was formed in the peat (Taylor et al., 1998).

Epigenetic pyrite is present as filling of open cell lumens and for example in porigelinite. Pyrite filling small fractures is present as well, but only in trace amounts. There is a tendency that pyrite content increases with increasing liptinite and huminite and with decreasing inertinite.

Carbonates are found in traces in fractures or cell lumen, mostly as blocky crystals. Clay minerals are usually dispersed, but some thin clay layers occur as well.

Ash contents based on weight are slightly higher, but generally less than 5 wt. % (see Figs. 2.5 and 2.6), correlating reasonably well with the mineral matter determined microscopically. Only some coal layers have high ash contents, which can reach 18.7 wt. %. Those layers are usually present in the basal and top parts of the seams. In Suban (B1) seam of TAL, one coal layer with high ash content is also present in the middle part of the seam. Coal layers with high ash content usually have also a high content of liptinite.

2.7.5 Coal microfacies

The petrographic composition of the coal has been studied in detail, in order to obtain a microfacies classification and to deduce paleoenvironments during peat deposition. The percentages of the three maceral groups, vitrinite, inertinite, and liptinite have been plotted in ternary diagrams (mineral-matter-free, mmf) for both deposits (TAL and BOB, Figs. 2.3 and 2.4) in order to provide the most basic information on coal deposition. Based on these diagrams four microfacies can be determined.

Facies I coals are those with high content of huminite and low contents of inertinite and liptinite. The percentage of huminite is greater than 65% mmf and that of inertinite is usually less than 10% mmf. Most of the studied TAL coals fall into this type (Fig. 2.3). Facies II coals have a huminite content lower than 75% mmf and an inertinite content between 10 and 20% mmf. Only two coal samples of TAL fall into this category. This facies is a transition type between facies I and III. The latter describes coals with huminite contents lower than 70% mmf and more than 20% mmf inertinite (inertinite-rich coals). Two studied TAL coals can be categorized into this type. All of those facies are usually characterized by liptinite contents of less than 25% mmf. There are only three coals of

TAL which have a liptinite content of more than 25 % mmf (facies IV). Two of them have a very high liptinite content of more than 50% mmf. BOB coals show only I and II facies (Fig. 2.4). BOB coals are even more homogeneous than TAL coals and are also dominated by facies I.

The petrological composition of coal seams is a key to understand the evolution of peat-forming depositional environments (Diessel, 1986, 1992; Cohen et al., 1987; Littke, 1987; Teichmüller, 1989, Calder et al., 1991; Lamberson et al. 1991; Wüst et al., 2001; Greb et al., 2002; Bechtel et al., 2003 and many other). However, the reconstruction and interpretation of TAL and BOB coals cannot be solely based on coal facies change (I-IV), as most coals were grouped as facies I. A slightly more detailed classification based on maceral composition of coal is made and used in this study to elicit more insight into changes during the peat stage of coal formation.

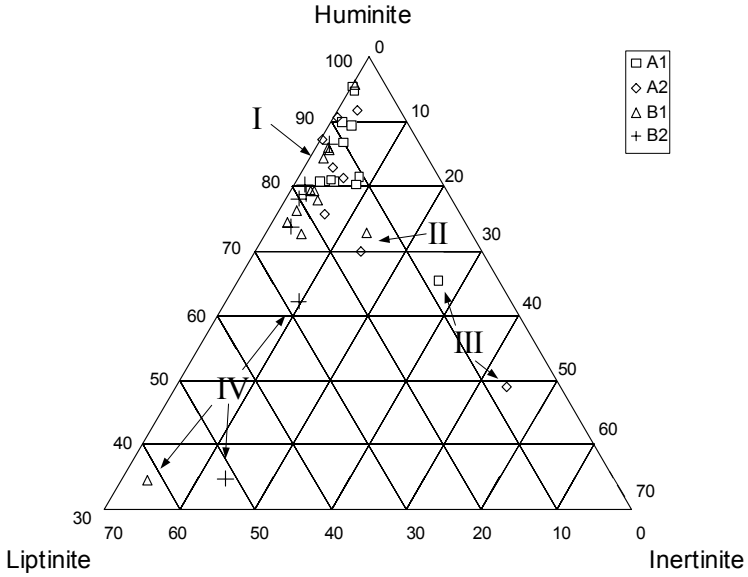

Fig. 2.3. Facies of TAL low rank coals based on their maceral group composition (mmf basis).

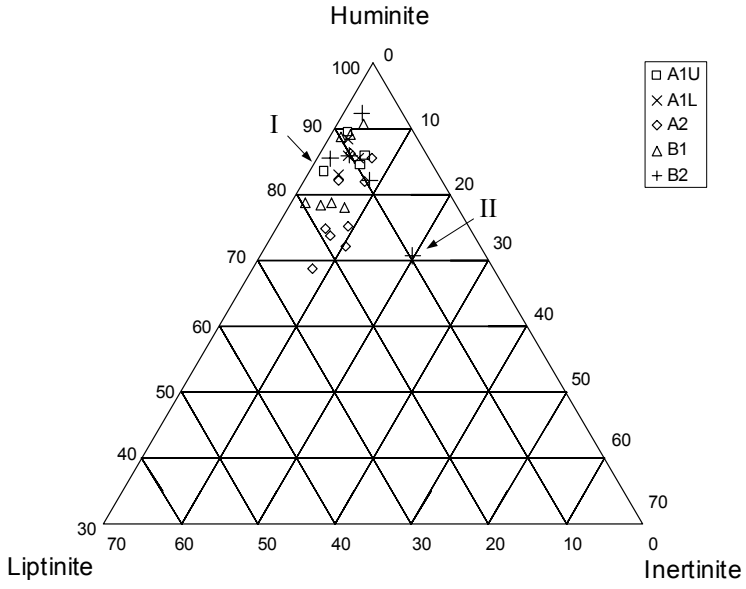

Fig. 2.4. Facies of BOB coals based on their maceral group composition (mmf basis).

The maceral assemblages classification is based on the composition of huminite and the variation in liptinite and inertinite content. The studied coal can be grouped into (1) humotelinite-rich group, (2) humodetrinite-rich group, (3) humocollinite-rich group, (4) inertinite-rich group and (5) humodetrinite–liptinite-rich group. The first, second and third groups correspond to the facies I and II coal, the fourth group to facies III coal and the fifth group to the facies IV coal (see Table 2.3). The characteristic of each group is described below:

Humotelinite-rich group – The humotelinite-rich group contains about 25 vol. % or more humotelinite (the highest amount is 55.7 vol. %). The amount of unstructured huminite can vary and the total amount of liptinite and inertinite is usually less than 20 vol. %. Texto-ulminite (partly gelified) is the predominant maceral of humotelinite in the studied coals. The percentage of eu-ulminite (completely gelified) reaches usually not more than half of that of texto-ulminite.

Humodetrinite-rich group – This is the most common maceral assemblage observed in the studied coals. The coal consists of about 35 – 70 vol. % humodetrinite, which is dominated by attrinite, and less than 25 vol. % humotelinite. The humocollinite amount varies and the total amount of liptinite and inertinite is only about 20 vol. % or less.

Humocollinite-rich group - This group contains about 40-65 vol. % humocollinite. The total amount of liptinite and inertinite is about 10 vol. %. Contents of humodetrinite and humotelinite are variable, but usually humotelinite is more abundant than humodetrinite. Corpohuminite appears as structureless cell fillings (either in situ or isolated) and dominates the humocollinite.

Inertinite-rich group - The inertinite-rich group is characterized by high contents of inertinite (more than 20 vol. %). Humotelinite does not exeed 20 vol. % and humocollinite is at less than 10 vol. %. The liptinite content is low (the highest content is only 8 vol. %).

Humodetrinite–liptinite-rich group - The striking characteristic of this group is its „high" content of liptinite of more than 20 vol. %. Humodetrinite content is usually between 30-55 vol. %. As in the humodetrinite group, attrinite also dominates the humodetrinite. Most of the liptinite in this group is derived from plant organs (sporinite, cutinite, suberinite and resinite).

Table 2.3. Criteria used for the classification of the low rank coal microfacies and their corresponding maceral assemblages

Microfacies [(a)]	Maceral assemblages [(b)]
Facies I: more than 65 vol. % huminite, less than 25 vol. % liptinite, around 10 vol. % or less inertinite	*Humotelinite-rich group*: 25 vol. % or more humotelinite, various amount of unstructured huminite, total amount of liptinite and inertinite is less than 20 vol. % *Humodetrinite-rich group*: 35 – 70 vol. % humodetrinite, less than 25 vol. % humotelinite, various amount of humocollinite, total amount of liptinite and inertinite is 20 vol. % or less
Facies II: less than 75 vol. % huminite, less than 20 vol. % liptinite, 10 - 20 vol. % inertinite	*Humocollinite-rich group*: 40 - 65 vol. % humocollinite, various amount of humotelinite and humodetrinite, total amount of liptinite and inertinite is about 10 vol. %
Facies III: less than 70 vol.% huminite, less than 10 vol. % liptinite, more than 20 vol. % inertinite	*Inertinite-rich group*: more than 20 vol. % inertinite, less than 20 vol. % humotelinite, less than 10 vol. % humocollinite, various amount of humodetrinite, less than 10 vol. % liptinite
Facies IV: more than 25 vol. % liptinite, various amount of huminite and inertinite	*Humodetrinite-liptinite-rich group*: more than 20 vol. % liptinite, 30 – 55 vol. % humodetrinite, various amount of humotelinite and humocollinite, various amount of inertinite

Note:
(a) calculated based on mineral matter free basis
(b) not calculated based on mineral matter free basis

2.8 Discussion

Peat and coal facies are controlled by the evolution of depositional environments. Factors such as temperature, rainfall, subsidence and morphology of the basin, lithology of rocks in the hinterland, volcanic activity, and the accumulation of peat itself control deposition and preservation of plants and minerals (Littke and Ten Haven, 1989). In the following, some of the factors will be discussed and their influence on microfacies and maceral assemblages will be reviewed. A comparison with modern peat environments will be used to reconstruct the depositional environment of the paleo-peat that formed the Mangus and Suban coal.

2.8.1 Comparison of maceral or pre-maceral composition of modern tropical peats with maceral assemblages of the studied coals

Maceral or pre-maceral composition studies on some modern domed peats in Indonesia give an overview about the development of maceral assemblages for such peat. Grady et al. (1993), who analyzed domed peat in Sumatra, found that the volume of huminite macerals representing well-preserved cell structures decreases upward. Huminite macerals representing severely degraded cellular debris increase uniformly from the base to the surface. This succession is believed to reflect a progression similar to the succession from telocollinite-rich, bright coal lithotypes in the lower benches upward to thin-banded/matrix collinite and desmocollinite in higher splint coal benches of the Stockton and other Middle Pennsylvanian Appalachian coal beds in West Virginia, USA and supports interpretations of an upward transition from planar to domed swamp accumulations.

Esterle and Ferm (1994) found in their study in Sarawak and Sumatra that the peat has overall low contents of liptinite and inertinite maceral precursors and a high average content of pre-huminite. They observed that at the base a sapric and fine hemic peat type dominates. Above those layers there are hemic, coarse hemic and fibric peat types. Sapric layers can be observed also at the surface of the peat margin. A shift from a forest to communities of smaller plants with extensive root systems can be denoted from the shift from large wood fragments in hemic peat to increasing proportion of small slender roots in coarse hemic material. They stated also that the fibric peats are least altered, contain very

little grain matrix and appear more as an array of loosely packed roots in a matrix of finer rootlets and rhizoids.

A similar pattern of peat development was also described by Dehmer (1993) for peat deposits in Kalimantan (Borneo) and by Supardi et al. (1993) for peat deposits in Sumatra. The general trend from sapric peats at the base to hemic and fibric peats in the overlying layers shows a change from topogenous and rheotrophic to ombrogenous and mesotrophic-oligotrophic conditions.

In their study, Shearer et al. (1994) stated that most thick coal beds, most of all Tertiary coals, are composed of multiple paleo-peat bodies, stacked one upon another. Three types of partings, which are inorganic partings, oxidized organic partings and organic, non-oxidized, degradative partings, can be used as boundaries to divide a single coal bed into component parts, or benches, each representing the accumulation of a different mire (Shearer et al., 1994; Greb et al., 2002).

2.8.1.1 Basal section

Typically, the basal section of each studied coal bench is represented by the humodetrinite-liptinite-rich group, and in some cases by the humodetrinite-rich group. This section might be derived from the sapric peat or fine hemic peat that often occurs at the base of recent tropical peats.

A high liptinite content in decomposed basal sapric peats was also observed by Dehmer (1993). In contrast, Esterle and Ferm (1994) did not recognize any high liptinite percentage in the sapric peat whereas Mukopadhyay (1991, unpublished data cited in Esterle and Ferm, 1994) found a high concentration of liptinite precursors, mostly cutinite and liptodetrinite, in sapric peats from the margin of the same deposit. Possibly, this peat section studied by Mukopadhyay may have developed under subaquatic conditions, as indicated by the abundance of liptodetrinite (Teichmüller, 1989). This fact also supports the assumption of a topogenic and rheotrophic genesis of the basal strata of the studied coal.

Another typical characteristic of basal coal benches is the high content of mineral matter. The continuous evolution from seat earth to coal has been observed often (e.g. Littke and Ten Haven, 1989; Grady et al., 1993). Studies on modern tropical peats by Dehmer (1993), Neuzil et al. (1993) and Esterle and Ferm (1994) confirm this trend, because such ash-rich layers were found. However, all the basal sections of the TAL and BOB benches have a very low mineral matter content determined by microscopic observation (less than 3 vol. %), most of which is pyrite.

The ash content of each basal section is generally also very low (2 wt. %, d.b. or less). A higher ash content is present, however, in the basal section of the Suban seam of TAL (7.3 wt. %, d.b. for B1 and 10.7 wt. %, d.b. for B2) and Suban B1 seam of BOB (9.7 wt. %, d.b.). The typical mineral-rich basal section probably occurs only in Suban B2 seam of TAL. This section contains 13.7 vol. % inertinite, which is dominated by inertodetrinite (5.9 vol. %). The liptinite content is also relatively high (51.6 vol. %). Liptodetrinite dominates the liptinite (38.6 vol. %).

According to Esterle and Ferm (1994) the absence of a high-ash or fine-grained coal type at the base of a sequence could be due to the following reasons:
(1) it never existed;
(2) thickness reduction due to compaction make this zone difficult to observe in coal,
(3) its high ash content and gradational nature results in its inclusion in the seat earth; or
(4) it is too thin to be noticed.

The sedimentary strata under each studied seam are carbonaceous claystones. The presence of this strata suggests an evolution from a seat earth to coal, as its composition is between that of claystone and coal. It is possible that the typical basal section of the coal is situated within the carbonaceous claystone or that it is very thin and therefore missed. It should be noted that formation of domed peat without any substrate of topogenous peat was reported by Grady et al. (1993) and there may not be a phase of transition from seat earth to coal.

2.8.1.2 Middle Section

The middle section of the coal benches usually consists of humotelinite- and humocollinite-rich groups. The precursors of these groups were hemic and fine hemic

peats. Previous studies have shown that both peat types are characterized by wood fragments and some logs and stumps (Dehmer, 1993; Supardi et al., 1993 and Esterle & Ferm, 1994). The matrix is compacted humic attritus (Anderson, 1983; Esterle & Ferm, 1994).

According to Diessel (1992), it can be assumed that the main precursors of humotelinite are woody and cortical cell tissues as herbaceous plants degrade rather quickly. He also described that wood tissues produced by gymnosperms are quite resistant as they have a relatively high content of resins and tannins. Prolonged humification would affect trees and other wood producing plants, so that they would disintegrate extensively and produce humodetrinite macerals.

For the middle sections of TAL and BOB coals, it can be deduced that the precursor peat was dominated by wood producing plants. The water level was probably fluctuating and there was mechanical degradation of wood taking place, which may be the reason why humotelinite is associated with humodetrinite in this section.

For modern tropical domed peats Dehmer (1993) documents that the tissue volume is high in the middle section. The enrichment of structured textinite in hemic peat, in the middle part of the peat section was also observed by Grady et al. (1993). Esterle and Ferm (1994) found that wood fragments, which are common in hemic samples, consist of structured huminite with some cell fillings (corpohuminite).

Humocollinite is also enriched in the middle section of the coals. It can be primarily liberated as excretions from living plant-cell walls (phlobaphinite) or be produced as secondary cell infillings from humic gels (pseudo-phlobaphinite; Taylor et al., 1998). The secondary infillings of tissue cavities by humic solutions precipitate as gels during peatification and early stages of coalification (Cohen et al., 1987; Taylor et al., 1998). Teichmüller (1989) stated that corpohuminite macerals other than phlobaphinite are products of the biochemical gelification which entered open cell lumens. Phlobaphinite is concentrated in peats derived from plant communities rich in wood (Cohen, 1968; Taylor et al., 1998). Thus it can be postulated that the humocollinite-rich coal was generated in a swamp rich in wood-producing trees. As mentioned above, high abundance of humocollinite in the TAL and BOB coal is usually associated with a high content of

humotelinite. This is also a supporting evidence that wood was a major component of the biomass in the middle coal sections.

2.8.1.3 Top Section

The top section of the coal bench is represented by the humodetrinite-rich group. This group is the counterpart of fibric peat type at the top of the modern peat analogues. In their study, Grady et al. (1993) found a high concentration of degraded textinite and humodetrinite in this peat type.

Esterle and Ferm (1994) stated that the fibric peat is essentially the climax of the dome sequence of ever decreasing nutrient levels, and hence plant size and arboresence. Remote nutrient sources and increasing acidity due to the absence of floodwater produce a shift towards increasingly non-arborescent and smaller plants. Dehmer (1993) reported a change of vegetation from mixed forest swamp to a poor stunted padang forest as the swamp became more rainwater dependent (ombrogenous).

Humodetrinite is derived mainly from easily decomposable (lignin-poor and cellulose-rich) herbaceous plants and from angiospermous woods (Teichmüller, 1989). Large amounts of detrovitrinite (the counterpart of humodetrinite in high rank coal) indicate a high degree of cell-tissue destruction. This group of coal samples mirrors a peat section that was dominated by the humification products of herbaceous-dominated plants in the upper part of a bog, probably representing ombrogenous peatland communities V and IV of Anderson (1983).

The top section of a domed peat can also be characterized by inertinite, mainly fusinite. The petrographic analysis conducted on domed mires in Kalimantan, Indonesia by Demchuck and Moore (1993) or Dehmer (1993) have shown significant increases in oxidized plant material near the top of the peat. Moore et al. (1996), who also examined peat deposit from Kalimantan, found that the high concentration of oxidized material can be generated through fungal mechanism in response to an abnormally fluctuating water table. This mechanism can lead to the formation of inertinite in coal.

In addition, forest fires could probably act as the agent that led to fusinite-rich coal in this section. Teichmüller (1989) stated that pyrofusinite or pyrosemifusinite, which is formed by charring of plant material or peat due to fires in coal swamps, represents the major form of inertinite in peat and brown coal. The peat was not developed permanently under water, since pyro/degrado-fusinite and -semifusinite are generally regarded as indications of a relatively dry environment of deposition (Teichmüller, 1989). The occurrence of widespread fires in coal measures would also mean either long periods of drought in the swamp or on the surrounding upland areas (Scott, 1989, 2000).

2.8.1.4 Peat development

According to comparisons with modern tropical peats, the model for domed paleo-peat development (from bottom to top) in this area is represented by a humodetrinite-liptinite-rich coal, overlain by humotelinite-rich and humocollinite-rich coal and finally humodetrinite-rich coal or inertinite-rich coal. This evolution also represents the change from a topogenous to an ombrogenous peat, but does not show a dulling up sequence as typical of many Carboniferous coals which developed towards ombrogenous peat. This fact has been described in detail by Esterle et al. (1989).

As illustrated by Figures 2.5 and 2.6, each seam can consist of more than one succession of paleo-peat development. Sometimes the succession is not complete, but the pattern can still be traced.

The occurrence of more than one succession in a coal seam may be linked with rise of the general water table. However, in the seams examined in this study, mineral-rich paleo-peats typical of topogeneous deposits did not develop. Cecil et al. (1993) observed that modern upland erosion and fluvial transport in Sumatra appear to be curtailed by the extensive vegetative cover of tropical rain forests. This fact is supported by a very low concentration of suspended sediment and absence of fluvial-derived bed load in the rivers. Nevertheless, some episodes of sediment deposition are indicated by the occurrence of thin carbonaceous claystones in the coal seams.

The most ideal coal seam that shows a complete ombrogenous peat development is Suban B2 seam of TAL. In this seam, the development from topogenous to ombrogenous peat can

be recognized from the maceral assemblage evolution. The other TAL seams show more than one succession of peat development. Suban B1 seam consists of three successions and Mangus A1 and A2 seam consists of two successions. The BOB seams also show more than one succession of peat development. The Suban B2 seam of BOB probably shows an incomplete ombrogenous peat development.

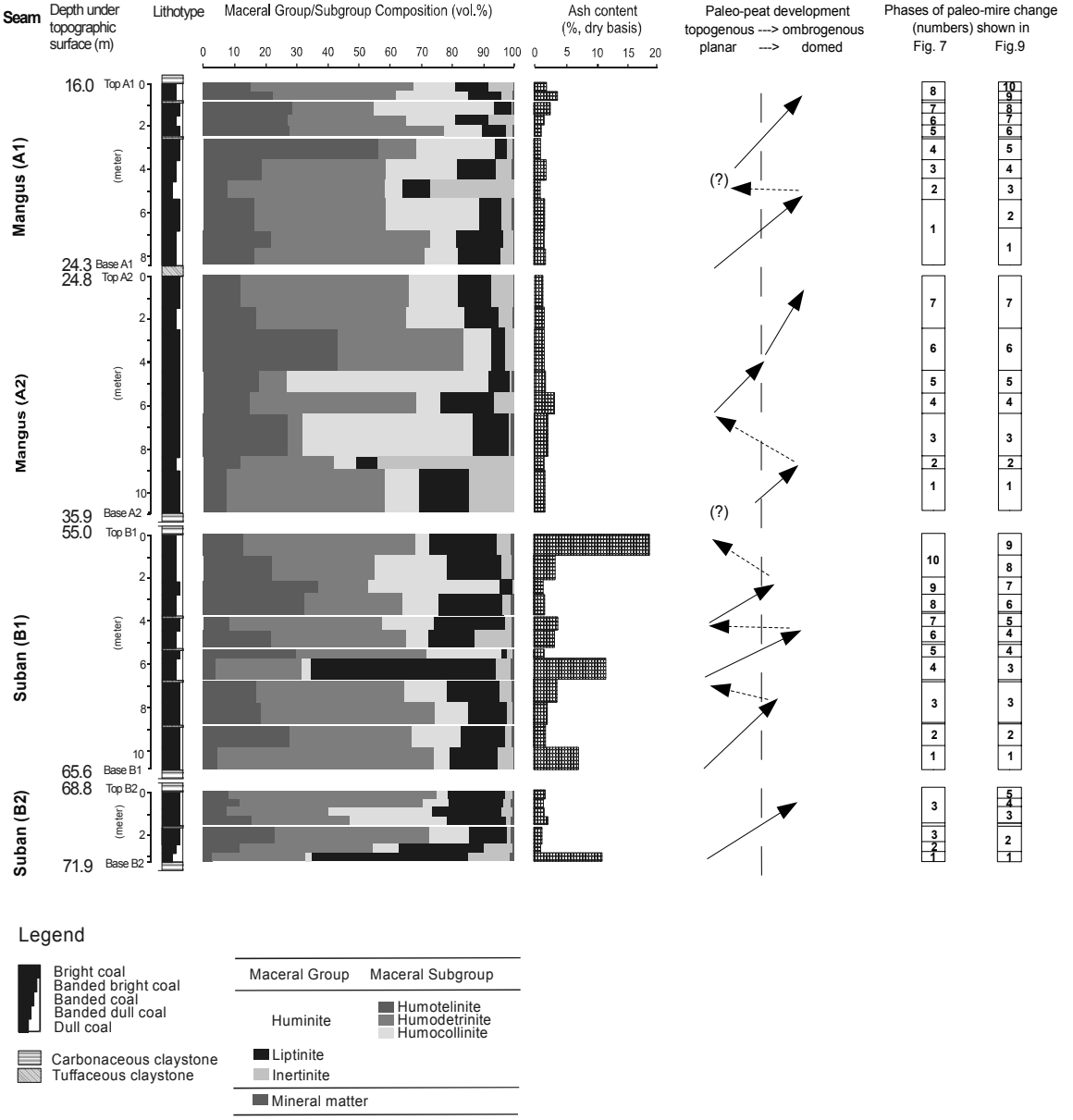

Fig. 2.5. Profile of maceral group/subgroup composition and paleo-peat development of Tambang Air Laya (TAL) coal.

The recognizable indicators of stacked paleo-peat bodies in this study are the coal layers which are characterized by humodetrinite-rich coal or inertinite-rich coal. These layers may represent the organic, non-oxidized, degradative partings and oxidized organic partings in sense of Shearer et al. (1994).

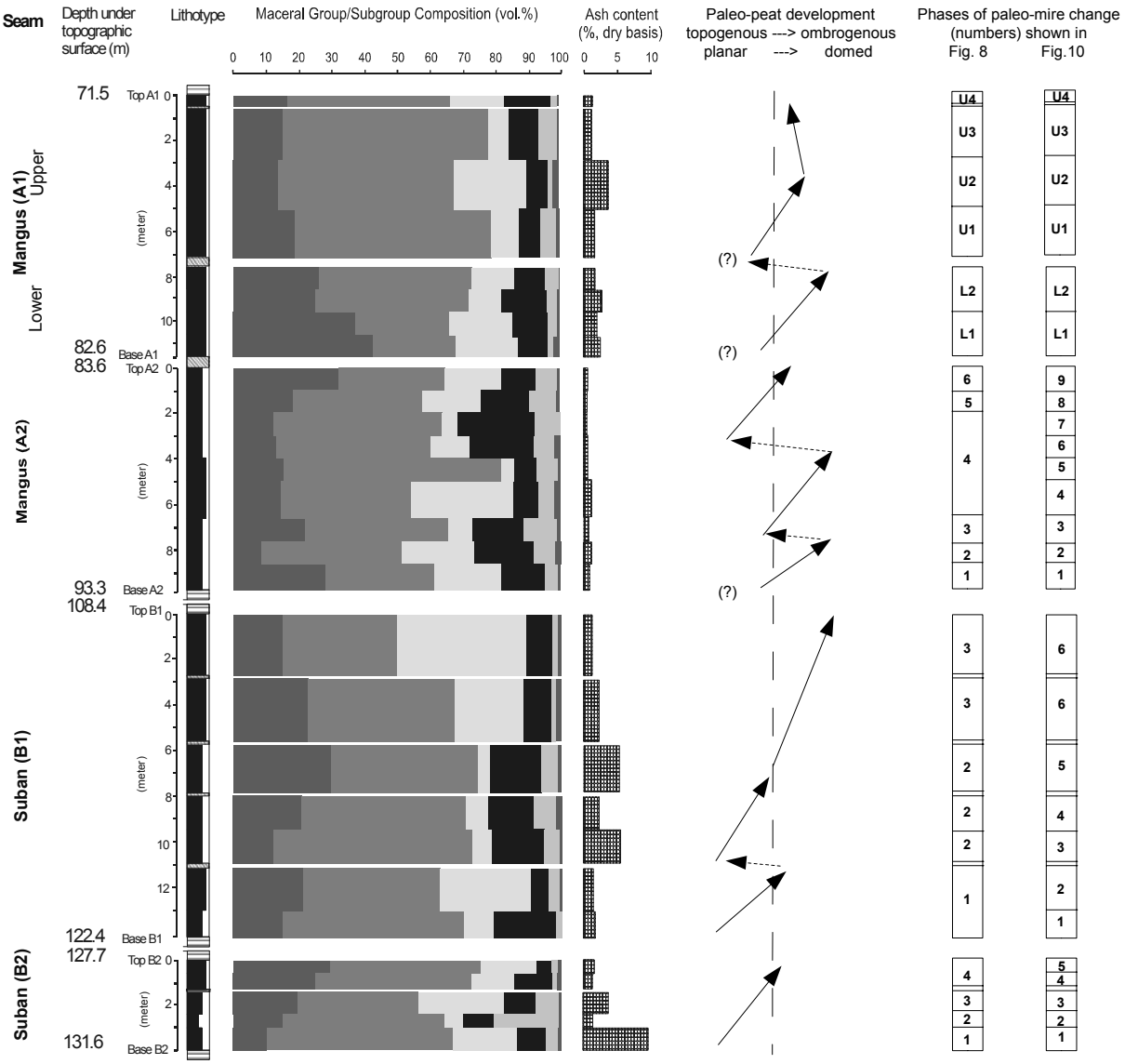

Fig. 2.6. Profile of maceral group/subgroup composition and paleo-peat development of Banko Barat (BOB) coal (legend see figure 2.5).

2.8.2 Mineral matter

The low content of mineral matter in the coals can be explained by three main processes, either the process of doming of the peat deposits, the leaching of mineral matter from previously deposited peat, or the deposition of peat on surfaces where inorganic sedimentation processes are not active. Doming of the peat is the most probable explanation, since low mineral matter content is typical for these modern peat deposits, especially where rainfall is higher than evaporation (Cohen et al., 1987). Moore (1987) stated that ombrotrophic mires (raised bog, blanket bog, bog forest) have less ash content than rheotrophic mires (fen, carr, swamp, swamp forest) or than wetlands (marsh, salt marsh), the latter being characterized by an even higher inorganic content in their sediments.

The low sulfur content of the studied coals clearly indicates that during deposition there was no significant marine influence; instead peat growth occurred in a fresh water environment (Price and Casagrande, 1991; Demchuck and Moore, 1993; Grady et al., 1993). Syngenetic pyrite content tends to increase with an increase in huminite and a decrease in inertinite content. This observation shows that the formation of (syngenetic) pyrite was more favorable under conditions in which huminite formation was also favorable. A similar relationship was also documented by Littke and Ten Haven (1989) for Carboniferous coals. The formation of pyrite requires the availability of sulfur. Raised bogs have only low sulfur contents (Cameron et al., 1989; Neuzil et al., 1993). Growth of domed peat established an acid and more oxidizing environment leading to conditions which were not favorable for pyrite formation.

2.8.3 Tissue Preservation and Gelification Index

Diessel (1986) developed the gelification index (GI) and tissue preservation index (TPI) based on coal facies analysis on Permian coals in Australia, in order to establish a correlation between coal facies indicators and the environment of coal formation. GI is the ratio of gelified and fusinitized macerals whereas TPI emphasizes the degree of tissue preservation versus destruction. TPI can be used as a measure of the degree of humification and GI is related to the continuity in moisture avaibility. Lamberson et al. (1991) made some modifications on GI and stated that an alternative way to view this

index is the inverse of an oxidation index. Those indices were also used and modified to define the depositional environment of coals from different areas and ages (e.g. Kalkreuth et al., 1991; Obaje et al., 1994; Bechtel et al., 2003 and many others).

Based on the modification by Lamberson et al. (1991), those indices were applied to the studied coal. However, a later modification was necessary, because TAL and BOB coals are of low rank. Therefore telovitrinite macerals were substituted by their precursors (humotelinite), detrovitrinite by humodetrinite and gelovitrinite by humocollinite. Fusinite, semifusinite and funginite are grouped as telo-inertinite, because they still show the plant cell structures, whereas macrinite and secretinite are grouped as gelo-inertinite because of the lack of plant cell structures. The modified formulas used are as follows:

$$TPI = \frac{\text{humotelinite} + \text{telo-inertinite}}{\text{humodetrinite} + \text{humocollinite} + \text{inertodetrinite} + \text{gelo-inertinite}} \quad (1)$$

$$GI = \frac{\text{huminite} + \text{gelo-inertinite}}{\text{inertinite (exclusive of macrinite und secretinite)}} \quad (2)$$

Coal facies diagrams for TAL and BOB coals are illustrated in Figures 2.7 and 2.8. Almost all the analyzed coals have a low TPI and high GI. In the Miocene coals of Sumatra, the low TPI is probably due to the fact that the central parts of domed peat in Indonesia are composed of thin stunted pole forest of tree-girths of about 1 m. These would be easier to decompose than those trees at the margin, which are more luxuriant, much thicker in diameter and reach 40 to 50 m in height (Anderson, 1983).

Cellulose-rich plant matter, such as that derived from herbaceous plants is more easily decomposed than lignin-rich wood (Teichmüller, 1989). Therefore a low TPI suggests either predominance of herbaceous plants in the mire or large scale destruction of wood because of extensive humification and mineralization (Diessel, 1992). The high GI, i.e. the high huminite/inertinite ratio, is also known to be typical of recent and ancient Indonesian peat and coal deposits (see Dehmer, 1995; Anggayana, 1996; Nas and Pujobroto, 2000).

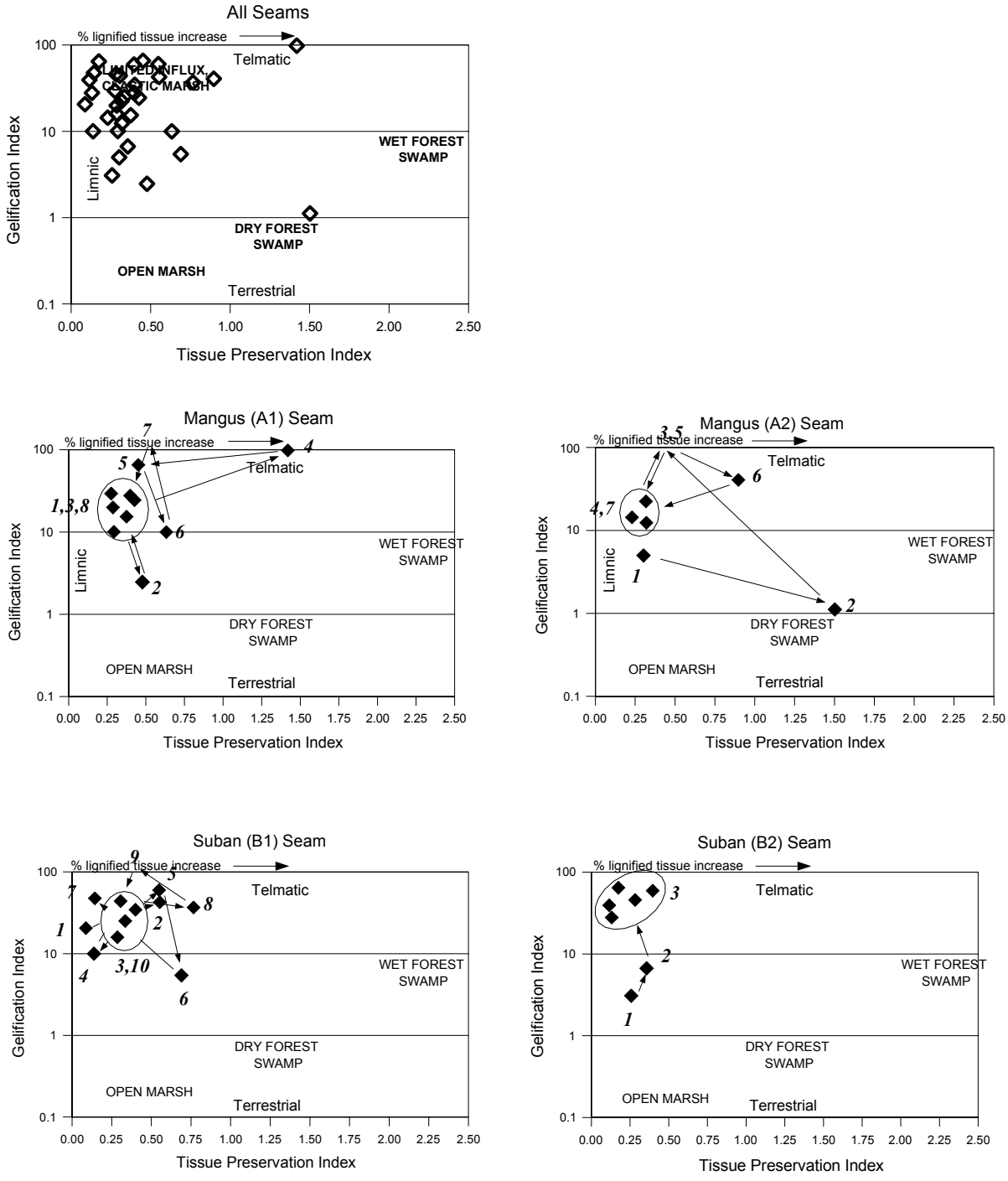

Fig. 2.7. Plot of Tissue Preservation Index and Gelification Index values of TAL low rank coals on modified Diessel's diagram (Lamberson et al., 1991). Arrows indicate the change of the depositional environment of the studied coal with time. Numbers indicate the phases of the paleo-mire change.

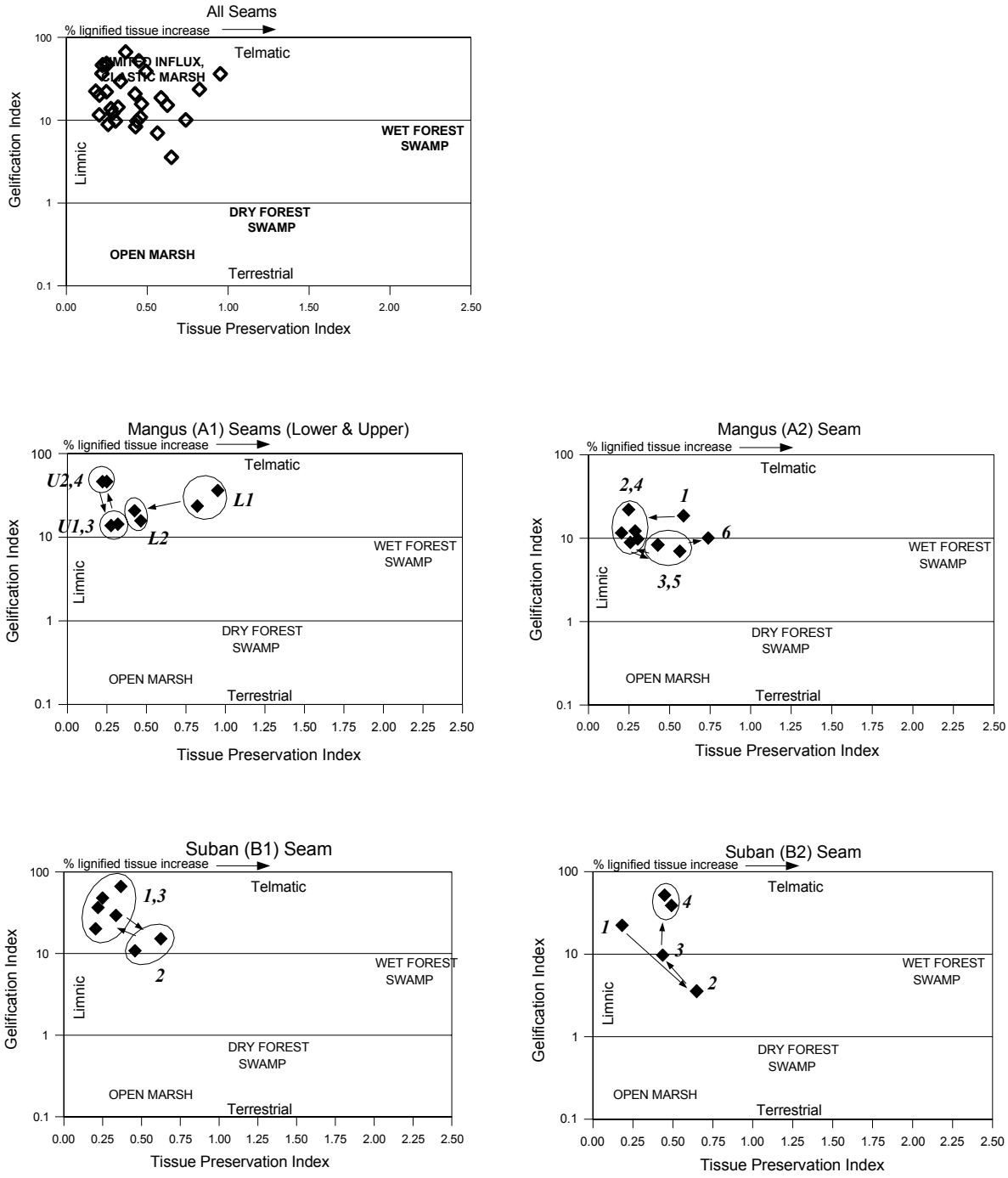

Fig. 2.8. Plot of Tissue Preservation Index and Gelification Index values of BOB coals on modified Diessel's diagram (Lamberson et al., 1991).

Whereas these indices are regarded as very helpful tools in analyzing the coal deposits, the related interpretation scheme (Figs. 2.7 and 2.8) does not fit to the Indonesian deposits, as the indices were developed for Permian coal of Australia, not for Tertiary coal of Indonesia. For example, the majority of the samples plot in the limited influx clastic marsh field. According to Diessel (1992, his table 5.2), coal with high GI and low TPI could originate from decomposed wood in forested peatlands or herbaceous plants in tree-less marshes, but both will usually generate coal with high ash content (which is not the case in TAL and BOB). Furthermore, the coal should be enriched in stable liptinite macerals (including sporinite and resinite) as well as dispersed residues of fusinite and semifusinite (in form of inertodetrinite), if the coal originated from highly decomposed forest swamp peat (Diessel, 1992). In fact, the amount of liptinite and inertinite in most of the coal samples is relatively low.

The term "marsh" is used to identify peat-forming areas which are or were predominantly covered by herbaceous plants (Martini and Glooschenko, 1984; Moore, 1987; Lamberson et al., 1991), but marsh is also considered as a kind of minerotrophic peatland (Martini and Glooschenko, 1984) with a large proportion of solid inorganic matter in the substrate (Clymo, 1987). The mineral matter content of studied coal is, however, low (see Table 2.2). Furthermore mineral matter is not dominated by clastic minerals, but by syngenetic pyrite. Therefore the paleoenvironmental interpretation as marsh in a strict sense as suggested by Figures 2.7 and 2.8 is not valid.

2.8.4 Vegetation and Groundwater Index

Another method of analysis to evaluate coal depositional environment was proposed by Calder et al. (1991) for Westphalian coal of Nova Scotia. They suggested a mire paleoenvironment diagram based on a groundwater influence index (GWI) and a vegetation index (VI) expressed as maceral ratios. The GWI evaluates the intensity of rheotrophic conditions as a ratio of strongly gelified to weakly gelified tissues. The VI is a measure of vegetation type by contrasting the macerals of forest affinity with those of herbaceous and marginal aquatic affinity. Later on, those indices were adapted to asses the development of paleo-mires in different areas (e.g. Obaje et al., 1994; Gruber and Sachsenhofer, 2001).

Modification was also necessary on Calder´s ratios for the purpose of this study. The macerals/submacerals of hard coals were substituted by their low-rank coal counterparts (see appendix in Calder et al. 1991). The ratios are expressed as:

$$GWI = \frac{\text{gelinite + corpohuminite + mineral matter}}{\text{texto-ulminite + (eu)ulminite + attrinite + densinite}} \quad (3)$$

$$VI = \frac{\text{texto-ulminite + (eu)ulminite + fusinite + semifusinite + suberinite + resinite}}{\text{attrinite + densinite + inertodetrinite + alginite + liptodetrinite + sporinite + cutinite}} \quad (4)$$

Plots of TAL and BOB coals are shown in Figures 2.9 and 2.10. Most of the studied coals lie in the area where both vegetation index and groundwater index values are low. Calder et al. (1991) proposed the GWI value of 3 as the border, above which the ecosystem is considered to be predominantly limno-telmatic. Most of the studied coal samples have GWI values of less than 0.5, indicating that the paleoenvironment was dominated by telmatic conditions. These low values indicate that groundwater ceased to be influential and the mire became solely rain-fed (ombrotrophic). Almost all the studied coal samples have low VI values of less than 1 and most plot in the marginal aquatic/herbaceous vegetation field in the diagram. This fact supports the view that forest vegetation was only a minor precursor of these coal samples.

The interpretation scheme used in Figures 2.9 and 2.10 suggests that the paleo-peat environment shifted between ombrotrophic and mesotrophic in most seams. In the Mangus A2 of TAL an elevated groundwater table drowned the bog and more forest plants developed. Therefore the mire once shifted into swamp forest (phase 3) or swamp (phase 5). A continuity from the Mangus A1 lower to upper seam of BOB is indicated by this analysis. Obviously, tuff deposition did not have a significant influence on paleo-mire character. In summary, the interpretation scheme in Figures 2.9 and 2.10 fits better to the facies interpretation deduced from the sum of petrographic information than the interpretation in Figures 2.7 and 2.8. Nevertheless, it does not seem to provide a complete and detailed description of seam evolution.

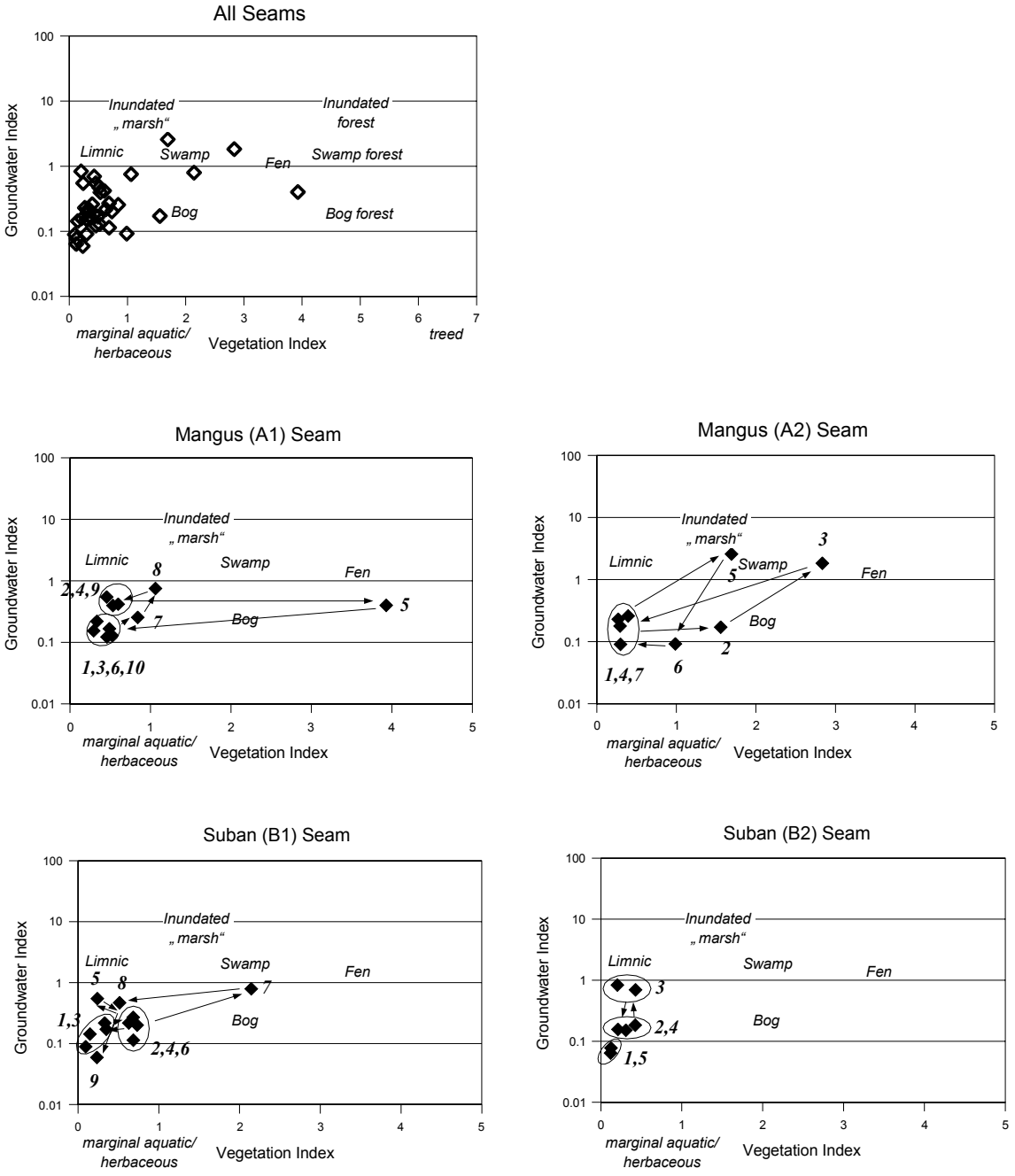

Fig. 2.9. Plot of Vegetation Index and Groundwater Index values of TAL low rank coals on mire paleoenvironment diagram (Calder et al., 1991) .

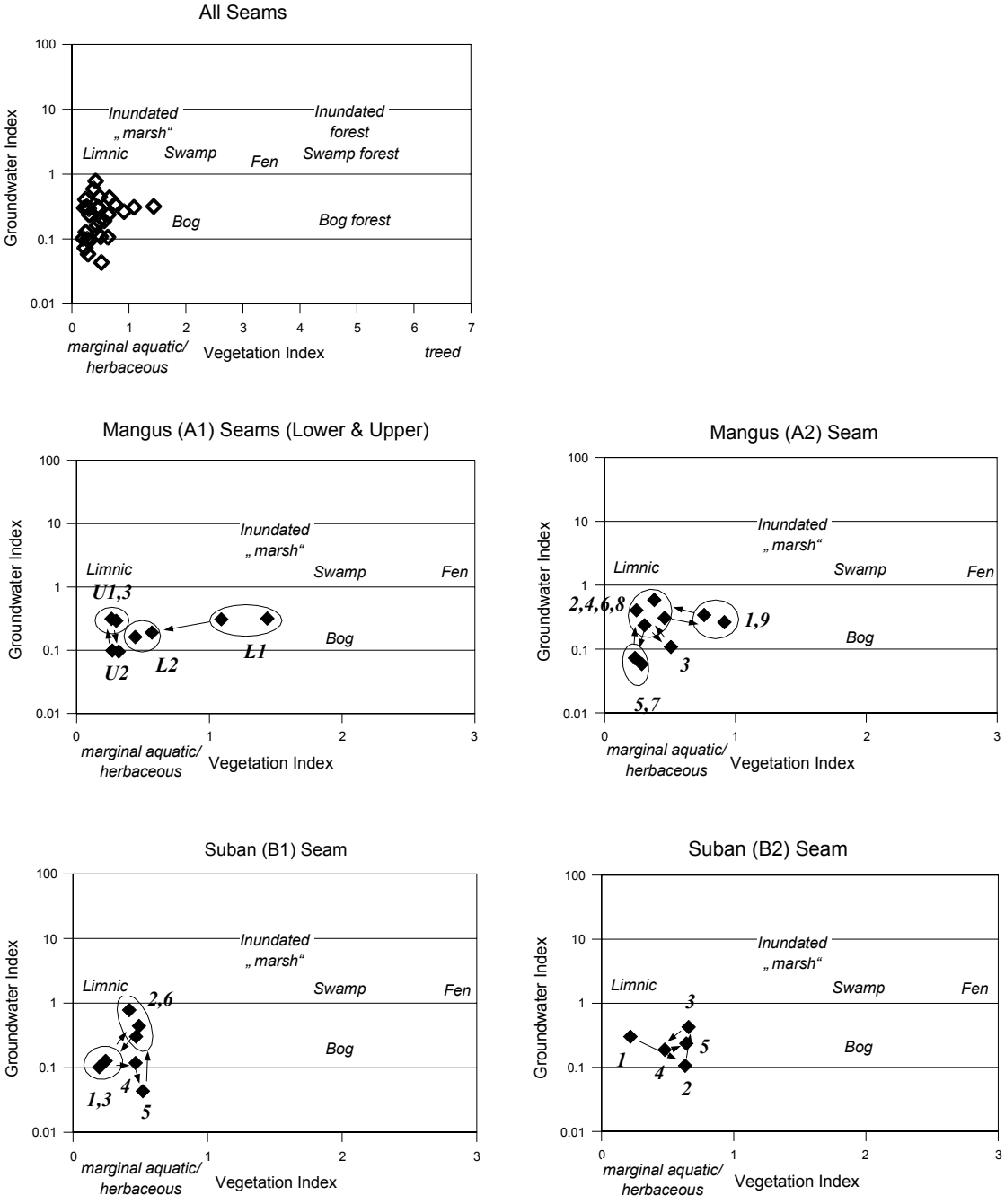

Fig. 2.10. Plot of Vegetation Index and Groundwater Index values of BOB coals on mire paleoenvironment diagram (Calder et al., 1991) .

Both the maceral ratio interpretation methods proposed by Diessel (1986) and Calder et al. (1991) fail to show the development of the paleo-mire in detail. The most obvious flaw in analysis is application of Pre-Tertiary models to Tertiary coals with very different vegetation and (in case of Permian coal) different climate. Some limitations of using the TPI and GI diagram have already been noted, for example by Crosdale (1993), Dehmer (1995), Nas and Pujobroto (2000), Wüst et al. (2001), Scott (2002) and Moore and Shearer (2003). Probably, peat paleo-depositional environments are too complex to be represented by relatively simple interpretation schemes. Furthermore, mineral matter (ash) content and composition is regarded as an additional important clue towards environmental interpretation, which is neglected by the above interpretation schemes. Especially the occurrence or lack of syngenetic pyrite and carbonate concretions, but also of fluvial layers witnessing flooding events can be a key towards an understanding of peat depositional environments. Nevertheless implementation of the indices applied above can be useful to develop an initial understanding of peat evolution through time.

2.9 Conclusions

The studied coals in the Tanjung Enim area are of low rank, except for some bituminous coals and anthracites which originate from contact metamorphism due to emplacement of an igneous intrusion. These low rank coals are rich in huminite and contain little liptinite, inertinite, and mineral matter. The maceral assemblage of the studied coals can be related to the maceral or pre-maceral composition that is observed in the modern tropical peat of Indonesia.

The ideal model of development of topogeous to ombrogenous peats (from bottom to the top) is represented by the series from humodetrinite–liptinite-rich coal at the base to humotelinite and humocollinite-rich coals in the middle and humodetrinite or inertinite-rich coal at the top. In some coal seams this depositional succession is incomplete or repeated several times. Moreover, the series appears to be similar to the succession changes seen in ombrogenous peats in modern tropical climates as clearly evidenced by low mineral matter, pyrite, and ash contents in all coal seams.

The application of the TPI–GI diagram proposed by Diessel (1986) and the GWI-VI diagram of Calder et al. (1991) to asses the paleoenvironment of the studied coal seams provided some interesting insight, for example with respect to the ratio of herbaceous to woody material, but failed to represent the peat evolution in detail.

The low content of mineral matter in paleo-peat can be explained by the doming of the deposit. By analogy to recent conditions, the influx of sediment from river water was probably limited, since only a very small amount of suspended sediment is transported by river water. Thus any overbank deposits remained thin, so that the peat was not enriched in mineral matter. During the deposition of the paleo-peat there was no significant marine influence as indicated by the low pyrite content of the coal.

Chapter 3 Properties of thermally metamorphosed coal from Tanjung Enim Area, South Sumatra Basin, Indonesia with special reference to the coalification path of macerals

3.1 Abstract

Thermally metamorphosed Tertiary age coals from Tanjung Enim in South Sumatra Basin have been investigated by means of petrographic, mineralogical and chemical analyses. These coals were influenced by heat from an andesitic igneous intrusion. The original coal outside the metamorphosed zone is characterized by high moisture content (4.13 – 11.25 wt.%) and volatile matter content (> 40 wt.%, daf), as well as less than 80 wt.% (daf) carbon and low vitrinite reflectance (VR_{max} = 0.52 - 0.76%). Those coals are of subbituminous and high volatile bituminous rank. In contrast the thermally metamorphosed coals are of medium-volatile bituminous to meta-anthracite rank and characterized by low moisture content (only < 3 wt.%) and volatile matter content (< 24 wt.%, daf), as well as high carbon content (>80 wt.%, daf) and vitrinite reflectance (VR_{max} = 1.87 - 6.20%). All the studied coals have a low mineral matter content, except for those which are highly metamorphosed, due to the formation of new minerals.

The coalification path of each maceral shows that vitrinite, liptinite and inertinite reflectance converge in a transition zone at VR_{max} of around 1.5%. Significant decrease of volatile matter occurs in the zone between 0.5 – 2.0% VR_{max}. A sharp bend occurs at VR_{max} between 2.0% and 2.5%. Above 2.5%, the volatile matter decreases only very slightly. Between VR_r = 0.5% and 2.0%, the carbon content of the coals is ascending drastically. Above 2.5% VR_r, the carbon content becomes relatively stable (around 95 wt.%, daf).

Vitrinite is the most abundant maceral in low rank coal (69.6 - 86.2 vol.%). Liptinite and inertinite are minor constituents. In the high rank coal, the thermally altered vitrinite composes 82.4 – 93.8 vol.%. Mosaic structures can be recognized as groundmasss and crack fillings. The most common minerals found are carbonates, pyrite or marcasite and clay minerals. The latter consist of kaolinite in low rank coal and illite and rectorite in high rank coal. Change of functional groups with rank increase is reflected most of all by the increase of the ratio of aromatic C-H to aliphatic C-H absorbances. The Oxygen

Index values of all studied coals are low (OI<5 mg CO_2/g TOC) and the high rank coals have a lower Hydrogen Index (< 130 mg HC/g TOC) than the low rank coals (about 300 mg HC/g TOC). T_{max} increases with maturity (420 - 440 °C for low rank coals and 475 - 551°C for high rank coals).

Based on the above data, it was calculated that the temperature of contact metamorphism reached 700 - 750ºC in the most metamorphosed coal.

Key words: coal, thermal metamorphism, South Sumatra, Indonesia, igneous intrusion

3.2 Introduction

Coal has become a very important resource in Indonesia since the government's energy diversification programs in the middle seventies. In 1998, coal contribution to electrical power generation was 33%, followed by natural gas (31%), oil (21%) and others (15%). The coal resources in Indonesia are estimated to exceed 38.8 billion tons. Most of the resources are located in East Kalimantan (35.5%) and South Sumatra (32.2%). Around 60% of the coal resources is lignite and subbituminous coal and only about 1% is anthracite (Directorate of Coal of Indonesia, 2000). The main coal deposits in Indonesia are of Tertiary age, although Paleozoic coal occurrences are known in Sumatra and Irian (Papua) (Koesoemadinata, 2000).

One of the high rank coal deposits in Indonesia can be found in Tanjung Enim area in the South Sumatra Basin. The rank increase of coal in this area was caused by igneous intrusions which initiated local metamorphism of the strata. This study is concerned with the properties of thermally metamorphosed Tanjung Enim coal. Thermally metamorphosed coal is also known by various names such as natural coke, geological coke, cinder coal or jhama (Taylor et al., 1998; Kwiecińska and Petersen, 2004). The organic petrographical, geochemical and mineralogical characteristics of those coals will be presented and discussed in the light of rank increase. Since the effects of heat from the igneous intrusion are mostly local and occur over short periods of time (see Taylor et al., 1998), the macerals are thought to be coalified following a different path as compared to macerals in normally coalified coal (i.e. through burial processes at moderate geothermal gradients). Therefore the focus of this study is particularly on a

comparison of various petrographic and geochemical properties of coals and coal macerals during coalification. The major goal is to provide a quantitative data base for the evolution of rapidly heated coal as compared to normally coalified coal.

3.3 Geological background

South Sumatra Basin is a back-arc basin, which was formed during east-west extension which took place during pre-Tertiary and early Tertiary times (de Coster, 1974; Daly et al., 1987). The stratigraphy of South Sumatra Basin is summarized in Adiwidjaja and de Coster (1973), de Coster (1974), Gafoer and Purbohadiwidjoyo (1986) and Darman and Sidi (2000). The coal bearing Muara Enim Formation (MEF) was deposited during the Late Miocene – Early Pliocene. It consists of claystones and siltstones with several sandstone layers and some coal beds (see Fig. 3.1). Boyd and Peacock (1986) interpreted the MEF as being deposited as part of a humid tropical deltaic system. Shell Mijnbouw (1976) divided MEF into two members, the lower called MPa (Middle Palembang 'a') and the upper MPb (Middle Palembang 'b'). Both members can be subdivided into M1 – M4 (Fig.3.2). The economically valuable coal seams are those from the upper part of MPa (Mangus, Suban and Petai seams). Figure 3.2 shows the geological situation of Tanjung Enim and a simplified lithological description of MEF.

The igneous intrusion in the Tanjung Enim area, which represents the late stage manifestation of post Miocene volcanic activity, is presumed to be of Pleistocene to early Quaternary age (Gafoer and Purbohadiwidjoyo, 1986; Darman and Sidi, 2000). This intrusion caused further uplift, faulting and folding as well as formation of some shallow domes, but most importantly the local metamorphism of the strata and rank increase of the coals from lignitic through to anthracitic grades in some areas. Pujobroto and Hutton (2000) report the occurrence of three main intrusive bodies near the main coalfields in Tanjung Enim (Air Laya and Suban). Those are the Bukit Asam dyke, Suban sill and a vertical parasitic cone to the west of Air Laya Dome (see Fig. 3.2). Bukit Asam dyke is the largest instrusive body and its outcrop forms a hill. Iskandar (1994) analyzed the chemistry of the igneous rock from the intrusion bodies and concluded that the intrusions are composed of basaltic andesite.

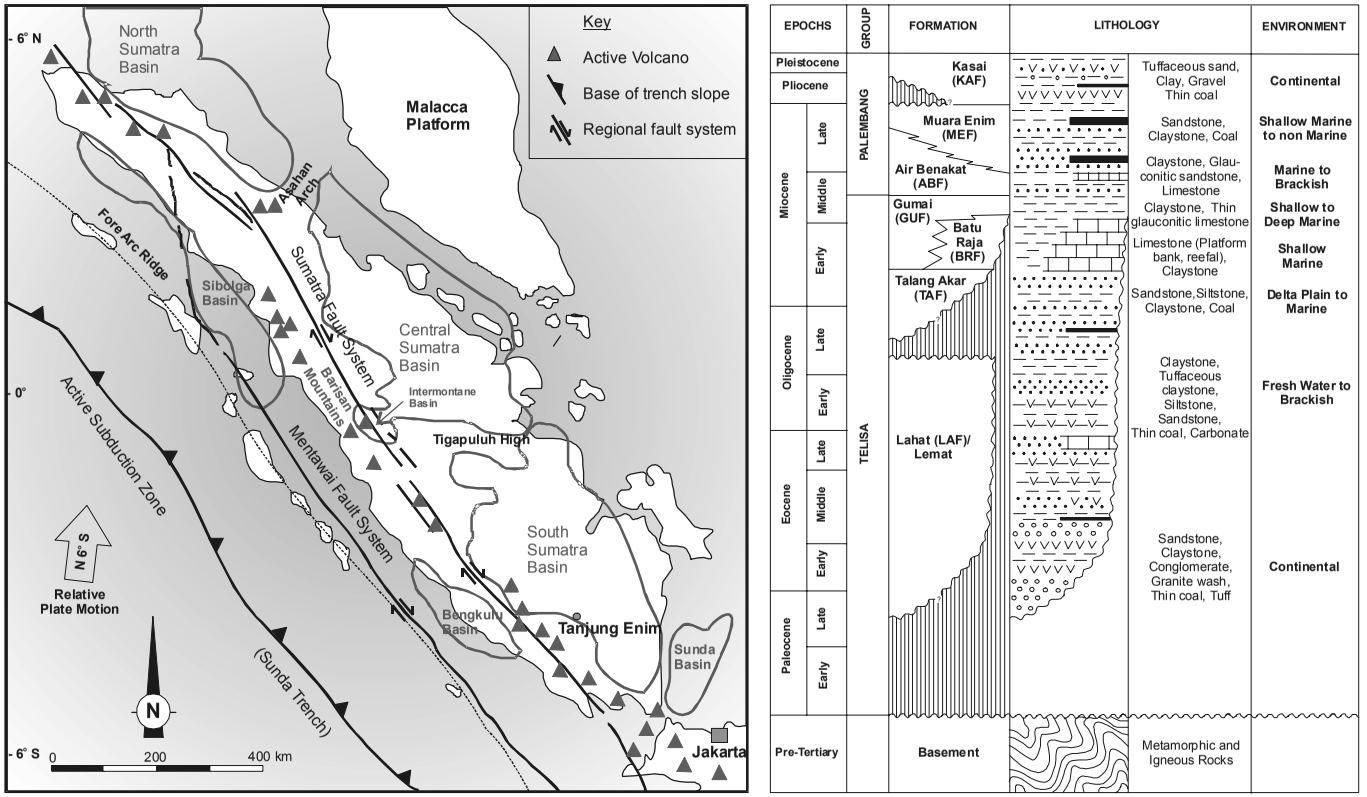

Fig. 3.1. Regional tectonic setting of Sumatra and general stratigraphy of South Sumatra Basin (modified from Darman & Sidi, 2000).

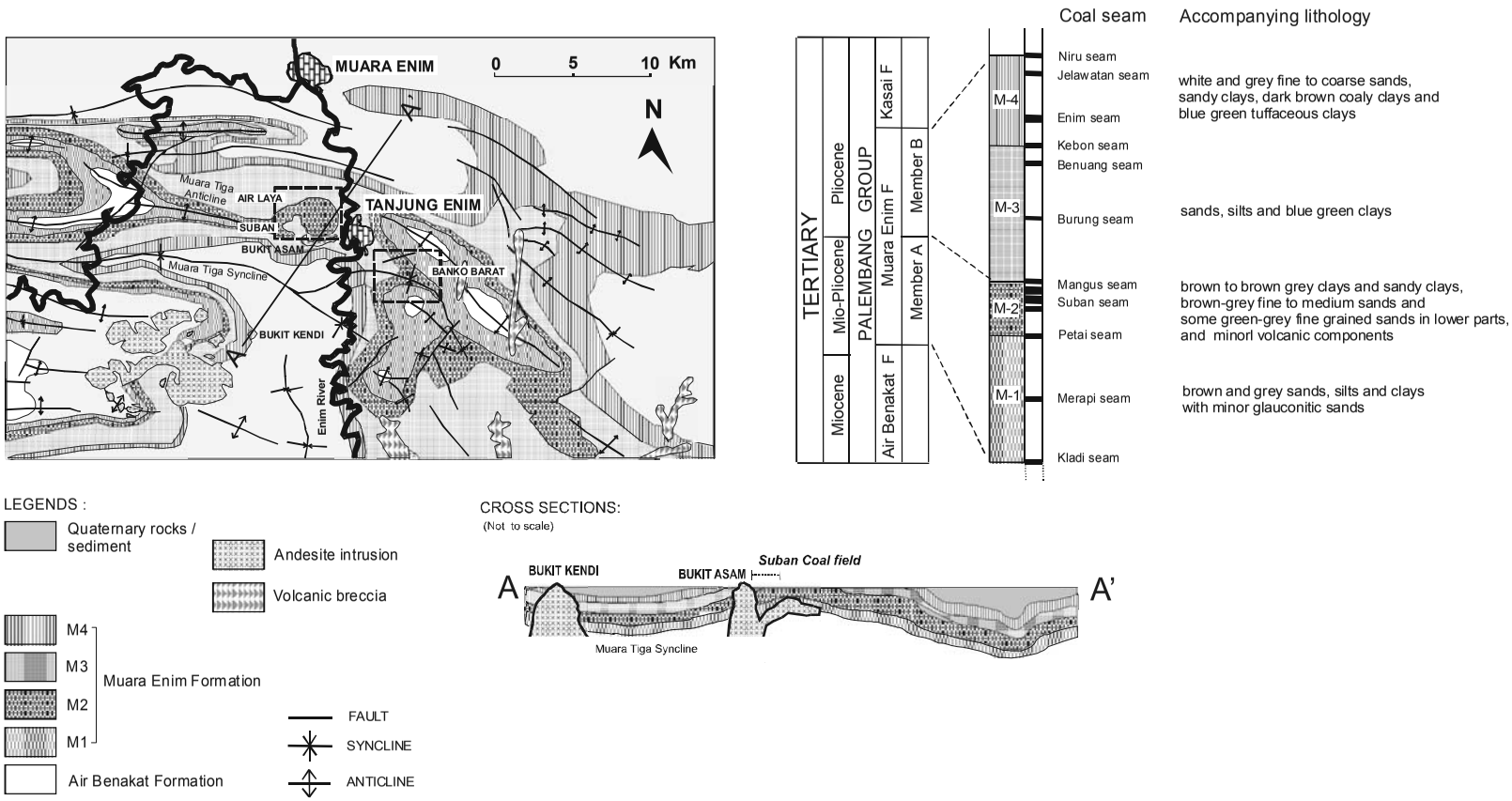

Fig. 3.2. Geological map and general stratigraphy of Tanjung Enim area (modified from Bamco, 1983 and Gafoer et al., 1986).

In general the coal of South Sumatra Basin is divided into normally coalified coal and heat affected coal. Here, "normally coalified" refers to the coals which underwent burial at moderate heat flows, whereas "heat affected" refers to coals which were rapidly heated by the igneous intrusion. The normally coalified coal has a VR_{max} of around 0.40 % to 0.50 %. Higher values of 0.60 % to 2.70 % are recorded for the heat-affected coal (Daulay et al., 2000; Pujobroto and Hutton, 2000). Almost all the low-rank coals from Tanjung Enim are dominated by huminite (around 35 - 95 vol. %; in Amijaya and Littke, 2005). Liptinite content varies from 4 vol.% up to 60 vol. % and inertinite (around 0.2 - 45 vol. %) is generally less abundant but can be high in some intervals. Minerals are found only in small amounts (0 - 2 vol.%). Ash contents are generally less than 5 wt. %, correlating reasonably well with the mineral matter determined microscopically. Only some samples have high ash contents, which can reach 18.7 wt.%. Those samples are usually present in the basal and top parts of the seams. The sulfur content of Tanjung Enim coal is very low. Anggayana (1996) reported that the sulfur content ranges between 0.1 – 2.1 % (dry basis; db). Other data by Bamco (1983) confirm these results reporting that coal from this area has a sulfur content of less than 1 % (as received; ar). Sulfur content of coal from the area affected by an igneous intrusion is slightly higher.

3.4 Samples and Methods

3.4.1 Samples

Samples were collected from an active mine, Suban, which is situated at the north east of the Bukit Asam hill. There, two main coal seams (Mangus and Suban seams) are mined. The Mangus and Suban seams split into two seams, namely Upper (A1) and Lower (A2) Mangus seams, Upper (B1) and Lower (B2) Suban seams, with average thickness of 2 to 7 m. In this coalfield, the Suban sill is outcropping and has also intruded some of the seams. The thermally metamorphosed coal samples from Suban seams were taken from the south-east side of the mine along a vertical section. In this location, the contact between the lowest seam (Suban B2) and the andesitic intrusion can be observed (see illustration in 3. 3). Coals which are unaffected or only slightly affected by the intrusion are represented by samples from Mangus A1 and A2 seams, which are located stratigraphically above the Suban seams. These latter samples were

taken from the north side of the mine. The vertical distance between individual samples depends on the macroscopic appearance of the coal.

In total there are 13 ply samples from Mangus seam and nine ply samples from Suban seam. Beside that, coals from Suban B2 seam were sampled in horizontal direction from the intrusion outcrop to south east – east along the strike. Six samples were taken with a distance of approximately 20 meters between each other. The first sample was taken directly at a the contact to the sill and the last sample at a distance of 100 m.

3.4.2 Proximate analysis and carbon content measurement

The measured moisture content in this study is the analysis moisture according to DIN 51718 (1978). Ash content determination on each sample was performed according to DIN 51719-A (1978). Volatile matter was determined by following the procedure in DIN 51720 (1978).

Carbon content was measured on powdered coal samples using a LECO multiphase C/H/H_2O analyzer (RC-412). This equipment permits the individual determination of inorganic and organic carbon in a single analytical run and does not require removal of carbonates by acid treatment for Total Organic Carbon (TOC) measurement.

3.4.3 Microscopy

The sample preparation and microscopic examination generally followed the procedures described in Taylor et al. (1998). Maceral reflectance measurement was performed under oil immersion on a Zeiss universal microscope equipped with SF photomultiplier. Maximum (R_{max}), minimum (R_{min}) and random reflectance (R_r) of each maceral group were taken on each sample at a wavelength of 546 nm. However, for later discussion on liptinite and inertinite only the R_{max} of both maceral groups will be used. Although the difference of maximum, minimum and random reflectance of liptinite in the low rank coal can hardly be distinguished, the term R_{max} of liptinite is used for convenience.

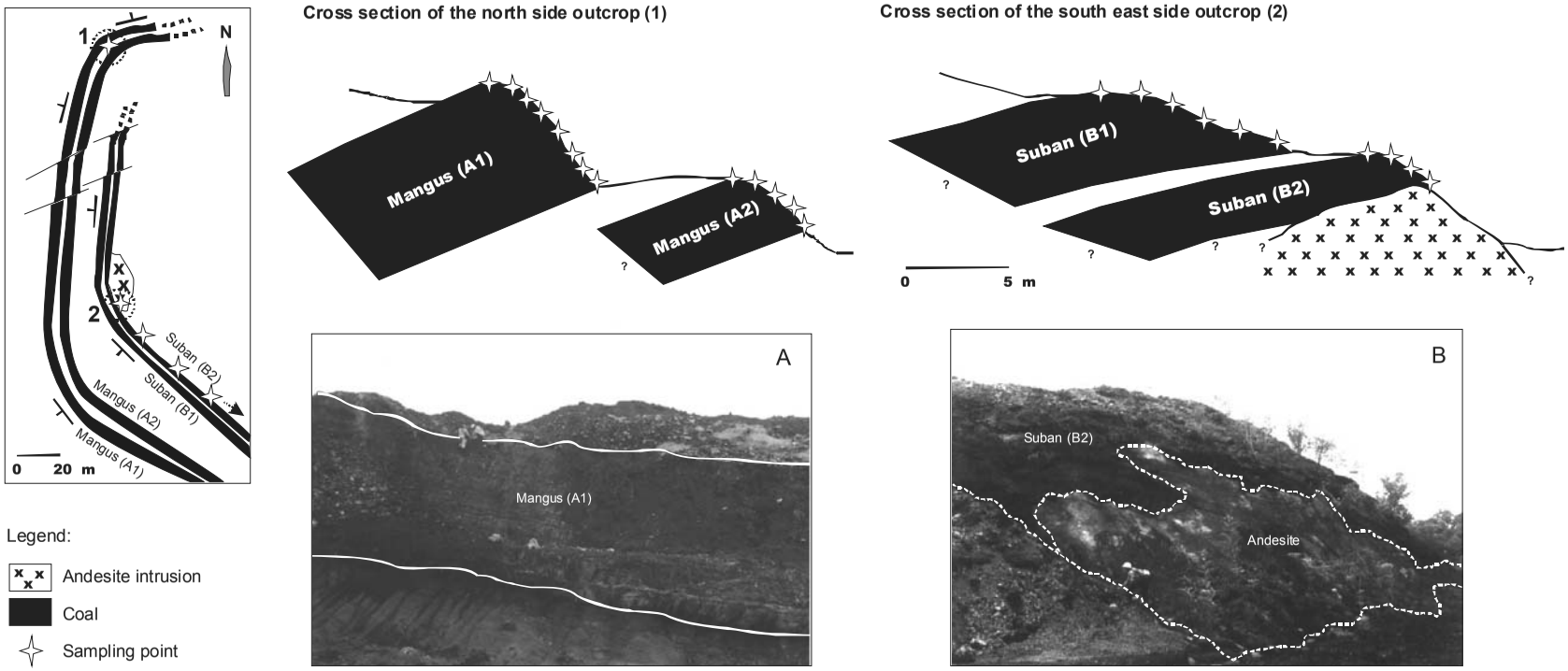

Fig. 3.3. Map showing the position of the andesitic intrusion relative to coal seams and the sampling points at studied location in Suban coal field. Photo A : Mangus (A1) seam exposed at the north-side outcrop. Photo B: Contact between andesite intrusion and Suban (B2) seam at the south-east side outcrop.

Reflectance was measured on macerals that have a visible botanical cell structure (telovitrinite for vitrinite and fusinite for inertinite). In very high-rank studied coals, almost all macerals were already homogenized. Therefore the measurement was performed on macerals, of which the remnant of the cell structure was still recognizable. Fifty reflectance measurements were made on the vitrinite per sample. If they were present, the reflectance measurement on liptinite in the low-rank coal samples was done on sporinite or cutinite. If there was no suitable sporinite or cutinite, the measurement other liptinite macerals were used. Traces of liptinite in very high rank coals (meta-liptinite) are still recognizable in some samples. For liptinite and inertinite, total measurement ranged from 2 to 20 per sample.

All of the studied coal samples were petrographically analyzed. For maceral analysis one thousand points with a minimum distance of 0.2 mm between each point were counted on each polished sample. The counting was conducted in reflected white light and in fluorescence irradiated by blue/violet light (Two-Scan method, Taylor et al., 1998) using a Zeiss Axioplan microscope with 50x magnification Epiplan objective lens and 10x magnification ocular lens. Coal rank determination and maceral classification outlined by Taylor et al. (1998) was followed. Attention was given to the coals with very high reflectance since most of them already show natural coke characteristics. Therefore the natural coke classification was also applied (see Gray, 1991; Taylor et al., 1998; Kwiecińska and Petersen, 2004).

In order to examine the appearance of the minerals in detail, some selected samples were analyzed using a Zeiss DSM 982 Gemini scanning electron microscope after coating with carbon. This method allows a lateral resolution up to 1.0 nm. The microscope is coupled with an energy-dispersive x-ray microanalyser (EDX-System Oxford Link ISIS with HPGe-Detector and UT-Window). Using this equipment, elemental analysis of microscopic volumes for all elements with atomic number > 4 can be conducted.

3.4.4 X-Ray Diffraction (XRD)

Bulk coal samples were analyzed using a Siemens D-500 X-Ray diffractometer to investigate the mineral species contained. Approximately 1 cm^3 powder sample is

required for XRD analysis. The sample is excited by a collimated beam of x-rays with diffraction angles (2θ) between 2° and 72°. These diffraction patterns are used to identify the mineral species, in particular clay minerals (Wilson, 1987; Moore and Reynolds, 1997). The examination of mineral content was done only qualitatively since the mineral content in coal is very low; thus most of them could not be detected by the equipment. Some samples which have high mineral matter content according to petrographic and ash content examination were selected to be analyzed.

3.4.5 Fourier Transform Infrared (FTIR) Spectroscopy

FTIR spectra of coal samples were measured on KBr pellets. Approximately 1 mg finely-ground air-dried coal and 200 mg KBr were mixed and ground again before transferred into a 13 mm mould. The powder was then pressed in a vacuum to form a pellet. The pressed pellets were dried in an oven (105 °C) overnight to minimize the contribution of water to the spectrum. Spectra were recorded on a Nicolet 505 spectrometer, collecting 256 scans per sample at a resolution of 4 cm^{-1}. Bands of adsorption were identified by comparing spectra with some published studies (e.g. Painter et al., 1981b; Sobkowiak and Painter, 1992). A series of samples varying in rank representing the normal and thermally metamorphosed coals were selected for FTIR analysis.

3.4.6 Rock-Eval pyrolysis

Rock-Eval pyrolysis was basically carried out following the procedure outlined by Espitalié et al. (1977a, 1977b) to determine the T_{max}, hydrogen index (HI) and the oxygen index (OI) values of some selected coal samples from low rank to high rank coals. The pyrolysis was conducted using a DELSI Inc. Rock-Eval II instrument. Approximately 20 mg of the powdered coal samples are pyrolyzed in a helium atmosphere in the absence of oxygen. The sample is first heated to 300 °C within several seconds and remains exposed to this temperature for 3 – 4 minutes. Subsequently pyrolysis proceeds in a temperature-programmed fashion by heating the samples to 550 °C at a heating rate of 25 °C/min.

3.5 Results and Discussion

3.5.1 Proximate analysis

The results of the proximate analysis from the studied coals are summarized in Table 3.1. The samples from Mangus seams have higher moisture content and volatile matter content than the samples from Suban seams. This data is the first indication that the Mangus coal has a lower rank than the Suban coal, since the moisture content and volatile matter generally decrease with increasing coal rank (see Teichmüller and Teichmüller, 1979). The volatile matter values decrease towards the intrusion body (Fig.3.4), indicating the increase of rank with increasing proximity to the intrusion. However, this trend cannot be deduced very well from the moisture content data.

The ash content varies widely, although most of the samples from Mangus seams have very low ash content. Only one sample, taken at the base section of Mangus A2 seam, produces 14.64 wt.% (db) ash. The ash content of the Suban coals is higher. The coals sampled horizontally along the strike have a relatively similar ash content, ranging between 2.61 wt.% to 4.76 wt.% (db). A wide range of ash content is displayed by the vertically collected samples of the Suban coals (5.03 – 23.65 wt.%, db). In particular, in the Suban B2 seam, the ash contents of coal are higher. This seam was sampled very close to the intrusion (see Fig. 3.3). The increase of the ash yield of coal from the unaltered part of the seam towards the intrusion has also been observed on other profiles, as some new minerals, especially carbonates, are formed (see for example Karayigit and Whateley, 1997; Golab and Carr, 2004).

3.5.2 Correlation of inter-maceral reflectance

The results of maceral reflectance measurements show that the studied coals can be classified into two groups. The coals from Mangus seams which have low to moderate maceral reflectance values (Table 3.2) can be categorized as subbituminous to high-volatile bituminous coals (VR_{max} less than 1%). The Mangus A1 seam does not show any tendency of increasing maceral reflectance from top to the bottom of the seam. Such a trend is, however, clearly recognized in the vitrinite reflectance data of Mangus A2 seam. The bottom part of Mangus A2 seam, which is closer to the intrusive

body, is characterized by a change in vitrinite reflectance (see Fig. 3.4). This trend cannot be found in the LR_{max} and IR_{max} values.

Table 3.1. Results of proximate analysis and carbon content measurement on the studied coals

Seam	Sample No.	Moisture content (wt.%)	Ash content (wt.%, db)	Volatile matter (wt.%, daf)	Total Carbon (wt.%, daf)
Mangus A1	03/1125	7.48	4.95	46.73	73.85
Mangus A1	03/1126	8.06	1.67	46.49	75.14
Mangus A1	03/1127	8.92	0.75	47.66	75.95
Mangus A1	03/1128	10.31	1.33	46.16	75.27
Mangus A1	03/1129	10.53	0.73	44.02	76.18
Mangus A1	03/1130	11.25	0.87	43.70	76.46
Mangus A1	03/1131	9.81	0.75	45.79	75.52
Mangus A1	03/1132	9.14	0.68	44.06	74.63
Mangus A2	03/1133	4.89	0.52	44.28	74.65
Mangus A2	03/1134	4.28	0.70	44.62	75.19
Mangus A2	03/1135	4.62	2.37	44.78	76.41
Mangus A2	03/1136	4.39	1.12	41.65	77.86
Mangus A2	03/1137	4.13	14.64	41.13	77.79
Suban B1	03/1138	2.79	14.38	14.16	90.31
Suban B1	03/1139	2.75	12.85	14.84	94.60
Suban B1	03/1140	2.01	6.65	12.99	89.12
Suban B1	03/1141	1.49	11.19	13.58	93.55
Suban B1	03/1142	1.53	11.26	12.96	93.46
Suban B1	03/1143	2.02	12.04	11.79	94.25
Suban B2	03/1144	1.89	5.03	9.63	91.16
Suban B2	03/1145	2.03	6.42	8.41	94.28
Suban B2	03/1146	1.95	13.77	5.77	95.37
Suban B2	03/1113	1.47	23.65	4.47	96.80
Suban B2	03/1117	1.72	3.18	14.01	90.01
Suban B2	03/1119	1.84	2.61	14.31	93.10
Suban B2	03/1120	2.22	4.22	14.52	83.47
Suban B2	03/1121	2.08	4.76	16.60	88.44
Suban B2	03/1123	1.92	2.63	23.63	84.78

Note: Samples are ordered from top to the bottom of each seam, except samples number 03/1113 to 03/1123 which were taken horizontally. Sample number 03/1113 was taken directly at the contact between Suban B2 seam and the intrusion body.

Table 3.2. Petrographical data of the studied coals from Mangus seams

Seam	Sample No.	VR_{max} (%)	VR_r (%)	VR_{min} (%)	LR_{max} (%)	IR_{max} (%)	Vitrinite (vol.%)	Liptinite (vol.%)	Inertinite (vol.%)	Mineral matter (vol.%)
Mangus A1	03/1125	0.53	0.52	0.50	0.13	0.86	80.48	12.60	3.37	3.56
Mangus A1	03/1126	0.57	0.55	0.53	0.13	0.89	83.29	12.00	3.96	0.75
Mangus A1	03/1127	0.52	0.52	0.49	0.11	0.89	86.23	10.60	2.43	0.75
Mangus A1	03/1128	0.53	0.51	0.50	0.12	0.90	81.51	14.60	3.33	0.56
Mangus A1	03/1129	0.55	0.52	0.50	0.11	0.84	77.25	10.80	11.77	0.18
Mangus A1	03/1130	0.56	0.54	0.53	0.12	0.94	81.79	7.40	10.03	0.79
Mangus A1	03/1131	0.52	0.51	0.48	0.16	0.89	81.94	11.20	6.30	0.56
Mangus A1	03/1132	0.54	0.53	0.52	0.12	0.87	85.93	7.20	6.68	0.19
Mangus A2	03/1133	0.59	0.58	0.57	0.21	0.95	78.95	13.40	7.65	0.00
Mangus A2	03/1134	0.61	0.59	0.58	0.18	0.89	73.24	13.80	12.58	0.38
Mangus A2	03/1135	0.59	0.57	0.56	0.18	0.84	85.53	8.40	4.70	1.37
Mangus A2	03/1136	0.69	0.66	0.65	0.23	0.96	82.73	9.40	7.29	0.58
Mangus A2	03/1137	0.76	0.73	0.71	0.17	0.99	69.62	8.60	13.22	8.56

In contrast, the coals from Suban seams contain macerals with high reflectance values (see Table 3.3). The coals from these seams can be classified into medium-volatile bituminous to anthracite coals (VR_{max} around 1.4% to more than 4%). The reflectance values of macerals of coals from Suban B2 seam, which is directly intruded by the andesite body (see Fig. 3.4) are higher than those of Suban B1 coals. In the sample which was taken directly at the contact with the intrusion, the VR_r value reaches 5.18%. Liptinite reflectance is higher than inertinite reflectance in all Suban samples. It should be noted that liptinite and inertinite are very rare, with the exception of small funginite. Liptinite and inertinite could not even be visually observed in the coal with highest vitrinite reflectance. It is clear that the optical characteristics of the coal have been greatly changed by the intrusion.

A

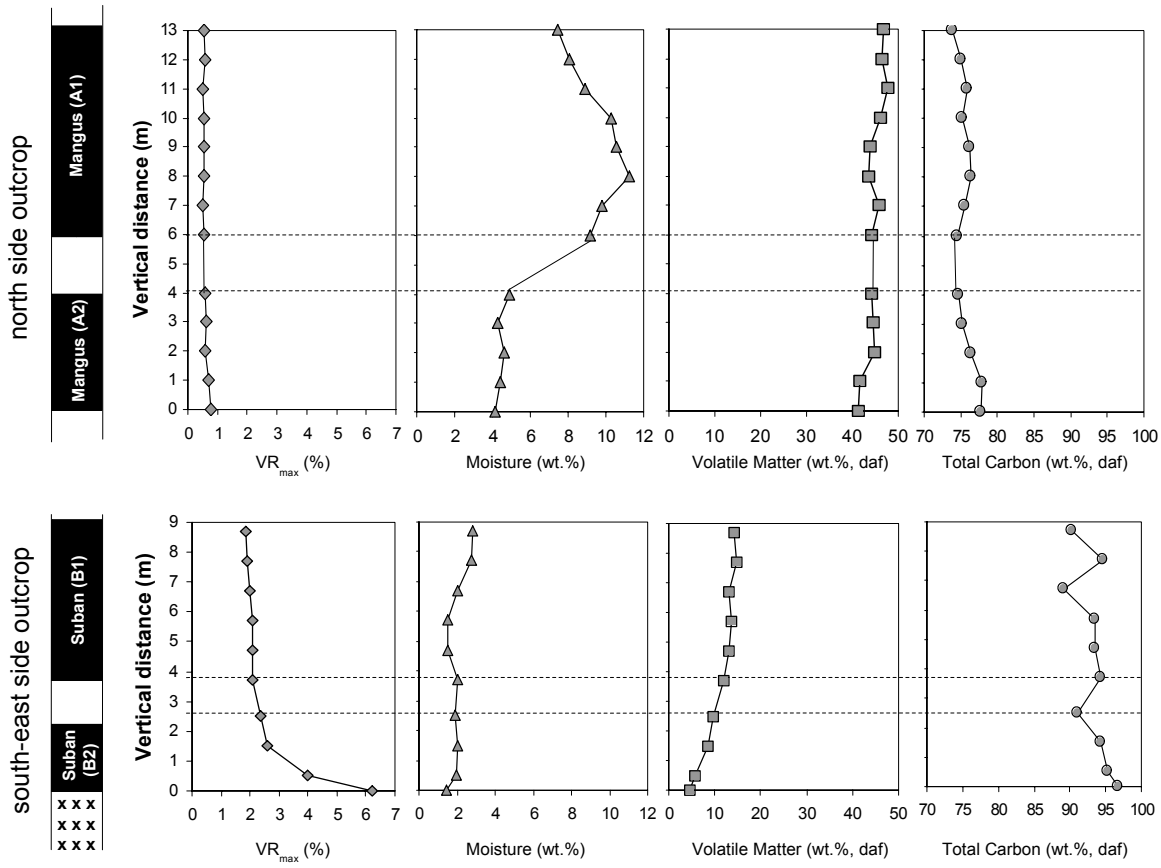

Fig. 3. 4. Change of some coal properties with (A) vertical depth and (B) horizontal distance toward the intrusion. Mangus A2 seam is located stratigraphically about 15 m above Suban B1 seam.

B

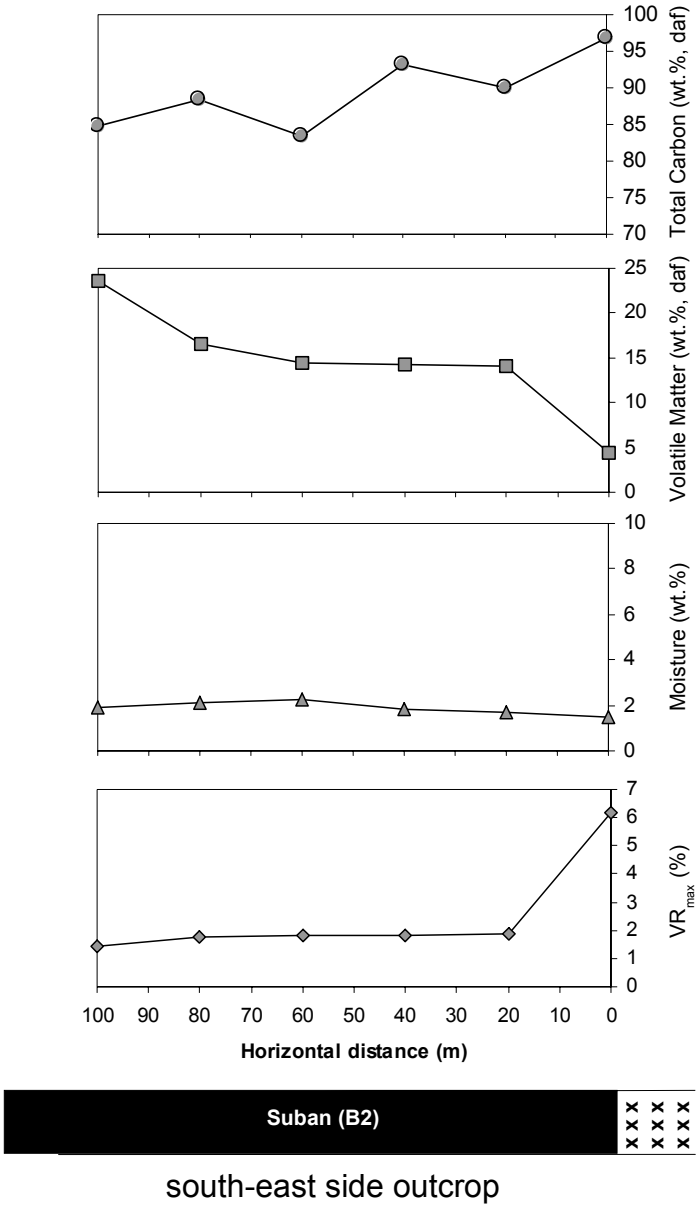

Fig. 3. 4. (*continued*)

In general, it has been observed that as the rank of the coal increases, the anisotropy of the macerals also increases, i.e. R_{max} - R_{min} of vitrinite is increasing. The vitrinite bireflectance values of the Mangus seam coals are only 0.02% to 0.05%, which basically is the range of standard deviation of VR_{max} and VR_{min} values (0.02 - 0.06%; standard error = 0.01 - 0.02%). In contrast, in the high rank Suban seam coals, the bireflectance of vitrinite increases from around 0.1% to 1.7% (see Fig. 3.5).

Table 3.3. Petrographical data of the studied coals from Suban seams

Seam	Sample No.	VR_{max} (%)	VR_r (%)	VR_{min} (%)	LR_{max} (%)	LR_{min} (%)	IR_{max} (%)	IR_{min} (%)	Vitrinite (vol.%)	(Meta-) Liptinite (vol.%)	Inertinite (vol.%)	Mineral matter (vol.%)	Mosaic structure (vol.%)
Suban B1	03/1138	1.87	1.85	1.76	1.98	1.76	1.78	1.64	91.20	0.40	2.00	6.40	-
Suban B1	03/1139	1.91	1.90	1.82	1.98	1.85	1.81	1.71	87.80	1.00	9.40	1.80	-
Suban B1	03/1140	1.99	1.90	1.88	2.06	1.98	1.90	1.69	84.20	0.80	11.60	3.40	-
Suban B1	03/1141	2.08	2.02	1.91	2.19	1.98	1.92	1.78	91.00	1.20	5.80	2.00	-
Suban B1	03/1142	2.09	2.02	1.89	2.12	1.98	1.91	1.76	89.40	0.60	8.00	2.00	-
Suban B1	03/1143	2.10	2.09	1.93	2.16	2.06	1.96	1.69	90.40	1.20	6.80	1.60	-
Suban B2	03/1144	2.38	2.33	2.19	2.46	2.27	2.22	2.08	90.60	0.20	7.20	2.00	-
Suban B2	03/1145	2.61	2.55	2.21	2.74	2.40	2.54	2.28	87.00	0.40	10.60	2.00	-
Suban B2	03/1146	3.99	3.69	3.33	-	-	3.72	2.35	90.60	0.00	1.00	8.40	-
Suban B2	03/1113	6.20	5.18	4.48	-	-	-	-	82.40	0.00	0.60	14.60	2.40
Suban B2	03/1117	1.86	1.78	1.64	1.93	1.77	1.76	1.50	91.40	1.80	6.60	0.20	-
Suban B2	03/1119	1.82	1.77	1.67	1.82	1.81	1.71	1.47	93.80	2.60	2.80	0.80	-
Suban B2	03/1120	1.80	1.78	1.73	1.84	1.79	1.69	1.60	92.80	0.40	2.60	4.20	-
Suban B2	03/1121	1.78	1.70	1.64	1.81	1.74	1.65	1.54	93.60	0.60	3.20	2.60	-
Suban B2	03/1123	1.45	1.42	1.33	1.25	1.15	1.49	1.42	91.80	0.40	5.60	2.20	-

Previous studies (Ragot, 1977; Diessel, 1983) document that there is a reversal of the VR_{min} curve in the meta-anthracite stage (about 6.% VR_{max}) when the pre-graphitization begins, so that the bireflectance value is tremendously high beyond that level. However, this pattern was observed on coals which underwent "normal" coalification by deep burial, although the vitrinite reflectance data of heat effected coals from Goodarzi and Gentzis (1990) show a similar trend. The data gained from this study on Tanjung Enim coals do not provide evidence for a decrease of VR_{min} at 6% VR_{max} although the curve tends to incline less steeply at that high rank stage (Fig. 3.5).

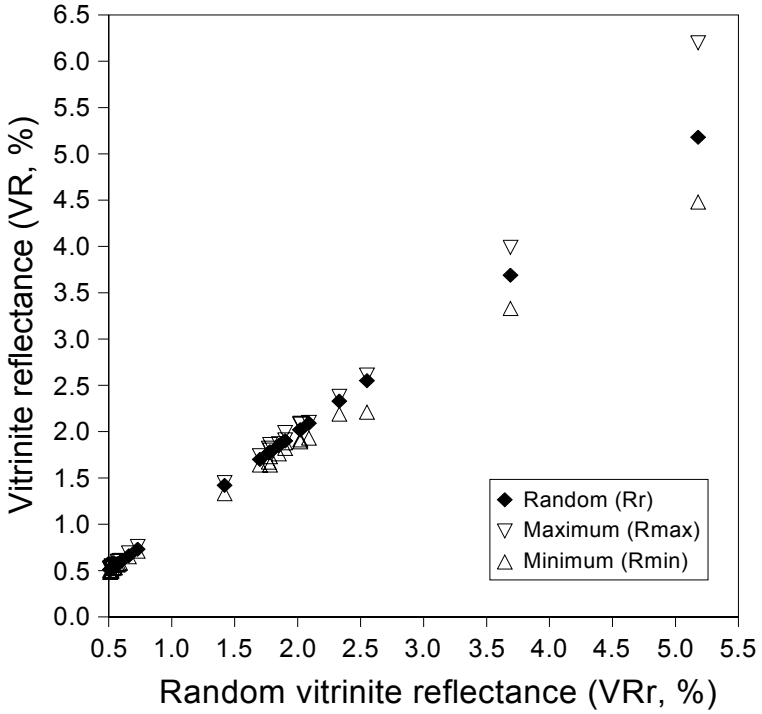

Fig. 3.5. Diagram showing the anisotropy of vitrinite caused by thermal metamorphism.

Hower and Davis (1999) found that in anthracites, the liptinite bireflectance is greater than the vitrinite bireflectance. In our study, this pattern could not be recognized because the liptinite bireflectance values of the high rank coals vary considerably, and liptinite cannot be observed in the coals with very high vitrinite reflectance (see Table 3.3).

During the "normal" coalification process, the reflectance anisotropy is caused by the progressive orientation of the aromatic nuclei into the bedding plane, as a consequence of load pressure (see Taylor et al., 1998). Our results indicate that in the absence of high pressure as typical for burial diagenesis, the increase in bireflectance with increasing maturity (rank) is less severe; i.e. there is some retardation of bireflectance increase and pre-graphitization relative to rank increase.

The trendlines of LR_{max} and IR_{max} of the studied samples in contrast to VR_{max} can be divided into three stages (Fig. 3.6). The first part is characterized by the typical reflectance trend of each maceral, where liptinite reflectance is lower than vitrinite reflectance and inertinite has the highest reflectance. This stage is typical of coals with VR_{max} of less than 1%. The second part can be observed at VR_{max} of 1.45%. At this stage, the maximum reflectance of inertinite begins to converge with the reflectance of accompanying vitrinite. Similarly, the liptinite reflectance value approaches the vitrinite reflectance value as well. The pattern of maceral reflectance distribution in the third part is contrary to that of the first stage. The LR_{max} of the coal is higher than VR_{max} and IR_{max}. This characteristic is shown by the samples which have VR_{max} of 1.7% and more. If a trend line is drawn for each maceral, all curves will cross each other at the transition stage.

The rapid increase of sporinite reflectance in the coking coal stage, as it approaches the reflectance of associated vitrinite, is known as the "coalification jump" (Stach, 1953). Alpern et al. (1972) showed that the coalification curve of liptinite converges with that of vitrinite at approximately 1.5% VR_{max}. Teichmüller (1974) recognized two liptinite (former term: exinite) coalification jumps at 0.6% and 1.2%. Smith and Cook (1980) argued that the coalification jump occurs only at 0.4 – 0.5% VR_{max}, and marks the beginning of measurable exinite coalification. The coalesence of liptinite curve and vitrinite curve at VR_{max} 1.1 – 1.5% is considered by them as "visual step" rather than coalification jump. In our study, the liptinite reflectance begins to exceed the vitrinite reflectance at the transition stage (VR_{max} around 1.5%). Looking at the trend of the increase of liptinite reflectance, no real "jump" can be observed. The liptinite reflectance increases progressively.

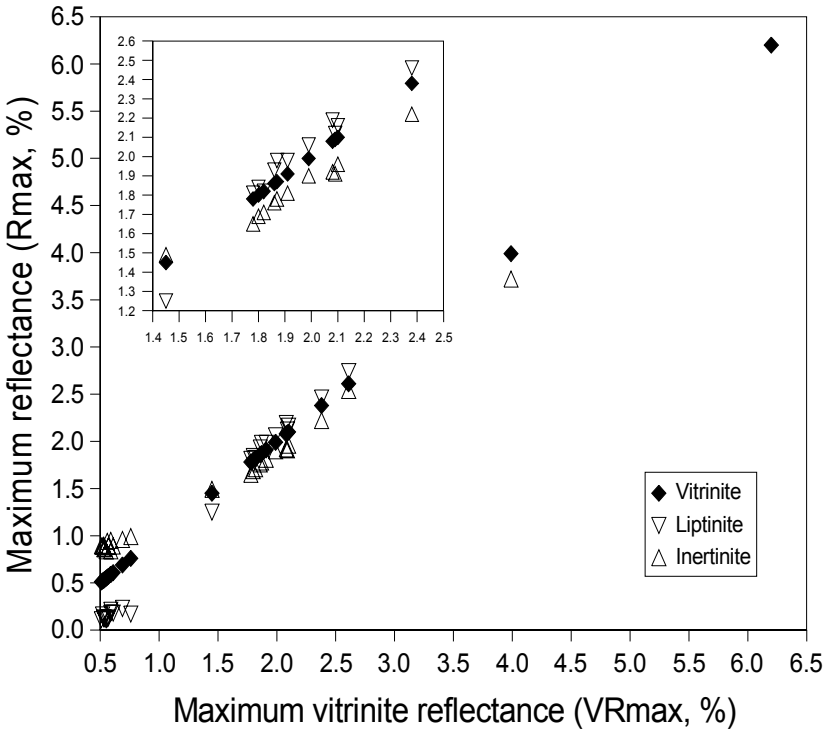

Fig. 3.6. Correlation between maximum reflectance of vitrinite, liptinite and inertinite. Inserted diagram shows the data in the range of 1.3 to 2.4 % VR_{max}.

Inertinite alters hardly during coalification because it is already "pre-coalified" (Taylor et al., 1998). Alpern et al. (1972) described that the reflectance of inertinite is always high, but at VR_{max} around 5%, its curve converges with the VR_{max} curve as the VR_{max} begins to increase rapidly. In their study, Smith and Cook (1980) showed that the reflectance of inertinite increases drastically in the range between brown coal and high volatile bituminous coal (0.2 - 0.9% VR_{max}), which is regarded as a coalification jump for inertinite. The measured samples in our study have VR_{max} of more than 0.5%, so that the development of inertinite reflectance in lower rank coal cannot be examined. Unlike the results of previous studies, vitritine reflectance already reaches inertinite reflectance at a moderate coal rank (around 1.5% VR_{max}). Above this stage, the reflectance of vitrinite is higher than that of inertinite, but differences between vitrinite and inertinite reflectance are minor.

3.5.3 Maceral reflectance in comparison to other coal properties

The typical trend of the decrease of volatile matter content with the increase of reflectance is observed in the studied coals (Fig. 3.7a). Although there is a lack of data for the high and medium volatile bituminous coals (25 – 40 wt.%, daf, volatile matter and around 1% VR_{max}), it can be seen that the content of volatile matter is decreasing by about 20 - 30 wt.% (daf) for each 1% VR_{max} increase in the range between 0.5 – 2.0% VR_{max}. A sharp bend occurs at VR_{max} between 2.0% and 2.5%. Above 2.5%, the volatile matter decreases only by 1 - 2 wt.% (daf) with each 1% VR_{max} increase (see Fig. 3.7b). The results of our study basically agrees with those of Bartenstein and Teichmüller (1974), which recognized a sharp bend of volatile matter content decrease at the anthracite stage (VR_{mean} = 2.5 - 3.0%; note: VR_{mean} has a same definition with VR_r used in this study). According to Taylor et al. (1998), volatile matter which derives predominantly from the non-aromatic fraction of coal, decreases rapidly as a result of the removal of aliphatic and alicyclic groups and the increasing aromatization of the humic complexes. Patrick and Walker (1991) found that during carbonization, the greatest weight loss occured between 380 – 550 ºC, i.e, the part of the plastic stage during which the major part of the optical anisotropy development takes place.

The reflectance values of liptinite and inertinite coalesce with those of vitrinite at 20 – 25 wt.% (daf) volatile matter, which is the transition between medium volatile bituminous and low volatile bituminous coals. The range of volatile matter content where the curve of vitrinite and liptinite reflectance merges is in agreement with results of Alpern et al. (1972). However, in contrast to the result of this study, they wrote that the values of inertinite reflectance are very high up to the meta-anthracite level and merge with the vitrinite reflectance values at less than 10 wt.% (daf) volatile matter.

A

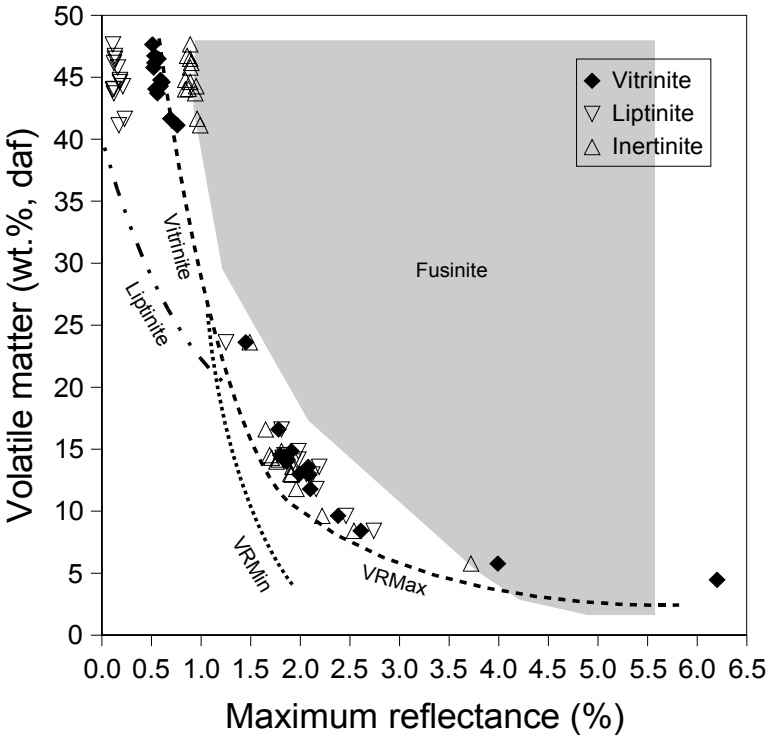

B

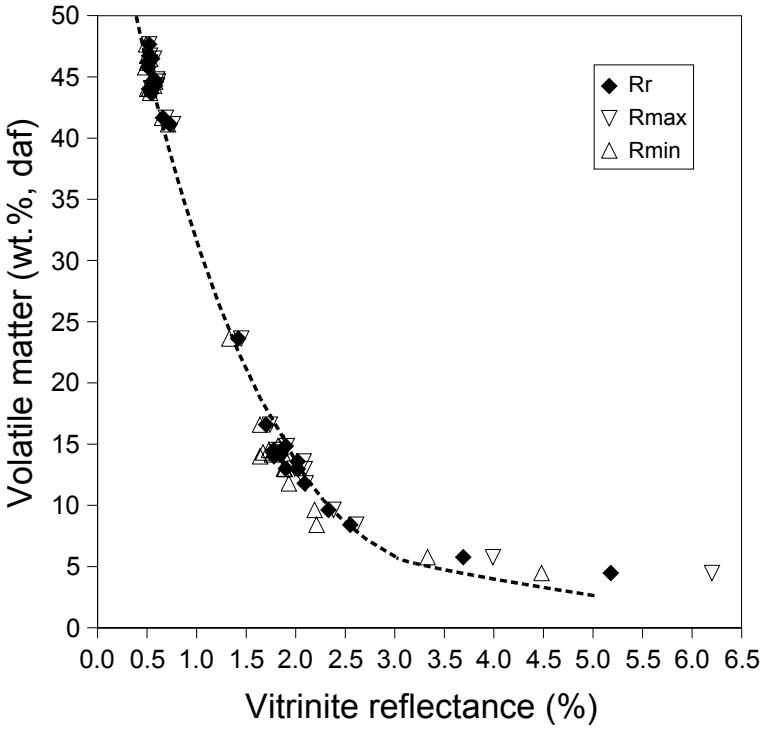

Fig. 3.7. (A) Correlation between volatile matter content and maceral reflectance of studied coals. Lines and shadowed areas display the diagenetic evolution of macerals shown in Alpern et al. (1972). (B) Relationship between volatile matter and reflectivity of vitrinite of studied coal in comparison with the trendline of volatile matter content versus mean vitrinite reflectance by Bartenstein and Teichmüller (1974) for "normally" coalified coal.

Another significant change of coal property that can be identified in the studied coals is the carbon content change. Between VR_{max} = 0.5% and 2.0%, the carbon content of the coals is ascending from around 75 wt.% to approximately 90 wt.% (daf). At the VR_{max} between 2.0% and 2.5%, the trend of ascending carbon content changes and above 2.5% VR_{max}, the carbon content ranges only between 94 wt.% and 96 wt.% (daf). A plot of carbon content versus VR_r is shown in Figure 3.8 indicating a much steeper gradient of C-increase with increasing vitrinite reflectance below 2% VR_r than above. This result agrees with earlier results which showed that with the increase of reflectance, the carbon content of coal increases very rapidly up to 90 wt.% (daf) at approximately 2.0% VR_{mean}. Above that level, there is only a minor increase of carbon content and it tends to be almost stable in the range of 90-95 wt.% (daf) carbon (Teichmüller and Teichmüller, 1979) .

It seems that the transition zone between medium volatile bituminous and low volatile bituminous coals is the range where the most severe change of optical, physical and chemical properties of coals occurs (see also Teichmüller and Teichmüller, 1979; Taylor et al., 1998 and other references therein). At 1.8 – 2.0 % VR_r, there is increased molecular orientation as the randomly small aromatic stacks found in low rank coal aggregate into bigger aromatic units (see Taylor et al., 1998; Prinz and Littke, 2005). This is possible because most of the aliphatic groups have disappeared. This process of molecular orientation is favored in material with higher hydrogen content (Taylor et al., 1998). It is possibly the reason why the reflectance of liptinite increases very rapidly and exceeds the reflectance of vitrinite at this stage, as liptinite contains more hydrogen than vitrinite (see Béhar and Vandenbrouke, 1987, Schenk et al., 1990).

In summary, the above described properties change systematically in very much the same way as described for coals which underwent normal burial diagenesis. The effect of rapid, short time heating to very high temperatures did not cause different relationships between these bulk parameters in comparison to coals which experienced gradual burial with slow and long time heating. An exception in this case, however, seems to be the bireflectance (see Section 4.2) which is less pronounced in the heat affected coals than in those which underwent normal burial and temperature histories.

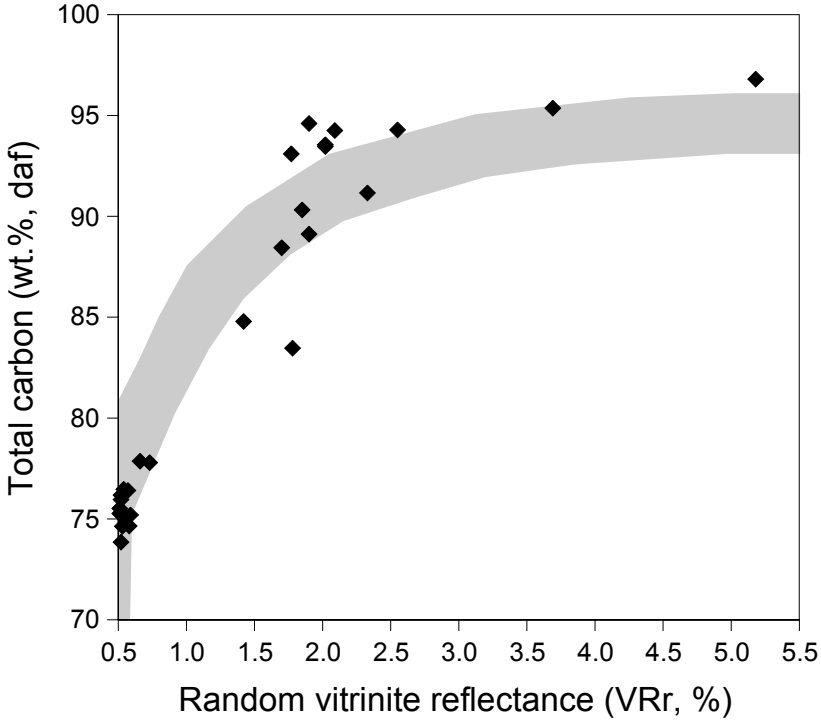

Fig. 3.8. Change of total carbon content as a result of coalification caused by the andesite intrusion. Shadowed area shows the relationship between vitrinite reflectance and carbon content by Teichmüller and Teichmüller (1979).

3.5.4 Petrographic constituents and natural coke morphology

The petrographic constituents of the studied coals from the Mangus seams are summarized in Table 3.2. The important macerals of vitrinite are collotelinite (up to 57.0 vol.%) and collodetrinite (up to 57.9 vol.%). The percentage of those gelified vitrinites is greater than that of ungelified vitrinite (telinite: max. 12.2 vol.%, vitrodetrinite: max. 13.5 vol.%). Gelovitrinite is composed predominatly by corpogelinite (2.5 – 8.5 vol.%). Gelinite composes only 0.6 – 5.4 vol.%. The common liptinite macerals are liptodetrinite, sporinite, cutinite, resinite and suberinite. Bituminite, which acts as a groundmass, can be found in some samples (up to 1.6 vol. %). In all samples, exsudatinite filling in small cracks or empty lumens is found (max. 2.8 vol.%). The least abundant maceral group is inertinite, composed mainly of fusinite, semifusinite and inertodetrinite. Funginite and other inertinite macerals are found only at less than 1 vol.%.

Samples from Suban seams (VR_{max} = 1.45 - 6.20 %) present different petrographical characteristics compared to those of the Mangus coals. In general most of the studied coals do not show sphere or mosaic microstructures which are the typical characteristics of natural coke (see Kisch and Taylor, 1966; Taylor et al., 1998; Kwiecińska and Petersen, 2004), except for the sample with the highest rank (sample 03/1113). Basically, the vitrinite group is homogenized, but the texture of some submaceral vitrinites are still recognizable. In the sense of Gray (1991), altered vitrinite can be categorized as pseudovitrinoids. The thermally altered vitrinite composes 82.4 – 93.8 vol.%.

The most obvious change observed in the thermally metamorphosed coals is the decrease of liptinite content. Almost all liptinite macerals can not be optically recognized anymore. Some residue of liptinite with very high reflectance can still be identified as meta-liptinite (Fig. 3.9a), but it comprises only 0.4 – 2.4 vol.%. In the two samples with the highest rank, no meta-liptinite was found. Inertinite (0.6 – 11.6 vol.%) usually maintains its unaltered texture and structure. The easiest inertinite macerals to be recognized are fusinite and funginite because their structures are best preserved (Fig. 3.9b). All the samples from Suban seams, including the sample with the lowest vitrinite reflectance, already show some microscopically visible pores and vesicles. These structures indicate that the rapid devolatilization process by the heat of the intrusion occurred in all the Suban samples.

As mentioned earlier, the typical microstructures of natural coke are only recognizable in the sample with the highest reflectance (VR_{max} = 6.20 %) which was taken at the contact of the coal seam with the intrusion. The coke microstructures, which mostly exhibit mosaic structure, compose only 2.4 vol.% of the microconstituents (see Table 3.3). Mosaic structures are formed as the mesophase spheres coalesce (Brooks and Taylor, 1968; Taylor et al., 1998). However, Patrick et al. (1973) stated that mosaic structures in cokes can be formed without any stage of growth and coalesence of spheres.

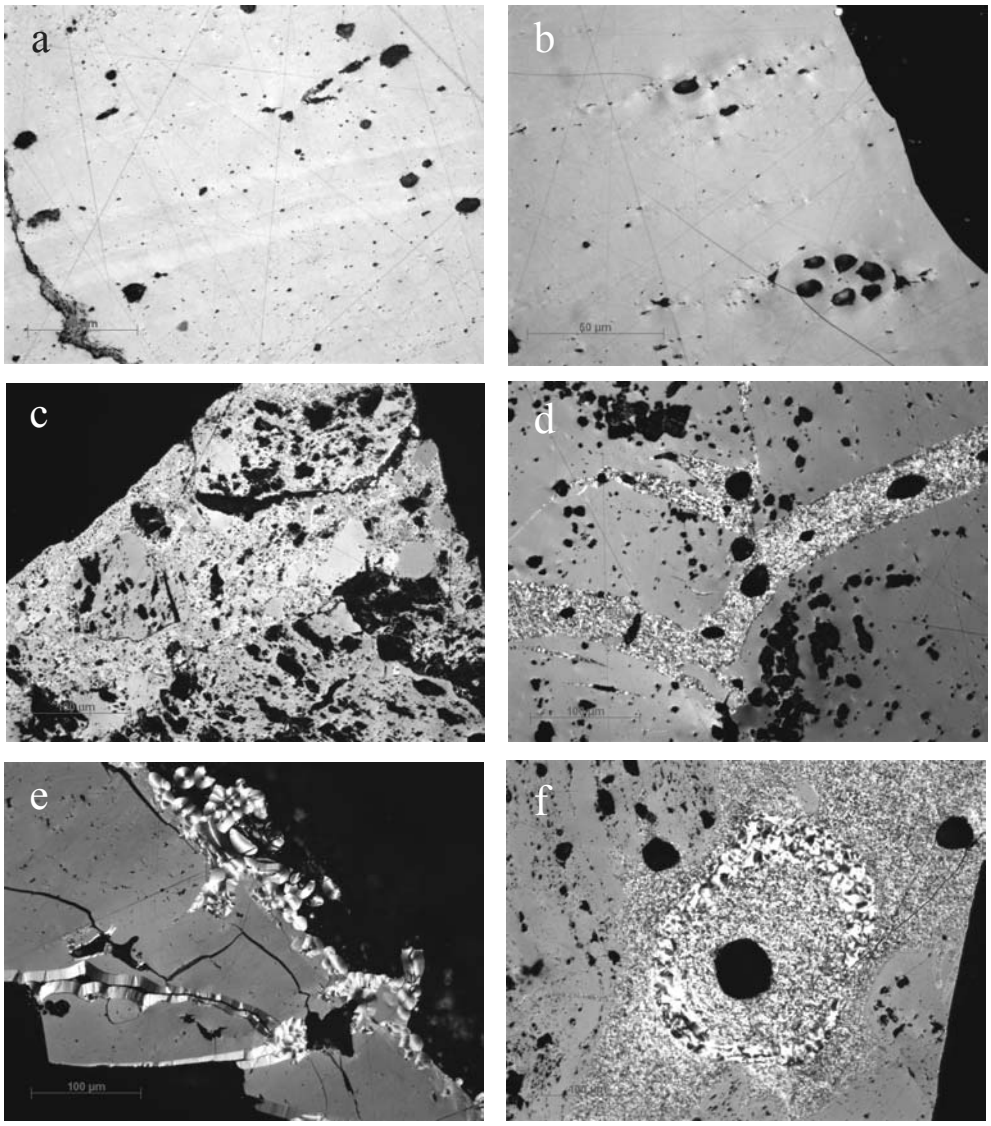

Fig. 3. 9. Photomicrographs of the thermally metamorphosed coal (under reflected light, oil immersion): (a) Meta-liptinite in coal with VR_{max}=2.61%. (b) Preserved funginite in high rank coal. (c) Mosaic structures mixed with the original constituents of coal. (d) Mosaic structures as cracks filling. (e) Spheres having circumferential structure in cracks. (f) Mosaic structures that build rings around a pore. Photos (c) to (f) were taken from the sample with the highest vitrinite reflectance (VR_{max}=6.20%).

The coke microstructures observed in the studied sample can be differentiated into two groups. The first group comprises microstructures which are mixed with the coal macerals. This structure was formed by total alteration of vitrinite or liptinite. The mosaics are usually very fine in dimension (Fig. 3.9c). The second group is composed of microstructures found in cracks of the coal (Fig. 3.9d). The dimension of each mosaic unit is usually similar to those of the first group. Besides that, spheres having

circumferential (radial) structures are also found in some cracks. This structure is one of the typical features of pyrolitic carbon. Pyrolytic carbon is deposited from the gas phase by chemical cracking of volatiles generated during the intrusion (Goodarzi and Gentzis, 1990; Taylor et al., 1998). A completely round sphere can have a diameter of about 20 microns (Fig. 3.9e).

An interesting mosaic pattern showing a continuous change of dimension surrounding a pore was observed as well (Fig. 3.9f). At the edge of the pore, the mosaic is very fine (mostly less than 3 microns in length or width). Between 40 to 80 microns from the pore edge, a ring of coarse mosaic is developed. The dimension of a mosaic is up to 20 microns in length and 10 microns in width. The mosaic becomes finer again inside the ring. Some small cracks in the vitrinite around this ring structure are filled with the fine mosaic structures. The structures were developed during the carbonization process as the growing liquid-crystal tends to flow over surfaces encountered within the carbonizing system, in this case the vesicles of gaseous volatiles (e.g. Brooks and Taylor, 1968; Marsh, 1973). This mosaic ring structure could indicate two phases of heating to different maximum temperatures, as the rate of heating and maximum temperature affect the size of anisotropic mosaic units (e.g. Marsh, 1973; Patrick et al., 1973). The coarse-grained pyrolitic carbon forms at higher temperature than the fine-grained pyrolitic carbon (Goodarzi and Gentzis, 1990).

3.5.5 Mineralogy

In the coals from Mangus seams, only minor amounts of minerals are petrographically observed (see Table 3.2). Most common are pyrite (or marcasite), which are dispersed throughout the coals. They occur as small, euhedral crystals or in framboidal concretionary form often associated with telinite. This type of pyrite is usually interpreted as syngenetic pyrite which was formed in the peat (Taylor et al., 1998). Carbonates are found in fractures or cell lumen, mostly as blocky crystals. Clay minerals are usually dispersed, but some thin clay layers occur as well. The highest content of mineral matter is present in the lowest sample from Mangus A2 seam (sample 03/1137). It should be noted that the mineral matter in this particular sample is composed mostly of carbonates (5.6 vol.%). This anomalous increase could be caused by the formation of new carbonate minerals as a result of the intrusion.

The highest content of visually observed mineral matter in Suban samples is 14.6 vol.% (see Table 3.3), the most common of which are carbonates. Like those in Mangus seams, carbonates are found in fractures or cell lumen, mostly as blocky crystals. The sample with the highest carbonate content (4.8 vol.%) is the sample which is situated directly at the intrusion. The carbonate content tends to decrease with the increase of distance from the intrusion. Clay minerals are found up to 9.6 vol. %. Pyrite and marcasite, which are dispersed throughout the coals, constitute only 0.2 – 1 vol.% of the coals. In some samples, quartz is observed but only in trace amount.

From EDX analysis, some details about mineral composition can be determined. The carbonate minerals in the studied coals are mostly calcite, but some dolomite is recognized as well. Calcite is deposited mostly in cracks and fissures and is usually a late-stage formation (Taylor et al., 1998). Dolomite can be derived from hydrothermal metasomatism initiated by magmatic activity (Deer et al., 1992). The iron disulfide minerals found in the examined samples are not only pyrite or marcasite. One sample has, in addition, a Cu-bearing iron disulfide, probably chalcopyrite. It is possible that chalcopyrite was formed during the intrusion by magmatic sulfide solutions (Deer et al., 1992). Figure 3.10 shows some identified minerals.

Only few minerals were identified by XRD, since almost all of them occur at low concentration. Figure 3.11 displays the X-ray diffractograms of two selected samples, representing the low rank (VR_{max} = 0.76%) and high rank coals (VR_{max} = 6.2%). Under XRD, the most prominent mineral identified is quartz, which can be found in both low and high rank coals. The peak at 3.34 Å and also weaker reflection at 4.26 Å spacing are characteristic for quartz. The other identified minerals are clay minerals. In the low rank coals, the identified clay mineral is kaolinite whereas it is illite and rectorite in high rank coal. Kaolinite is recognized by the intense reflections at ~7.1 Å and ~3.57 Å. In general, the illite minerals yield strong reflections at ~10Å, which can be seen in the diffractogram of the highly metamorphosed coal. From the XRD data, it seems that illite occurs as illite-1M polytype. The other clay mineral identified, rectorite, is a mixed-layered clay mineral that consists of dioctahedral mica and smectite (Wilson, 1987; Moore and Reynolds, 1997). The typical reflection of rectorite is found at 25Å and ~13.3 Å. It should be noted that an organic hump occurs as well. This hump is usually found in the area between 15º – 33º 2θ (Mandile and Hutton, 1995). As also

documented by other authors, the high rank humic coal produces a broader organic hump than low rank coal

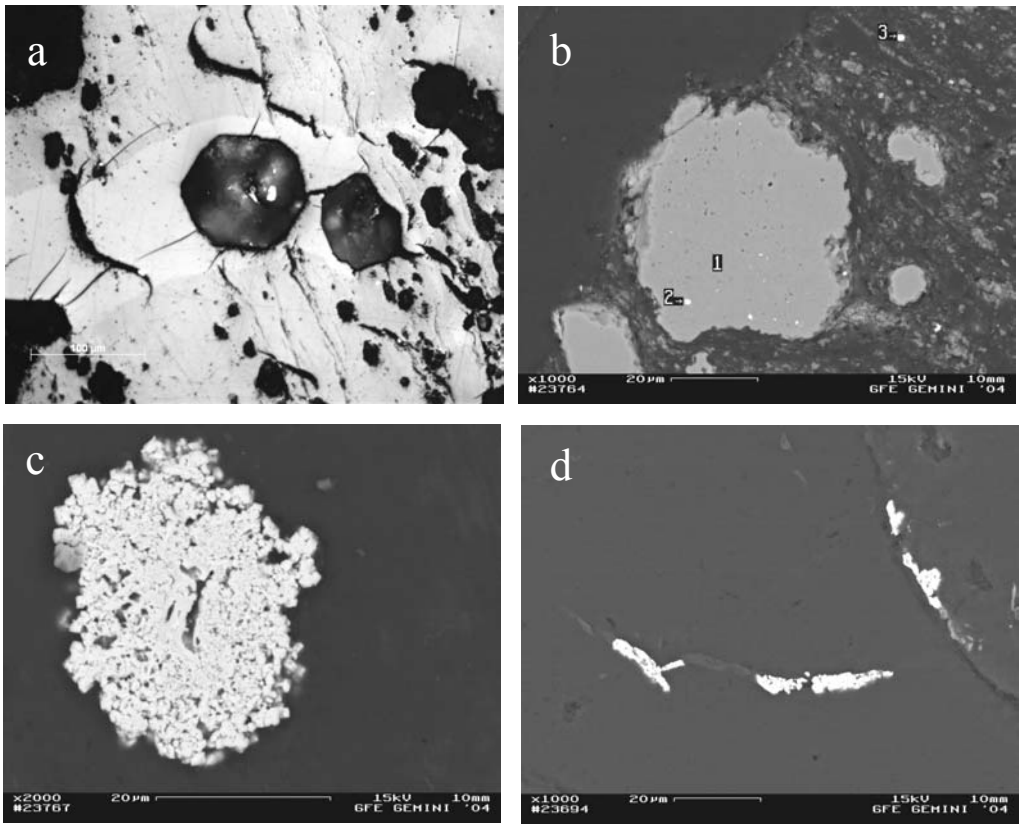

.

Fig. 3.10. Photomicrographs of some minerals found in studied high rank coals: (a) Carbonate mineral as pore filling. (b) Quartz *(1)* and chalcopyrite which fill vesicles in quartz *(2)* and as individual particle in the groundmass *(3)*. (c) Framboidal concretion of pyrite. (d) Pyrite as crack filling. Photo (a) was taken under reflected light in oil immersion. Photos (b) to (d) were taken under SEM, backscaterred electron mode.

3.5.6 Functional group distribution and its changes with rank

Figure 3.12 shows the FTIR spectra of the selected studied coals. The broad bands in the 3600 – 3100 cm^{-1} range indicate the occurrence of hydroxyl (OH) groups. The relative amount of hydroxyl groups in the low rank coal tends to be much higher than in the high rank coals. Those broad bands are thought to be related also to water which is still bound in the coal itself. This water content decreases with rank (Painter et al., 1981b).

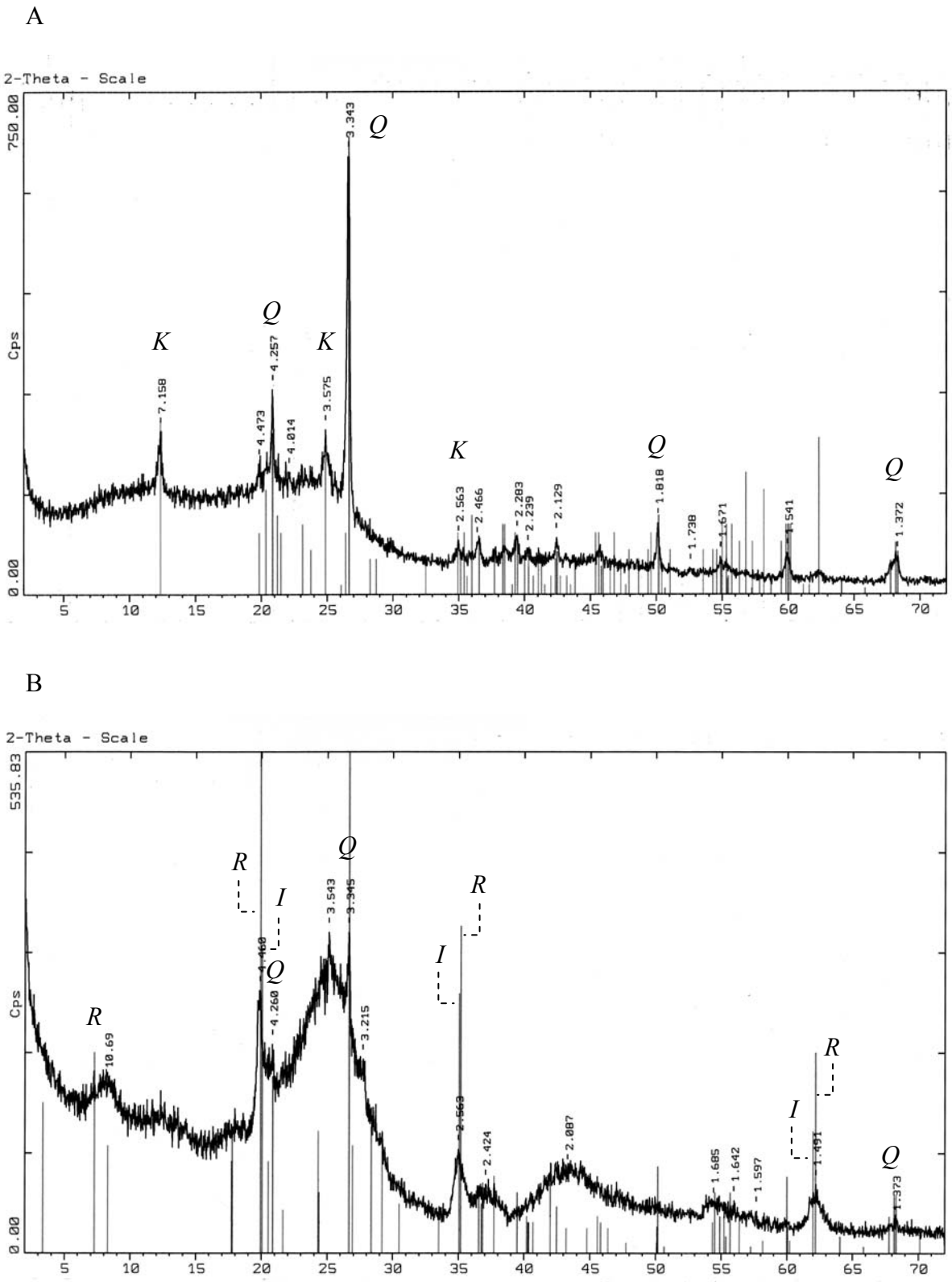

Fig. 3.11. X-ray diffractogram of (A) low rank coal (VR_{max} = 0.76%) and (B) high rank coal (VR_{max}=6.20%). Q = quartz, K = kaolinite, I = illite, R = rectorite.

A distinct aromatic C-H signal in the aromatic stretching region (3000 – 3100 cm^{-1}) is clearly recognizable in the subbituminous and bituminous coals. However, by semi-anthracite rank and beyond, it begins to be reduced in intensity and is only marginally detectable, as also shown by other studies (e.g. Ibarra et al., 1996; Radlinski et al., 2004). Prominent aliphatic C-H stretch is revealed in the 3000 – 2700 cm^{-1} zone. Two peaks at around 2900 cm^{-1} and 2850 cm^{-1} which are both related to CH_2 and to a lesser extent CH_3, are dominant. There is a progressive decrease in the aliphatic hydrogen content of the coal as the rank increases from high volatile bituminous to meta anthracite. In the aliphatic C-H bend region (1450 cm^{-1}), the absorbances are also the highest in low rank coals and decrease with rank. The distribution of out-of-plane aromatic C-H in the 900 – 700 cm^{-1} range is also modified during maturation. Its absorbance increases with rank. This result indicates that aromaticity increases with rank, which agrees with many previous works (e.g. Kuehn et al., 1982; Mastalerz and Bustin, 1993; Ibarra et al., 1996; Radlinski et al., 2004).

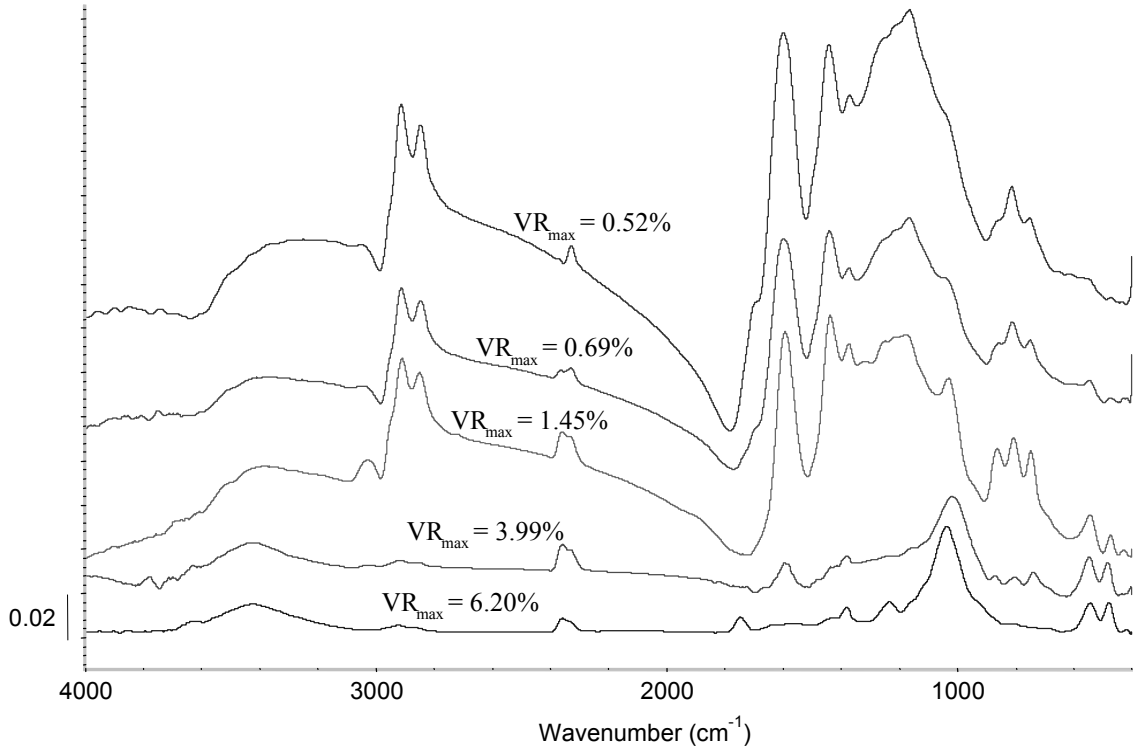

Fig. 3.12. FTIR spectra of studied coals varying in rank.

From low rank to high rank coals there is a decrease in the intensity of the ~1600 cm^{-1} band, which is assigned to an aromatic ring (C=C) stretch. This band is very intense in the low rank coals but relatively weak in the high rank coals, which are supposed to contain more aromatic material. This phenomenon has been discussed by Painter et al. (1981b). They concluded that the absorbance is enhanced by the presence of phenolic groups or may be the result of a linkage of aromatic entities by methylene and possibly ether bridges. In low rank coal, there is also an adsorption near 1580 cm^{-1} due to COO^{-} groups. The occurrence of the carbonyl or carboxyl groups at around 1650 cm^{-1} should be noted as well. The decrease of absorbance in the 1600 cm^{-1} band is probably a consequence of the loss of phenolic O-H with rank as also observed by Vasallo et al. (1991) than by the change of aromatic ring content.

Beside the changes mentioned above, significant changes of the other oxygen containing functional groups can be observed in general in the 1800 – 1100 cm^{-1} zone. The C-O-R structures visible in the 1100 cm^{-1} range are also modified during coalification. Basically they tend to decrease with increasing coalification. However, comparison of absorbance bands in the 1000 – 1300 cm^{-1} zone is difficult because the absorbance is a composite of organic C-O groups and mineral matter (Mastalerz and Bustin, 1993). In the anthracite and meta-anthracite coals, noticeable absorbances are detected in the 1800 – 1700 cm^{-1}, ~ 1400 cm^{-1}, 1300 – 1200 cm^{-1} , 1100 – 1000 cm^{-1} and below 600 cm^{-1} ranges. It seems that mineral matter, mainly clay minerals and quartz, are responsible for producing this absorbance (see Painter et al., 1981a; Rochdi and Landais, 1991). The microscopic and XRD analysis results also indicate the occurrence of quartz and clay minerals (illite and kaolinite) in the studied samples.

Many methods have been proposed to quantify the aromaticity of coal based on FTIR spectra (e.g. Kuehn et al., 1982; Riesser et al., 1984; Schenk et al., 1990; Cagniant et al., 1991). To assess the aromaticity of the studied coals, the ratio of the aromatic CH stretching area (3100 - 2990 cm^{-1}) to aliphatic CH streching area (2990 – 2700 cm^{-1}) was calculated and compared to selected coalification parameters (Fig. 3.13). Both bands were selected since the organic matter spectra with lower wave number (most of all <1500 cm^{-1}) could be strongly masked by mineral matter spectra bands since the samples were taken as ply samples. The result shows that the aromaticity parameter is also increasing with increasing coalification, except at the meta-anthracite stage, where

the aromaticity parameter is very low since the CH spectra bands almost disappear. Van Vucht et al. (1955; see also van Krevelen, 1993) observed that the aromatic and aliphatic CH absorption bands disappear at the anthracite stage (> 94% carbon content) because of increasing electronic absorption which also points to a transition into a graphitic structure. From above discussion, it seems that the quantification of coal aromaticity based on FTIR analysis is only applicable for coals which have not reached anthracite rank, as also observed in this study.

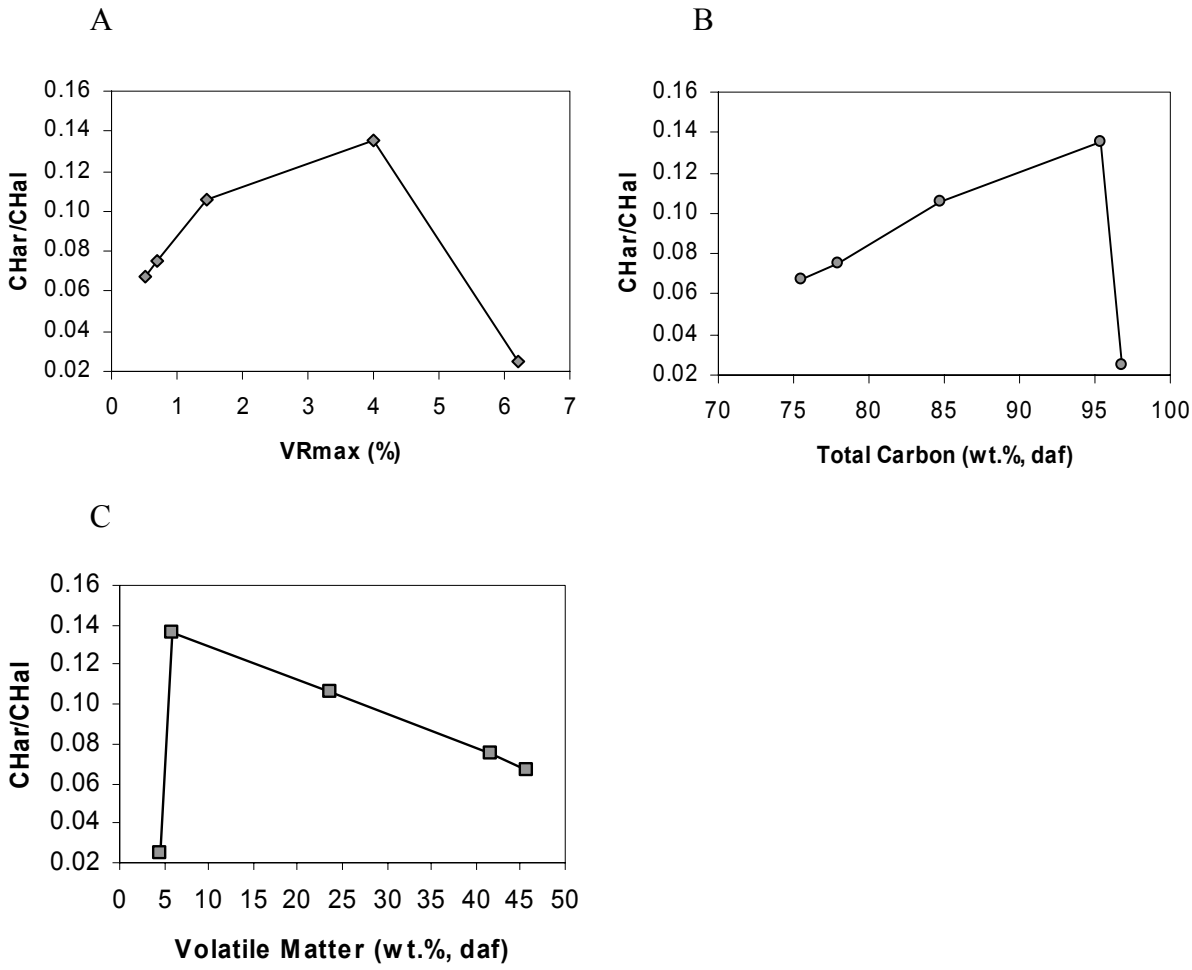

Fig. 3.13. Change of the ratio of aromatic CH (CH_{ar}) to aliphatic CH (CH_{al}) with increasing coalification indicated by (A) VR_{max}, (B) total carbon content and (C) volatile matter content.

3.5.7 Rock-Eval parameters

Results of the total organic carbon (TOC) and Rock-Eval pyrolysis measurements on selected coals are presented in Table 3.4. The plot of OI versus HI of the studied coals is illustrated in Figure 3.14a. Samples from the Mangus seams and Suban seams show a different response to Rock-Eval pyrolysis. Basically, the OI of all studied coals is low (less than 5 mg CO_2/g TOC). The distinction between both groups of coals is apparent in their respective HI values. The Mangus coals are characterized by HI values of around 300 mg HC/g TOC, whereas the Suban seam coals possess lower HI values (< 130 mg HC/g TOC).

By plotting the T_{max} against HI as proposed by Espitalié et al. (1985a), the two groups of coal plot in fields of different maturity (Fig. 3.14b). The Mangus coals plot in the immature and early mature ranges since their T_{max} values vary between 420 and 440 °C. In contrast, Suban coals have very high T_{max} values (475 - 551°C) and plot in the postmature field. It should be noted that the coal samples 03/1113 and 03/1146, which have more than 95 wt.% (daf) total carbon, are not included because their S2 peaks were beyond the detection limit of the equipment.

As depicted in both diagrams, the studied Mangus and Suban coals are located at the conjugation line of the coalification paths of kerogen type I, II and III. Humic coal is usually expected to fall into the kerogen type III. However, coal can also plot between type II and III kerogens because coal generally does not respond in the same way as dispersed type III organic matter (see Espitalié et al., 1985b; Peters, 1986; Littke et al., 1989). The Rock-Eval pyrolysis study on coals from various basins by Katz et al. (1991) showed that most of the coals fall between type II and III kerogens including the Muara Enim coals from South Sumatra Basin.

Table 3.4. Rock-Eval pyrolysis results of selected coals from Mangus and Suban seams

Seam	Sample No.	TOC (wt.%)	Tmax (°C)	S1 (mg HC/g coal)	S2 (mg HC/g coal)	S3 (mg CO_2/g coal)	Oxygen Index (mg CO_2/g TOC)	Hydrogen Index (mg HC/g TOC)
Mangus A1	03/1125	64.5	426	2.88	186.90	3.14	4.87	289.86
Mangus A1	03/1126	67.7	422	4.41	197.34	2.18	3.22	291.45
Mangus A1	03/1127	68.6	423	5.00	218.61	2.77	4.04	318.86
Mangus A1	03/1129	67.5	426	3.33	173.54	2.91	4.31	257.29
Mangus A1	03/1131	67.4	430	7.59	213.92	3.13	4.64	317.39
Mangus A2	03/1133	70.4	433	5.17	223.14	2.63	3.74	317.19
Mangus A2	03/1134	70.2	433	4.92	236.21	2.58	3.68	336.72
Mangus A2	03/1136	73.1	437	4.50	218.80	3.40	4.79	308.47
Mangus A2	03/1137	63.1	437	4.50	173.82	1.86	2.95	275.55
Suban B1	03/1139	79.5	524	1.30	40.00	0.62	0.82	52.98
Suban B1	03/1140	76.8	524	1.32	35.39	0.49	0.64	46.07
Suban B1	03/1142	80.4	525	0.95	32.07	0.55	0.71	41.43
Suban B1	03/1143	78.9	530	1.71	27.15	0.58	0.76	35.78
Suban B2	03/1144	81.2	551	1.02	15.14	1.12	1.38	18.65
Suban B2	03/1145	79.8	550	1.42	9.69	1.07	1.34	12.14
Suban B2	03/1117	81.8	509	2.37	49.12	1.34	1.64	60.04
Suban B2	03/1120	75.4	504	3.03	52.48	1.09	1.45	69.57
Suban B2	03/1121	81.7	494	4.09	68.18	1.46	1.79	83.49
Suban B2	03/1123	80.2	476	7.47	101.18	1.23	1.53	126.11

Note: Very low OI value of coal also had been documented by other studies (for example see Espitalié et al., 1985b; Bostick and Daws, 1994).

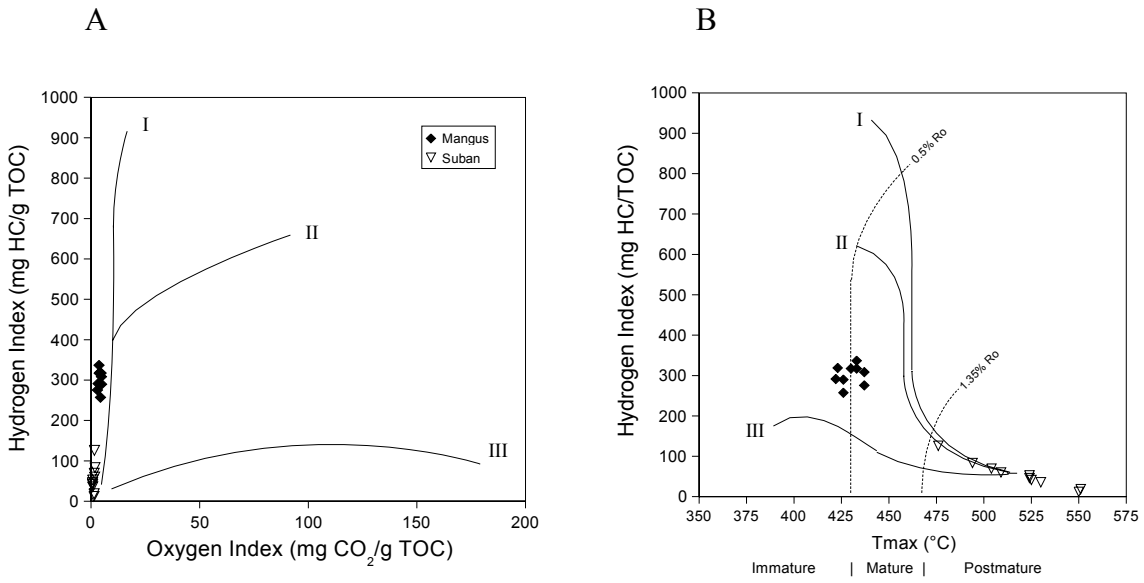

Fig.3.14. Plot of (A) Oxygen Index versus Hydrogen Index and (B) T_{max} versus Hydrogen Index of the studied coals.

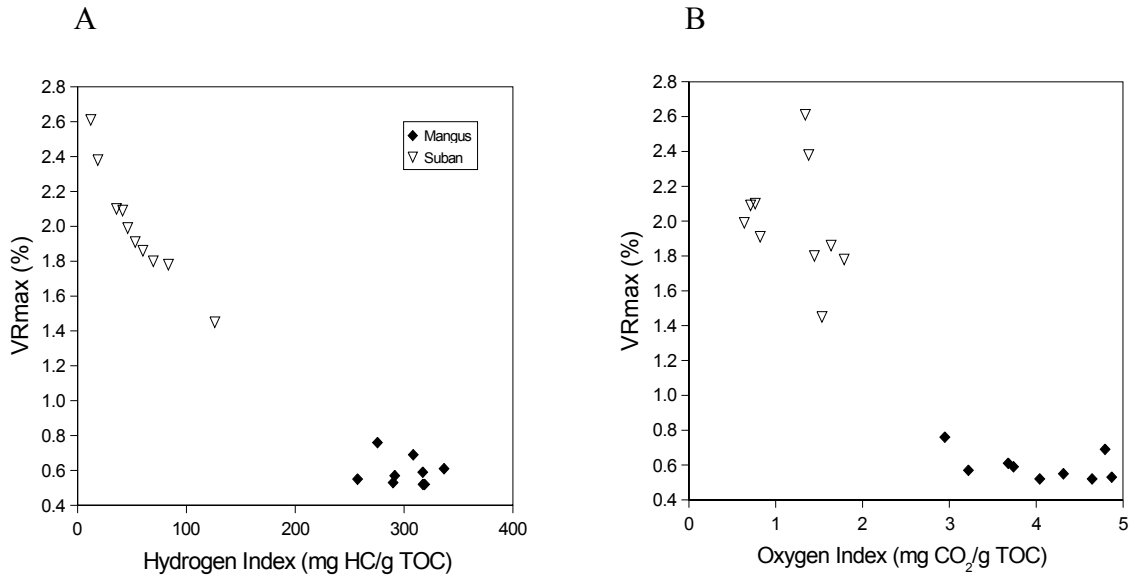

Fig.3.15. Diagrams showing the change of (A) HI and (B) OI with maturity indicated by VR_{max}.

To assess the changes of HI and OI with maturity, both parameters were plotted against VR_{max} (Figs 3.15a-b). In general, the HI of the coals are decreasing with the increase of vitrinite reflectance, although there is a broad scatter of HI in the low rank coals. The same pattern is observed in the OI – VR_{max} correlation, but contrary to the HI, a slightly broader scatter of OI is visible in the high rank coals. This result seems to support the

fact that loss of oxygen is characteristic for the coalification of low rank coal, whereas loss of hydrogen becomes relatively more important for higher rank coal (Teichmüller and Teichmüller, 1979; Teichmüller and Durand, 1983; Taylor et al., 1998; Prinz et al., 2004).

The fact that T_{max} varies with thermal evolution of coal can also be seen in the plot of T_{max} against vitrinite reflectance, total carbon content and volatile matter (see Figs 3.16a-c). In this study, a clear correlation can be recognized between those coal maturity parameters and T_{max}. This result corresponds very well with the results of other studies (see for example Teichmüller and Durand, 1983; Bostick and Daws, 1994). However, at maturity levels above 1.2% VR_r T_{max} values are higher by 10 – 20°C than predicted by Teichmüller and Durand (1983). Whether this is an effect of rapid heating remains to be studied in future.

3.5.8 Metamorphism temperature during the intrusion

Artificial coalification by a carbonization experiment has been widely used to estimate the temperature of contact metamorphism of various coals (see for example Goodarzi and Gentzis, 1990; Kwiecińska et al., 1992). A well known study of evaluating temperature of carbonized or thermally metamorphosed coals using vitrinite reflectance was done by Chandra (1963, 1965). The method is valid for carbonized or thermally metamorphosed coals at low pressure. The application to the studied Tanjung Enim coals seems appropriate, since the precursor coals have not been subjected to advanced pressure in nature. The evaluation is based on the relation of maximum and minimum reflectance and presumed that the precursor coals are at low rank stage (even lower than the lowest value measured from coal here). If the reflectance values are plotted in Chandra`s diagram, it can be deduced that the coal directly at the intrusion was subjected to a temperature of around 700ºC.

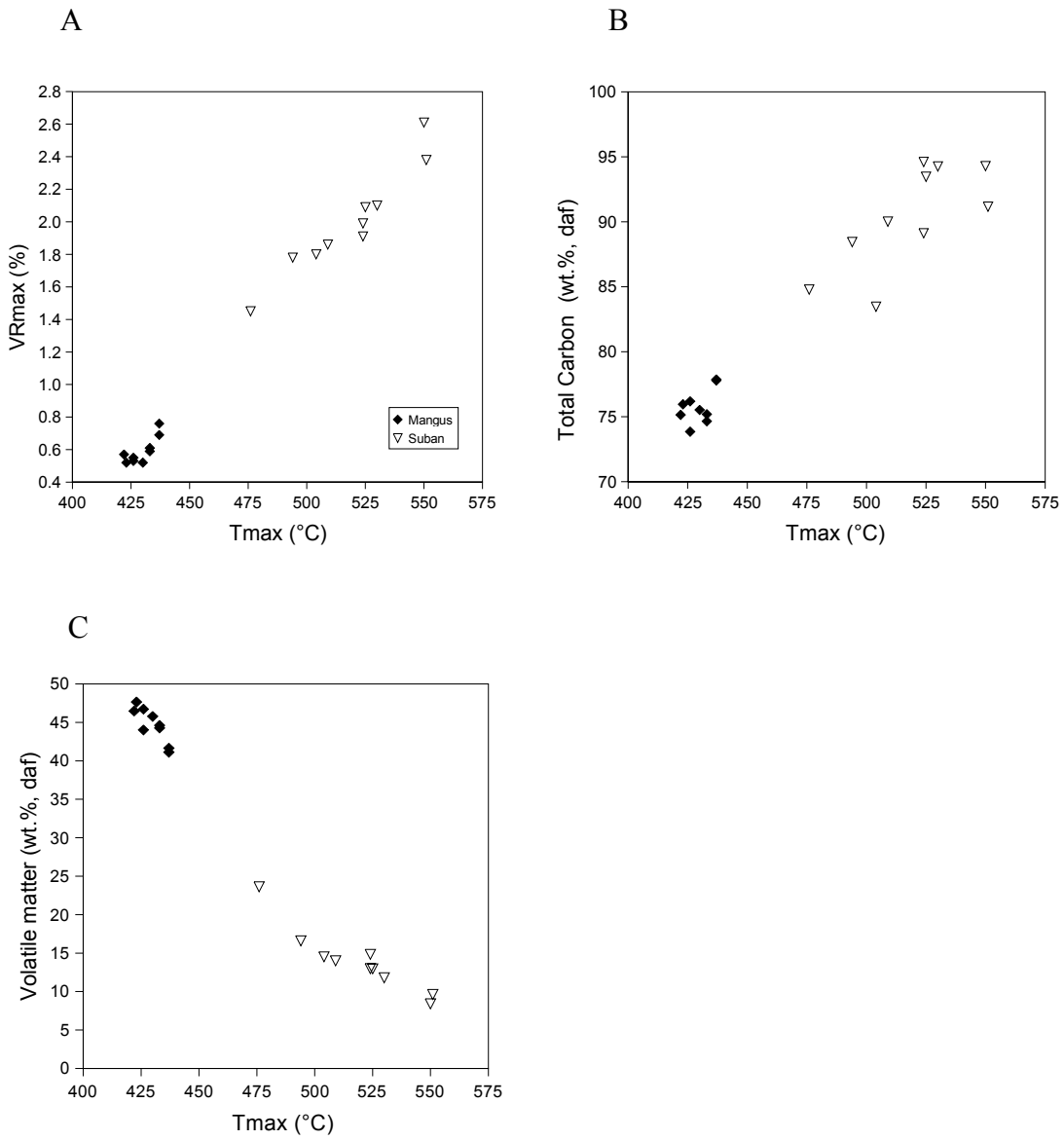

Fig.3.16. The variation of T_{max} with thermal evolution of studied coals indicated by (A) VR_{max} , (B) total carbon content and (C) volatile matter content.

A similar method of comparing coal properties and carbonization temperature has been applied by Goordazi and Murchinson (1972) and Patrick and Walker (1991). According to their studies, the reflectance of vitrinite increases very rapidly at carbonization temperatures greater than 400ºC. The lowest carbon content of precursor coals used by those authors is around 82 wt.%. The trend lines published in those studies suggest that coals with lower carbon content would show a similar reaction when subjected to carbonization as the 82 wt.% carbon-coal. Maximum vitrinite reflectance of around 6% (as shown by the most thermally metamorphosed coal in Tanjung Enim) would be

reached if the coal is carbonized at approximately 750ºC (Goordazi and Murchinson, 1972). Patrick and Walker (1991) found that a lower temperature (approximately 700ºC) is needed to reach that value of VR_{max}. The measured bireflectance of around 1.5% would only occur at a temperature of around 800ºC.

According to the models proposed by the above authors, coals from the Mangus seams probably have not experienced temperatures above 400ºC, since their reflectances are low. Iskandar (1994) also found that based on the clay mineral analysis, there is an extreme temperature decrease from approximately 1000ºC at the intrusion's contact to less than 560ºC within a distance of only 4 m. Mangus seams and the accompanying sedimentary strata were probably not directly affected by heating from the andesite intrusion, but they may have been coalified by hydrothermal metamorphism. Hydrothermal fluid is known to have an important role on coal metamorphism (see for example Hower and Gayer, 2002). In our study, hydrothermal fluids may have transferred heat from the intrusion to the surrounding rock. The compelling evidence of this process is the formation of new minerals, which are thought to have been introduced by hydrothermal activity (see Section 4.5). Using the algorithm suggested by Baker and Pawlewicz (1994), a random vitrinite reflectance of 0.73% (highest VR_r value of coals from Mangus seams) indicates a peak temperature of only 112ºC for these coals.

3.6 Conclusions

The andesitic intrusion close to the Tertiary coal seams in Tanjung Enim area in South Sumatra Basin, Indonesia has caused some significant changes of petrographic and chemical coal properties. The rank of the coals increases from sub-bituminous and high volatile bituminous to medium - low volatile bituminous and even anthracite and meta-anthracite.

The intrusion has also caused the formation of some new minerals, particularly in the coals which are highly metamorphosed. This mineralization is indicated by high mineral matter and ash contents. Beside that the hydrothermal solution produced by the intrusion probably caused precipitation of new minerals i.e. dolomite and chalcopyrite. There are also differences in clay mineralogy among the samples studied.

The coalification path of maceral groups can be described from their reflectance change during coalification. No liptinite or inertinite coalification jump can be recognized, since the reflectance increases progressively. Interestingly, the bireflectance is less pronounced in the most metamorphosed anthracites than what is found in naturally coalified anthracites.

A good correlation between maceral reflectance and volatile matter content can be deduced. A significant decrease of volatile matter occurs in the range < 2.0% VR_{max}. Above 2.5% VR_{max}, the volatile matter content decreases only very slightly. The carbon content correlates to vitrinite reflectance positively. Between 0.5 - 2.0% VR_r, there is a strong increase of carbon content. Above 2.5% VR_r, the carbon content increases only slightly. The transition zone between medium volatile bituminous and low volatile bituminous coals is the range where optical, physical and chemical properties of coals change strongly. This change is recorded in the abundance of functional groups. As the rank of coal increases, there is a decrease of hydroxyl groups and aromatic ring (C=C) stretch and also an increase of aromatic C-H absorbances. Based on the Rock-Eval pyrolysis data, the studied coals are characterized by a low OI. The high rank coals have a lower HI than the low rank coals.

Vitrinite is the major maceral in the low rank coal samples in this study. In the high rank coal samples, vitrinite has been thermally altered. Mosaic structures can only be recognized in the coal which is most affected by the intrusion, and it occurs as groundmass or as crack fillings. It seems that the coals were subjected to at least two cycles of heating, as indicated by the size of anisotropic units.

Based on the coal characteristics, a maximum temperature of contact metamorphism of 700 - 750ºC has been calculated for the coals directly adjacent to the intrusion. However, the temperatures decreased strongly at a distance of just a few meters from the intrusion.

Chapter 4 Organic geochemistry of Lower Suban coal seam, South Sumatra Basin, Indonesia: paleoecological and thermal metamorphism implications

4.1 Abstract

Extracted hydrocarbons of the Tertiary age coals from Lower Suban seam, South Sumatra Basin, Indonesia have been investigated by GC and GC/MS. Low rank (vitrinite-huminite reflectance ~0.41-0.45%) coals from the Tambang Air Laya mine represent different maceral assemblages of an ideal succession of ombrogenous paleo-peat development in a vertical section. High rank coals (vitrinite reflectance ~1.42 to 5.18%) from the Suban mine are thermally metamorphosed by an andesitic intrusion.

Variations in the distributions of *n*-alkanes, isoprenoids, and saturated and aromatic biomarkers in extracts of the low rank coals reflect variations in local source input and paleomire conditions. Terpenoid biomarkers, such as cadinane- and eudesmane-type sesquiterpenoids and oleanane- and ursane-type triterpenoids, indicate the predominance of angiosperm plants in the paleomire, particularly *Dipterocarpaceae*. The distribution of hopanoids is affected by the organic facies of the coal and their maturity, and correlates with the paleomire evolution as derived from petrological studies.

Close to the igneous intrusion, rapid thermal stress has destroyed most of the biomarkers, but variations in n-alkane distributions, attributable to paleomire conditions, remain. Reversals in the trends of molecular parameters based on aliphatic hydrocarbons (*n*-alkane distribution and pristane/phytane ratio) and aromatic hydrocarbons (methylphenanthrene) with coal rank are observed.

Key words: coal, maceral, biomarker, paleoecology, vitrinite reflectance, thermal metamorphism, South Sumatra Basin, Indonesia

4.2 Introduction

The dynamics of depositional environments and the coalification process have been studied by many physical and chemical methods. Petrographic analysis is widely applied and gives very useful insight into depositional environments of coals (e.g. Diessel, 1992; Calder et al., 1991 and others). However, collaborative study with paleobotany and organic geochemistry is needed to elucidate fully the origin of coal (Teichmüller, 1989). A wide variety of organic geochemical indicators reflect paleoenvironmental and paleoecological conditions (see for example Tissot and Welte, 1984; Peters and Moldowan, 1993; Hunt, 1996). Biological marker (biomarker) analysis can provide clues about environmental conditions and botanical and bacterial input in the paleomire and has been applied to many coal deposits from different areas and ages and also to recent peat deposits that may act as analogues for ancient coal-forming mires (e.g. Dehmer, 1993, 1995; Jiamo et al., 1990; Bechtel et al., 2003, and many others).

This study deals with the organic geochemical characterization of the Tertiary Lower Suban coal seam in the South Sumatra Basin, Indonesia, which is one of the important oil and coal producing sedimentary basins in Indonesia. Some studies characterized the coal from this basin in detail (Daulay and Cook, 1988; Anggayana, 1996; Daulay et al., 2000; Pujobroto, 2000; Pujobroto and Hutton, 2000; Nas and Pujobroto, 2000). The purpose of this study is to compare the molecular characteristics of the studied coal with petrographical data described in detail in Amijaya and Littke (2005) and to deduce information of paleoecological conditions.

Another important aspect is that thermal alteration affects the molecular composition of coal (e.g. Hayatsu et al., 1978; Radke et al., 1982; Dzou et al., 1995). The heating of organic-rich sediments is not always caused by regional basin subsidence, but can also be initiated by igneous activity. The effect of igneous activity on the molecular composition of different types of organic matter has become the subject of many studies (e.g. Raymond and Murchison, 1992; Farrimond et al., 1999; Meyers and Simoneit, 1999). In this study, we examine the effects of andesitic intrusions on Lower Tertiary coals from the South Sumatra Basin.

4.3 Geological background

Lower Suban coal seam is a part of the lower MPa (Middle Palembang 'a'), member of the Late Miocene–Early Pliocene Muara Enim Formation (MEF) in the South Sumatra Basin, Indonesia (Fig. 4.1), a back-arc basin formed during the pre-Tertiary and early Tertiary (de Coster, 1974; Daly et al., 1987). Boyd and Peacock (1986) described that MEF was deposited as a part of a humid tropical deltaic system. The detailed aspects of tectonic history and stratigraphy of this basin are given in Adiwidjaja and de Coster (1973), de Coster (1974), Gafoer and Purbohadiwidjoyo (1986), Daly et al. (1987) and Darman and Sidi (2000).

The economically valuable coal seams (Mangus, Suban and Petai) crop out mostly in the Tanjung Enim area. The Suban seam splits into two: the Upper Suban (also known as Suban B1) and the Lower Suban (Suban B2) seams. The thickness of the Lower Suban seam varies between 2 and 3 m. In this area, the coal-bearing strata were subjected to invasion by plug-like masses of basaltic andesite (Iskandar, 1994) that are presumed to be of Pleistocene to early Quaternary age (Gafoer and Purbohadiwidjoyo, 1986; Darman and Sidi, 2000). The intrusions caused local thermal metamorphism of the strata and increased the rank of the coals from lignite through to anthracite in some areas.

4.4 Samples and Methods

4.4.1 Samples

Coal samples from the Lower Suban seam were collected from two active surface mines, Tambang Air Laya (TAL) and Suban (SUB), situated in the Tanjung Enim area (Fig. 4.1). Random vitrinite (huminite) reflectance (VR_r) of coal samples from TAL range between 0.41% and 0.45% that are characteristic of low rank coal (in this case lignite) and have no signs of extreme heating from the intrusion. In contrast, thermally metamorphosed coals from SUB show high random vitrinite reflectance values (VR_r) up to 5.18%.

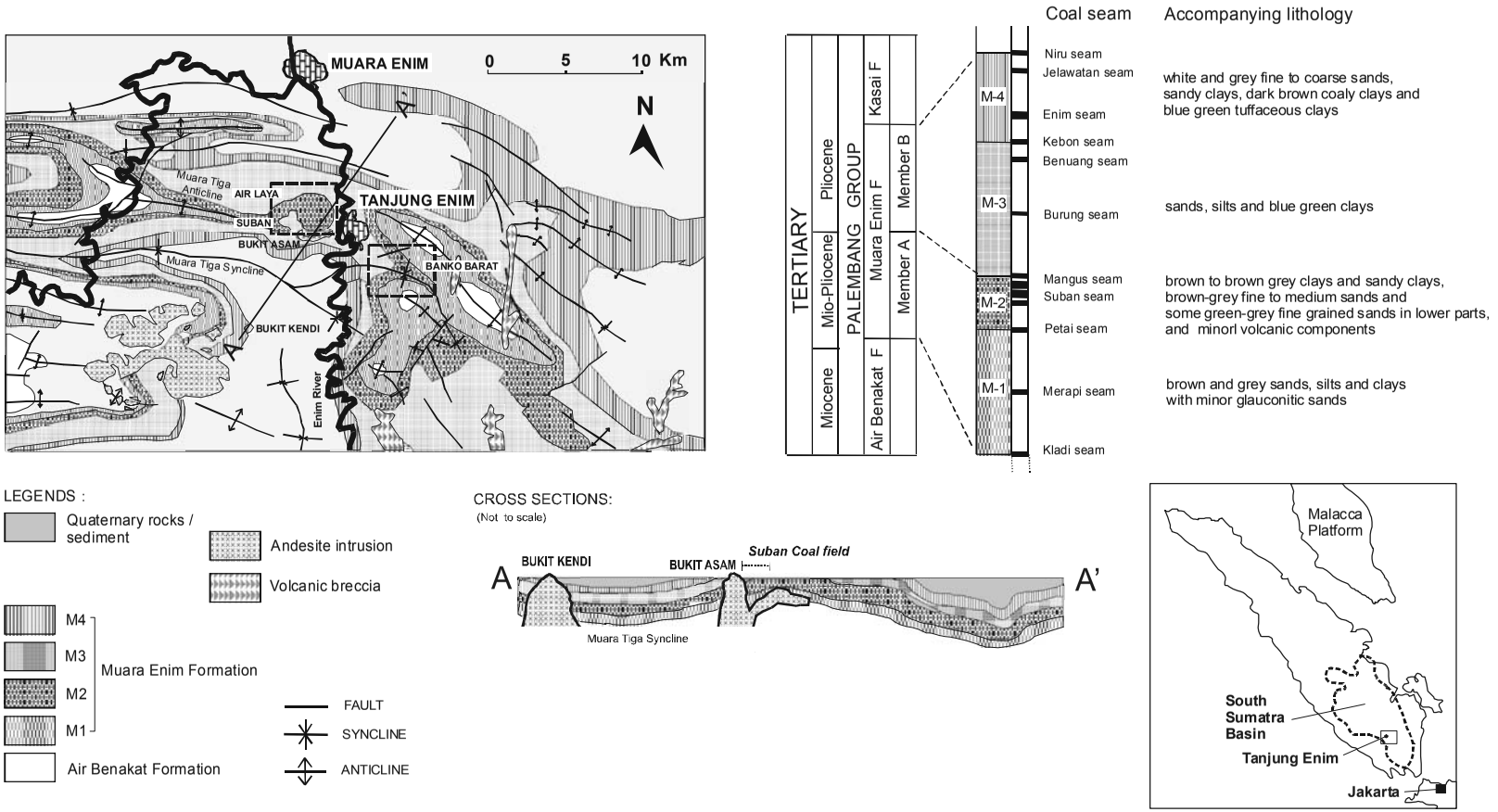

Fig. 4.1. Geological map and general stratigraphy of Tanjung Enim area (modified from Bamco, 1983 and Gafoer et al., 1986). Broken rectangles show the location of the main coal fields. The position of Tanjung Enim in South Sumatra Basin is displayed on the inserted location map.

Four selected samples of Lower Suban seam from TAL were examined. These samples contain different maceral assemblages representing an ideal vertical succession of ombrogenous paleo-peat development. From base to top, the coal seam is composed of humodetrinite-liptinite rich coal, overlain by humotelinite-rich and humocollinite-rich coal, and finally humodetrinite-rich coal (Amijaya and Littke, 2005). The petrographical composition of the low rank coals from TAL are presented in Table 4.1.

Four samples of varying rank were taken from SUB. These coals were thermally metamorphosed as the Lower Suban seam was penetrated by the andesitic sill. One sample was taken directly at the contact to the sill. Two samples were sampled 1.5 m and 2.5 m above the sill. One sample was collected at a distance of approximately 100 m in a horizontal direction from the intrusion outcrop along the strike. The composition of the thermal metamorphosed coal is dominated by homogenized vitrinite, although the texture of some vitrinite is still recognizable. Liptinite macerals are largely absent. Inertinite usually presents an unaltered structure, although it is difficult to recognize in the coal with high vitrinite reflectance. Typical microstructure of natural coke (mosaic structure) is recognizable in the sample with the highest reflectance. Table 4. 2 shows the petrographical characteristics of the high rank coals.

Table 4.1. Petrographical data of the studied low rank coals from Lower Suban seam at Tambang Air Laya (TAL)

Sample No.	VRr (%)	Huminite (vol.%)	Liptinite (vol.%)	Inertinite (vol.%)	Mineral matter (vol.%)	Maceral assemblages*
02/767	0.45	78.6	18.6	2.3	1.0	Humodetrinite-rich
02/769	0.42	73.7	23.2	2.8	0.4	Humocollinite-rich
02/771	0.44	85.9	11.6	1.6	1.0	Humotelinite-rich
02/773	0.41	34.7	50.8	13.6	1.6	Humodetrinite-liptinite-rich

Note: samples are listed from top to the base of the seam
* detail description in Amijaya and Littke (2005)

4.4.2 Gas chromatography and gas chromatography/mass spectrometry

Prior to organic geochemical analysis, coal powders (approximately 10 gram for each sample) were extracted in a Soxhlet apparatus for 24 hours using an azeotropic mixture of acetone (47 vol.%), methanol (23 vol.%) and chloroform (30 vol.%) as solvent. Solvent was evaporated with a rotary evaporator after extraction. The extracts were then

separated by column chromatography over activated silica gel and eluted sequentially into six fractions using *n*-pentane (fraction 1), *n*-pentane/dichloromethane (95/5 v/v, fraction 2), *n*-pentane/dichloromethane (90/10 v/v, fraction 3), *n*-pentane/dichloromethane (40/60 v/v, fraction 4), dichloromethane (fraction 5) and methanol (fraction 6). Details of the procedure of liquid column chromatography are described elsewhere (see Franke et al., 1995; Schwarzbauer et al., 2000). In this study, only the first, second, and fourth fractions were analyzed.

Gas chromatography (GC) was carried out with a Carlo Erba 8000 gas chromatograph equipped with a 30 m x 0.25 mm ID x 0.25 μm film Zebron - ZB 5 fused silica column. The oven temperature was programmed from 60 to 300 °C at a rate of 3 °C/min and 20 min isothermal period at 300 °C. Injection was performed in a split/splitless mode with a splitless time of 60s. Hydrogen was used as carrier gas (injector temperature: 270 °C). GC/MS analysis was done on a Finnigan MAT 8222 mass spectrometer linked to a HP 5890 gas chromatograph. A 30 m x 0.25 ID x 0.25 μm film Varian CP Sil - 8CB fused silica column was used. Helium was used as carrier gas. The temperature program was the same as described above. For low resolution mass spectra, the mass spectrometer was operated at a resolution of 1000 in EI^+-mode (70eV), source temperature 200°C, scanning from 35 to 700 amu with a rate of 1s/decade and an inter-scan time of 0.1 s.

Table 4.2. Petrographic composition of the studied high rank coals from Lower Suban seam at Suban (SUB)

Sample No.	VRr (%)	Vitrinite (vol.%)	Liptinite (vol.%)	Inertinite (vol.%)	Mineral matter (vol.%)	Coke mosaic structure (vol.%)	Distance to intrusion
03/1123	1.42	91.8	0.4	5.6	2.2	-	100 m from contact in horizontal direction
03/1143	2.09	90.4	1.2	6.8	1.6	-	2.5 m above
03/1145	2.55	87.0	0.4	10.6	2.0	-	1.5 m above
03/1113	5.18	82.4	-	0.6	14.6	2.40	directly at contact

Note: trace of liptinite is identified as meta-liptinite (altered liptinite with very high reflectance)

4.5 Results

4.5.1 Molecular composition of the low rank coal extracts

4.5.1.1 n-Alkanes and isoprenoids

The *n*-alkanes observed in the low rank coals range from C_{13} to C_{33} (Fig. 4.2). Unimodal *n*-alkane distributions were observed in humotelinite-rich coal (maximum at *n*-C_{27}) and humodetrinite-liptinite-rich coal (maximum at *n*-C_{25}). The second type of *n*-alkane distribution is bimodal, which is clearly recognized in humocollinite-rich coal. The first maximum occurs at *n*-C_{14} and the long-chain *n*-alkanes exhibit a distribution maximum at *n*-C_{24}. It is noteworthy that the *n*-alkane pattern of humodetrinite-rich coal maximizes at *n*-C_{14}, *n*-C_{22} and C_{25}.

The long chain *n*-alkanes compose more than 50% of total *n*-alkanes in all studied low rank coals, which is characteristic of their low thermal maturity. Except for the extract from the humodetrinite-liptinite-rich coal, the long chain *n*-alkanes exhibit an odd predominance with Carbon Preference Index (CPI) values higher than 1 (Table 4.3). If the CPI is calculated on the full range of *n*-alkanes, the values are close to 1. The studied coal samples are also characterized by low LHCPI values (<1, except sample 03/771) indicating the dominance of long chain *n*-alkanes.

Pristane (C_{19}) is the most dominant acyclic isoprenoid while phytane (C_{20}) and the smaller isoprenoid molecules are present in lower concentration than pristane. The pristane/phytane ratio (Pr/Ph) is high and varies considerably (see Table 4.3). C_{16}-isoprenoid (2,6,10-trimethyltridecane) is present in relatively higher concentration in humodetrinite- and humocollinite-rich coals.

4.5.1.2 Sesquiterpenoids and diterpenoids

The saturated sesquiterpanes that occur in high concentration in the studied samples are of cadinane and eudesmane types (based on Philp, 1985). The aromatic sesquiterpenoids are dominated by cadalene, with lower amounts of 5,6,7,8-tetrahydrocadalene and calamene (see Fig.4.3).

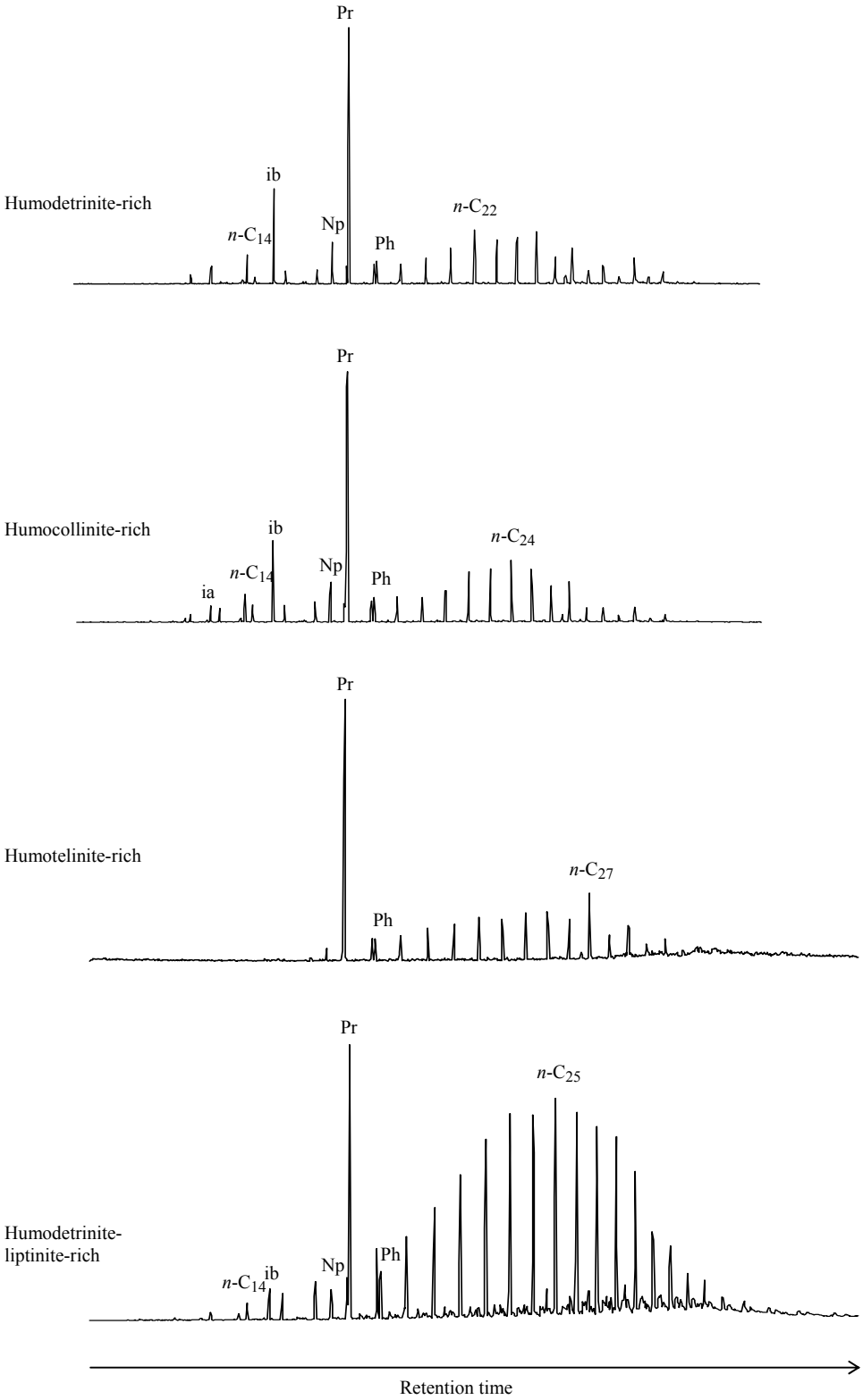

Fig. 4.2. Mass fragmentograms for m/z 57 of the aliphatic fraction of the low rank coals (VR_r = 0.41-0.45%) showing the *n*-alkanes and acyclic isoprenoids. ia = 2,6,10-trimethylundecane; ib = 2,6,10-trimethyltridecane; Np = Norpristane; Pr = Pristane; Ph = Phytane

Table 4.3. Molecular parameters used for paleoenvironment and maturity assessment of the studied coals

Sample No.	CPI (BE)[1]	CPI (H)[2]	CPI All[3]	LHCPI[4]	Pr/Ph	Pr/*n*-C_{17}	Ph/*n*-C_{18}	Oleanane Index[5]	22S/(22S+22R) Homohopane[6]	Ts/(Ts+Tm)	Tm/Ts	MPR[7]	MPI[8]	1-MP/9-MP[9]
Low rank														
02/767	1.9	1.5	1.2	0.5	14.7	24.4	1.5	0.2	0.3	0.5	1.2	1.4	0.8	0.3
02/769	1.7	1.4	1.2	0.8	11.8	19.1	1.5	0.3	0.4	0.4	1.4	0.4	0.5	1.0
02/771	2.2	1.8	1.2	1.2	18.2	21.2	1.1	0.3	0.3	0.5	1.0	1.6	1.0	0.4
02/773	0.8	0.7	0.8	0.4	7.1	8.4	0.8	0.2	0.4	0.5	1.0	1.2	0.6	0.2
High rank														
03/1123	1.1	1.0	1.0	1.7	4.4	0.8	0.2	n.d.	n.d	n.d	n.d	1.5	2.1	1.2
03/1143	1.4	1.1	0.9	5.3	4.6	0.5	0.2	n.d.	n.d	n.d	n.d	5.5	5.1	1.3
03/1145	1.3	1.1	1.0	1.8	7.0	1.6	0.3	n.d.	n.d	n.d	n.d	7.3	3.4	1.2
03/1113	1.1	1.0	1.0	6.7	7.2	0.1	0.02	n.d.	n.d	n.d	n.d	2.9	2.6	1.3

Note: n.d. = not detected

Explanation:

1. CPI according to Bray and Evans (1961)

$$CPI = \tfrac{1}{2}\left(\frac{C_{25}+C_{27}+C_{29}+C_{31}+C_{33}}{C_{24}+C_{26}+C_{28}+C_{30}+C_{32}} + \frac{C_{25}+C_{27}+C_{29}+C_{31}+C_{33}}{C_{26}+C_{28}+C_{30}+C_{32}+C_{34}}\right)$$

2. CPI according to Hunt (1996)

$$CPI = \frac{(\%C_{25}\text{-}C_{33}\text{ odd}) + (\%C_{23}\text{-}C_{31}\text{ odd})}{2(\%C_{24}\text{-}C_{32}\text{ even})}$$

3. CPI of all *n*-alkanes, calculated according to Marzi et al. (1993)

$$CPI = \frac{\sum_{i=n}^{m} C_{2i+1} + \sum_{I=n+1}^{m+1} C_{2i+1}}{\sum_{I=n+1}^{m+1} C_{2i}}$$

n = starting *n*-alkane # divided by 2; m = ending *n*-alkane # divided by 2; i = index

5. LHCPI $= \frac{C_{17}+C_{18}+C_{19}}{C_{27}+C_{28}+C_{29}}$ (see Littke et al., 1998)

4. Oleanane Index $= \frac{18\alpha(H)+18\beta(H)-oleanane}{17\alpha(H),21\beta(H)-hopane}$ (see Peters and Moldowan, 1993)

5. 22S/(22S+22R) ratio for C_{31}-homohopane (see Peters and Moldowan, 1993)

6. MPR (Methylphenanthrene Ratio) $= \frac{[2-MP]}{[1-MP]}$ (Radke et al., 1982)

7. MPI (Methylphenanthrene Index) $= \frac{1.5([2-MP]+[3-MP])}{[P]+[1-MP]+[9-MP]}$ (Radke et al., 1982)

8. [1-MP]/[9-MP] ratio (Alexander et al., 1992)

Two aromatic compounds with methylated tetrahydronaphthalene skeletons have also been identified, ionene (1,1,6-trimethyltetraline) and 1,6,8-trimethyltetraline. Pentamethylindan, identified in other brown coals (Hayatsu et al., 1978; Wang and Simoneit, 1990), is present in relatively high concentrations.

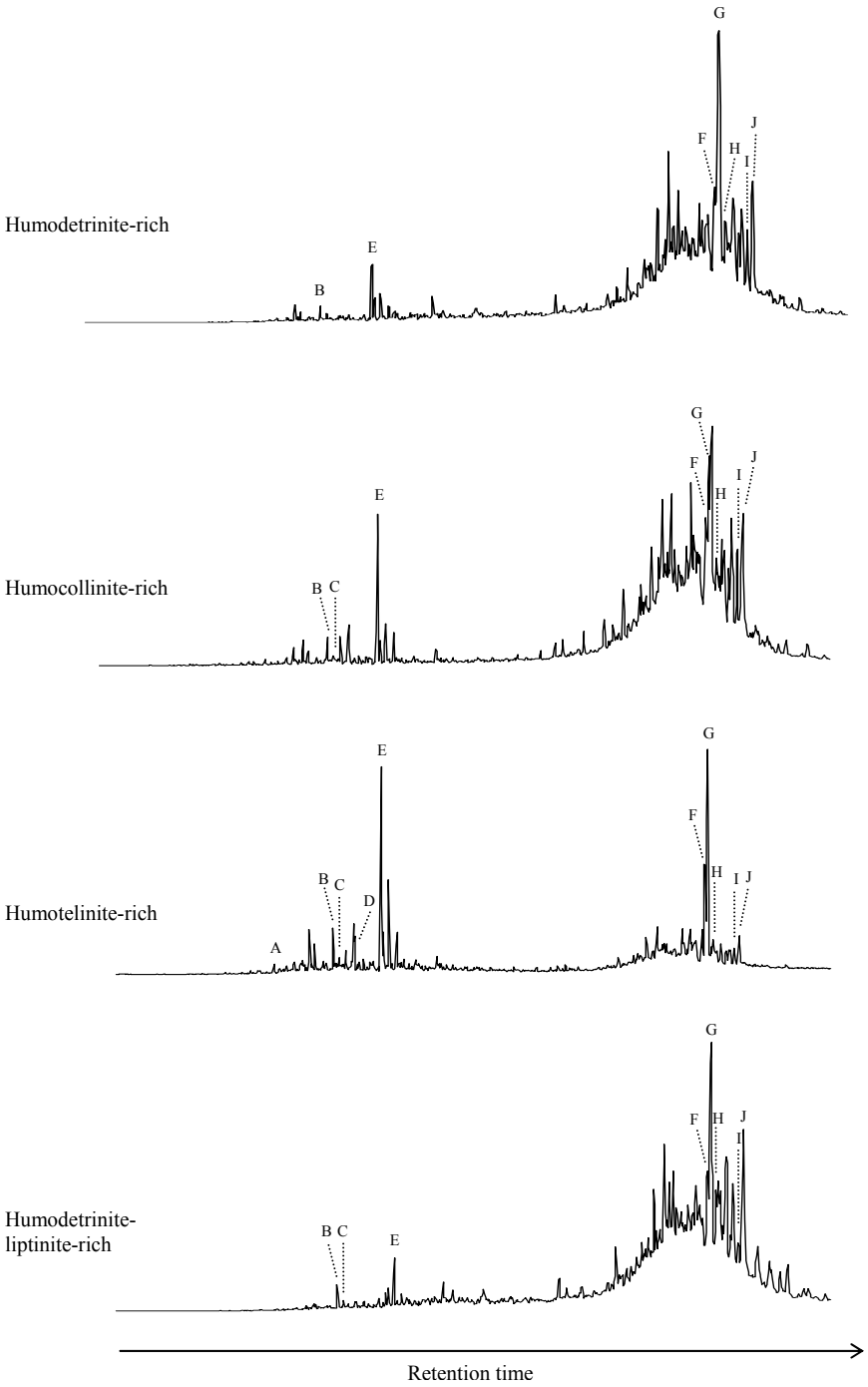

Fig. 4.3. Some identified biomarkers in total ion chromatograms of the aromatic fraction of the low rank coals. Annotations correspond to Table 4. 4.

Table 4.4. Peak assignment for biomarkers identified in the aromatic fractions (Fig.4.3) and hopanoids in the aliphatic fractions (Fig. 4.5) of low rank coal from TAL.

Peak	Compound
	Aromatic hydrocarbons
A	Ionene
B	Pentamethylindan
C	5,6,7,8-Tetrahydrocadalene
D	Calamene
E	Cadalene
F	2,2,4a,9-Tetramethyl-1,2,3,4,4a,5,6,14b-octahydropicene
G	1,2,4a,9-Tetramethyl-1,2,3,4,4a,5,6,14b-octahydropicene
H	2,2-Dimethyl-1,2,3,4-tetrahydropicene
I	1,2,9-Trimethyl-1,2,3,4-tetrahydropicene
J	2,2,9-Trimethyl-1,2,3,4-tetrahydropicene
	Hopanoids
a	18α(H)-22,29,30-Trisnorneohopane (Ts)
b	17α(H)-22,29,30-Trisnorhopane (Tm)
c	17α(H),21ß(H)-30-Norhopane
d	17ß(H),21α(H)-30-Normoretane
e	17α(H),21ß(H)-Hopane
f	17ß(H),21α(H)-Moretane
g	17α(H),21ß(H)-30-Homohopane (22S)
h	17α(H),21ß(H)-30-Homohopane (22R)
i	17ß(H),21ß(H)-Hopane
j	17α(H),21ß(H)-30,31-Bishomohopane (22S)
k	17α(H),21ß(H)-30,31-Bishomohopane (22R)
l	17ß(H),21α(H)-30,31-Bishomomoretane

Note: Compound identification is based on relative retention times and published mass spectral data.

Diterpenoids have not been found or occur only in trace concentrations in the studied coals. Other previous studies on Tertiary coals and recent peats from Indonesia (Dehmer, 1993; Anggayana, 1996; Stankiewicz et al., 1996) also indicate this phenomenon. In the case of TAL coals, only in one sample (humocollinite-rich coal), a major peak of abietane has been identified.

4.5.1.3 Sesterterpenoids, non-hopanoid triterpenoids and steroids

The only identified sesterterpenoid in the Suban seam low rank coal is de-A-lupane (identification based on Philp, 1985) in humocollinite-rich coal. Sesterterpenoids are no major natural products and, therefore, their occurrence in the sedimentary record is limited (Simoneit, 1986).

Non-hopanoid triterpenoids found in the coal extracts have an oleanane or ursane structure (based on Philp, 1985; Rullkötter et al., 1994). The prominent compounds identified on the m/z 410 mass fragmentogram are olean-13(18)-ene, oleane-12-ene, oleane-18-ene, and urs-12-ene. 18α-oleanane, which probably coelutes with 18ß-oleanane, also is identifiable in the m/z 412 mass fragmentogram (Fig. 4.4). Elution of 18α- + 18ß-oleanane with lupane should be considered (see Nytoft et al., 2002). However, a clear indication of the presence of lupane could not be recognized. The aromatic pentacyclic triterpenoids of oleanane and ursane type are found mostly in the form of alkylated-tetrahydro- or octahydropicenes (Fig. 4.3).

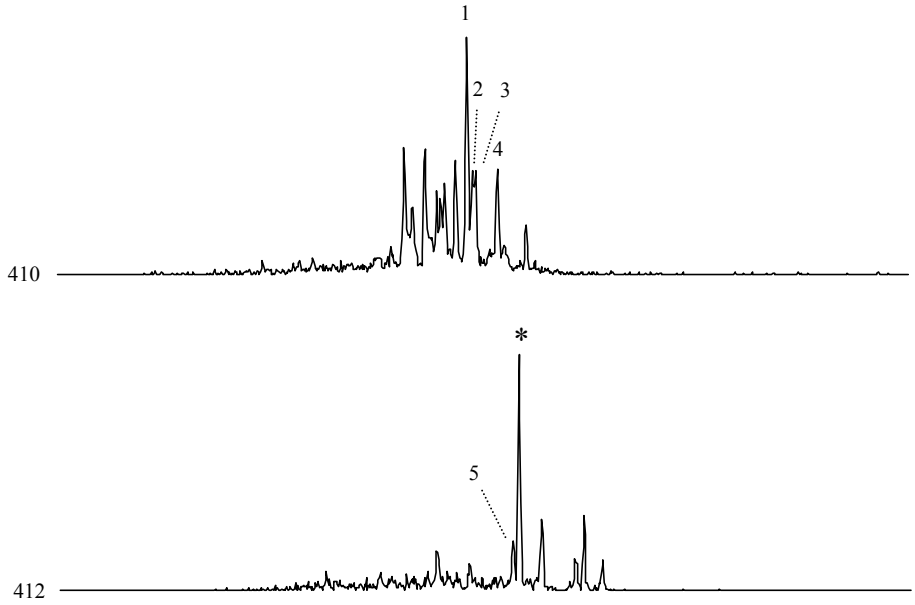

Fig. 4.4. The m/z 410 and 412 mass fragmentograms of sample 02/773 (humodetrinite-liptinite-rich coal) showing typical sesquiterpenoid distribution for the low rank coal. Identified compounds: 1 = Olean-13(18)-ene; 2 = Olean-12-ene; 3 = olean-18-ene; 4 = Urs-12-ene; 5 = 18α(H) + 18ß(H)-oleanane; * = 17α(H),21ß(H)-hopane.

Steroid compounds do not occur in the studied samples, which is consistent with observations by Anggayana (1996) on several Indonesian Tertiary coals and coals in general (see Chaffee et al., 1986; Wang and Simoneit, 1990). However, some recent studies by Lu and Kaplan (1992) and Bechtel et al. (2003) have indicated the occurrence of steroid compounds in some coals. Chaffee et al. (1986) reasoned that the absence of steroids may be due to preferential removal or incorporation into the soluble matrix of

components during diagenetic transformation of coal. It is also possible that sterols are either absent in the starting material or have not yet been converted to steranes or sterenes (Lu and Kaplan, 1992).

4.5.1.4 Hopanoids

The hopanoids of the studied coals are characterized by the presence of a series of hopane homologues from C_{27} to C_{33}, with bisnorhopanes (C_{28}) being absent (see Fig. 4.5, based on retention time and mass spectral data published in Seifert and Moldowan, 1978; Philp, 1985; Lu and Kaplan, 1992). C_{27} - 17α(H)-trisnorhopane (Tm) and its isomer 18α(H)-trisnorneohopane (Ts) have been identified. The values of the Ts/(Ts+Tm) ratio of the studied samples range between 0.43 - 0.50.

The predominant hopanoid in the low rank TAL coals is the C_{31} 17α(H)-homohopane. The presence of C_{31} hopanes in high concentrations is characteristic of many peats and coals (see for example Lu and Kaplan, 1992; Dehmer, 1993, 1995; Anggayana, 1996; Bechtel et al., 2003). Both epimers (22R and 22S) of C_{31} 17α(H)-homohopane occur. The ratio of 22S/[22S+22R] ranges between 0.3 and 0.4, which is consistent with low maturity sediments and well below the equilibrium value (approximately 0.6) that occurs at a vitrinite reflectance of around 0.5 – 0.6% (see Waples and Machihara, 1990; Peters and Moldowan, 1993). The occurrence of 17ß(H),21(ß)-hopane is consistent with the low maturity of the TAL coals (Ensminger et al., 1974; Volkman et al., 1983).

4.5.2 Molecular composition of the high rank coal extracts

4.5.2.1 Aliphatic hydrocarbons

High rank coals from the Lower Suban seam in the Suban area were subjected to varying degrees of thermal stress by the intrusion of the andesitic sill. Extracts exhibit various *n*-alkane distributions although the concentration is low (Fig. 4.6). *n*-Alkanes with unimodal distributions are exhibited by the coal at VR_r = 1.42% (*n*-alkanes maximum at *n*-C_{16}) and by the coal with the highest VR_r (5.18%, *n*-alkanes maximum at *n*-C_{17}). Coals that have intermediate VR_r values are characterized by bimodal *n*-alkane distributions.

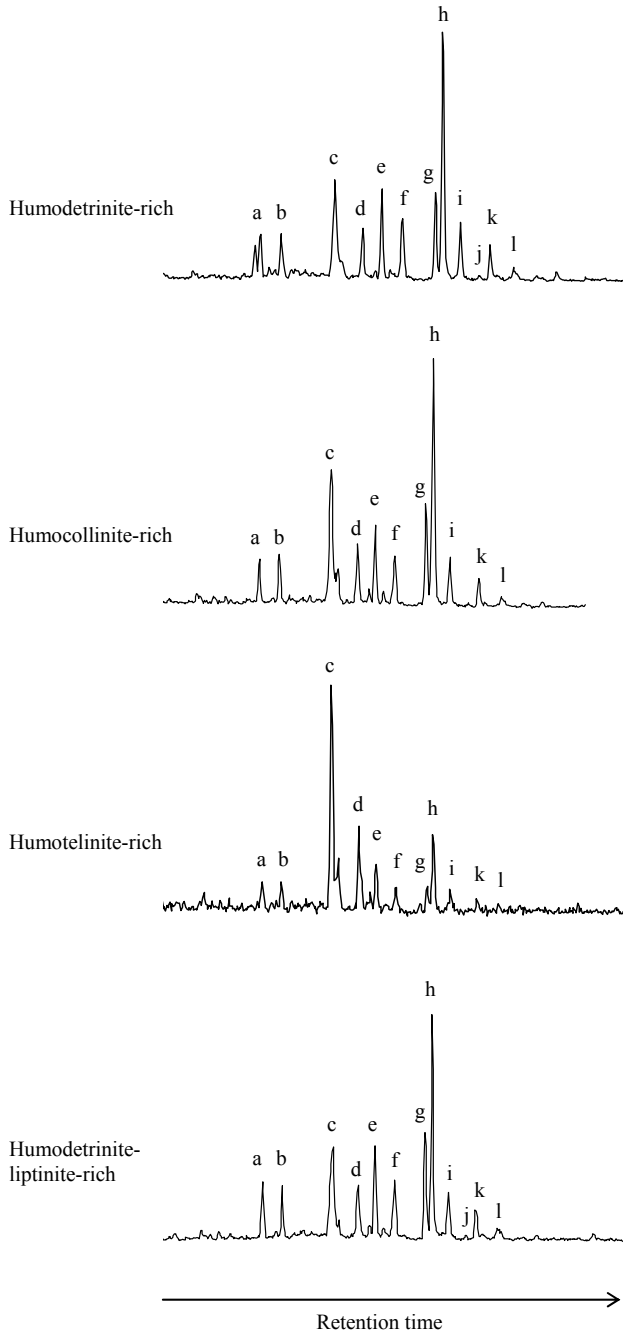

Fig. 4.5. Hopanoid distribution according to the m/z 191 mass fragmentogram of the low rank coals (peaks assignment see Table 4.4).

The relative abundance of light *n*-alkanes to heavy *n*-alkanes also exhibits a broad variation in the high rank Suban area coals. The LHCPI values vary between 1.7 to 6.7 and do not show any particular pattern (see Table 4.3 and Fig. 4.7). The CPI of high molecular weight *n*-alkanes and the full range of n-alkanes is ~1, consistent with high thermal maturity.

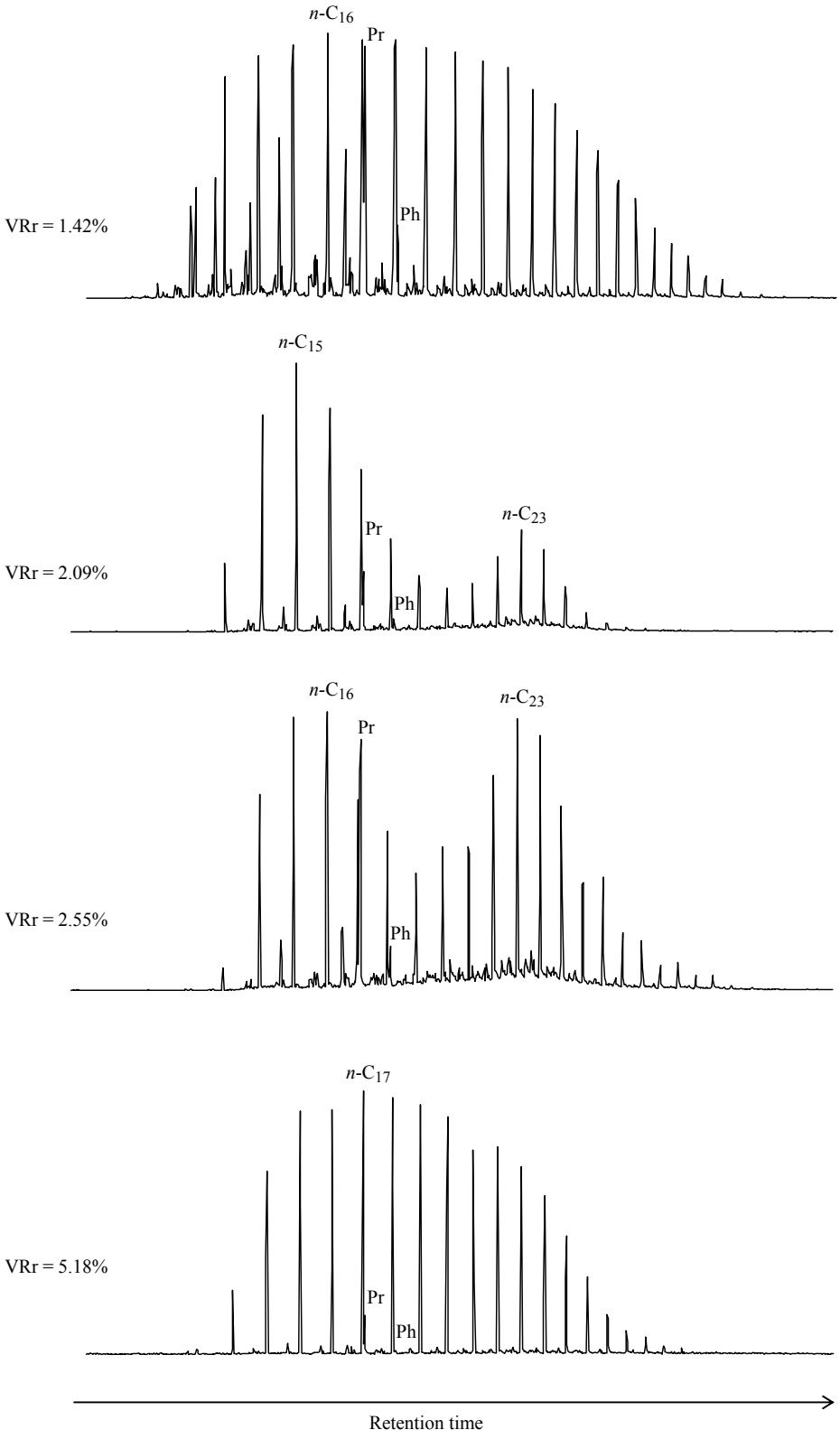

Fig. 4.6. Total ion chromatograms of the aliphatic fraction of the high rank coals.

The ratios of pristane to phytane are low compared to values seen in the lower rank TAL coals (Fig. 4.7). The Pr/nC_{17} and Ph/nC_{18} ratios of the low rank coals are appreciably higher than those of the high rank coals. Other smaller acyclic isoprenoid molecules, such as norpristane or farnesane, are identified in the coal with VR_r = 1.42%. The saturated cyclic isoprenoids are absent, except in the coal with VR_r = 1.42%, in which sesquiterpenoids are still present but are not identifiable. The cyclic isoprenoids appear to have been aromatized completely as a result of extreme heating by the intrusion.

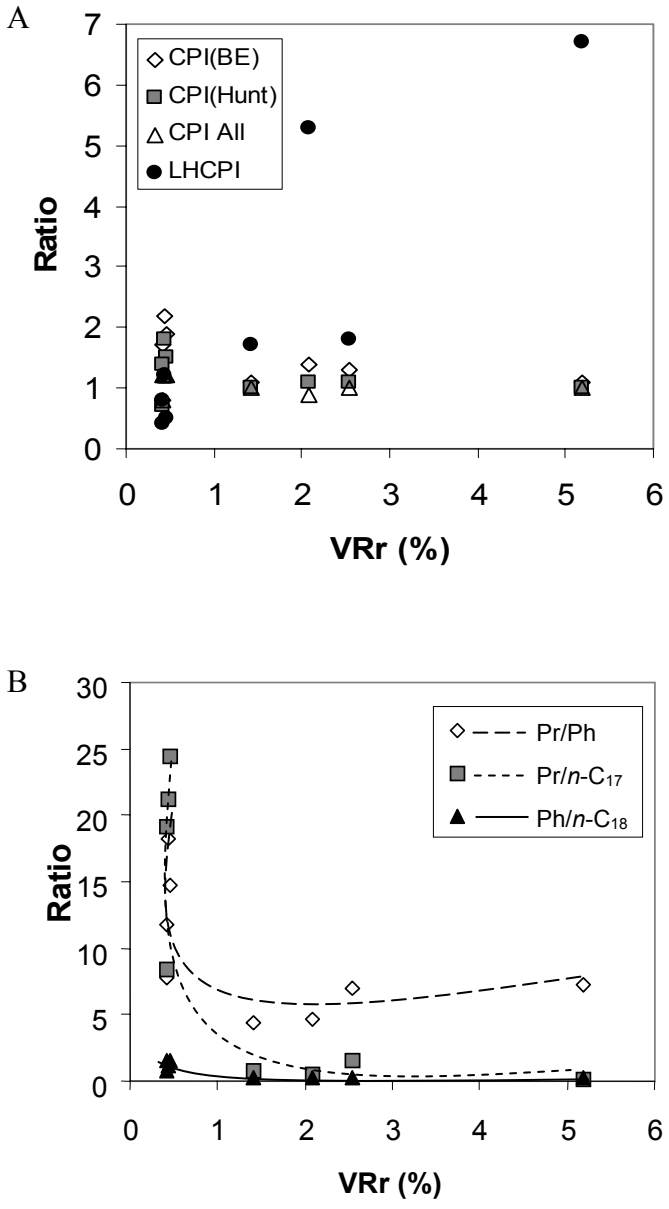

Fig. 4.7. Graphic showing the change of (A) CPI and (B) Pr/Ph, Pr/nC_{17} and Ph/nC_{18} ratios with increasing thermal maturity indicated by random vitrinite reflectance of the studied coals.

4.5.2.2 Aromatic hydrocarbons

Various aromatic hydrocarbon compounds are detected in the thermally metamorphosed Suban area coals. Distributions of the isomers of the main compounds (methylnaphthalene, dimethylnaphthalene, trimethylnaphthalene, phenanthrene, methylphenanthrene, dimethylphenanthrene, trimethylphenanthrene) are presented in Figure 4. 8.

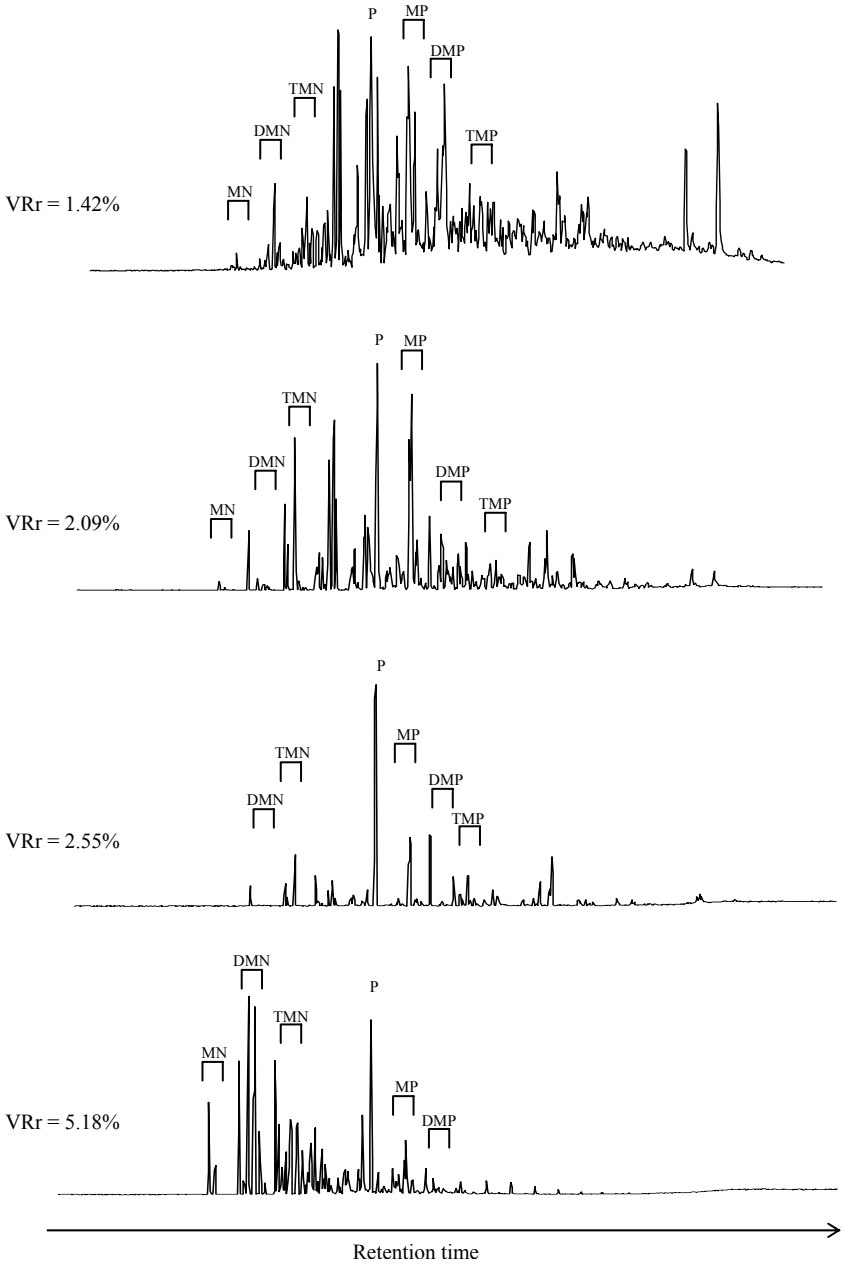

Fig. 4.8. Total ion chromatograms of the aromatic fraction of the high rank coals and indication of the position of some important aromatic hydrocarbon compounds. MN = Methylnaphthalene; DMN = Dimethylnaphthalene; TMP = Trimethylnaphthalene; P = Phenanthrene; MP = Methylphenanthrene; DMP = Dimethylphenanthrene; TMP = Trimethylphenanthrene.

A reversal pattern is shown by the relative abundance of the naphthalene isomers relative to phenanthrene. In general, there is a decrease in the abundance of naphthalenes relative to the phenanthrene with increasing rank between VR_r = 1.42 to 2.55%. However, in the coal taken directly at the intrusion contact (VR_r = 5.18%), the naphthalene isomers are more abundant than phenanthrene.

Several maturity indices have been formulated based upon the distribution of methyl-subtituted aromatic compounds. MPR (Methylphenanthrene Ratio), MPI (Methylphenanthrene Index) both proposed by Radke et al. (1982) and 1-MP/9-MP ratio (see Alexander et al., 1992) have been calculated for the Lower Suban coals (Table 4.3 and Fig. 4.9). The values of MPR, MPI and 1-MP/9-MP vary considerably in low rank coal. MPR and MPI increase with rank before decreasing at very high rank (above VR_r ≈ 2.5%), whereas the 1-MP/9-MP value of the high rank coals is invariable at about 1.2 - 1.3 (Table 4.3 and Fig. 4.10).

4.6 Discussion

4.6.1 Paleoecological and paleoenvironmental conditions

The formation of paleo-peat is known to be related to the environmental conditions of the paleomire. Petrographic analysis of the studied Lower Suban seam had confirmed the development of a raised paleo-peat bog (Amijaya and Littke, 2005). The organic geochemical analysis is intended for providing information on plant input, bacterial activity and the interaction with the paleoenvironment, which basically encompass the paleoecological conditions of the coal precursor.

It is well known that the dominance of long-chain over short-chain *n*-alkanes is typical for immature coals composed of higher land plant organic matter (Wang and Simoneit, 1990; Stout, 1992; Zhang et al., 1993; Petersen et al., 2001; Bechtel et al., 2003) and, specifically, cuticular waxes (Eglinton and Hamilton, 1967). The bimodal distribution could indicate a mixture of terrigenous higher land plant material and an algal/bacterial source (Moldowan et al., 1985). However, abundant algal material was not microscopically identified in the studied coals (Amijaya and Littke, 2005). The abundance of smaller *n*-alkanes is likely attributable to microbial activity.

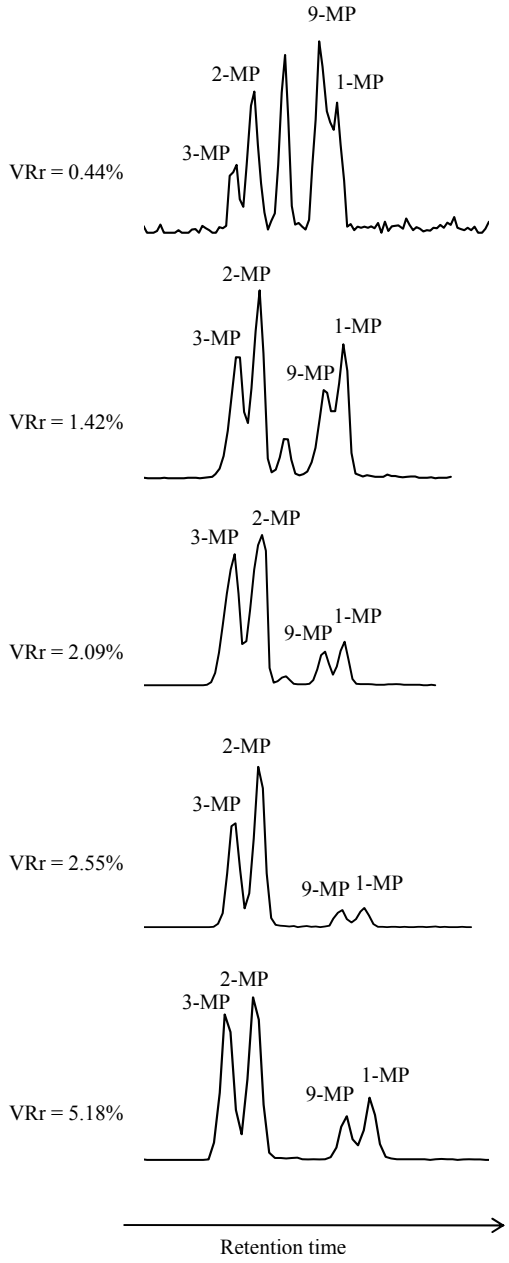

Fig. 4.9. Methylphenanthrene distribution of coal samples of different rank.

The isoprenoids are mainly derived from the phytol side chain of chlorophyll in phototrophic organisms although other sources such as archaebacteria are also known (see Volkman and Maxwell, 1986 and references therein). The presence of a C_{16}-isoprenoid with high concentration in humodetrinite- and humocollinite-rich coals supports the possibility of enhanced microbial activity in the top section of paleopeat. In this case, the bacteria may either act as direct source of acyclic isoprenoids or as degradation agent.

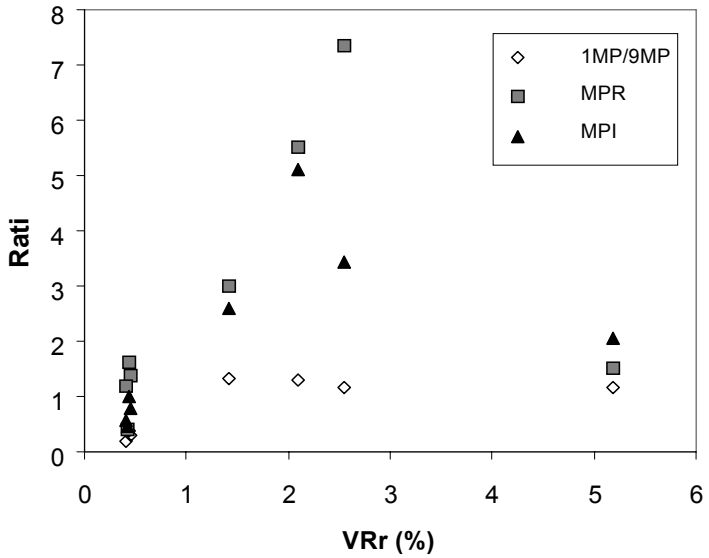

Fig. 4.10. Graphic showing the change of the1-MP/9-MP and Methylphenanthrene ratios and Methylphenanthrene index with increasing thermal maturity indicated by random vitrinite reflectance of the studied coals.

The biomarker composition of the coals indicates that the paleo-peat was formed from angiosperm vegetation. As mentioned earlier, cadinane and eudesmane dominate the saturated sesquiterpanes in the studied samples. Cadinane is regarded as the product of depolymerization and subsequent hydrogenation of polycadinene, a compound found in dammar resins of angiosperms, most of all the *Dipterocarpaceae* family, which inhabits Southeast Asia (van Aarssen et al., 1992, 1994). This finding agrees with the pollen analysis that identifies *Dipterocarpaceae* in Tertiary coal and recent peat of Indonesia. One of its genera, *Shorea*, is a typical plant found in modern ombrogenous tropical lowland peat swamps in Indonesia, especially in Sumatra and Kalimantan (Anderson and Muller, 1975; Morley, 1981; Demchuck and Moore, 1993). The presence of a sesquiterpanoid with a eudesmane skeleton, probably 4ß(H)-eudesmane, is also consistent with input from higher land plants (Alexander et al., 1984).

The precursors of the aromatic sesquiterpenoids identified in Lower Suban coals (cadalene, tetrahydrocadalene and calamene) are found mostly in dammar resins of angiosperms (Bendoraitis, 1974; Simoneit and Mazurek, 1982; Wang and Simoneit, 1990; van Aarssen et al., 1992). Depolymerization of polycadinene during catagenesis initiated an aromatization that led to the formation of those compounds (van Aarssen et al., 1992).

The identified ionene (1,1,6-trimethyltetraline) and 1,6,8-trimethyltetraline probably are derived from degraded and cyclized carotenoids (Wang and Simoneit, 1990). Carotenoids have been proposed to constitute sporopollenins derived from some higher plant pollen and ionene was identified in pyrolysates of sporopollenins derived from some higher plant pollen and spore coal (Achari et al., 1973).

Abietane has been found in the humotellinite-rich coal. Diterpenoids are predominant constituents of higher plant resins, mostly from gymnosperms (see Simoneit, 1986; Chaffee et al., 1986; Killops et al., 1995; Otto et al., 2005), though diterpenoids are also found in some species of angiosperms, such as in the family *Burseraceae* (Sukh Dev, 1989). Compounds with abietane skeleton are found mostly in conifer resins and lipids in form of abietic acid, abietinol or ferruginol (Laflamme and Hites, 1979; Sukh Dev, 1989).

The absence of diterpenoids in most of the samples can be correlated with an absence of gymnosperm precursors at the time of deposition, since angiosperms are the predominant plants in Tertiary coals and recent ombrogenous peats of the Malay-Indonesian region (Anderson and Muller, 1975; Morley, 1981; Demchuck and Moore, 1993). However, Anderson and Muller (1975) identified some conifer pollen grains (*Dacrydium* and *Podocarpus*) in peat deposits and *Burseraceae* pollen grains in clay underlying a peat deposit in NW Kalimantan. A species of *Dacrydium* is prominent in a peat swamp forest in one locality in that area. Although there is no palynological evidence in the studied area, the occurrence diterpenoid compounds in one of the studied coals is likely due to such local variations in biotic input at the time of deposition.

The role of angiosperms as paleo-peat-forming vegetation of Lower Suban coal is also revealed by the occurrence of triterpenes, especially the defunctionalized, unsaturated and monoaromatic oleanane or ursane, which are found mostly in the *Dicotylodonea,* angiosperm dicots. Only a few gymnosperm species containing these compounds are known (Simoneit, 1986; Sukh Dev, 1989; Otto et al., 2005; Stefanova et al., 2005). Ten Haven et al. (1992) suggested that olean-12-ene and urs-12-ene are mainly alteration products from ß- and α-amyrin. Oleananes are formed through diagenetic and catagenetic alteration of various 3ß-functionalized angiosperm triterpenoids (see

Rullkötter et al., 1994; Murray et al., 1997) or the catalytic hydrogenation of oleanene (Rullkötter et al., 1994).

Aromatic pentacyclic triterpenoid compounds with picene structure are considered biomarkers for angiosperms, since they have been identified in lignite from angiosperms (Stout, 1992). These structures may result from the microbial aromatization of triterpenoids (Wakeham et al., 1980; Stout, 1992). Dehmer (1988) identified several compounds with the same structures in peat deposits in Indonesia indicating that the dehydrogenation of triterpenoids does not require long periods of time nor high temperatures.

De-A-lupane, which is the only identified sesterterpenoid with significant concentration has been considered as a product of photochemical or photomimetic degradation at ring-*A* commencing with the oxygen functionality at C-3 of certain triterpenoids (but not hopanes) from higher plants (Corbet et al., 1980; Simoneit, 1986).

The presence of hopanoids in the studied coals points to microbial input due to their primary origin (Simoneit, 1986). The identified major hopanoid, 17α(H)-homohopane, results from the oxidative and subsequent decarboxylation reactions of bacteriohopanetetrol and other precursors; and α,ß C_{31}-hopanes are often the major hopanes in coals derived from peat deposited in acidic environments (Van Dorselaer et al., 1977). This finding agrees with the fact that an acidic environment is typical for domed peat deposits in Indonesia (Neuzil et al., 1993; Dehmer, 1993). Noteworthy is the dominance of 17α(H),21ß(H)-30-norhopane in humotelinite-rich coal. Lu and Kaplan (1992) observed an enrichment of norhopanes with increasing temperature. However, in this TAL low rank coal, the variation of hopane distribution is likely source-dependent.

Dydik et al. (1978) proposed that Pr/Ph values reflect the redox conditions during organic matter deposition. Accordingly, the humodetrinite-, humocollinite-, and humotelinite-rich coals (higher Pr/Ph) were developed under more oxic conditions than the humodetrinite-liptinite-rich coal, which is acceptable since the humodetrinite-liptinite-rich is a typical coal facies for planar-topogenous paleomires whereas the other coal facies are typical for domed-ombrogenous paleomires in this area (Amijaya and

Littke, 2005). Similar variations of Pr/Ph ratio had been observed by Bechtel et al. (2002; 2003) on lignite seams in Austria and Slovenia. Other interpretations of Pr/Ph ratios (e.g. ten Haven et al., 1987) take other sources into account but are probably less relevant in the case of peat and coal. The role of liptinite macerals to reduce the value of Pr/Ph is also a matter of debate, because liptinite-rich coals could have a wide range of Pr/Ph ratios (see Püttmann et al., 1986).

The influence of maturation on the variability of Pr/Ph values can also be ruled out in this low rank coal, because the samples are at the same maturity level (VRr = 0.41-0.45%). Nevertheless, a bacterial origin of phytane (Volkman and Maxwell, 1986) can not be excluded. High pristane/*n*-C_{17} ratios (>1) are also indications of sediment deposition in inland peat-swamp environments (Lijmbach, 1975), which agrees with the depositional environment of the studied coals (Boyd and Peacock, 1986; Amijaya and Littke, 2005).

The Tm/Ts ratio may reflect the redox potential of the paloenvironment with higher Tm/Ts ratios indicating oxic conditions during sedimentation (Moldowan et al., 1986). This explanation is consistent with the Pr/Ph ratio of the TAL coal samples as the coals with higher Tm/Ts ratios are those that were deposited in the upper part of the ombrogenous paleomire under prolonged oxic conditions. However, it is also possible that the small variation of the ratio of Ts to Tm is related to the difference in the maceral composition of the coals. The highest ratio is found in the humocollinite-rich coal, which is composed mostly by corpohuminite (Amijaya and Littke, 2005). Corpohuminite originates from primary cell excretions, tannins, which later convert to phlobaphenes by oxidation or condensation (Taylor et al., 1998; Sýkorová et al., 2005). The process of corpohuminite formation could possibly drive an advance production of Tm.

4.6.2 Effect of the thermal metamorphism caused by the intrusion

Varying degrees of thermal stress by the andesitic intrusion had changed the *n*-alkane distributions of the studied coals. A reversal pattern of *n*-alkane distribution from unimodal to bimodal and back to unimodal with increasing maturity has been noted in this study. George (1992) observed a similar phenomenon in a shale horizon intruded by

a sill in Scotland and suggested that the unusual modification of *n*-alkane distributions is probably due to the rapid heating of an immature organic matter. The result of our study on SUB coals supports that suggestion.

However, the influence of precursor material as seen in the lower rank TAL samples should not be neglected. Unfortunately, such influence can not be recognized microscopically because the macerals of the high rank coals are homogenized.

Heating by the intrusion greatly lowers the ratio of pristane to phytane compared to values seen in the lower rank TAL coals (Fig. 4.7). The Pr/Ph ratio, however, does not directly correlate with thermal exposure as the ratio first decreases then increases at the highest level of maturation. Some studies indicate that Ph/Pr ratio reaches a maximum at medium rank (VR_r = 0.7 – 1.0%, Radke et al., 1980; Littke et al., 1990). The trend of Pr/Ph ratio for the Suban area coals may be typical for rapid coalification of low rank coal caused by the igneous intrusion, which was also also found by Norgate et al. (1999) in their study on New Zealand coals.

As presented in Figure 4.8, a decrease in the abundance of the methyl-subtituted phenanthrenes relative to phenanthrene occurs with increasing rank, which is in agreement with the transformation pattern of tricyclic diterpenoids with increasing coal rank as described by Hayatsu et al. (1978). As mentioned earlier, a reversal pattern is shown by the relative abundance of the naphthalene isomers relative to phenanthrene. It should be noted that for type III kerogen, the change of distribution of naphthalene isomers with increasing rank is a less reliable thermal indicator than that of phenanthrene isomers (Radke et al., 1986; Raymond and Murchinson, 1992).

The result of MPR change with rank observed in this study is basically in agreement with the study by Radke et al. (1984), which inferred a gradient reversal between 1.7 – 2.5% VR_r for MPR. However, unlike the data from Radke et al. (1982), which indicated a reversal of MPI at $VR_r \approx 1.3\%$, the reversal of MPI in this thermally metamorphosed coal occurs at a higher vitrinite reflectance (above 2.5%). This data supports the suggestions from Raymond and Murchison (1992) which indicate that MPI is highly susceptible to differences in heating rate and organic matter type and thus considered as unreliable maturity parameter. However, the trend observed in MPI for the Lower

Suban coals is similar to that described by them. They also found that rapidly heat-affected organic matter exhibits a more immature molecular signature than organic matter exposure to normal geothermal gradients at the same vitrinite reflectance. Change of the molecular characteristic of Lower Suban coals caused by rapid heating due to igneous activity confirms this fact.

In the oil window range, the value of the 1-MP/9-MP ratio of the sediment extracts increases with rank (Alexander et al., 1992). Our study shows that the low rank coals of TAL have a low 1-MP/9-MP ratio, even though one sample has an anomalously high value. The high rank coals from SUB show similar values. This observation possibly indicates that an equilibrium of 1-MP/9-MP ratio can be reached at a certain rank, possibly close to VR_r = 1.4%.

4.7 Conclusions

A number of conclusions can be drawn from the preserved biomarkers in the coal and their response to the thermal metamorphism caused by the igneous intrusion.

The *n*-alkane distribution is correlated with the different maceral assemblages of the low rank coals. It should be noted, however, that this distribution could be due to the different intensity of microbial activity at each part of the paleomire.

In this case, the pristane/phytane ratio can be used to draw conclusions on the redox conditions within paleomire, because it is consistent with the paleoenvironmental interpretation based on maceral assemblages. The humodetrinite-liptinite-rich coal, which is the typical coal facies for planar-topogenous paleomires, shows the lowest Pr/Ph ratio in comparison to the other coal facies, which were deposited in domed-ombrogenous paleomires (see Amijaya and Littke, 2005).

The composition of terpenoid biomarkers (especially cadinane and eudesmane type sesquiterpenoids and oleanane and ursane type triterpenoids) indicates an abundant contribution of angiosperm plants to the Late Miocene/Early Pliocene paleoecology of the paleomire in this area.

The distribution of hopanoids is influenced by the organic facies of the coal and their maturity. The pattern of the Tm/Ts ratio reflects the paleomire conditions since a higher Tm/Ts ratio is shown by the coals which were more oxidized and deposited as the upper part of the ombrogenous paleomire. The predominant hopanoids in most of the studied low rank coals are the 22R and 22S epimers of 17α(H)-homohopane, which is a common characteristic of many peats and coals deposited in acidic environments.

There is a reversal pattern in the trends of molecular maturity parameters based on the aliphatic hydrocarbons (*n*-alkane distribution and pristane/phytane ratio) and the aromatic hydrocarbons (methylphenanthrene) with coal rank. CPI equilibrium at ~1 is reached at a maturity with vitrinite reflectance lower than 1.4%, whereas the Pr/Ph ratio decreases with thermal maturity but increases again in the anthracite stage. The values of methylphenanthrene ratios MPR, MPI, and 1-MP/9-MP vary considerably in low rank coal. In the high rank coal, the MPR and MPI increase with rank before decreasing at very high maturity (above $VR_r \approx 2.5\%$). However, the 1-MP/9-MP ratio of the high rank coals remains quite constant.

Chapter 5 Final Discussion

Each study described in the previous chapter shows that the petrological and geochemical characteristics of the Tanjung Enim coals are the implications of various factors involved during (1) deposition of coal precursor, especially the paleoenvironment and paleoecology, and (2) coalification process, particularly as the result of thermal metamorphism caused by the igneous intrusion. In the following section, the important results of all studies are discussed comprehensively.

5.1 Deposition of coal precursor (paleoenvironment and paleoecology)

Climate, depositional environment, mire type and vegetation type dictate peat composition (see review in Scott, 1987). The same factors govern the development of paleo-peat, which in turn produced a coal deposit. This means that the inter-correlation of those aspects can not be neglected in an attempt to characterize a particular coal deposit.

Petrographic investigations of modern tropical peat deposits have contributed valuable information about paleoenvironment and paleoecological setting of a paleomire. In the case of Tertiary Tanjung Enim coals, comparison between the identified maceral assemblages and the pre-maceral assemblages of some studied modern peat in the Malay-Indonesia region have been very useful to reconstruct the paleoenvironment of the coals. These conclusions benefited also from the fact that the tectonic setting and climatic condition during the deposition of the studied coal and modern tropical peat in Indonesia were similar. Moreover, the plant communities did not significantly change during Tertiary to Quartenary times (see explanation in Chapter 2).

The vertical alignment of peat type (from sapric peats at the base to hemic and fibric peats in the overlying layers) is a typical evolution of modern tropical peat from a topogenous to an ombrogenous peat or from rheotrophic to mesotrophic-oligotrophic conditions. Typical maceral assemblages for certain coal sections can be also distinguished in this study. The basal section is represented by the humodetrinite-liptinite-rich group, correlating with sapric or fine hemic peat often occurring at the base of modern peats. The middle section is characterized by humotelinite-rich and

humocollinite-rich groups. The precursors of these groups were hemic and fine hemic peats. The top section is typically represented by the humodetrinite-rich or inertinite-rich group. These groups are the counterparts of fibric peat at the top of the modern peats. Therefore, the sequence of maceral assemblages in the studied coals also represents the change of topogenous to ombrogenous paleo-peat and the development of a raised peat bog.

The result of microfacies analysis is in agreement with results of GC/GC-MS analysis showing that the humodetrinite-, humocollinite-, and humotelinite-rich coals have higher Pr/Ph ratios than humodetrinite-liptinite-rich coal. This points out that they were deposited under relatively more oxic conditions than the humodetrinite-liptinite-rich coal. This could be the effect of ombrogenous environment (deposition near to groundwater table, supply of nutrients dominantly from rain water), whereas the humodetrinite-liptinite-rich coal was deposited in a topogenous environment (under stagnant water).

It should be noticed that most thick coal beds are composed of multiple paleo-peat bodies, stacked one upon another. Each seam can consist of more than one succession of paleo-peat development. The occurrence of more than one succession in a coal seam may be linked with the dynamics of the general water table. In the studied seams, three types of partings which separate the paleo-peat bodies have been identified. Those are inorganic partings (thin clastic sediment layer), oxidized organic partings (inertinite-rich coal) and organic, non-oxidized, degradative partings (humodetrinite-rich coal). Figure 5.1 illustrates the possible formation of a coal seam formed by stacked paleo-peat bodies in the studied area.

Biological marker (biomarker) analysis is basically performed to identify the molecular fossils of flora or fauna. Some important biomarkers in the studied samples are cadinane- and eudesmane-type sesquiterpenoids and oleanane- and ursane-type triterpenoids. Those compounds are typical biomarkers from angiosperms, most of all the *Dipterocarpaceae* family. *Dipterocarpaceae* family is well known as the predominant plant in the tropical peats in Southeast Asia (see references in Chapter 4). Moreover, *Dipterocarpaceae* dominates tree communities in the dry lowland forest located between mire margin and mire center in a modern tropical peat (Wüst et al.,

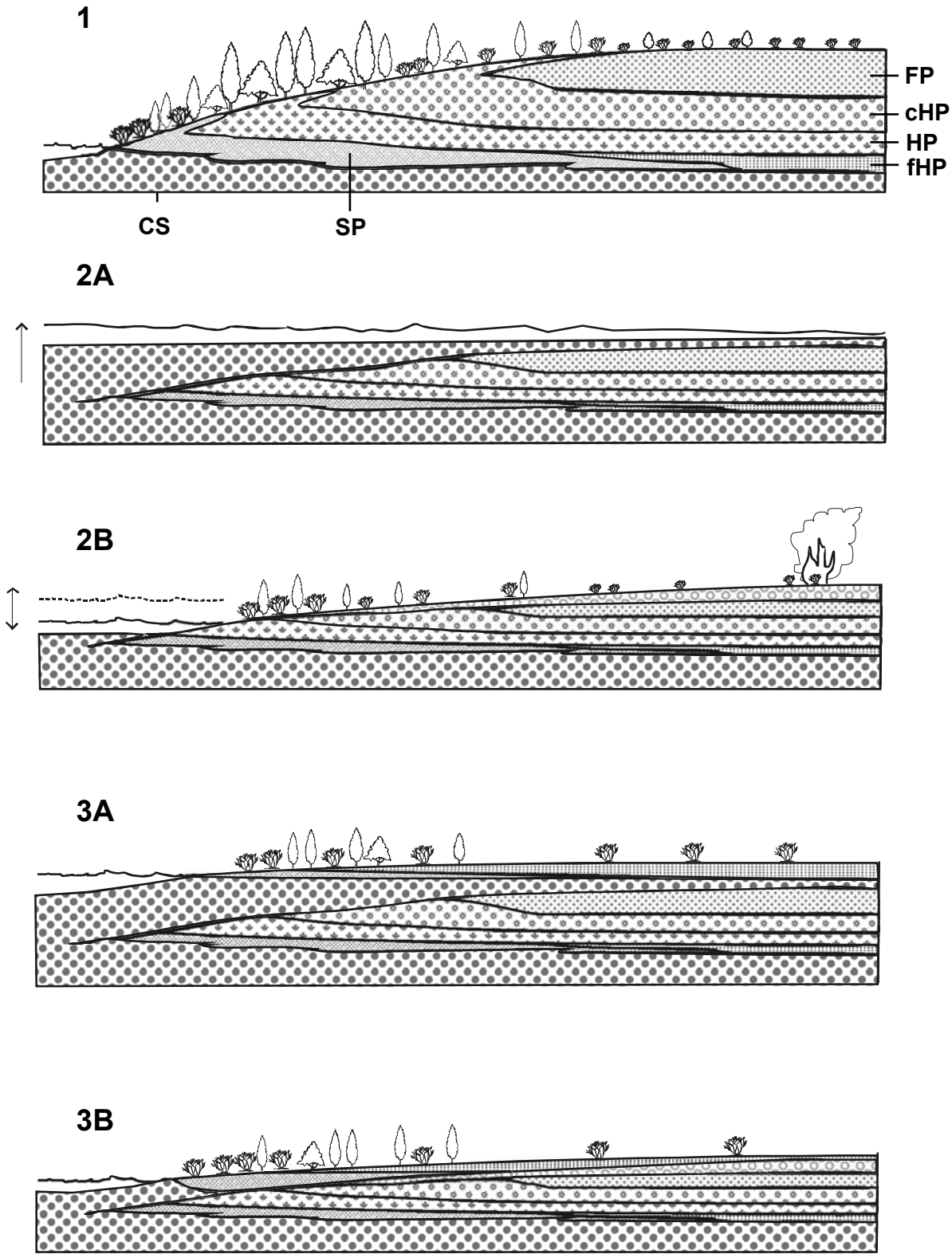

Figure 5.1. Scheme of possible formation of stacked paleo-peat bodies in studied area. (1) Original ombrogenous peat. (2) Formation of partings: (A) inorganic parting by increasing general water table or (B) oxidized organic parting by fire/water table fluctuation or non-oxidized degradative parting by severe plant degradation. (3A and 3B) Reinitialization of mire. Note : FP = fibric peat, cHP = coarse hemic peat, HP = hemic peat, fHP = fine hemic peat, SP = sapric peat, CS = clastic sediments. Figures are not to scale.

2001; Greb et al., 2002). This is also a supporting indication that the studied seams came from an ombrogenous paleo-peat.

5.2 Coalification process (effect of thermal metamorphism)

The conducted study indicates that besides the normal coalification process, the rapid heating as the result of andesite intrusion had extensively changed the coal optical and chemical properties. Moreover, some changes in the mineralogy had been identified as well. This study clarified that the transition zone between medium volatile bituminous and low volatile bituminous coals is the range where the most severe change of coal properties occurs. At this stage, the molecular orientation of compounds in coals transforms significantly from randomly small aromatic stacks into bigger aromatic units (see explanation in Chapter 3), which in turn affected the optical appearance of studied coal too. Those aspects are summarized below.

5.1 Changes in petrology

Based on vitrinite reflectance measurement, the studied coals can be classified into two groups. First there are coals with low to moderate maceral reflectance (VR_r less than 0.8%). These coals were not or not directly affected by thermal metamorphism. Second there are coals which were thermally metamorphosed. The vitrinite reflectance values of these coals are very high (VR_r reaches 5.2%). With increasing maturity, the bireflectance value (VR_{max} - VR_{min}) is increasing too. However, in this case the increase in bireflectance with increasing maturity is less severe in comparison to that caused by normal burial diagenesis. This difference may be connected with the absence of high pressure.

The effect of rapid heating can be seen not only on vitrinite, but also on the coalification path of liptinite and inertinite. In coals with $VR_{max} < 1\%$, liptinite reflectance is lower than vitrinite reflectance and inertinite has the highest reflectance. At $VR_{max} \sim 1.45\%$ the reflectances of liptinite and inertinite begin to converge with the reflectance of vitrinite. Finally, in the samples which have VR_{max} of 1.7% and more, liptinite shows the highest reflectance and contrary to that, inertinite has the lowest reflectance value among the maceral groups. However, no “liptinite coalification” jump can be

recognized, since liptinite reflectance increases progressively. As mentioned earlier, vitritine reflectance already reaches inertinite reflectance at a moderate coal rank, which is much lower than the usual reflectance value of vitrinite-inertinite optical convergence in the normally coalified coal.

The typical microstructures of natural coke, which mostly exhibits mosaic structure, are recognizable in the sample which was taken at the contact of the coal seam with the intrusion. The microstructures could have been formed by total alteration of vitrinite or liptinite or as result of the deposition from the fluid phase in the cracks. A continuous change of mosaic dimension surrounding a pore could be an evidence that the coals surrounding the intrusion were probably subjected to at least two phases of heating with different maximum temperatures.

5.2 Changes in geochemistry

One important elemental change in the studied coals due to thermal metamorphism is the carbon content change. This study shows that the total carbon content increases very rapidly with rank increase, up to 90 wt.% (daf) at approximately 2.0% VR_r. Above that level, there is only a minor increase of carbon content and it tends to be almost stable in the range of 94 -96 wt.% (daf) carbon.

Rock-Eval pyrolysis was conducted to examine the variation of hydrogen and oxygen content in coals with respect to the organic carbon content (Hydrogen Index and Oxygen Index). The thermal metamorphism basically did not have a significant effect on the amount of oxygen in coals, since the relative amount of released oxygen from coals (in form of CO_2) during pyrolysis only differs slightly in all studied coals (indicated by low OI values). The heating has, however, decreased the relative amount of hydrogen (in form of HC) in coals. The low rank coals are characterized by higher HI values than the high rank coals. This indicates that the hydrogen has been released from coals during the heating process. The thermal stability of studied coals has increased also, which is shown by increasing T_{max} as the coal reaches a higher maturity rank.

A further change in geochemistry of studied Tanjung Enim coals is the loss of volatile matter with increasing rank. This phenomenon is very obvious in Suban mine, where

the volatile matter values of coals decrease towards the intrusion body. High volatile matter content (> 40 wt.%, daf) is the characteristic of the original low rank coal. In contrast, the thermally metamorphosed coals are characterized by low volatile matter content (< 24 wt.%, daf). The liberated components consist predominantly of the non-aromatic fraction of coal, which are produced by the removal of aliphatic and alicyclic groups and the increasing aromatization of the humic complexes in coal with increasing temperature (Ward, 1984; Taylor et al., 1998).

The dependence of molecular compound distributions on the maturity of organic matter has been recognized in this study. Moreover, the rapid heating initiated by andesite intrusion has produced some significant changes on the molecular compound distribution with increasing rank, which slightly differs from the expected change on normally coalified coals. Based on GC/GC-MS analysis, the *n*-alkane distribution in organic matter with high maturity is commonly expected to have an unimodal pattern. The strongly bimodal distribution of *n*-alkanes of the high maturity sediment is unusual. In this study, however, bimodality of *n*-alkane distribution in a certain maturity range of the high rank coal is observed. The effect of organic facies and maturity on *n*-alkane distribution can be also represented by the variability of the CPI. The low rank coals show a wide range of CPI values, but the CPI of the high rank coals have almost the same value (~ 1). This indicates that thermal degradation generates new alkanes without any odd or even predominance. Awareness should be given on using CPI as maturity indicator because it seems that a CPI-equilibrium is reached at a maturity corresponding to a vitrinite reflectance lower than 1.4 %.

The application of Pr/Ph ratio as maturity parameter should also be noticed in the case of coalification by rapid heating. The Pr/Ph values of the low rank coals are high and also vary considerably, but at the high rank coal range the values become lower and finally tend to increase again. One should be aware that this pattern could be typical pattern for Pr/Ph ratios of thermally metamorphosed coals.

A “reversal” trend is the typical trend of the relative abundance of aromatic hydrocarbon compounds with increasing coal rank. This pattern is shown by:

(1) the ratio of the aromatic CH stretching area to aliphatic CH stretching area (FTIR analysis). The values of this parameter increase with increasing coalification, except at the meta-anthracite stage, where the value is very low.
(2) the relative abundance of the naphthalene isomers relative to phenanthrene. From GC/GC-MS analysis, it is observed that the abundance of naphthalenes relative to phenanthrene decreases with increasing rank. However, the naphthalene isomers are more abundant than phenanthrene in the coal taken directly at the intrusion contact.
(3) MPR (Methylphenanthrene Ratio), MPI (Methylphenanthrene Index) and 1-MP/9-MP calculated from GC-MS fragmentograms. MPR and MPI increase with rank before decreasing at very high rank, whereas the 1-MP/9-MP value of the high rank coals is invariant (possibly indicating an equilibrium of 1-MP/9-MP ratio at a certain rank close to VR_r = 1.4%).

One should notice that the application of various maturity parameters based on the molecular composition for coal should be done with caution if very high rank coals are involved.

5.3 Changes in mineralogy

The impact of the igneous intrusion on the mineralogy of the studied coals includes two aspects, which are the composition and the amount of minerals. Differences in the mineralogical composition and their relative amount have been observed in the intrusion-affected coals in comparison to the unaltered coals. In the unaltered coals, only minor amounts of minerals are petrographically observed (<4 vol.%). Most common are pyrite (or marcasite), carbonates and clay minerals. An increase of carbonate amount is recognized in the intrusion-affected coals as the formation of new carbonates occurred (total mineral amount is up to 14.6 vol.%). The increase of the ash yield of coal from the unaltered part of the seam towards the intrusion is also an evidence of the formation of minerals as an effect of the igneous intrusion.

EDX analysis indicates that the carbonate minerals in the studied coals are mostly calcite, but some dolomite is recognized in the thermally metamorphosed coals, as a consequence of the hydrothermal metasomatism initiated by magmatic. There is also a change in chemical composition of the iron disulfide minerals. Most of the iron

disulfide minerals found are pyrite or marcasite, but in one intrusion-affected sample, a Cu-bearing iron disulfide, probably chalcopyrite is recognized. It is possible that chalcopyrite was formed during the intrusion by magmatic sulfide solutions.

Change in clay mineralogy is identified by XRD analysis. In the low rank coals, the prominently identified clay mineral is kaolinite whereas it is illite and rectorite in high rank coal. This transformation is an indication that the heating by igneous intrusion had changed the mineralogy of clay. The transformation is related to the dehydration process of clay minerals initiated by temperature increase.

Chapter 6 Outlook

Many studies have been done to characterize the coals of various Indonesian coal basins. However, the studies usually deal only with the optical and some basic physical or chemical properties of coals in the framework of coal quality assessment for mining purpose. More research is still needed to comprehensively study the coals especially in light of coal petrology and geochemistry to inquire the aspects of coal genesis and coalification in more detail. A complete understanding of the characteristics of Indonesian coal will allow the development of new and sophisticated exploration and production strategies. Beneath are some important issues which can be further studied, mostly based on some problems recognized in this study.

6.1 Coal Petrology

The macroscopic description of humic coal is usually following the lithotype classification, which is based on the qualitative or semi-quantitative differentiation of recognizable bright and dull bands (vitrain, clarain, durain and fusain) in coals (see Bustin et al., 1989; Diessel, 1992; Taylor et al., 1998). Some problems have been encountered as the lithotype classifications are applied to the studied coals. The studied coals and other Tertiary Indonesian coals are mainly composed of attrital matrix which does not contain vitrain bands, so that the coals have a relatively homogeneous appearance (Chapter 2; also see Shearer, 1995). These coals can not be classified based on brown coal lithotypes (which includes matrix coal) either, because they already show a bituminous coal–like appearance. A modification of the lithotype classification or a special classification is needed to accommodate that particular characteristic. Therefore, a detail study on the lithotype characteristics of Tertiary Indonesian coals would be beneficial.

Coal petrography may provide data on the maceral percentages of a coal together with reflectance values, which can be used to indicate the depositional environment and the coalification process. The use of various petrographic indices to interpret paleoenvironment has been an important subject in coal petrography. Some limitations have been noted in applying the well known maceral ratio interpretation methods (for example from Diessel, 1986 and Calder et al., 1991), most of all for paleoenvironmental

study of Tertiary coals or Neogene peats which were deposited in a tropical area (Chapter 2). Some authors concluded that using maceral ratios to indicate depositional setting or climate should be unacceptable (see review in Scott, 2002). However, a study to compare the microscopic constituents of Tertiary coals with those of modern tropical peat in Indonesia and to make a model of depositional conditions should be carried out. To formulate a special maceral ratio concept is also probably worth in future. This should be possible because most of the Tertiary coals and modern tropical peats in Indonesia were deposited in a similar tectonic setting and under similar climatic conditions and are basically composed by similar plant communities (see Chapters 2 and 4).

An interesting subject in this study is the effect of the igneous intrusion on the coalification path of the coal macerals. The macerals were in fact coalified following a slightly different path in comparison to macerals in normally coalified coal (Chapter 3). The result of this study can still be improved by analyzing more coal samples, because there is still some lack of data at certain coal maturity ranges. This would increase the reliability of the results. Moreover, results can be used to derive a model of maceral coalification paths for thermally metamorphosed coal.

Another important issue with respect to a coal thermal-metamorphism study is the calculation of paleotemperature of the igneous rock intrusion. Carbonization experiments have been conducted in many studies to simulate coalification processes. Besides that, some vitrinite reflectance - temperature models have been proposed by some authors (Chapter 3). However, the estimation of the paleotemperature in a contact zone is still somewhat speculative since a lot of parameters (for example the original condition of coal during intrusion and thermal diffusivity of original coal), which should be taken into account, are usually simplified. More work needs to be done on vitrinite-reflectance geothermometry in a contact metamorphism situation.

6.2 Organic Geochemistry

Coal organic geochemistry as a tool to study the coal genesis and coalification process has not caught enough attention in Indonesian coal research yet, although nowadays more coal geochemical study have been conducted in the framework of coal utilization

analysis. A lot of organic geochemical studies in Indonesia were focused on petroleum and only some research pay some limited interest on coal (some of the previous studies are cited in Chapters 3 and 4).

Biological marker (biomarker) analysis has become a very useful method to determine paleoenvironmental and paleoecological conditions of coal. Although biomarker analysis has been applied for many coal deposits from different areas and ages, its application to paleoenvironmental and paleoecological studies of South Sumatra coal or Indonesian coal in general is still limited (see Chapter 4). One should also realizes that advances in organic geochemical techniques have led to a better understanding of the relationship of plants and coal macerals (see review by Scott, 2002). The results of this study show that the reconstruction of depositional and ecological conditions of coal enormously benefited from the identification of the redox conditions during deposition based on molecular compounds and the recognition of molecular plant fossils in coals. For further studies, it is suggested that a molecular plant fossil stratigraphy in coal seams is made by analyzing more samples. This can lead us to a better understanding of the plant evolution in a paleomire and its relation with the paleoecological interpretation based on petrographical analysis.

It is also well known that the degree of thermal alteration caused by igneous intrusions affects the organic geochemical characteristics of the Tanjung Enim coal (Chapters 3 and 4). The variation of the chemistry of coal with different rank has been detected by some analysis in this study (proximate/ultimate, Rock-Eval pyrolysis, FTIR and GC/GC-MS). With respect to the gained results, improvement should be reached by analyzing more coal samples and a more complete coal maturity range, so that the path of the organic geochemical characteristics change can be determined properly and completely. This kind of study will be very useful because previously, many other studies only used samples with VR_{max} of less than 2 %. The organic molecular change of the coals within higher rank is less well known. Moreover, other methods of organic geochemical analysis (for example nuclear magnetic resonance, electron spin resonance, etc) could be applied to increase the knowledge.

6.3 Paleobotany/paleopalynology

Our recent study shows that an integration of a variety of approaches is necessary to understand the genesis of coal and coal bearing strata in Indonesia. Paleobotanical and palynological studies have been considered to play a major role in the study of coals. Among the most important factors controlling the petrographic composition and facies characteristics of coal are the types and relatives abundance of plants that composed the peat. Macro- and microfossils of plant are important constituents of coals, especially in the Tertiary coals, both as petrographic components and as distinctive indicators of the nature of the depositional environment where the coal-forming peat accumulated. Furthermore, floras can be indicative of the conditions of climate, water depth, chemistry or nutrient supply. The nature of the vegetation and the botanical affinity of dominant species may have contributed to variations in peat/coal thickness and quality (see review by Scott, 1991; Nichols, 1995).

In Indonesia, paleobotanical or palynological analysis on coal receives only minor interest in comparison to microscopic maceral analysis. Only few studies have been conducted to comprehensively investigate the paleoenvironment and paleoecology of Indonesian coals, also in South Sumatra Basin, based on paleobotanical or palynological assessment (some of them are cited in Chapters 2 and 4). Indonesian coal geologists should consider the fact that the floristic composition of mire vegetation is a crucial factor in the origin of a coal deposit and this can be determined to a large extent from its paleobotanical/palynological records. Therefore a considerable progress in paleobotanical or palynological studies is needed to complete the geological data on Indonesian coals and to improve the understanding of their genesis.

References

van Aarssen, B.G.K., Hessels, J.K.C., Abbink, O.A., de Leeuw, J.W., 1992. The occurrence of polycyclic sesqui-, tri-, and oligoterpenoids derived from a resinous polymeric cadinene in crude oils from southeast Asia. Geochimica et Cosmochimica Acta 56, 1231-1246.

van Aarssen, B.G.K., de Leeuw, J. W., Collinson, M., Boon, J. J, Goth, K., 1994. Occurrence of polycadinene in fossil and recent resins. Geochimica et Cosmochimica Acta 58 (1), 223-229.

Achari, R.G., Shaw, G., Holleyhead, R., 1973. Identification of ionene and other carotenoid degradation products from the pyrolysis of sporopollenins derived from some pollen exines, a spore coal and the Green River shale. Chemical Geology 12, 229-234.

Adiwidjaja, P., de Coster, G.L., 1973. Pre-tertiary paleotopography and related sedimentation in South Sumatra. Proceedings Indonesian Petroleum Association 2nd Annual Convention, Jakarta, pp. 89-103.

Alexander, R., Kagi, R.I., Noble, R., Volkman, J.K., 1984. Identification of some bicyclic alkanes in petroleum. Organic Geochemistry 6, 63-70.

Alexander, R., Kagi, R.I., Rowland, S.J., Sheppard, P.N., Chirila, T.V., 1985. The effects of thermal maturity on distributions of dimethylnaphthalenes and trimethylnaphthalenes in some ancient sediments and petroleums. Geochimica et Cosmochimica Acta 49, 385-395.

Alexander, R., Larcher, A.V., Kagi, R.I., Price, P.L., 1992. An oil-source correlation study using age-specific plant-derived aromatic biomarkers. In: Moldowan, J.M., Albrecht, P., Philp, R.P. (Eds), Biological markers in sediments and petroleum. Prentice Hall, New Jersey, pp. 201-220.

Alpern, B., Durand, B., Espitalié, J.,1972. Localisation, caracterisation et classification petrographique des substances organiques sedimentaires fossiles. Advances in Organic Geochemistry 1971, Pergamon Press, Oxford – Braunschweig, pp.1-28.

Amijaya, H., Littke, R., 2005. Microfacies and depositional environment of Tertiary Tanjung Enim low rank coal, South Sumatra Basin, Indonesia. International Journal of Coal Geology 61 (3/4), 197-221.

Anderson, J.A.R., 1964. The structure and development of the peat swamps of Sarawak and Brunei. Journal of Tropical Geography 18, 7-16.

Anderson, J.A.R., 1983. The tropical peat swamps of western Malesia. In: Gore, A.J.P. (Ed), Ecosystems of the world 4B, Mires: Swamp, Bog, Fen and Moor. Elsevier, Amsterdam, pp.181-198.

Anderson, J.A.R., Muller, J., 1975. Palynological study of a Holocene peat and a Miocene coal deposit from NW Borneo. Review of Palaeobotany and Palynology 19, 291-351.

Anggayana, K., 1996. Mikroskopische und organisch-geochemische Untersuchungen an Kohlen aus Indonesien, ein Beitrag zur Genese und Fazies verschiedener Kohlenbecken. Dissertation, RWTH Aachen, Germany, 224 pp.

Baker, C.E., Pawlewicz, M.J., 1994. Calculation of vitrinite reflectance from thermal histories and peak temperatures: A comparison method. In Mukhopadhyay, P.K., Dow, W.G. (Eds.), Vitrinite reflectance as a maturity parameter, Applications and limitations. ACS Symposium Series 570, pp.217-229.

Bamco (Bukit Asam Mine Constructors), 1983. Bukit Asam Drilling Campaign, Report on geology-coal quality. Bukit Asam Coal Mining Development and Transportation Project, Morrison-Knudsen International Company Inc. and Rheinbraun-Consulting GmbH, Cologne, 90 pp. (unpublished)

Bartenstein, H., Teichmüller, M., 1974. Inkohlungsuntersuchungen, ein Schlüssel zur Prospektierung von paläozoischen Kohlenwasserstoff-Lagerstätten? Fortschritte in der Geologie von Rheinland und Westfalen 24, 129-160.

Bechtel, A., Gruber, W., Sachsenhofer, R.F., Gratzer, R., Lücke, A., Püttman, W., 2003. Depositional environment of Late Miocene Hausruck lignite (Alpine Foreland Basin): insights from petrography, organic geochemistry, and stable carbon isotopes. International Journal of Coal Geology 53, 153-180.

Bechtel, A., Sachsenhofer, R.F., Kolcon, I., Gratzer, R., Otto, A., Püttmann, W., 2002. Organic geochemistry of the Lower Miocene Oberdorf lignite (Styrian basin, Austria): its relation to petrography, palynology and the paleoenvironment. International Journal of Coal Geology 51, 31-57.

Bechtel, A., Sachsenhofer, R.F., Markic, M., Gratzer, R., Lücke, A., Püttmann, W., 2003. Palaeoenvironmental implication from biomarker and stable isotope investigations on the Pliocene Velenje lignite seam (Slovenia). Organic Geochemistry 34, 1277-1298.

Béhar, F., Vandenbroucke, M., 1987. Chemical modeling of kerogens. Organic Geochemistry 11 (1), 15-24.

Bendoraitis, J.G., 1974. Hydrocarbons of biogenic origin in petroleum – aromatic triterpenes and bycyclic sesquiterpenes. In: Tissot, B., Bienner, F. (Eds), Advances in Organic Geochemistry 1973, Editions Technip., Paris, 209-224.

Bostick, N.H., Daws, T.A., 1994. Relationship between data from Rock-Eval pyrolysis and proximate, ultimate, petrographic, and physical analyses of 142 diverse U.S coal samples. Organic Geochemistry 21 (1), 35-49.

Boyd, J.D., Peacock, S.G., 1986. Sedimentological analysis of a Miocene deltaic system: Air Benakat and Muara Enim Formations, Central Merangin Block, South Sumatra. Proceedings Indonesian Petroleum Association 15th Annual Convention, Jakarta, pp. 245-258.

Bray, E.E., Evans, E.D., 1961. Distribution of n-paraffins as a clue to recognition of source beds. Geochimica et Cosmochimica Acta 22, 2-15.

Brooks, J.D., Taylor, G.H., 1968. The formation of some graphitizing carbons. In Walker, P.L., Jr., (Ed), Chemistry and physics of carbon. Marcel Dekker Inc., New York, pp. 243-286.

Bustin, R.M., Cameron, A.R., Grieve, D.A., Kalkreuth, W.D., 1989. Coal petrology: Its principles, methods and applications. Geological Association of Canada Short Course Notes Vol. 3, 230 pp.

Cagniant, D., Gruber, R., Lacordaire, C., Legrand, A.P., Sderi, D., Sfihi, H., Tougne, P., Quinton, M.F., Bunte, G., Jasienko, S., Machinkowska, H., 1991. Characterization of coals and their macerals by solid state ^{13}C n.m.r. and FT-i.r. Fuel 70, 675-681.

Calder, J.H., Gibling, M.R., Mukopadhyay, P.K., 1991. Peat formation in a Westphalian B piedmont setting, Cumberland Basin, Nova Scotia: implications for the maceral-based interpretation of rheotrophic and raised paleo-mires. Bull. Soc. Geol. France 162/2 , 283-298.

Cameron, C.C., Esterle, J.S., Palmer, C.A., 1989. The geology, botany and chemistry of selected peat-forming environments from temperate and tropical latitudes. International Journal of Coal Geology 12, 105-156.

Cecil, C.B., Dulong, F.T., Cobb, J.C., Supardi, 1993. Allogenic and autogenic controls on sedimentation in the Central Sumatra Basin as an analogue for Pennsylvanian coal-bearing strata in the Appalacian basin. In: Cobb, J.C., Cecil, C.B. (Eds), Modern and ancient coal-forming environment, Geological Society of America Special Paper 286, pp. 3-22.

Chadwick, J., 2001. World coal report. Mining Magazine, September 2001. 102-110.

Chaffee, A.L., Hoover, D.S., Johns, R.B., Schweighardt, F.K., 1986. Biological markers extracable from coal. In: John, R.B. (Ed), Biological markers in the sedimentary record. Elsevier, Amsterdam, pp. 311-345.

Chandra, D., 1963. Reflectance of thermally metamorphosed coals. Fuel 42, 69-74.

Chandra, D., 1965. Use of reflectance in evaluating temperature of carbonized or thermally metamorphosed coals. Fuel 44, 171-176.

Clymo, R.S., 1987. Rainwater-fed peat as a precursor of coal. In: Scott, A.C. (Ed), Coal and Coal-bearing Strata: Recent Advances, Geological Society Special Publication No.32, pp. 17-23.

Cohen, A.D., 1968. The petrology of some peats of southern Florida (with special reference to the origin of coal). PhD Thesis, Pennsylvania State University, USA, 352 pp. (unpublished)

Cohen, A.D., Spackman, W., Raymond, R.,Jr., 1987. Interpreting the characteristics of coal seams from chemical, physical and petrographic studies of peat deposits. In: Scott, A.C. (Ed), Coal and Coal-bearing Strata: Recent Advances. Geological Society Special Publication No.32, pp. 107-125.

Corbet, B., Albrecht, P., Ourisson, G., 1980. Photochemical or photomimetic fossil triterpenoids in sediments and petroleum. Journal of American Chemical Society, 1711-1173.

de Coster, G.L., 1974. The geology of Central and South Sumatra Basins. Proceedings Indonesian Petroleum Association 3rd Annual Convention, June 1974, Jakarta, pp. 77-110.

Crosdale, P.J., 1993. Coal maceral ratios as indicators of environment of deposition: do they work for ombrogenous mires? An example from the Miocene of New Zealand. Organic Geochemistry 20, 797-809.

Daly, M.C., Hooper, B.G.D., Smith, D.G., 1987. Tertiary plate tectonics and basin evolution in Indonesia. Proceedings of the 6th Regional Congress on Geology, Mineral and Hydrocarbon Resources of Southeast Asia (GEOSEA VI), Jakarta, pp.1-28.

Darman, H., Sidi, F.H., 2000. An outline of the geology of Indonesia. Indonesian Association of Geologists, Jakarta, 254 pp.

Daulay, B., Cook, A.C., 1988. The petrology of some Indonesian coals. Journal of Southeast Asian Earth Sciences 2 (2), 45-64.

Daulay, B., Ningrum, N.S., Cook, A.C., 2000. Coalification of Indonesian coal. Proceedings of Southeast Coal Geology Conference, Directorate General of Geology and Mineral Resources of Indonesia, Bandung, pp. 85-92.

Deer, W.A., Howie, R.A., Zussman, J., 1992. An Introduction to the Rock-forming Minerals. 2nd Ed., Longman Scientific and Technical, London, 696 pp.

Dehmer, J., 1988. Petrographische und organisch-geochemische Untersuchungen an rezenten Torfen und tertiären Braunkohlen – Ein Beitrag zur Fazies und Genese gebänderter Braunkohlen. Dissertation, RWTH Aachen, 340 pp.

Dehmer, J., 1993. Petrology and organic geochemistry of peat samples from a raised bog in Kalimantan (Borneo). Organic Geochemistry, 20 (2), 349-362.

Dehmer, J., 1995. Petrological and organic geochemical investigation of recent peats with known environments of deposition. International Journal of Coal Geology 28, 111-138.

Demchuck, T., Moore, T.A., 1993. Palynofloral and organic characteristics of a Miocene bog-forest, Kalimantan, Indonesia. Organic Geochemistry 20 (2), 119-134.

Diessel, C.F.K., 1983. Carbonization reactions of inertinite macerals in Austalian coals. Fuel 63, 883-892.

Diessel, C.F.K., 1986. On the correlation between coal facies and depositional environments. Proceeding of 20th Symposium of Deparment of Geology, University Newcastle, NSW, pp. 19-22.

Diessel, C.F.K., 1992. Coal-Bearing Depositional Systems. Springer Verlag, Berlin-Heidelberg, 721 pp.

DIN 51718, 1978. Prüfung fester Brennstoffe – Bestimmung des Wassergehaltes. Deutsches Institut für Normung e.V., Beuth Verlag, Berlin-Köln, 2 pp.

DIN 51719-A, 1978. Prüfung fester Brennstoffe – Bestimmung des Aschegehaltes. Deutsches Institut für Normung e.V., Beuth Verlag, Berlin-Köln, 5 pp.

DIN 51720, 1978. Prüfung fester Brennstoffe – Bestimmung des Gehaltes an Flüchtigen Bestandteilen. Deutsches Institut für Normung e.V., Beuth Verlag, Berlin-Köln, 4 pp.

Directorate of Coal of Indonesia, 2000. Indonesian coal statistics, Special Edition 2000. Directorate General of Mines, Ministry of Mines and Energy of Indonesia, Jakarta, 20 pp.

van Dorsselaer, A., Albrecht, P., Conan, J., 1977. Changes in composition of polycyclic alkanes by thermal maturation (Yallourn Lignite, Australia). In: Campos, R., Goni, J. (Eds.), Advances in Organic Geohemistry 1975. Enadimsa, Madrid, pp. 53-59.

Dydik, B.M., Simoneit, B.R. T., Brassell, S.C., Eglinton, G., 1978. Organic geochemical indicators of palaeoenvironmental conditions of sedimentation. Nature 272, 216-222

Dzou, L.I.P., Noble, R.A., Senftle, J.T., 1995. Maturation effects on absolute biomarker concentration in a suite of coals and associated vitrinite concentrates. Organic Geochemistry 23 (7), 681-697.

Eglinton, G., Hamilton, R.J., 1967. Leaf epicuticular waxes. Science 156, 1322-1335.

Ensminger, A., van Dorsselaer, A., Spyckerelle, C., Albrecht, P., Ourisson, G., 1974. Pentycyclic triterpenes of the hopane type as ubiquitous geochemical markers: Origin and significance. In: Tissot, B., Bienner, F. (Eds), Advances in Organic Geochemistry 1973, Editions Technip., Paris, 245-260.

Espitalié, J., Deroo, G., Marquis, F., 1985a. La Pyrolyse Rock-Eval et ses applications, Première partie, Revue de L'Institut Français du Petrole 40 (5), 563-579.

Espitalié, J., Deroo, G., Marquis, F., 1985b. La Pyrolyse Rock-Eval et ses applications, Deuxième partie, Revue de L'Institut Français du Petrole 40 (6), 755-784.

Espitalié, J., Laporte, J.L., Madec, M., Marquis, F., Leplat, P., Paulet, J., Boutefeu, A.,1977a. Méthode rapide de caractérisation des roches mères de leur potentiel pétrolier et de leur degré d'évolution. Revue de L'Institut Français du Petrole 32, 23-42.

Espitalié, J., Madec, M., Tissot, B.,1977b. Source rock characterization method for petroleum exploration. Proceedings 9th Offshore Technology Conference Vol.3, Houston, pp.439-444.

Esterle, J.S., Ferm, J.C., 1994. Spatial variability in modern tropical peat deposits from Sarawak, Malaysia and Sumatra, Indonesia: analogues for coal. International Journal of Coal Geology 26, 1-41.

Esterle, J.S., Ferm, J.C., Yiu-Liong, T., 1989. A test for the analogy of tropical domed peat deposits to 'dulling up' sequences in coal beds – Preliminary results. Organic Geochemistry 14, 333-342.

Farrimond, P., Bevan, J.C., Bishop, A.N., 1999. Tricyclic terpane maturity parameters: response to heating by an igneous intrusion. Organic Geochemistry 30, 1011-1019.

Franke, S., Hildebrandt, S., Schwarzbauer, J., Link, M., Francke, W., 1995. Organic compounds as contaminants of Elbe river and its tributaries. Fresenius Journal of Analitical Chemistry 353, 39-49.

Gafoer, S., Cobrie, T., Purnomo, J., 1986. Geologic Map of the Lahat Quadrangle, South Sumatra. Geological Research and Development Centre, Directorate General of Geology and Mineral Resources of Indonesia, Bandung.

Gafoer, S., Purbohadiwidjoyo, M.M., 1986. The geology of Southern Sumatra and its bearing on the occurrence of mineral deposits. Bulletin of the Geological Research and Development Center, No.12, Directorate General of Geology and Mineral Resources of Indonesia, Bandung, pp.15-30.

George, S.C., 1992. Effect of igneous intrusion on the organic geochemistry of a siltstone and an oil shale horizon in the Midland Valley of Scotland. Organic Geochemistry 18 (5), 705-723.

Golab, A.N., Carr, P.F., 2004. Changes in geochemistry and mineralogy of thermally altered coal, Upper Hunter Valley, Australia. International Journal of Coal Geology 57, 197-210.

Goodarzi, F., Gentzis, T., 1990. The lateral and vertical reflectance and petrological variation of a heat-affected bituminous coal seam from southeastern British Columbia, Canada. International Journal of Coal Geology 15, 317-339.

Goordazi, F., Murchinson, D.G., 1972. Optical properties of carbonized vitrinites. Fuel 51, 322-328.

Gore, A.J.P., 1983. Introduction. In: Gore, A.J.P. (Ed), Ecosystems of the world 4A, Mires: Swamp, Bog, Fen and Moor. Elsevier, Amsterdam, pp.1-34.

Grady, W.C., Eble, C.F., Neuzil, S.G., 1993. Brown coal maceral distributions in a modern domed tropical Indonesian peat and a comparison with maceral distribution in Middle Pennsylvanian-age Appalacian bituminous coal beds. In: Cobb, J.C., Cecil, C.B. (Eds), Modern and ancient coal-forming environment, Geological Society of America Special Paper 286, pp. 63-82.

Gray, R.J., 1991. Some petrographic applications to coal, coke and carbons. Organic Geochemistry 17 (4), 535-555.

Greb, S.F., Eble, C.F., Hower, J.C., Andrews, W.M., 2002, Multiple-bench architecture and interpretations of original mire phases - Examples from the Middle Pennsylvanian of the Central Appalachian Basin, USA. International Journal of Coal Geology 49, 147-175.

Gruber, W., Sachsenhofer, R.F., 2001. Coal deposition in the Noric Depression (Eastern Alps): raised and low lying mires in Miocene pull-apart basin. International Journal of Coal Geology 48, 89-114.

Hall, R., 1995. Plate tectonic reconstruction of the Indonesian region. Proceedings Indonesian Petroleum Association 24th Annual Convention, Jakarta, pp. 72-84.

Hayatsu, R., Winans, R.E., Scott, R.G., Moore, L.P., Studier, M.H., 1978. Trapped organic compounds and aromatic units in coals. Fuel 57, 541-548.

Hower, J.C., Davis, A., 1999. Reflectance of liptinites in anthracite: Examples from the Southern Anthracite Field, Pennsylvania. TSOP Newsletter 16 (1), 15 - 17.

Hower, J.C., Gayer, R.A., 2002. Mechanisms of coal metamorphism: case studies from Paleozoic coalfields. International Journal of Coal Geology 50, 215-245.

Hunt, J.M., 1996. Petroleum Geochemistry and Geology, 2nd Ed.,W.H. Freeman and Company, New York, 743 pp.

Ibarra, J.V., Munoz, E., Moliner, R., 1996. FTIR study of the evolution of coal structure during the coalification process. Organic Geochemistry 24 (6/7), 725-735.

International Committee for Coal and Organic Petrology, 2001. The new inertinite classification (ICCP System 1994). Fuel 80, 459-471.

Iskandar, E., 1994. Thermometamorphose im Bukit Asam Kohlenrevier, Südsumatra, Indonesien. Dissertation, University of Cologne, Germany, 117 pp.

Jiamo, F., Guoying, S., Jiayou, X., Eglinton, G., Gowar, A.P., Rongfen, J., Shanfa, F., Pingan, P., 1990. Applications of biological markers in the assessment of paleoenvironment of Chinese non-marine sediments. Organic Geochemistry 16 (4-6), 769-779.

Kalkreuth, W., Kotis, T., Papanicolaou, C., Kokkonakis, P., 1991. The geology and coal petrology of a Miocene lignite profile at Meliadi Mine, Katerini, Greece. International Journal of Coal Geology 17, 51-67.

Karayigit, A.I., Whateley, M.K.G., 1997. Properties of a lacustrine subbituminous (k1) seam, with special reference to the contact metamorphism, Soma-Turkey. International Journal of Coal Geology 34, 131-155.

Katz, B.J., Kelley, P.A., Royle, R.A., Jorjorian, T., 1991. Hydrocarbon products of coals as revealed by pyrolysis-gas chromatography, Organic Geochemistry 17 (6), 711-722.

Killops, S.D., Raine, J.I., Woolhouse, A.D., Weston, R.J., 1995. Chemostratigraphic evidence of higher-plant evolution in the Taranaki Basin, New Zealand. Organic Geochemistry 23 (5), 429-445.

Kinhill-Otto Gold Joint Venture, 1986. South Sumatra coal exploration project, Banko Barat feasibility study. Directorate General of Mines of Republic Indonesia, 78 pp. (unpublished)

Kisch, H.J., Taylor, G.H., 1966. Metamorphism and alteration near an intrusive-coal contact. Economic Geology 61, 343-361.

Koesoemadinata, R.P., 2000. Tectono-stratigraphic framework of Tertiary coal deposits of Indonesia. Proceedings of Southeast Coal Geology Conference, Directorate General of Geology and Mineral Resources of Indonesia, Bandung, pp.8-16.

van Krevelen, D.W., 1993., Coal, Typology-Physics-Chemistry-Constitution, 3rd Ed., Elsevier, Amsterdam, 979 pp.

Kuehn, D.W., Snyder, R.W., Davis, A., Painter, P.C., 1982. Characterization of vitrinite concentrates, 1. Fourier transform infrared studies. Fuel 61, 682-694.

Kwiecińska, B., Hamburg, G., Vleeskens, J.M., 1992. Formation temperatures of natural coke in the lower Silesian coal basin, Poland. Evidence from pyrite and clays by SEM-EDX. International Journal of Coal Geology 21, 217-235.

Kwiecińska, B., Petersen, H.I., 2004. Graphite, semi-graphite, natural coke and natural char classification – ICCP system. International Journal of Coal Geology 57, 99-116.

Laflamme, R.E., Hites, R.A., 1979. Tetra- and pentacyclic, naturally-occuring, aromatic hydrocarbons in recent sediments. Geochimica et Cosmochimica Acta 43, 1687-1691.

Lamberson, M.N., Bustin, R.M., Kalkreuth, W., 1991. Lithotype (maceral) composition and variation as correlated with paleo-wetland environments, Gates Formations, Northeastern British Columbia, Canada. International Journal of Coal Geology 18, 87-124.

Lijmbach, G.W.M., 1975. On the origin of petroleum. Proceedings 9th World Petroleum Congress Vol.2, Applied Science Publishers, London, 357-369.

Littke, R., 1987. Petrology and genesis of Upper Carboniferous seams from the Ruhr region, West Germany. International Journal of Coal Geology 7, 147-184.

Littke, R., Horsfield, B., Leythaeuser, D., 1989. Hydrocarbon distribution in coals and in dispersed organic matter of different maceral compositions and maturities. Geologische Rundschau 78 (1), 391-410.

Littke, R., Leythaeuser, D., Radke, M., Schaefer, R.G., 1990. Petroleum generation and migration in coal seams of the Carboniferous Ruhr Basin, northwest Germany. Organic Geochemistry 16 (1-3), 247-258.

Littke, R., Lückge, A., Wilkes, H., 1998. Organic matter in Neogene sediments of the Southern Canary Channel, Canary Island (Sites 955 and 956). In: Weaver, P.P.E., Schminke, H.-U., Firth, J.V., Duffield, W. (Eds), Proceedings of the ODP Scientific Results 157, 361-372.

Littke, R., Ten Haven, H.L., 1989. Palaeoecologic trends and petroleum potential of Upper Carboniferous coal seams of Western Germany as revealed by their petrographic and organic geochemical characteristics. International Journal of Coal Geology 13, 529-574.

Lu, S.T., Kaplan, I.R., 1992. Diterpanes, triterpanes, steranes, and aromatic hydrocarbons in natural bitumens and pyrolysates from different humic coals. Geochimica et Cosmochimica Acta 56, 2761-2788.

Mandile, A.J., Hutton, A.C., 1995. Quantitative X-ray diffraction analysis of mineral and organic phases in organic-rich rocks. International Journal of Coal Geology 28, 51-69.

Marsh, H., 1973. Carbonization and liquid-crystal (mesophase) development: Part 1. The significance of the mesophase during carbonization of coking coals. Fuel 52, 205-212.

Martini, I.P., Glooschenko, W., 1984. Cold climate environments of peat formation in Canada. Advances in the Study of the Sydney Basin 18, Newcastle Symposium Proceeding., Deparment of Geology, University of Newcastle, pp. 18-28

Marzi, R., Torkelson, B.E., Olson, R.K., 1993. A revised carbon preference index. Organic Geochemistry 20 (8), 1303-1306.

Mastalerz, M., Bustin, R.M.,1993. Electron microprobe and micro-FTIR analyses applied to maceral chemistry. International Journal of Coal Geology 24, 333-345.

Meyers, P.A., Simoneit, B.R.T., 1999. Effects of extreme heating on the elemental and isotopic compositions of an Upper Cretaceous coal. Organic Geochemistry 30, 299-305.

Moldowan, J.M., Seifert, W.K., Gallegos, E.J., 1985. Relationship between petroleum composition and depositional environment of petroleum source rocks. AAPG Bulletin 69, 1255-1268.

Moldowan, J.M., Sundararaman, P., Shoell, M., 1986. Sensitivity of biomarker properties to depositional environment an/or source input in the Lower Toarcian of S.W. Germany. Organic Geochemistry 10, 915-926.

Moore, D.M., Reynolds, R.C., Jr., 1997. X-Ray diffraction and the identification and analysis of clay minerals. 2nd Ed., Oxford University Press, New York, 378 pp.

Moore, P.D., 1987. Ecological and hydrological aspects of peat formation. In: Scott, A.C. (Ed), Coal and Coal-bearing Strata: Recent Advances, Geological Society Special Publication No.32, pp. 7-15.

Moore, T.A., Shearer, J.C., 2003. Peat/coal type and depositional environment – are they related? International Journal of Coal Geology 56, 233-252.

Moore, T.A., Shearer, J.C., Miller, S.L., 1996. Fungal origin of oxidised plant material in the Palangkaraya peat deposit, Kalimantan Tengah, Indonesia: Implication for 'inertinite' formation in coal. International Journal of Coal Geology 30, 1-23.

Morley, R.J., 1981. Development and vegetation dynamics of a lowland ombrogenous peat swamp in Kalimantan Tengah, Indonesia. Journal of Biogeography 8, 383-404.

Morley, R.J., 1998. Palynological evidence for tertiary plant dispersals in the SE Asian region in relation to plate tectonics and climate. In: Hall, R., Holloway, J.D. (Eds), Biogeography and Geological Evolution of SE Asia, Backhuys Publishers, Leiden, pp. 211-234.

Morley, R.J. 2000. Tertiary ecological history of Southeast Asian Peat Mires. Proceedings of Southeast Coal Geology Conference, Directorate General of Geology and Mineral Resources of Indonesia, Bandung, pp.44-47.

Murray, A.P., Sosrowidjojo, I.B., Alexander, R., Kagi, R.I., Norgate, C.M., Summons, R.E., 1997. Oleananes in oils and sediments: Evidence of marine influence during early diagenesis? Geochimica et Cosmochimica Acta 61 (6), 1261-1276.

Murrel, F.J., 1996. Coal mining in Indonesia. Mining Engineering, October 1996, 19-13.

Nas, C., Pujobroto, A., 2000. Vitrinite macerals in Indonesian coal. Proceedings of Southeast Coal Geology Conference, Directorate General of Geology and Mineral Resources of Indonesia, Bandung, pp.215-226.

Neuzil, S.G., Supardi, Cecil, C.B., Kane, J.S., Soedjono, K., 1993. Inorganic Geochemistry of domed peat in Indonesia and its implication for the origin of mineral matter in coal. In: Cobb, J.C., Cecil, C.B. (Eds), Modern and ancient coal-forming environment, Geological Society of America Special Paper 286, pp. 23-84.

Nichols, D.J., 1995. The role of palynology in paleoecological analyses of tertiary coals. International Journal of Coal Geology 28, 139-159.

Norgate, C.M., Boreham, C.J., Wilkins, A.J., 1999. Changes in hydrocarbon maturity indices with coal rank and type, Buller Coalfield, New Zealand. Organic Geochemistry 30, 985-1010.

Nytoft, H.P., Bojesen-Koefeld, J.A., Christiansen, F.G., Fowler, M.G., 2002. Oleanane or lupane? Reappraisal of the presence of oleanane in Cretaceous-Tertiary oils and sediments. Organic Geochemistry 33 (2), 1225-1240.

Obaje, N.G., Ligouis, B., Abaa, S.I., 1994. Petrographic composition and depositional environments of Cretaceous coals and coal measures in the Middle Benue Trough of Nigeria. International Journal of Coal Geology 26, 233-260.

Otto, A., Simoneit, B.R.T., Rember, W.C., 2005. Conifer and angiosperm biomarkers in clay sediments and fossil plants from the Miocene Clarkia Formation, Idaho, USA, Organic Geochemistry 36 (6), 907-922.

Painter, P.C., Rimmer, S.M., Snyder, R.W., Davis, A., 1981a. A fourier transform infrared study of mineral matter in coal: The application of a least squares curve-fitting program. Applied Spectroscopy 35 (1), 102-106.

Painter, P.C., Snyder, R.W., Starsinic, M., Coleman, M.M., Kuehn, D.W., Davis, A., 1981b. Concerning the application of FT-IR to the study of coal: A critical assessment of band assignments and the application of spectral analysis programs. Applied Spectroscopy 35 (5), 475-485.

Patrick, J.W., Reynolds, M.J., Shaw, F.H., 1973. Development of optical anisotropy in vitrains during carbonization. Fuel 52, 198-204.

Patrick, J.W., Walker, A.,1991. The relation between vitrain properties and the development of optical anisotropy during carbonization. Fuel 70, 465-470.

Peters, K.E., 1986. Guidelines for evaluating petroleum source rock using programmed pyrolysis. AAPG Bulletin 70 (3), 318-329.

Peters, K.E., Moldowan, J.M., 1993. The biomarker guide, Interpreting molecular fossils in petroleum and ancient sediments. Prentice Hall, Englewood Cliffs, New Jersey, 363 pp.

Petersen, H.I., Andersen, C., Anh, P.H., Bojesen-Koefeld, J.A., Nielsen, L.H., Nytoft, H.P., Rosenberg, P., Thanh, L., 2001. Petroleum potential of Oligocene lacustine mudstones and coals at Dong Ho, Vietnam – an outcrop analogue to terrestrial source rocks in the greater Song Hong Basin. Journal of Asian Earth Sciences 19, 135-154.

Philp, R.P., 1985. Fossil fuel biomarkers, Applications and spectra. Elsevier, Amsterdam-New York, 294 pp.

Price, F.T., Casagrande, D.J., 1991. Sulfur distribution and isotopic composition in peats from the Okefenokee Swamp, Georgia and the Everglades, Florida. International Journal of Coal Geology 17, 1-20.

Prijono, A., 1989. Overview of the Indonesian coal development. Journal of the Indonesian Association of Geologists 12 (1), 253-278.

Prinz, D., Littke, R., 2005. Development of the micro- and ultramicroporous structure of coals with rank as deduced from the accessibility to water. Fuel 84, 1645-1652.

Prinz, D., Pyckhout-Hintzen, W., Littke, R., 2004. Development of the meso- and macroporous structure of coals with rank as analysed with small angle neutron scattering and adsorption experiments. Fuel 83, 547-556.

Pujobroto, A., 2000. Vertical distribution of elements in the A1 seam, Muara Enim Formation in the Bukit Asam mine area. Proceedings of Southeast Coal Geology Conference, Directorate General of Geology and Mineral Resources of Indonesia, Bandung, pp.152-166.

Pujobroto, A., Hutton, A.C., 2000. Influence of andesitic intrusions on Bukit Asam coal, South Sumatra Basin Indonesia. Proceedings of Southeast Coal Geology Conference, Directorate General of Geology and Mineral Resources of Indonesia, Bandung, pp.81-84.

Püttmann, W., Wolf, M., Wolff-Fischer, E., 1986. Chemical characteristics of liptinite macerals in humic and sapropelic coals. Advances in Organic Geochemistry 1985, Organic Geochemistry 10, 625-632.

Radke, M., Leythaeuser, D., Teichmüller, M., 1984. Relationship between rank and composition of aromatic hydrocarbons for coals of different origins. Organic Geochemistry 6, 423-430.

Radke, M., Schaefer, R.G., Leythaeuser, D., Teichmüller, M., 1980. Composition of soluble organic matter in coals: relation to rank and liptinite fluoresence. Geochimica et Cosmochimica Acta 44, 1787-1800.

Radke, M., Welte, D.H., Willsch, H., 1986. Maturity parameters based on aromatic hydrocarbons: Influence of the organic matter type. Advances in Organic Geochemistry 1985, Organic Geochemistry 10, 51-63.

Radke, M., Willsch, H., Leythaeuser, D., Teichmüller, M., 1982. Aromatics components of coal: relation of distribution pattern to rank. Geochimica et Cosmochimica Acta 46, 1831-1848.

Radlinski, A.P., Mastalerz, M., Hinde, A.L., Hainbuchner, M., Rauch, H., Baron, M., Lin, J.S., Fan, L., Thiyagarajan, P., 2004. Application of SAXS and SANS in evaluation of porosity, pore size distribution and surface area of coal. International Journal of Coal Geology 59, 241-271.

Ragot, J.P., 1977. Contribution à l'évolution des substances carbonées dans les formations géologiques. Thesis, P. Sabatier University, Toulouse, 150 pp.

Raymond, A.C., Murchison, D.G., 1992. Effect of igneous activity on molecular-maturation indices in different types of organic matter. Organic Geochemistry 18 (5), 725-735.

Riesser B., Starsinic, M., Squires, E., Davis, A., Painter, P.C., 1984. Determination of aromatic and aliphatic CH groups in coal by FT-i.r. : 2. Studies of coals and vitrinite concentrates. Fuel 63, 1253-1261.

Rochdi, A., Landais, P., 1991. Transmission micro-infrared spectroscopy: An efficient tool for microscale characterization of coal. Fuel 70, 367-371.

Rullkötter, J., Peakman, T.M., ten Haven, H.L., 1994. Early diagenesis of terrigenous triterpenoids and its implications for petroleum geochemistry. Organic Geochemistry 21 (3/4), 215-233.

Schenk, H.J., Witte, E.G., Littke, R., Schwochau, K., 1990. Structural modeling of vitrinite and alginite concentrates during pyrolytic maturation at different heating rates. A combined infrared, ^{13}C NMR and microscopical study. Advances in Organic Geochemistry 1989, Organic Geochemistry 16 (4-6), 943-950.

Schwarzbauer, J., Littke, R., Weigelt, V., 2000. Identification of specific organic contaminants for estimating the contribution of the Elbe river to the pollution of German Bight. Organic Geochemistry 31, 1713-1731.

Scott, A.C. (Ed.), 1987. Coal and Coal-bearing Strata: Recent Advances. Geological Society Special Publication No.32, 332pp.

Scott, A.C., 1989. Observations on the nature and origin of fusain. International Journal of Coal Geology 12, 443-475.

Scott, A.C., 1991. An introduction to the applications of palaeobotany and palynology to coal geology. Bulletin de la Société Géologique de France 162 (2), 145-153.

Scott, A.C., 2000. The Pre-Quaternary history of fire. Palaeogeography, Palaeoclimatology, Palaeoecology 164, 281-329.

Scott, A.C., 2002. Coal petrology and the origin of coal macerals: a way ahead? International Journal of Coal Geology 50, 119-134.

Seifert, W.K., Moldowan, J.M., 1978. Application of steranes, terpanes and monoaromatics to the maturation, migration and source of crude oils. Geochimica et Cosmochimica Acta 42, 77-95.

Shearer, J.C., Staub, J.R., Moore, T.A., 1994. The conundrum of coal bed thickness: A theory for stacked mire sequences. Journal of Geology 102, 611-617.

Shearer, J.C., Moore, T.A., Demchuk, T.D., 1995. Delineation of the distinctive nature of tertiary coal beds. International Journal of Coal Geology 28, 71-98.

Shell Mijnbouw N.V., 1976. Geological study of the Bukit Asam coal mines, Jakarta, 18 pp. (unpublished)

Simoneit, B.R.T., 1986. Cyclic terpenoids of the geosphere. In: John, R.B. (Ed), Biological markers in the sedimentary record. Elsevier, Amsterdam, pp. 43-99.

Simoneit, B.R.T., Grimalt, J.O., Wang, T.G., Cox, R.E., Hatcher, P.G., Nissenbaum, A., 1986. Cyclic terpenoids of contemporary resionous plant detritus and of fossil woods, ambers and coals. Organic Geochemistry 10, 877-889.

Simoneit, B.R.T., Mazurek, M.A., 1982. Organic matter of the troposphere – II. Natural background of biogenic lipid matter in aerosols over the rural western United States. Atmospheric Enivronment 16 (9), 2139-2159.

Smith, G.C., Cook, A.C., 1980. Coalification paths of exinite, vitrinite and inertinite. Fuel 59, 641-646.

Sobkowiak, M., Painter, P., 1992. Determination of aliphatic and aromatic CH contents of coal by FT-i.r. studies of coal extracts. Fuel 71, 1105-1125.

Soehandojo, 1989. Coal exploration and exploitation review in Indonesia. Journal of the Indonesian Association of Geologists 12 (1), 279-325.

Stach, E., 1953. Der Inkohlungssprung im Ruhrkarbon. Brennstoffe Chemie 34, 353-355.

Stankiewicz, B.A., Kruge, M.A., and Mastalerz, M. 1996. A geochemical study of macerals from a Miocene lignite and an Eocene bituminous coal, Indonesia. Organic Geochemistry 24(5) , 531-545.

Stefanova, M., Markova, K., Marinov, S., Simoneit, B.R.T., 2005. Molecular indicators for coal-forming vegetation of the Miocene Chukurovo lignite, Bulgaria. Fuel 84, 1830-1838.

Stout, S.A., 1992. Aliphatic and aromatic triterpenoid hydrocarbons in a Tertiary angiospermous lignite. Organic Geochemistry 18 (1), 51-66.

Sukh Dev, 1989. Terpenoids. In: Rowe, J.W. (Ed.), Natural products of Woody Plants I. Springer Verlag, Berlin, pp. 691-807.

Supardi, Subekty, A.D., Neuzil, S.G., 1993. General geology and peat resources of the Siak Kanan and Bengkalis Island peat deposits, Sumatra, Indonesia. In: Cobb, J.C., Cecil, C.B. (Ed), Modern and ancient coal-forming environment, Geological Society of America Special Paper 286, pp. 45-62.

Sýkorová, I., Pickel, W., Chistanis, K., Wolf, M., Taylor, G.H., Flores, D., 2005. Classification of huminite – ICCP System 1994. International Journal of Coal Geology 62, 85-106.

Taylor, G.H., Teichmüller, M., Davis, A., Diessel, C.F.K., Littke, R., Robert, P., 1998. Organic Petrology, Gebrüder Borntraeger, Berlin-Stuttgart, 704 pp.

Teichmüller, M., 1974. Entstehung und Veränderung bituminöser Substanzen in Kohlen in Beziehung zur Entstehung und Umwandlung des Erdöls. Fortschritte in der Geologie von Rheinland und Westfalen 24, 65-112.

Teichmüller, M. , 1989. The genesis of coal from the viewpoint of coal petrology. International Journal of Coal Geology 12, 1-87.

Teichmüller, M., Durand, B.,1983. Fluorescence microscopical rank studies on liptinites and vitrinites in peat and coals, and comparison with results of the Rock-Eval pyrolysis, International Journal of Coal Geology 2, 197-230.

Teichmüller, M., Teichmüller, R., 1979. Diagenesis of coal (coalification). In Larsen, G., Chilingar, G.V. (Eds), Diagenesis in Sediments and Sedimentary Rocks, Elsevier, Amsterdam, pp. 207-246.

Ten Haven, H.L., de Leeuw, J.W., Rullkötter, J., Sinninghe Damsté, J.S., 1987. Restricted utility of the pristane/phytane ratio as a palaeoenvironmental indicator. Nature 330, 641-643.

Ten Haven, H.L., Peakman, T.M., Rullkötter, J., 1992. Δ^2-Triterpenes: Early intermediates in the diagenesis of terrigenous triterpenoids. Geochimica et Cosmochimica Acta 56, 1993-2000.

Tissot, B.P., Welte, D.H., 1984. Petroleum Formation and Occurrence, 2nd Ed. Springer Verlag, Berlin-Heidelberg, 599 pp.

Vasallo, A.M., Liu, Y.L., Pang, L.S.K., Wilson, M.A., 1991. Infrared spectroscopy of coal maceral concentrates at elevated temperatures. Fuel 70, 635-639.

Volkman. J.K., Alexander, R., Kagi, R.I., 1983. GC-MS characterisation of C_{27} and C_{28} triterpanes in sediments and petroleum. Geochimica et Cosmochimica Acta 47, 1033-1040.

Volkman, J.K., Maxwell, J.R., 1986. Acyclic isoprenoids as biological markers. In: John, R.B. (Ed), Biological markers in the sedimentary record. Elsevier, Amsterdam, pp. 1-42.

van Vucht, H.A., Reitveld, B.J., van Krevelen, D.W., 1955. Chemical structure and properties of coal VIII – Infra red absorption spectra. Fuel 34, 50-59.

Wakeham, S.G., Schaffner, C., Giger, W., 1980. Polycyclic aromatic hydrocarbons in Recent lake sediments – II. Compounds derived from biogenic precursors during early diagenesis. Geochimica et Cosmochimica Acta 44, 415-429.

Wang, T.G., Simoneit, B.R.T., 1990. Organic geochemistry and coal petrology of Tertiary brown coal in the Zhoujing mine, Baise Basin, South China. Fuel 69, 12-20.

Waples, D.W., Machihara, T. , 1990. Applications of sterane and triterpane biomarkers in petroleum exploration. Bulletin of Canadian Petroleum Geology 38 (3), 357-380.

Ward, C.R., 1984. Coal geology and coal technology. Blackwell Scientific Publications, Melbourne, 345 pp.

Wilson, M.J., 1987. X-ray powder diffraction methods. In Wilson, M.J. (Ed), A handbook of determinative methods in clay mineralogy. Blackie and Son Ltd., Glasgow and London, pp.26-98.

Wüst, R.A.J., Hawke, M.I., Bustin, R.M., 2001. Comparing maceral ratios from tropical peatlands with assumptions from coal studies: do classic coal petrographic interpretation methods have to be discarded? International Journal of Coal Geology 48, 115-132.

Zhang, E., Hatcher, P.G., Davis, A., 1993. Chemical composition of pseudo-phlobaphinite precursors: implications for the presence of aliphatic biopolymers in vitrinite from coal. Organic Geochemistry 20 (6), 721-734.

Appendix 1 Petrographical data

Table.A1.1. Random reflectance (Rr) values of huminite in the studied coals from Tambang Air Laya (TAL).

Sample Number	Seam	Rr (%)	SD
02/732	Mangus (A1)	0.35	0.02
02/733		0.38	0.02
02/734		0.40	0.02
02/735		0.36	0.02
02/736		0.36	0.02
02/737		0.39	0.02
02/738		0.37	0.04
02/739		0.38	0.02
02/740		0.38	0.02
02/741		0.38	0.02
02/742		0.38	0.02
02/743	Mangus (A2)	0.39	0.02
02/744		0.39	0.03
02/745		0.43	0.02
02/746		0.41	0.02
02/747		0.42	0.03
02/748		0.41	0.02
02/749		0.42	0.04
02/750		0.43	0.04
02/754	Suban (B1)	0.40	0.02
02/755		0.41	0.03
02/756		0.43	0.03
02/757		0.41	0.03
02/758		0.44	0.04
02/759		0.40	0.03
02/760		0.44	0.03
02/761		0.42	0.03
02/762		0.43	0.03
02/763		0.45	0.03
02/764		0.44	0.03
02/765		0.45	0.03
02/767	Suban (B2)	0.45	0.03
02/768		0.43	0.03
02/769		0.42	0.03
02/770		0.45	0.03
02/771		0.44	0.04
02/772		0.46	0.03
02/773		0.41	0.04
02/777	Petai (C)	1.99	0.05
02/778		2.01	0.07
02/779		2.06	0.08
02/780		2.01	0.02
02/781		2.04	0.08

Note: SD = standard deviation

Table.A1.2. Random reflectance (Rr) values of huminite in the studied coals from Banko Barat (BOB).

Sample Number	Seam	Rr (%)	SD
02/851	Mangus (A1)	0.41	0.03
02/852		0.41	0.03
02/853		0.41	0.03
02/854		0.42	0.02
02/856		0.41	0.03
02/857		0.41	0.03
02/858		0.39	0.03
02/859		0.40	0.02
02/861	Mangus (A2)	0.44	0.03
02/862		0.43	0.03
02/863		0.42	0.03
02/864		0.42	0.03
02/865		0.40	0.03
02/866		0.39	0.03
02/867		0.40	0.03
02/868		0.43	0.02
02/869		0.39	0.03
02/872	Suban (B1)	0.40	0.03
02/873		0.39	0.03
02/874		0.41	0.02
02/875		0.41	0.03
02/876		0.41	0.03
02/877		0.43	0.02
02/878		0.40	0.03
02/880	Suban (B2)	0.40	0.04
02/881		0.42	0.03
02/882		0.41	0.03
02/883		0.42	0.03
02/884		0.39	0.03

Table.A1.3. Reflectance values of vitrinite in the studied coals from Suban .

Sample Number	Seam	Rmax (%)	SD	Rr (%)	SD	Rmin (%)	SD
03/1113	Suban (B2)-H	6.20	0.29	5.18	0.26	4.48	0.55
03/1117		1.86	0.04	1.78	0.05	1.64	0.10
03/1119		1.82	0.03	1.77	0.04	1.67	0.07
03/1120		1.80	0.02	1.78	0.04	1.73	0.03
03/1121		1.74	0.03	1.70	0.05	1.64	0.03
03/1122		1.45	0.01	1.42	0.03	1.38	0.04
03/1123		1.45	0.01	1.42	0.04	1.33	0.02
03/1125	Mangus (A1)	0.53	0.04	0.52	0.04	0.50	0.05
03/1126		0.57	0.04	0.55	0.02	0.53	0.03
03/1127		0.51	0.05	0.51	0.05	0.49	0.04
03/1128		0.53	0.04	0.51	0.04	0.50	0.05
03/1129		0.55	0.03	0.52	0.04	0.50	0.05
03/1130		0.56	0.02	0.54	0.05	0.53	0.02
03/1131		0.52	0.04	0.51	0.05	0.48	0.05
03/1132		0.54	0.06	0.53	0.04	0.52	0.05
03/1133	Mangus (A2)	0.60	0.03	0.58	0.04	0.57	0.02
03/1134		0.61	0.03	0.59	0.06	0.58	0.02
03/1135		0.60	0.03	0.57	0.05	0.56	0.03
03/1136		0.69	0.03	0.66	0.05	0.65	0.03
03/1137		0.76	0.02	0.73	0.03	0.71	0.01
03/1138	Suban (B1)	1.87	0.03	1.85	0.04	1.76	0.08
03/1139		1.91	0.07	1.90	0.03	1.82	0.06
03/1140		1.99	0.05	1.90	0.06	1.88	0.07
03/1141		2.08	0.06	2.02	0.06	1.91	0.07
03/1142		2.09	0.05	2.02	0.05	1.89	0.10
03/1143		2.10	0.03	2.09	0.05	1.93	0.09
03/1144	Suban (B2)	2.38	0.06	2.33	0.07	2.19	0.09
03/1145		2.61	0.10	2.55	0.09	2.21	0.07
03/1146		3.99	0.15	3.69	0.12	3.33	0.22

Note : H = samples were taken in horizontal direction

Table.A1.4. Reflectance values of liptinite in the studied coals from Suban .

Sample Number	Seam	Rmax (%)	SD	Rr (%)	SD	Rmin (%)	SD
03/1113	Suban (B2)-H	n.o.	n.o.	n.o.	n.o.	n.o.	n.o.
03/1117		1.93	0.01	1.79	0.06	1.77	0.17
03/1119		1.82	0.09	1.81	0.07	1.81	0.12
03/1120		1.84	0.01	1.79	0.03	1.79	0.01
03/1121		1.81	0.02	1.74	0.05	1.74	0.03
03/1122		1.25	0.04	1.25	0.05	1.15	0.02
03/1123		1.30	0.03	1.24	0.08	1.14	0.04
03/1125	Mangus (A1)	0.13	0.08	0.13	0.04	0.12	0.07
03/1126		0.13	0.04	0.13	0.05	0.11	0.04
03/1127		0.11	0.02	0.11	0.05	0.10	0.03
03/1128		0.12	0.04	0.12	0.05	0.11	0.03
03/1129		0.11	0.02	0.11	0.07	0.09	0.02
03/1130		0.12	0.03	0.12	0.06	0.11	0.03
03/1131		0.16	0.09	0.14	0.04	0.14	0.08
03/1132		0.12	0.02	0.12	0.05	0.09	0.01
03/1133	Mangus (A2)	0.21	0.03	0.21	0.05	0.18	0.02
03/1134		0.18	0.02	0.18	0.05	0.13	0.03
03/1135		0.18	0.05	0.18	0.07	0.17	0.04
03/1136		0.23	0.04	0.23	0.05	0.16	0.07
03/1137		0.17	0.02	0.17	0.06	0.12	0.05
03/1138	Suban (B1)	1.98	0.10	1.76	0.03	1.76	0.07
03/1139		1.98	0.06	1.85	0.04	1.85	0.05
03/1140		2.06	0.03	1.98	0.05	1.98	0.03
03/1141		2.19	0.05	1.98	0.02	1.98	0.03
03/1142		2.12	0.03	1.98	0.03	1.98	0.05
03/1143		2.16	0.02	2.10	0.07	2.06	0.03
03/1144	Suban (B2)	2.46	0.05	2.39	0.04	2.27	0.09
03/1145		2.74	0.03	2.52	0.05	2.40	0.06
03/1146		n.o.	n.o.	n.o.	n.o.	n.o.	n.o.

Note: n.o.= not observed

Table.A1.5. Reflectance values of inertinite in the studied coals from Suban .

Sample Number	Seam	Rmax (%)	SD	Rr (%)	SD	Rmin (%)	SD
03/1113	Suban (B2)-H	n.o.	n.o.	n.o.	n.o.	n.o.	n.o.
03/1117		1.78	0.04	1.74	0.01	1.50	0.04
03/1119		1.71	0.08	1.67	0.06	1.47	0.03
03/1120		1.69	0.02	1.64	0.05	1.60	0.07
03/1121		1.65	0.09	1.65	0.06	1.54	0.09
03/1122		1.49	0.02	1.42	0.05	1.42	0.04
03/1123		1.39	0.04	1.34	0.05	1.21	0.02
03/1125	Mangus (A1)	0.86	0.04	0.85	0.08	0.82	0.04
03/1126		0.89	0.03	0.87	0.05	0.85	0.04
03/1127		0.89	0.09	0.85	0.09	0.79	0.09
03/1128		0.89	0.12	0.86	0.05	0.86	0.12
03/1129		0.84	0.03	0.83	0.05	0.80	0.03
03/1130		0.94	0.05	0.86	0.08	0.85	0.07
03/1131		0.86	0.05	0.80	0.05	0.79	0.06
03/1132		0.87	0.06	0.83	0.07	0.81	0.06
03/1133	Mangus (A2)	0.95	0.06	0.89	0.04	0.88	0.03
03/1134		0.89	0.04	0.86	0.05	0.79	0.04
03/1135		0.84	0.05	0.83	0.05	0.75	0.06
03/1136		0.96	0.05	0.96	0.04	0.89	0.06
03/1137		0.99	0.05	0.98	0.04	0.94	0.06
03/1138	Suban (B1)	1.78	0.07	1.70	0.05	1.64	0.05
03/1139		1.81	0.06	1.76	0.07	1.71	0.08
03/1140		1.90	0.03	1.78	0.06	1.69	0.05
03/1141		1.92	0.02	1.78	0.06	1.78	0.07
03/1142		1.91	0.05	1.76	0.07	1.76	0.09
03/1143		1.96	0.07	1.81	0.08	1.69	0.08
03/1144	Suban (B2)	2.22	0.12	2.22	0.13	2.08	0.11
03/1145		2.54	0.14	2.42	0.07	2.28	0.09
03/1146		3.72	0.08	3.01	0.05	2.35	0.13

Note: n.o.= not observed

Table.A1.6. Petrographical composition of the studied low rank coals from Tambang Air Laya (TAL) (in vol. %).

Sample No.	Seam	Huminite									Total
		Humotelinite			Humodetrinite			Humocollinite			
		T-Ulm	Ulm	Total	Att	Den	Total	Cor	Gel	Total	
02/732	Mangus (A1)	7.89	7.89	15.78	42.64	8.45	51.09	14.46	0.00	14.46	81.34
02/733		18.04	4.27	22.31	33.75	5.24	38.99	23.86	0.78	24.64	85.93
02/734		26.68	2.34	29.01	25.51	0.00	25.51	40.11	0.00	40.11	94.63
02/735		24.59	2.06	26.66	30.60	6.76	37.35	15.77	0.56	16.33	80.34
02/736		20.46	7.02	27.48	29.04	20.46	49.50	12.08	0.39	12.47	89.45
02/737		55.67	0.00	55.67	11.90	0.00	11.90	26.68	0.00	26.68	94.26
02/738		14.74	4.29	19.03	29.66	9.14	38.80	21.83	0.56	22.39	80.22
02/739		5.97	2.24	8.21	37.51	12.13	49.64	6.53	0.93	7.46	65.31
02/740		14.39	3.03	17.42	39.01	1.51	40.52	29.54	1.51	31.06	89.00
02/741		13.94	8.25	22.20	49.16	0.73	49.90	8.62	0.00	8.62	80.71
02/742		8.17	8.88	17.05	39.96	13.32	53.28	10.12	0.53	10.66	80.98
02/743	Mangus (A2)	9.18	2.30	11.48	33.72	21.01	54.74	15.01	0.00	15.01	81.22
02/744		15.26	2.57	17.84	45.79	2.39	48.18	16.00	0.55	16.55	82.57
02/745		26.87	15.70	42.57	24.60	17.03	41.62	7.19	0.57	7.76	91.95
02/746		17.39	0.37	17.76	7.21	0.37	7.58	59.57	5.36	64.93	90.28
02/747		12.60	2.32	14.92	36.63	17.90	54.52	6.30	0.00	6.30	75.74
02/748		27.22	0.37	27.59	3.15	0.19	3.33	53.89	1.48	55.38	86.30
02/749		10.00	2.64	12.64	26.41	2.83	29.24	6.79	0.38	7.17	49.05
02/750		8.02	0.00	8.02	36.02	15.20	51.22	9.90	0.68	10.59	69.83
02/754	Suban (B1)	11.91	1.41	13.33	42.33	13.33	55.65	3.29	0.00	3.29	72.27
02/755		16.55	4.93	21.47	26.58	6.16	32.74	24.64	0.18	24.82	79.03
02/756		32.06	5.38	37.44	13.63	2.30	15.94	42.43	0.00	42.43	95.81
02/757		27.46	4.26	31.72	31.21	0.85	32.07	10.92	0.51	11.43	75.22
02/758		6.54	1.87	8.41	36.28	3.58	39.86	25.22	0.62	25.84	74.11
02/759		20.95	0.74	21.69	43.75	0.00	43.75	6.86	0.19	7.04	72.48
02/760		16.63	13.23	29.86	30.76	10.19	40.95	15.02	0.00	15.02	85.83
02/761		2.30	0.00	2.30	28.23	0.58	28.81	3.46	0.00	3.46	34.57
02/762		16.28	1.40	17.68	47.25	0.35	47.60	13.83	0.00	13.83	79.10
02/763		9.72	9.54	19.26	39.40	14.49	53.88	8.83	3.53	12.37	85.50
02/764		27.31	1.25	28.56	37.84	0.18	38.02	17.14	0.00	17.14	83.72
02/765		3.78	0.69	4.46	50.28	16.82	67.10	5.15	1.03	6.18	77.74
02/767	Suban (B2)	2.00	5.33	7.32	46.44	20.64	67.08	3.50	0.67	4.16	78.57
02/768		10.84	0.35	11.19	56.82	1.92	58.75	8.92	0.00	8.92	78.85
02/769		4.82	2.18	7.00	22.23	11.19	33.43	31.09	2.18	33.27	73.69
02/770		15.76	0.68	16.44	28.47	1.36	29.83	30.51	0.68	31.19	77.46
02/771		18.26	5.24	23.50	42.84	7.05	49.89	12.11	0.36	12.47	85.87
02/772		9.46	0.92	10.37	43.17	0.92	44.08	7.63	0.00	7.63	62.08
02/773		2.01	0.34	2.35	25.05	6.26	31.31	1.01	0.00	1.01	34.66

Note : T-Ulm = Texto-Ulminite; Ulm = Ulminite; Att = Attrinite; Den = Densinite; Cor = Corpohuminite; Gel = Gelinite

Table.A1.6. *(continued)*

Sample No.	Seam	Liptinite									Total
		Spo	Cut	Res	Sub	Alg	Lip	Bit	Exu	Flu	
02/732	Mangus (A1)	0.80	0.60	0.80	0.40	0.00	7.20	0.00	0.40	0.20	10.40
02/733		0.20	1.60	1.40	0.60	0.00	5.00	0.00	1.00	0.00	9.80
02/734		0.00	0.00	0.40	0.00	0.00	2.00	0.00	1.80	0.00	4.20
02/735		0.40	0.20	2.20	0.80	0.00	5.80	0.00	2.00	0.00	11.40
02/736		0.40	1.80	0.40	0.00	0.00	5.80	0.00	0.20	0.00	8.60
02/737		0.00	0.00	0.40	0.00	0.00	1.60	0.00	2.40	0.00	4.40
02/738		1.00	1.80	1.00	1.60	0.00	6.00	0.00	2.60	0.00	14.00
02/739		0.80	1.20	0.60	1.00	0.00	2.80	0.00	1.40	0.20	8.00
02/740		0.40	1.40	1.40	0.00	0.00	3.80	0.00	0.40	0.00	7.40
02/741		1.40	1.00	1.60	1.20	0.00	8.20	0.60	1.80	0.00	15.80
02/742		2.00	2.00	1.00	0.60	0.20	7.40	0.20	1.00	0.00	14.40
02/743	Mangus (A2)	0.80	1.00	1.40	0.00	0.00	6.40	1.40	1.60	0.00	12.60
02/744		1.40	1.40	1.40	1.00	0.00	6.60	0.40	1.00	0.00	13.20
02/745		0.00	2.00	0.20	0.00	0.00	1.60	0.40	1.20	0.00	5.40
02/746		0.00	0.00	1.80	0.00	0.00	3.60	0.00	3.40	0.00	8.80
02/747		0.80	1.40	1.20	0.60	0.00	11.00	0.40	2.40	0.00	17.80
02/748		0.20	0.00	0.00	0.00	0.00	6.20	0.40	5.60	0.00	12.40
02/749		0.40	1.80	0.20	0.20	0.20	3.60	0.60	0.00	0.00	7.00
02/750		1.20	4.40	0.60	0.40	0.00	7.60	0.20	1.60	0.00	16.00
02/754	Suban (B1)	2.80	2.80	0.60	0.00	0.00	13.80	1.00	1.40	0.00	22.40
02/755		1.80	4.80	1.40	0.20	0.00	8.00	0.00	1.60	0.00	17.80
02/756		0.00	0.00	0.40	0.00	0.00	1.80	0.00	1.80	0.00	4.00
02/757		2.20	2.20	1.40	0.40	0.00	11.20	1.20	2.60	0.00	21.20
02/758		1.20	2.60	0.60	3.20	0.00	9.40	0.00	5.80	0.60	23.40
02/759		0.80	1.60	0.80	1.40	0.00	8.20	0.60	0.40	0.00	13.80
02/760		0.60	3.40	0.80	0.40	0.00	5.00	0.00	1.80	0.20	12.20
02/761		3.40	4.80	5.80	0.00	0.00	32.20	6.40	8.40	0.40	61.40
02/762		1.20	4.00	0.80	0.00	0.00	9.80	0.00	1.60	0.00	17.40
02/763		0.80	1.60	0.60	1.60	0.00	5.80	0.00	1.80	0.00	12.20
02/764		1.20	1.20	1.20	0.60	0.00	6.60	0.00	0.00	2.80	13.60
02/765		1.40	3.00	1.00	0.40	0.00	10.20	0.20	1.60	0.00	17.80
02/767	Suban (B2)	1.00	2.80	0.40	1.60	0.00	11.40	0.40	0.80	0.20	18.60
02/768		1.00	3.20	1.00	2.40	0.20	8.80	0.00	1.40	0.00	18.00
02/769		1.40	1.20	0.40	0.60	0.00	9.40	0.40	9.80	0.00	23.20
02/770		1.20	3.40	0.60	1.00	0.00	9.40	0.20	3.80	0.40	20.00
02/771		0.40	1.40	0.80	0.00	0.00	8.20	0.00	0.80	0.00	11.60
02/772		1.40	3.80	0.40	1.60	0.40	16.20	0.40	3.60	0.20	28.00
02/773		8.40	1.40	1.00	0.20	0.40	38.00	1.00	0.40	0.00	50.80

Note: Spo = Sporinite; Cut = Cutinite; Res = Resinite; Sub = Suberinite; Alg = Alginite; Lip = Liptodetrinite; Bit = Bituminite; Exu = Exsudatinite; Flu = Fluorinite

Table.A1.6. *(continued)*

Sample No.	Seam	Inertinite							Total	Mineral matter		Total Mm
		Mic	Mac	Sfu	Fus	Fun	Sec	Ine		Py/Ma	Other	
02/732	Mangus (A1)	0.00	0.00	0.00	4.13	0.38	0.00	3.57	8.08	0.20	0.00	0.20
02/733		0.00	0.19	0.97	2.13	0.00	0.00	0.00	3.30	0.80	0.20	1.00
02/734		0.00	0.00	0.00	0.00	0.00	0.00	0.19	0.19	0.20	0.80	1.00
02/735		0.00	0.00	2.06	5.44	0.19	0.19	0.38	8.26	0.00	0.00	0.00
02/736		0.19	0.00	0.39	0.19	0.19	0.00	0.58	1.56	0.40	0.00	0.40
02/737		0.00	0.00	0.00	0.00	0.19	0.00	0.77	0.96	0.40	0.00	0.40
02/738		0.00	0.00	0.37	3.92	0.00	0.00	0.93	5.22	0.60	0.00	0.60
02/739		0.19	0.00	2.80	18.47	0.19	0.00	5.04	26.69	0.00	0.00	0.00
02/740		0.00	0.00	0.57	1.89	0.00	0.00	0.57	3.03	0.60	0.00	0.60
02/741		0.00	0.00	0.73	2.20	0.00	0.00	0.37	3.30	0.20	0.00	0.20
02/742		0.18	0.18	0.36	0.71	0.89	0.00	2.13	4.44	0.20	0.00	0.20
02/743	Mangus (A2)	0.35	0.00	0.35	3.88	0.53	0.00	0.88	6.00	0.00	0.20	0.20
02/744		0.00	0.00	1.29	1.47	0.18	0.00	0.74	3.68	0.60	0.00	0.60
02/745		0.19	0.19	0.19	1.89	0.00	0.00	0.19	2.65	0.00	0.00	0.00
02/746		0.00	0.00	0.00	0.00	0.18	0.00	0.37	0.55	0.40	0.00	0.40
02/747		0.17	0.17	0.99	2.82	1.16	0.00	1.16	6.46	0.00	0.00	0.00
02/748		0.00	0.00	0.00	0.00	0.19	0.00	0.00	0.19	1.00	0.20	1.20
02/749		0.00	0.00	4.15	38.86	0.19	0.00	0.75	43.95	0.00	0.00	0.00
02/750		0.17	0.00	1.54	9.05	0.85	0.00	2.56	14.17	0.00	0.00	0.00
02/754	Suban (B1)	0.16	0.00	0.47	3.29	0.00	0.00	0.78	4.70	0.20	0.60	0.80
02/755		0.35	0.00	0.53	1.06	0.18	0.00	0.53	2.64	0.40	0.20	0.60
02/756		0.00	0.00	0.00	0.19	0.00	0.00	0.00	0.19	0.00	0.00	0.00
02/757		0.17	0.17	0.34	1.19	0.34	0.00	0.17	2.39	1.00	0.40	1.40
02/758		0.47	0.00	0.31	0.31	0.47	0.00	0.47	2.02	0.20	0.40	0.60
02/759		0.00	0.00	0.74	12.61	0.00	0.00	0.00	13.35	0.40	0.00	0.40
02/760		0.18	0.00	0.54	0.00	0.54	0.00	0.36	1.61	0.00	0.40	0.40
02/761		0.00	0.00	0.00	2.30	0.00	0.00	1.15	3.46	0.00	1.00	1.00
02/762		0.00	0.00	0.35	1.93	0.70	0.00	0.18	3.15	0.40	0.00	0.40
02/763		0.18	0.00	0.00	0.53	0.71	0.00	0.71	2.12	0.00	0.20	0.20
02/764		0.00	0.00	0.00	1.79	0.18	0.00	0.00	1.96	0.60	0.20	0.80
02/765		0.51	0.00	0.69	1.37	0.00	0.00	1.72	4.29	0.20	0.00	0.20
02/767	Suban (B2)	0.33	0.00	0.00	0.67	0.33	0.00	1.00	2.33	0.40	0.20	0.60
02/768		0.17	0.00	0.00	0.70	0.00	0.00	0.52	1.40	1.80	0.20	2.00
02/769		0.16	0.00	0.31	1.09	0.47	0.00	0.78	2.80	0.20	0.20	0.40
02/770		0.00	0.00	0.51	0.51	0.00	0.00	0.68	1.69	1.00	0.00	1.00
02/771		0.18	0.00	0.36	0.90	0.00	0.00	0.18	1.63	0.80	0.20	1.00
02/772		0.15	0.00	1.07	7.17	0.15	0.00	0.92	9.46	0.40	0.20	0.60
02/773		0.22	0.00	2.46	4.70	0.34	0.00	5.93	13.64	0.40	1.20	1.60

Note : Mic = Micrinite; Mac = Macrinite; Sfu = Semifusinite; Fus = Fusinite; Fun = Funginite; Sec = Secretinite; Ine = Inertinite; Py/Ma = Pyrite or Marcasite; Mm = Mineral matter

Table.A1.7. Petrographical composition of the studied high rank coals from Tambang Air Laya (TAL) (in vol. %).

Sample No.	Seam	Vitrinite	Meta-Liptinite	Inertinite	Mineral matter		Total Mm
					Py/Ma	Other	
02/777	Petai (C)	98.00	0.00	2.00	0.00	0.00	0.00
02/778		98.20	0.00	1.40	0.40	0.00	0.40
02/779		96.80	0.40	2.00	0.20	0.60	0.80
02/780		98.20	0.00	1.40	0.40	0.00	0.40
02/781		95.20	0.40	3.40	1.00	0.00	1.00

Note : Py/Ma = Pyrite or Marcasite, Mm = Mineral matter

Table.A1.8. Petrographical composition of the studied low rank coals from Banko Barat (BOB) (in vol. %).

Sample No.	Seam	Huminite									Total
		Humotelinite			Humodetrinite			Humocollinite			
		T-Ulm	Ulm	Total	Att	Den	Total	Cor	Gel	Total	
02/851	Mangus (A1)	12.05	3.96	16.01	43.88	5.04	48.91	18.34	0.00	18.34	83.26
02/852		13.53	2.04	15.56	51.51	9.82	61.33	7.41	0.00	7.41	84.30
02/853		5.30	9.46	14.76	22.52	31.23	53.76	18.93	0.00	18.93	87.45
02/854		14.56	4.48	19.03	55.98	3.55	59.53	7.09	0.00	7.09	85.66
02/856		15.73	10.11	25.84	37.45	8.61	46.06	12.36	1.12	13.48	85.38
02/857		18.74	5.77	24.50	38.56	8.65	47.20	9.91	0.72	10.63	82.34
02/858		9.76	27.64	37.40	7.05	21.50	28.55	19.15	0.18	19.33	85.28
02/859		31.56	11.08	42.64	23.26	1.48	24.73	19.57	0.00	19.57	86.94
02/861	Mangus (A2)	27.55	4.41	31.96	27.55	5.33	32.88	15.98	0.73	16.71	81.55
02/862		15.20	2.15	17.34	30.76	9.66	40.41	16.63	0.18	16.81	74.57
02/863		9.66	2.25	11.91	44.09	8.21	52.30	4.67	0.00	4.67	68.88
02/864		11.73	0.35	12.08	47.27	0.86	48.13	12.42	0.00	12.42	72.63
02/865		11.67	3.01	14.68	58.72	7.53	66.25	4.33	0.00	4.33	85.26
02/866		14.33	0.18	14.51	39.50	0.37	39.86	30.31	0.37	30.68	85.06
02/867		15.13	6.26	21.39	42.08	1.91	44.00	5.91	0.35	6.26	71.64
02/868		6.38	1.38	7.76	43.46	2.24	45.70	20.35	0.17	20.52	73.98
02/869		18.76	9.64	28.40	29.80	3.16	32.96	19.11	1.23	20.34	81.69
02/872	Suban (B1)	9.31	5.77	15.08	31.46	3.54	35.00	38.17	0.37	38.54	88.62
02/873		18.98	3.76	22.74	44.92	0.75	45.67	19.17	0.00	19.17	87.58
02/874		19.40	10.86	30.26	38.81	6.76	45.57	2.49	0.00	2.49	78.33
02/875		19.26	1.07	20.33	49.22	0.71	49.93	7.13	0.00	7.13	77.40
02/876		2.82	8.45	11.27	57.57	2.46	60.04	6.69	0.00	6.69	78.00
02/877		18.11	2.50	20.61	38.14	4.24	42.38	27.35	0.00	27.35	90.35
02/878		12.21	2.19	14.40	51.05	4.38	55.42	8.39	0.55	8.93	78.76
02/880	Suban (B2)	26.30	3.14	29.44	39.06	6.28	45.34	15.31	1.57	16.88	91.66
02/881		22.53	2.70	25.23	45.59	1.44	47.03	12.25	0.00	12.25	84.52
02/882		15.07	4.65	19.72	35.72	2.23	37.95	24.00	0.00	24.00	81.67
02/883		14.35	2.08	16.42	46.62	1.13	47.75	5.66	0.19	5.85	70.03
02/884		8.54	1.90	10.44	48.99	6.84	55.82	15.95	2.85	18.80	85.06

Note: Abbrevation see Table A1.6

Table.A1.8. *(continued)*

Sample No.	Seam	Liptinite									Total
		Spo	Cut	Res	Sub	Alg	Lip	Bit	Exu	Flu	
02/851	Mangus (A1)	0.40	2.00	1.00	0.00	0.00	8.00	0.00	2.60	0.40	14.40
02/852		1.20	0.80	0.00	0.00	0.00	6.60	0.00	0.80	0.00	9.40
02/853		0.40	1.60	0.00	0.00	0.00	5.20	0.00	0.80	0.20	8.20
02/854		1.20	0.80	0.20	0.00	0.00	5.60	0.00	0.20	0.00	8.00
02/856		1.20	0.80	0.40	2.00	0.00	4.60	0.00	0.00	0.00	9.00
02/857		0.60	1.00	0.80	0.20	0.00	8.20	0.00	2.00	0.00	12.80
02/858		0.20	0.00	0.00	0.20	0.00	7.00	0.00	2.80	0.00	10.20
02/859		0.00	0.40	0.40	0.00	0.00	4.00	0.20	3.80	0.20	9.00
02/861	Mangus (A2)	0.00	1.80	0.20	0.20	0.00	5.20	0.00	2.60	0.00	10.00
02/862		2.00	2.20	0.40	0.00	0.00	9.60	0.00	1.40	0.00	15.60
02/863		1.00	3.20	0.80	1.00	0.00	15.00	0.20	2.00	0.20	23.40
02/864		1.60	3.40	0.80	0.60	0.00	10.60	0.00	1.40	0.00	18.40
02/865		0.40	1.40	0.20	0.20	0.00	4.20	0.00	1.00	0.00	7.40
02/866		0.20	1.60	0.40	0.00	0.00	4.60	0.00	3.00	0.00	9.80
02/867		1.20	1.40	0.60	0.20	0.00	11.00	0.00	2.60	0.40	17.40
02/868		1.00	2.00	0.60	0.60	0.00	10.20	0.00	4.20	0.00	18.60
02/869		0.40	1.40	0.00	0.00	0.00	5.40	0.00	6.20	0.00	13.40
02/872	Suban (B1)	0.00	2.40	0.40	0.00	0.00	1.40	0.00	4.20	0.00	8.40
02/873		0.20	4.20	0.20	0.80	0.00	2.80	0.00	1.20	0.20	9.60
02/874		1.00	2.40	0.60	0.00	0.00	9.80	0.20	1.20	0.60	15.80
02/875		0.60	4.40	1.00	1.40	0.00	6.40	0.00	0.60	0.00	14.40
02/876		1.60	2.40	0.60	0.60	0.00	10.60	0.20	1.60	0.00	17.60
02/877		0.60	0.80	0.00	0.00	0.00	2.40	0.00	2.00	0.00	5.80
02/878		1.00	5.60	0.40	1.00	0.00	8.20	0.20	2.80	0.40	19.60
02/880	Suban (B2)	0.00	1.20	0.20	0.80	0.00	2.60	0.20	0.20	0.00	5.20
02/881		1.20	1.00	0.40	0.40	0.00	8.00	0.00	1.60	0.00	12.60
02/882		0.20	0.80	1.00	0.20	0.00	3.60	0.00	3.60	0.00	9.40
02/883		0.80	0.00	0.40	0.20	0.00	6.80	0.00	1.20	0.00	9.40
02/884		1.00	0.80	0.20	0.60	0.00	7.00	0.20	0.20	0.00	10.00

Note: Abbrevation see Table A1.6

Table.A1.8. *(continued)*

Sample No.	Seam	Inertinite							Total	Mineral matter		Total Mm
		Mic	Mac	Sfu	Fus	Fun	Sec	Ine		Py/Ma	Other	
02/851	Mangus (A1)	0.36	0.00	0.36	0.54	0.00	0.00	0.54	1.80	0.40	0.20	0.60
02/852		0.56	0.00	0.37	3.33	0.19	0.00	1.67	6.11	0.20	0.00	0.20
02/853		0.00	0.00	0.00	1.32	0.19	0.00	0.38	1.89	2.20	0.40	2.60
02/854		0.75	0.00	1.12	1.68	0.19	0.00	2.24	5.97	0.20	0.20	0.40
02/856		0.56	0.00	0.37	2.43	0.00	0.00	2.06	5.43	0.20	0.00	0.20
02/857		0.54	0.00	0.00	0.72	0.36	0.00	2.34	3.96	1.00	0.00	1.00
02/858		0.00	0.00	0.00	2.35	0.36	0.00	0.90	3.61	1.00	0.00	1.00
02/859		0.00	0.00	0.18	0.74	0.00	0.00	1.48	2.40	1.80	0.00	1.80
02/861	Mangus (A2)	0.55	0.00	1.29	4.41	0.18	0.00	1.65	8.08	0.40	0.00	0.40
02/862		0.00	0.00	0.72	6.97	0.00	0.00	1.25	8.94	0.80	0.20	1.00
02/863		0.64	0.00	0.80	2.90	0.00	0.00	3.38	7.72	0.00	0.00	0.00
02/864		0.00	0.00	0.35	5.87	0.35	0.00	0.86	7.42	1.80	0.00	1.80
02/865		0.38	0.00	0.56	5.08	0.19	0.00	0.75	6.96	0.40	0.00	0.40
02/866		0.00	0.00	0.55	2.39	0.18	0.00	0.73	3.86	1.00	0.40	1.40
02/867		0.35	0.00	2.96	5.04	0.00	0.00	1.91	10.26	0.80	0.00	0.80
02/868		0.00	0.00	1.72	3.79	0.34	0.00	0.52	6.38	1.00	0.20	1.20
02/869		0.18	0.00	0.35	2.45	0.53	0.00	0.88	4.38	0.60	0.00	0.60
02/872	Suban (B1)	0.19	0.00	0.37	0.74	0.19	0.00	0.93	2.42	0.60	0.00	0.60
02/873		0.00	0.00	0.19	0.94	0.00	0.00	0.19	1.32	1.60	0.00	1.60
02/874		1.07	0.00	0.18	0.89	0.36	0.00	2.67	5.16	0.80	0.00	0.80
02/875		0.00	0.00	0.89	5.35	0.00	0.00	0.89	7.13	1.20	0.00	1.20
02/876		0.88	0.00	0.88	1.41	0.18	0.00	0.53	3.87	0.60	0.00	0.60
02/877		0.00	0.00	0.19	1.93	0.77	0.19	0.19	3.27	0.60	0.00	0.60
02/878		0.00	0.00	0.00	1.28	0.36	0.00	0.00	1.64	0.00	0.00	0.00
02/880	Suban (B2)	0.00	0.00	0.79	0.79	0.00	0.00	0.79	2.36	0.80	0.00	0.80
02/881		0.00	0.00	0.00	1.44	0.00	0.00	0.18	1.62	1.40	0.00	1.40
02/882		0.00	0.00	1.30	6.33	0.00	0.00	0.74	8.37	0.20	0.40	0.60
02/883		0.00	0.00	1.51	16.99	0.38	0.00	0.76	19.63	1.00	0.00	1.00
02/884		0.00	0.00	2.09	0.95	0.19	0.00	0.57	3.80	1.20	0.00	1.20

Note: Abbrevation see Table A1.6

Table.A1.9. Petrographical composition of the studied medium rank coals from Suban (in vol. %).

Sample No.	Seam	Vitrinite									Total
		Telovitrinite			Detrovitrinite			Gelovitrinite			
		Tel	Colt	Total	Vitd	Cold	Total	Corg	Gel	Total	
03/1125	Mangus (A1)	4.68	34.25	38.93	1.12	34.25	35.37	4.30	1.95	6.18	80.48
03/1126		2.83	34.86	37.69	3.58	35.43	39.01	4.33	2.28	6.60	83.29
03/1127		4.11	39.01	43.11	1.68	30.42	32.10	8.40	2.63	11.01	86.23
03/1128		1.48	29.64	31.12	2.41	34.09	36.49	8.52	5.41	13.89	81.51
03/1129		11.59	34.02	45.61	4.60	19.31	23.91	4.78	2.95	7.72	77.25
03/1130		12.19	57.01	69.20	1.97	4.33	6.29	3.15	3.17	6.29	81.79
03/1131		6.12	46.90	53.02	0.74	21.88	22.62	4.26	2.05	6.30	81.94
03/1132	Mangus (A2)	2.48	51.75	54.23	1.15	24.06	25.20	5.16	1.34	6.49	85.93
03/1133		3.17	35.65	38.82	0.93	34.71	35.65	2.99	1.49	4.48	78.95
03/1134		2.25	19.53	21.78	13.52	29.48	43.01	7.89	0.57	8.45	73.24
03/1135		1.37	23.68	25.05	7.05	49.52	56.56	2.74	1.19	3.91	85.53
03/1136		0.77	17.28	18.04	3.46	57.97	61.42	2.50	0.77	3.26	82.73
03/1137		0.58	8.95	9.53	3.31	50.56	53.87	5.06	1.29	6.22	69.62

Note : Tel = Telinite; Colt = Collotelinite; Vitd = Vitrodetrinite; Cold = Collodetrinite; Corg = Corpogelinite; Gel = Gelinite

Table.A1.9. *(continued)*

Sample No.	Seam	Liptinite									Total
		Spo	Cut	Res	Sub	Alg	Lip	Bit	Exu	Flu	
03/1125	Mangus (A1)	0.80	2.60	0.60	0.40	0.00	6.20	0.20	1.80	0.00	12.60
03/1126		0.40	4.00	0.40	1.60	0.00	5.00	0.20	0.40	0.00	12.00
03/1127		0.80	0.80	0.20	1.00	0.00	5.80	0.40	1.60	0.00	10.60
03/1128		1.60	1.60	0.80	1.00	0.00	8.60	0.00	0.80	0.20	14.60
03/1129		0.80	1.20	0.80	0.40	0.20	4.00	0.00	2.80	0.60	10.80
03/1130		0.60	1.80	0.00	0.20	0.00	3.20	0.00	1.60	0.00	7.40
03/1131		0.80	0.60	0.40	0.80	0.20	6.80	0.40	1.00	0.20	11.20
03/1132	Mangus (A2)	0.80	1.20	0.00	0.00	0.00	4.00	0.00	1.20	0.00	7.20
03/1133		1.60	1.60	1.20	0.60	0.00	7.40	0.20	0.80	0.00	13.40
03/1134		1.40	1.60	0.80	0.40	0.00	5.80	1.60	2.20	0.00	13.80
03/1135		1.20	0.40	0.40	0.40	0.20	3.20	1.40	1.20	0.00	8.40
03/1136		1.20	1.60	0.80	0.80	0.00	4.40	0.00	0.60	0.00	9.40
03/1137		1.00	2.60	1.00	0.00	0.20	3.00	0.40	0.40	0.00	8.60

Note: Abbrevation see Table A1.6

Table.A1.9. *(continued)*

Sample No.	Seam	Inertinite							Total	Mineral matter			Total Mm
		Mic	Mac	Sfu	Fus	Fun	Sec	Ine		Py/Ma	Carb	Other	
03/1125	Mangus (A1)	0.00	0.00	0.75	2.06	0.37	0.00	0.19	3.37	2.25	0.94	0.37	3.56
03/1126		0.00	0.00	0.19	2.45	0.75	0.00	0.57	3.96	0.38	0.19	0.19	0.75
03/1127		0.00	0.00	0.37	1.12	0.37	0.19	0.37	2.43	0.56	0.00	0.19	0.75
03/1128		0.00	0.00	0.74	1.11	0.00	0.00	1.48	3.33	0.37	0.00	0.19	0.56
03/1129		0.00	0.37	2.39	6.44	0.00	0.00	2.57	11.77	0.18	0.00	0.00	0.18
03/1130		0.00	0.20	1.77	5.90	0.20	0.00	1.97	10.03	0.59	0.20	0.00	0.79
03/1131		0.00	0.37	1.30	2.78	0.56	0.00	1.30	6.30	0.56	0.00	0.00	0.56
03/1132	Mangus (A2)	0.00	0.00	0.95	3.44	0.95	0.00	1.34	6.68	0.19	0.00	0.00	0.19
03/1133		0.00	0.37	0.19	3.73	0.75	0.00	2.61	7.65	0.00	0.00	0.00	0.00
03/1134		0.38	0.00	1.31	6.20	0.75	0.00	3.94	12.58	0.19	0.00	0.19	0.38
03/1135		0.00	0.00	0.59	1.37	0.59	0.00	2.15	4.70	0.00	0.78	0.59	1.37
03/1136		0.00	0.00	0.58	3.07	0.58	0.00	3.07	7.29	0.19	0.19	0.19	0.58
03/1137		0.00	0.00	2.53	7.97	0.58	0.00	2.14	13.22	0.58	5.64	2.33	8.56

Note: Carb = Carbonate, other abbreviation see Table A1.6

Table.A1.10. Petrographical composition of the studied high rank coals from Suban (in vol. %).

Sample No.	Seam	Vitrinite	Meta-Liptinite	Inertinite	Mineral matter					Total Mm	Mosaic Structure
					Py/Ma	Carb	Clay	Qu	Other		
03/1113	Suban (B2)-H	82.40	0.00	0.60	0.40	4.80	9.40	0.00	0.00	14.60	2.40
03/1117		91.40	1.80	6.60	0.00	0.20	0.00	0.00	0.00	0.20	0.00
03/1119		93.80	2.60	2.80	0.20	0.60	0.00	0.00	0.00	0.80	0.00
03/1120		92.80	0.40	2.60	1.00	1.60	1.60	0.00	0.00	4.20	0.00
03/1121		93.60	0.60	3.20	0.20	1.40	1.00	0.00	0.00	2.60	0.00
03/1123		91.80	0.40	5.60	0.20	1.60	0.40	0.00	0.00	2.20	0.00
03/1138	Suban (B1)	91.20	0.40	2.00	0.40	4.60	1.20	0.20	0.00	6.40	0.00
03/1139		87.80	1.00	9.40	0.20	1.60	0.00	0.00	0.00	1.80	0.00
03/1140		84.20	0.80	11.60	0.40	1.60	1.40	0.00	0.00	3.40	0.00
03/1141		91.00	1.20	5.80	0.20	0.60	1.20	0.00	0.00	2.00	0.00
03/1142		89.40	0.60	8.00	0.40	0.80	0.80	0.00	0.00	2.00	0.00
03/1143		90.40	1.20	6.80	0.20	0.60	0.80	0.00	0.00	1.60	0.00
03/1144	Suban (B2)	90.60	0.20	7.20	0.40	1.60	0.00	0.00	0.00	2.00	0.00
03/1145		87.00	0.40	10.60	0.20	1.40	0.40	0.00	0.00	2.00	0.00
03/1146		90.60	0.00	1.00	0.20	2.00	6.00	0.20	0.00	8.40	0.00

Note : Py/Ma = Pyrite or Marcasite; Carb = Carbonate; Qu = Quartz, Mm = Mineral matter

Appendix 2 Geochemical data

Mass spectra of identified biomarkers in the studied coals

A2.1 Isoprenoids

2,6,10-Trimethylundecane

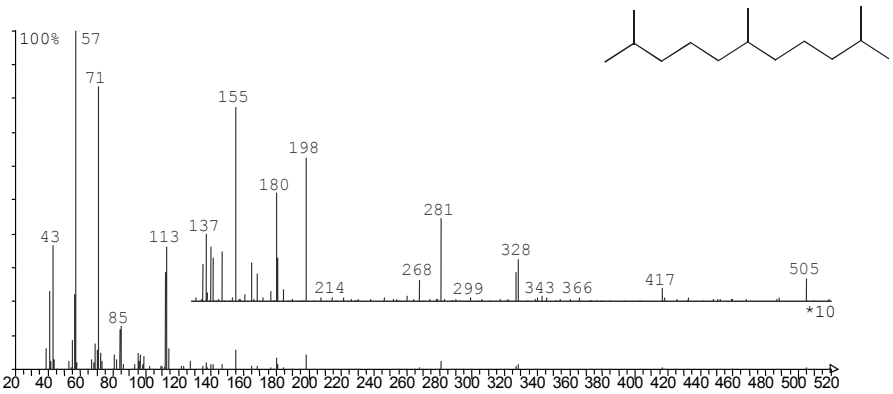

2,6,10-Trimethyltridecane

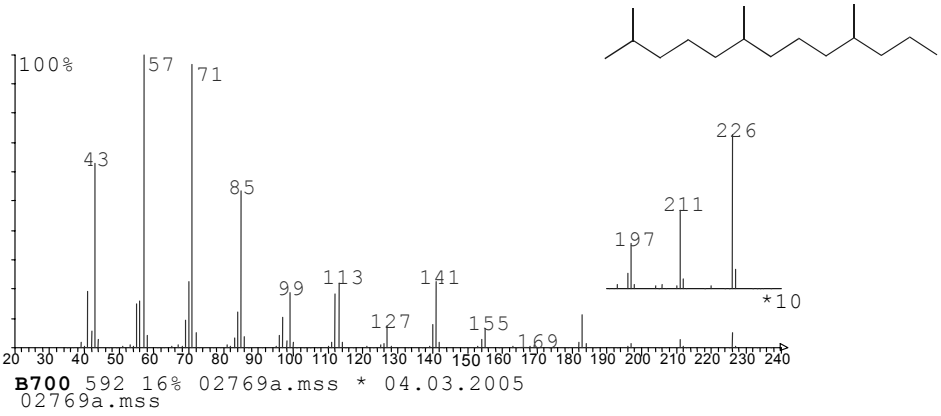

Norpristane

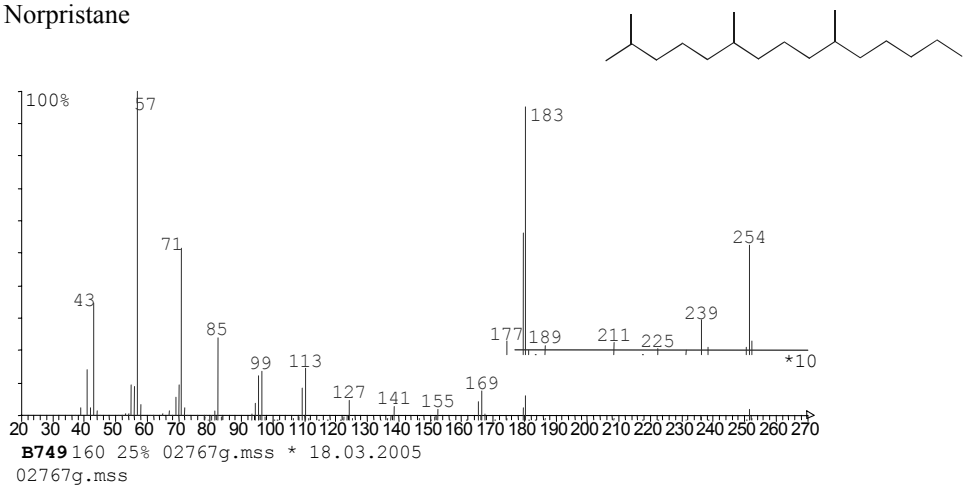

Pristane

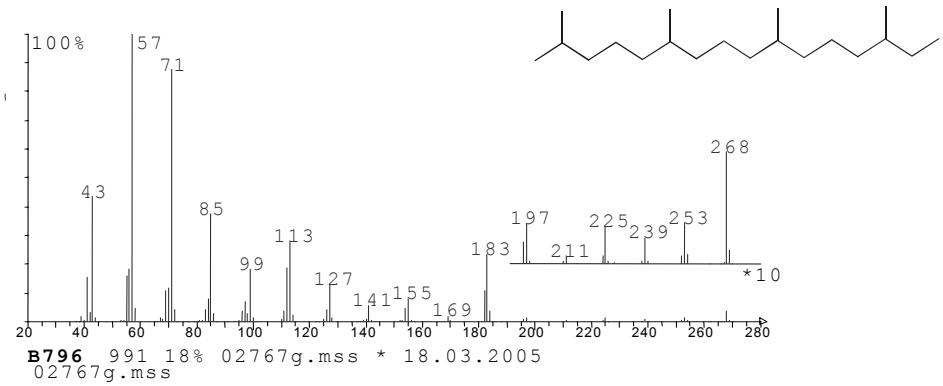

Phytane

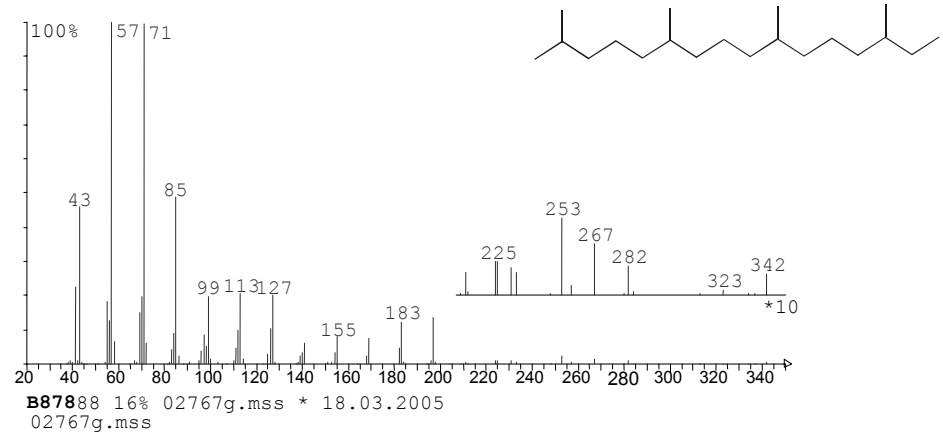

A2.2 Sesquiterpenoids

Cadinane

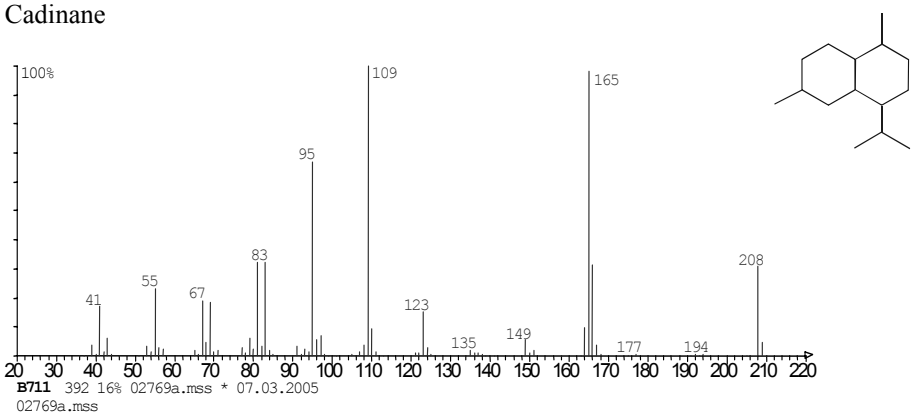

Trans-Cadinane

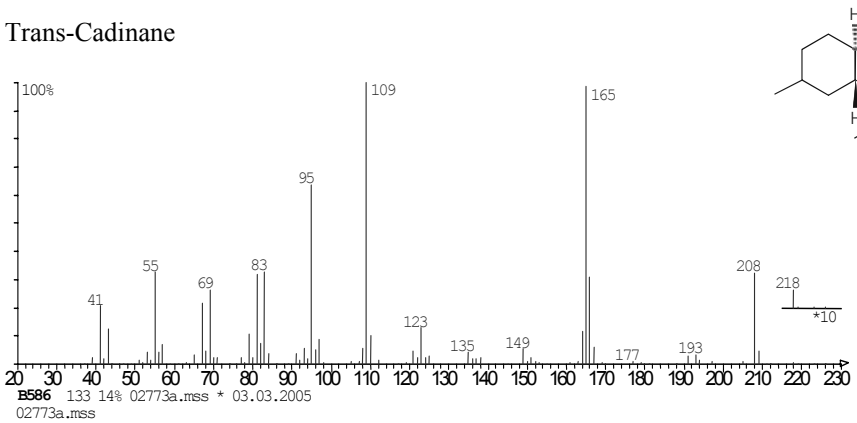

4ß(H) -Eudesmane

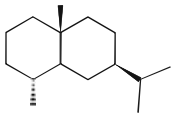

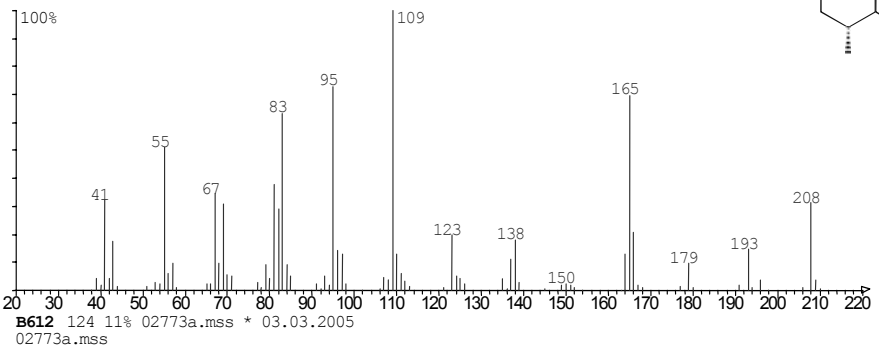

Ionene (1,1,6-Tetramethyltetraline)

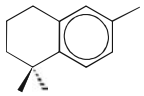

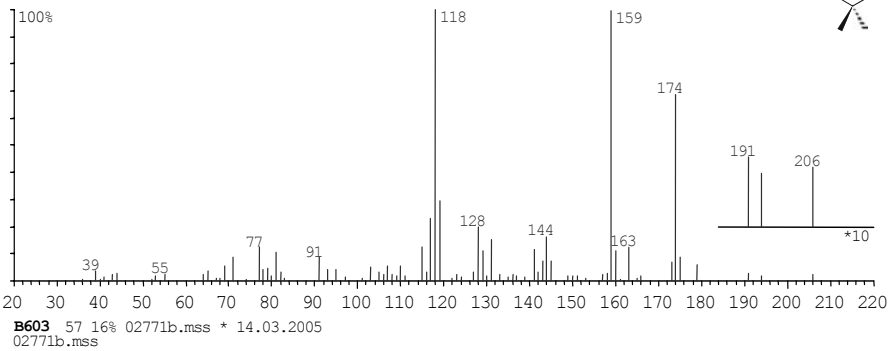

Pentamethylindan

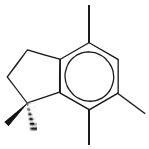

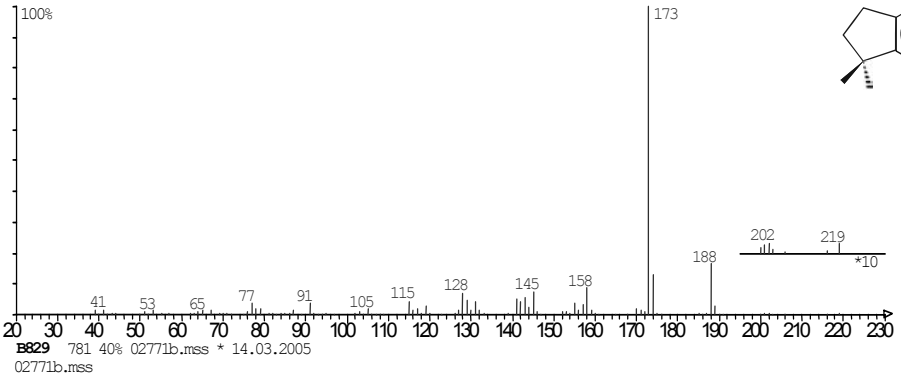

Calamene

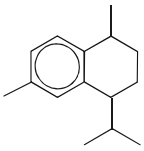

Cadalene

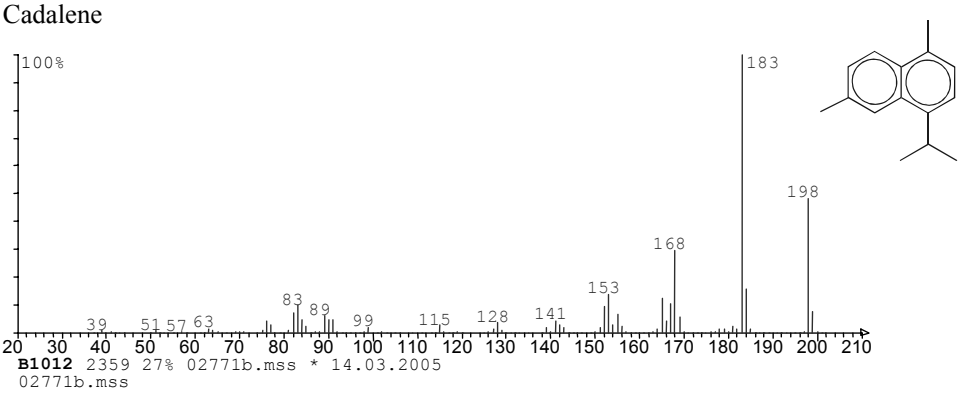

5,6,7,8-Tetrahydrocadalene

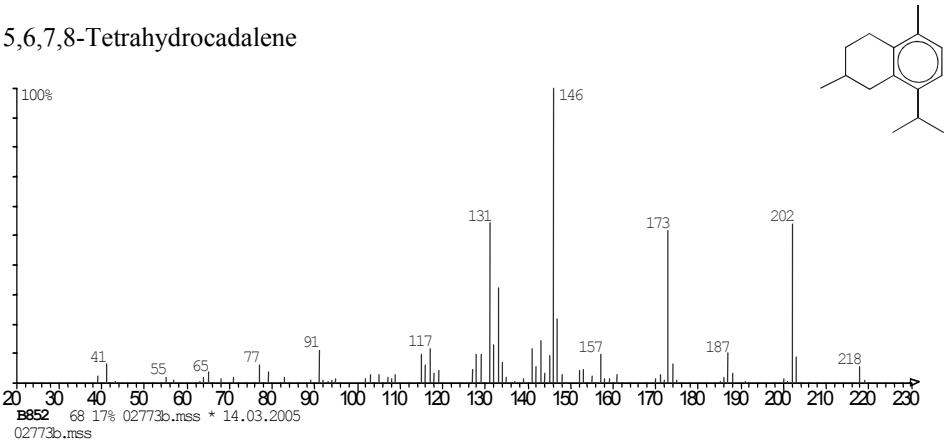

A2.3 Diterpenoids

Abietane

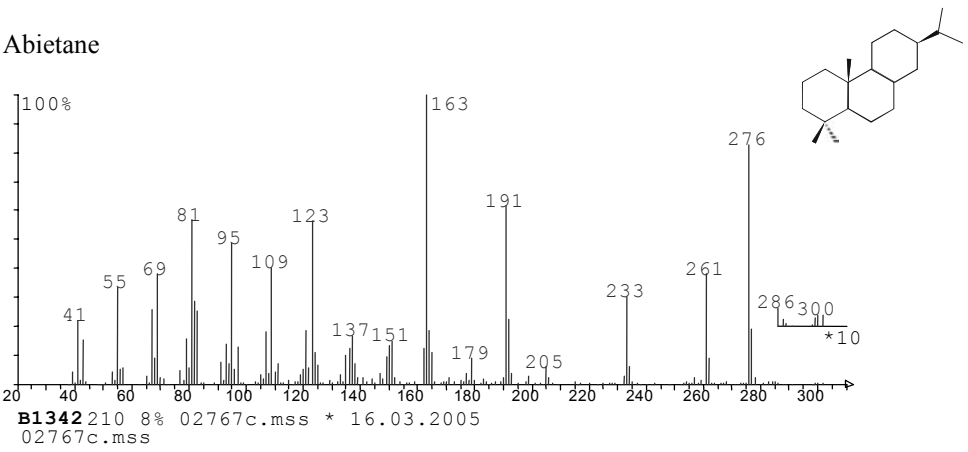

A2.4 Sesterterpenoids

De-A-lupane

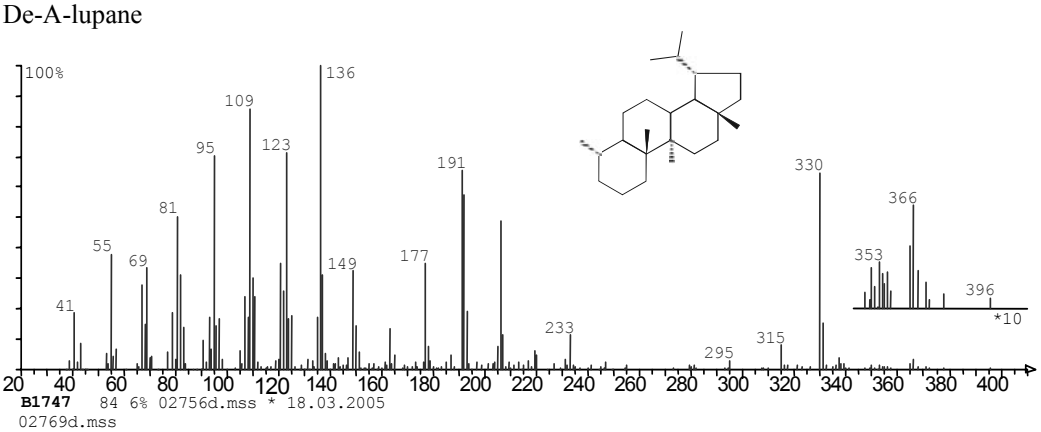

A2.5 Non-hopanoid triterpenoids

Olean-13(18)-ene

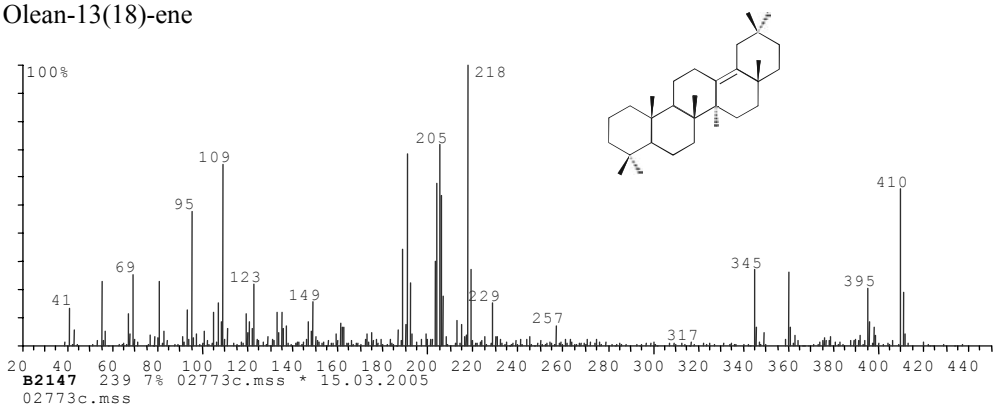

Olean-12-ene

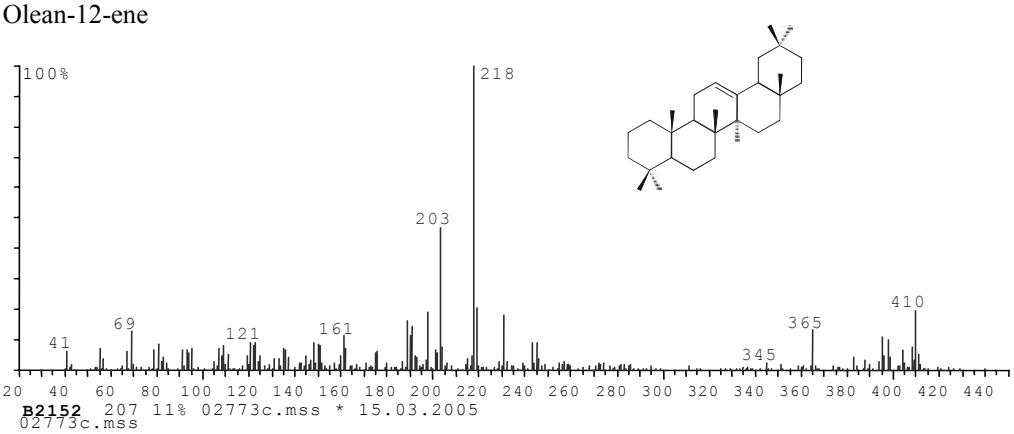

Olean-18-ene

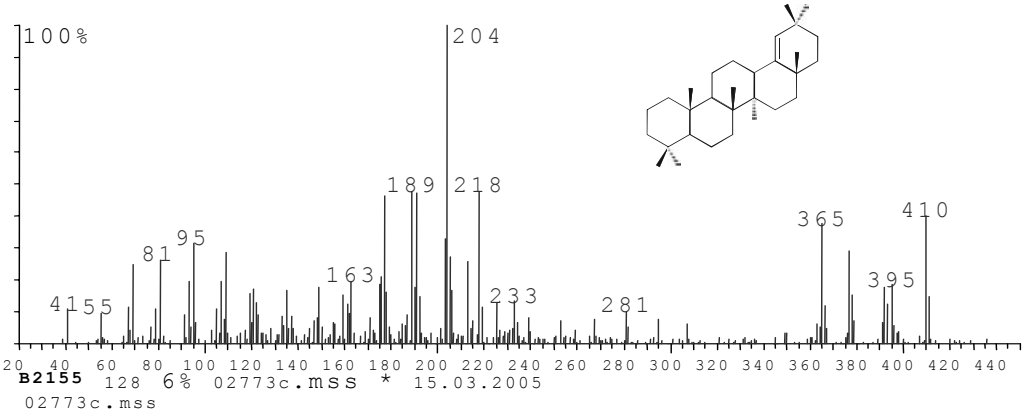

Urs-12-ene

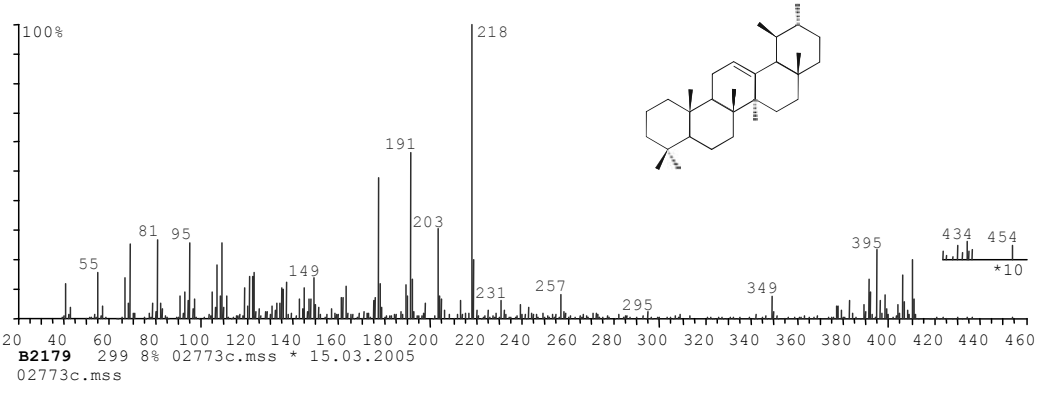

18α(H)- + 18ß(H)-Oleanane

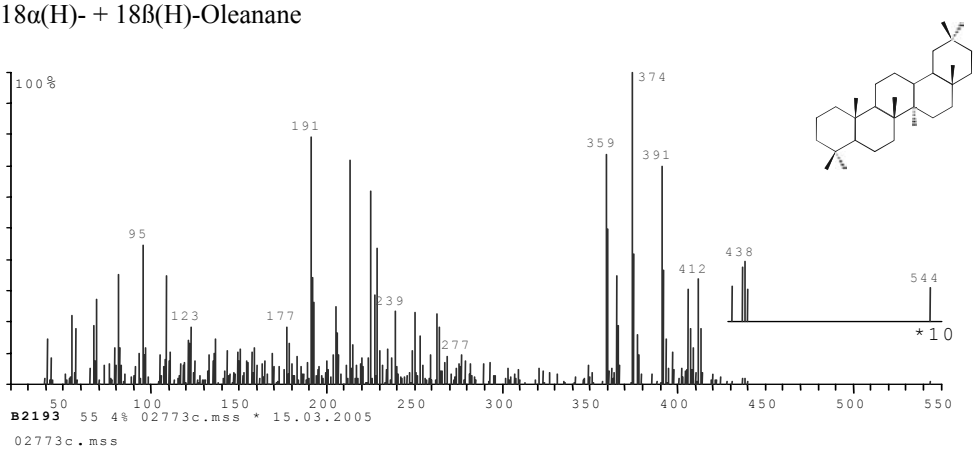

2,2,4a,9-Tetramethyl-1,2,3,4,4a,5,6,14b-octahydropicene

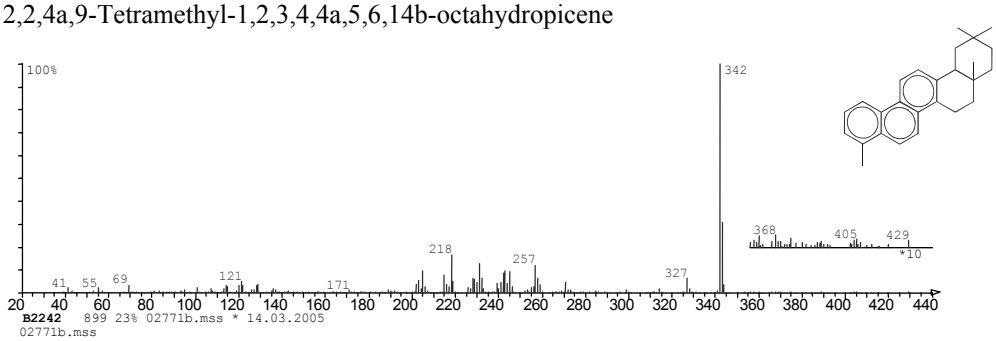

1,2,4a,9-Tetramethyl-1,2,3,4,4a,5,6,14b-octahydropicene

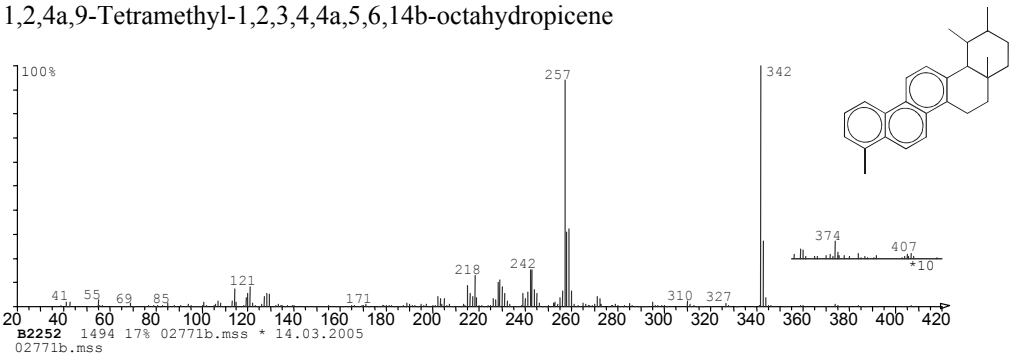

2,2,-Dimethyl-1,2,3,4-tetrahydropicene

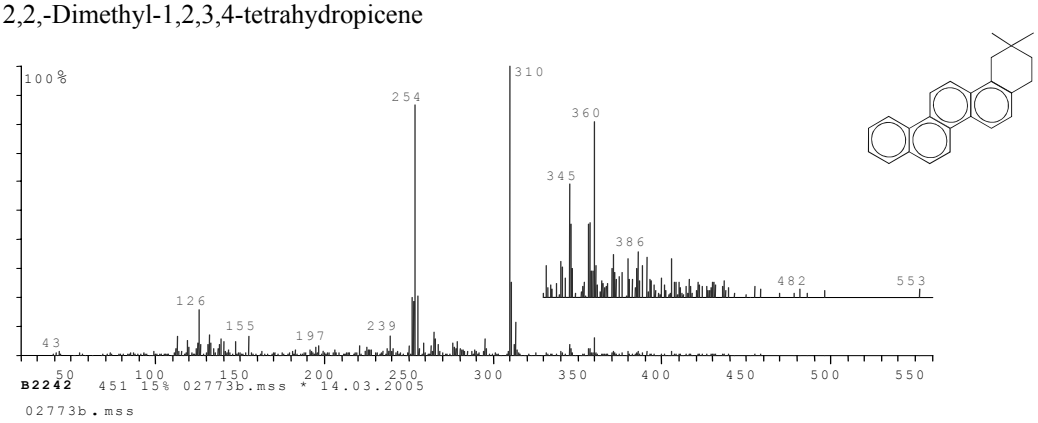

1,2,9-Trimethyl-1,2,3,4-tetrahydropicene

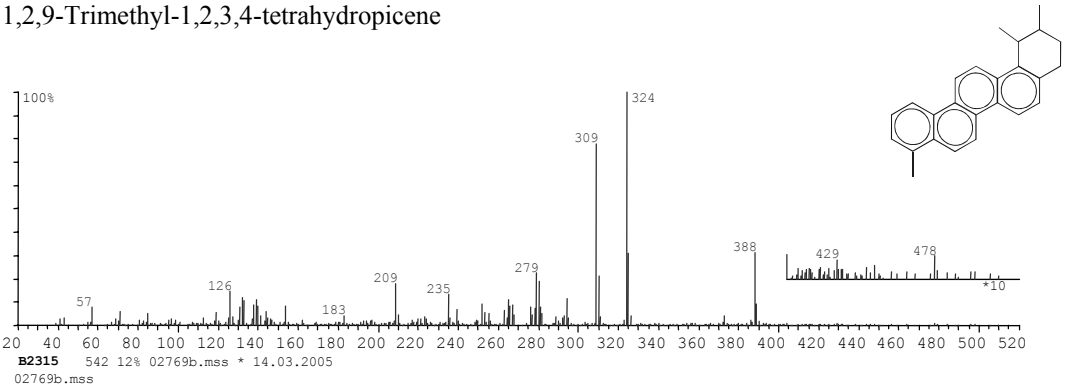

2,2,9-Trimethyl-1,2,3,4-tetrahydropicene

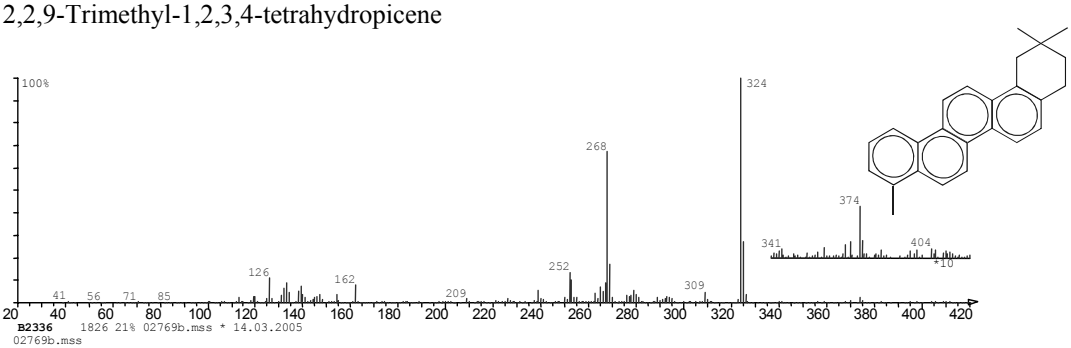

A2.5 Hopanoids

18α(H)-22,29,30-Trisnorneohopane (Ts)

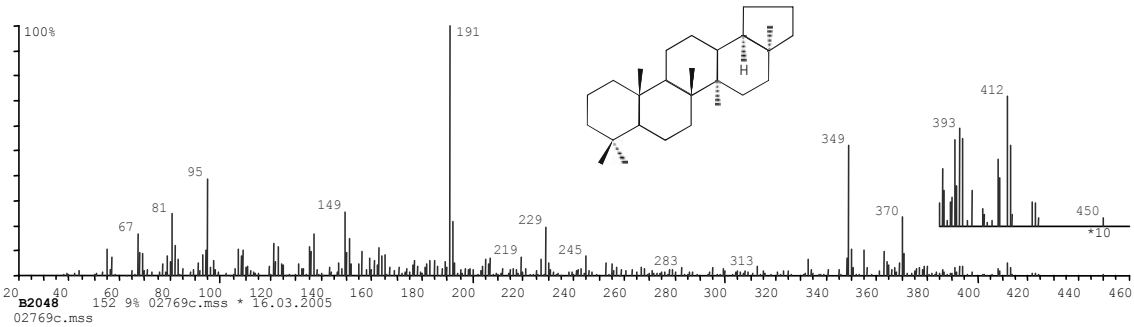

17α(H)-22,29,30-Trisnorhopane (Tm)

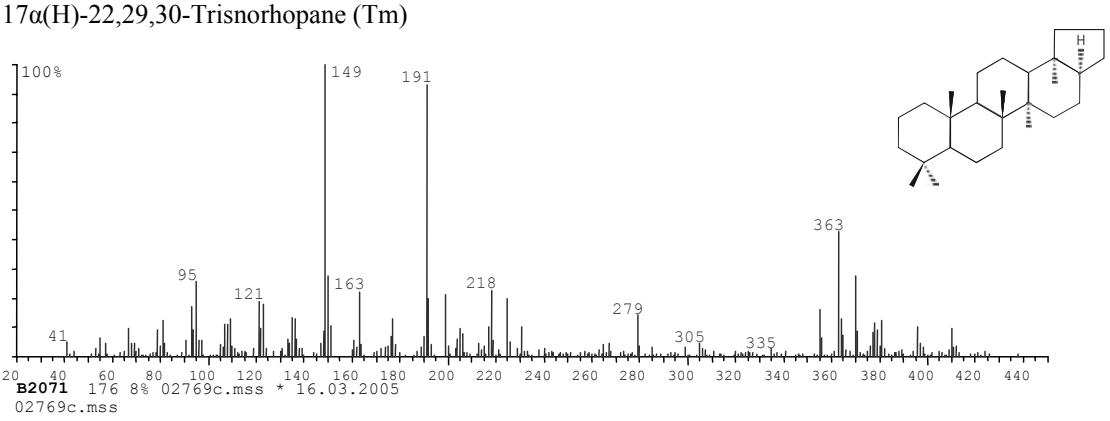

17α(H)-21ß(H)-Hopane

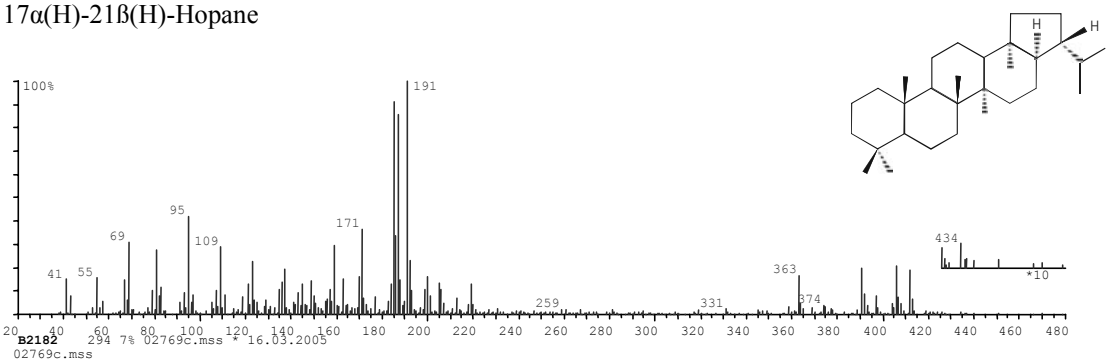

17ß(H)-21α(H)-Moretane

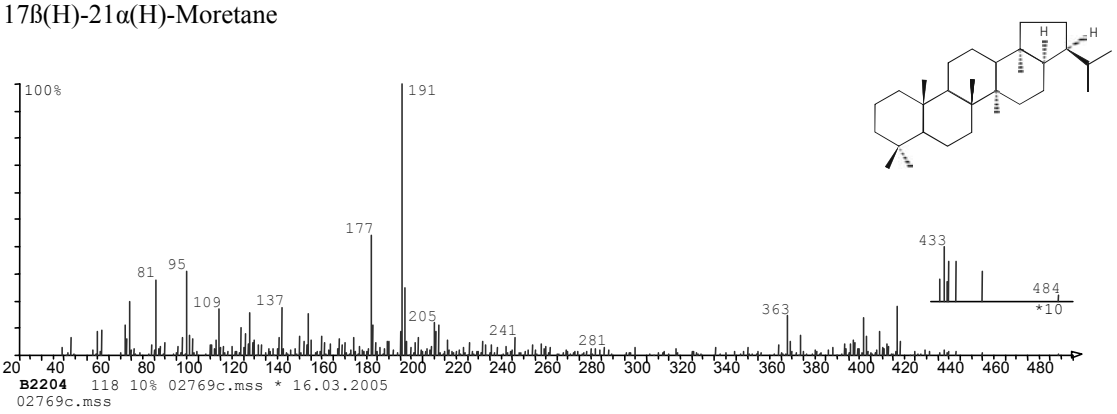

17α(H)-21ß(H)-30-Homohopane (22S)

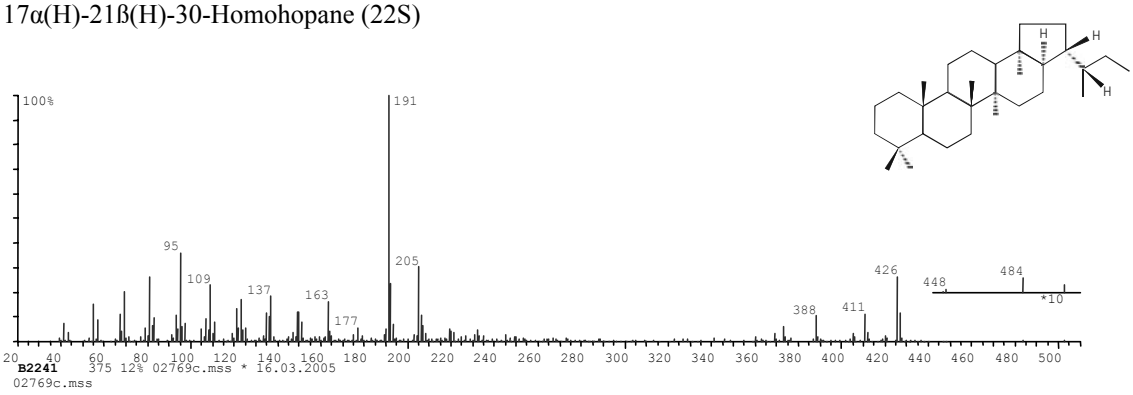

17α(H)-21ß(H)-30-Homohopane (22R)

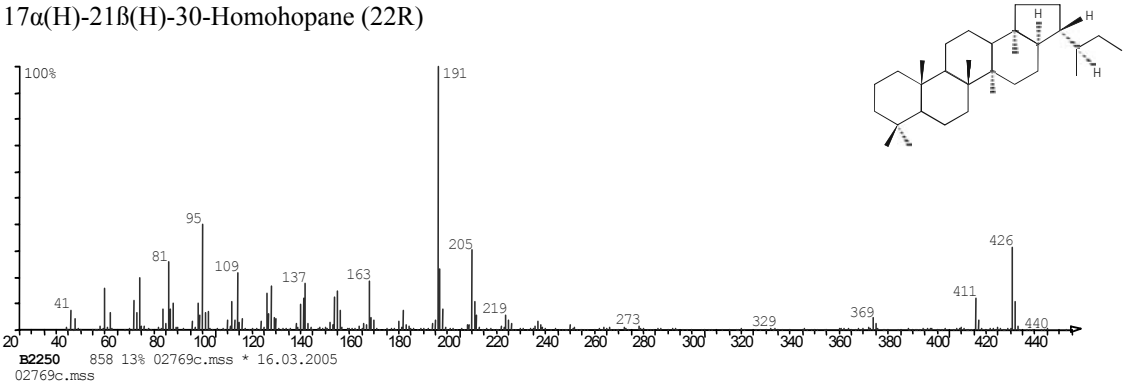

17ß(H)-21ß(H)-Hopane

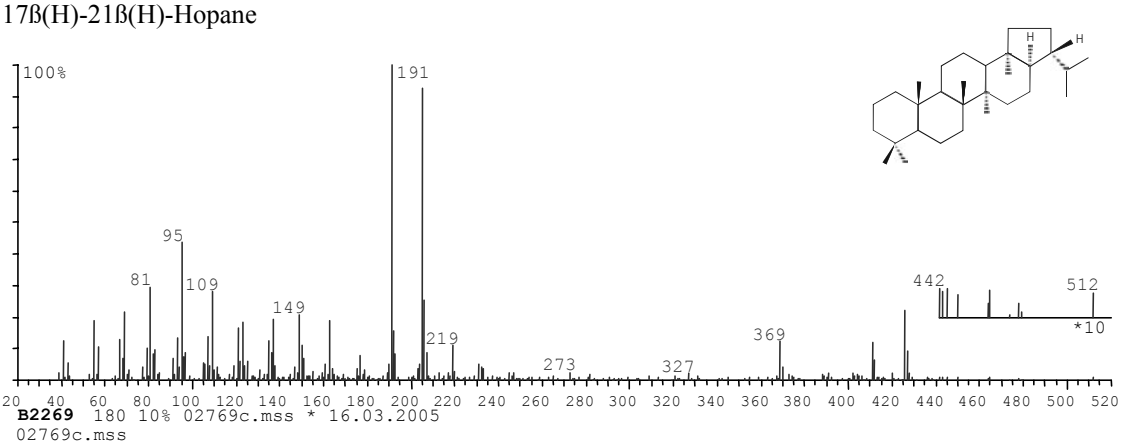

17α(H)-21ß(H)-30,31-Bishomohopane (22S)

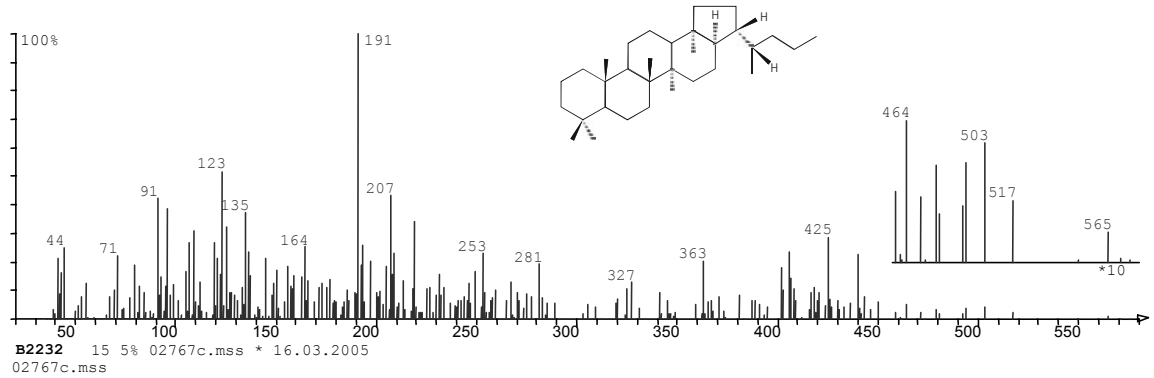

17α(H)-21ß(H)-30,31-Bishomohopane (22R)

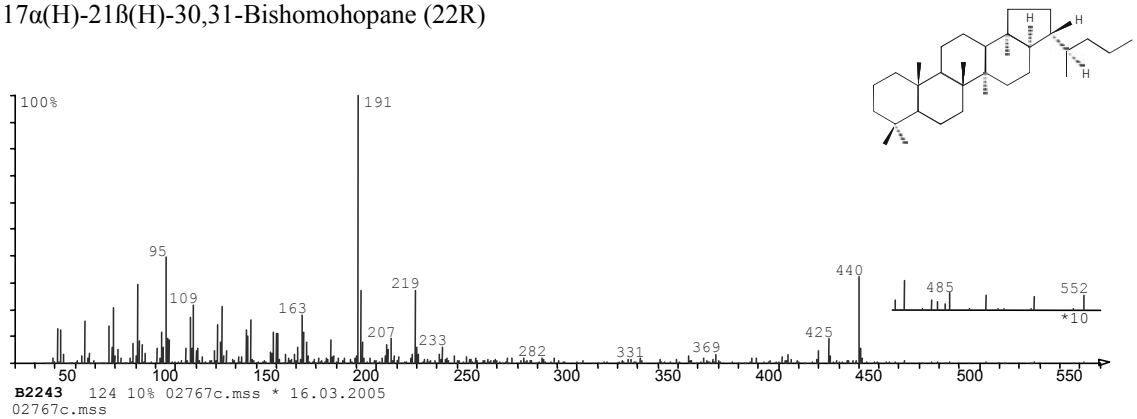

17ß(H)-21α(H)-30,31-Bishomomoretane

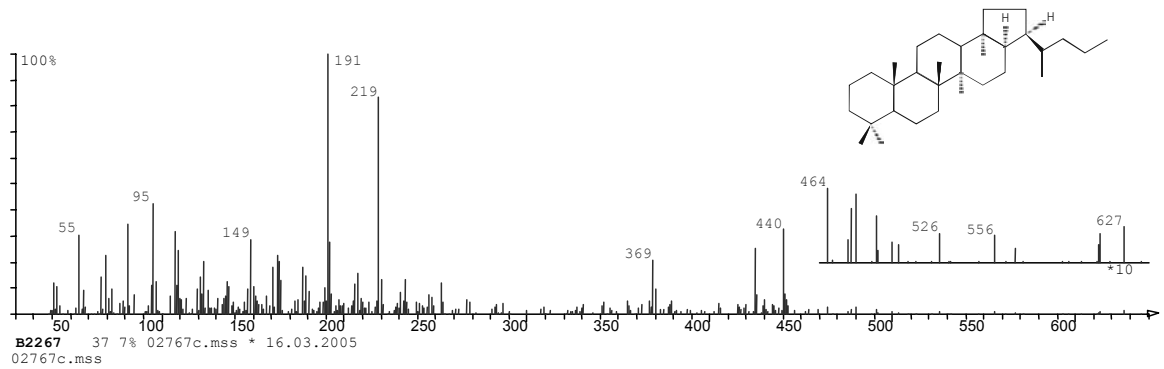

CURRICULUM VITAE

Personal Details

Name	: Donatus Hendra Amijaya
Place and date of birth	: Yogyakarta, August 7, 1974
Gender	: Male
Marital status	: Married

Education

2001 - 2005	Promotion at Institute of Geology and Geochemistry of Petroleum and Coal, Aachen University, Germany Subject of interest: coal petrology and geochemistry
1998 - 2001	Graduate study at Department of Geological Engineering, Gadjah Mada University, Yogyakarta, Indonesia; "Magister Teknik" degree in Geological Engineering Subject of interest: sedimentology
1992 - 1998	Undergraduate study at Department of Geological Engineering Gadjah Mada University, Yogyakarta, Indonesia; "Sarjana Teknik"(Bachelor) degree in Geological Engineering
1989 - 1992	Senior High School at SMA Negeri 3, Yogyakarta
1986 - 1989	Junior High School at SMP Pangudi Luhur 2, Yogyakarta
1980 - 1986	Elementary School at SDK Baciro, Yogyakarta

Additional course

January 2004	AAPG Winter Education Conference in Houston, USA. Course subject: *Practical mapping of surfaces/Reservoir characterization, Essentials of subsurface mapping and Coal-bed methane*
July 2003	*Fluid Inclusion* course at Department of Mineralogy, Würzburg University, Germany
March 2003	*Stable Isotopes* course at Department of Geology, Heidelberg Universty, Germany
June 2000	*Organic petrography* course at Manpower Development Center for Mines in Bandung, Indonesia
1997 - 1998	*Coal Exploration* course at Manpower Development Center for Mines in Bandung, Indonesia with practical course as coal exploration geologist at PT. Tambang Batubara Bukit Asam (PTBA) in Tanjung Enim, Sumatra

Work experience

2002 - 2005	Organic petrographer at Institute of Geology and Geochemistry of Petroleum and Coal, Aachen University, Germany
1999 - 2001	Lecture and research assistant at Laboratory of Sedimentography, Department of Geological Engineering Gadjah Mada University, Yogyakarta
1995 -1997	Student assistant for laboratory work of mineralogy and petrology at Laboratory of Mineral Resources, Department of Geological Engineering and for field geology at Department of Geophysics, Gadjah Mada University, Yogyakarta.

Scholarship

2001 - 2005	German Academic Exchange (DAAD) scholarship for postgraduate education at Aachen University, Germany
1998 - 2000	University Research for Graduate Education (URGE) scholarship from The World Bank for graduate education at Gadjah Mada University, Indonesia